uni.lu

UNIVERSITÉ DU LUXEMBOURG

DISSERTATION

Defence held on 08/05/2024 in Luxembourg

to obtain the degree of

DOCTEUR DE L'UNIVERSITÉ DU LUXEMBOURG

EN SCIENCES DE L'INGÉNIEUR

by

Pëllumb ZOGU

Born on 25 August 1992 in Gllogoc, (Republic of Kosovo)

SAFETY & RELIABILITY ASSESSMENT OF COMPOSITE COLUMNS IN STEEL AND CONCRETE USING NONLINEAR STOCHASTIC FINITE ELEMENT ANALYSIS

Dissertation defence committee

Prof. Dr.-Ing. Markus Schäfer, dissertation supervisor
Professor, Université du Luxembourg

Prof. Dr. Giovanni Muciaccia
Professor, Politecnico di Milano

Prof. Dr.-Ing. Stefan Maas, Chairman
Professor, Université du Luxembourg

Prof. Dr. Andreas Taras
Professor, ETH Zürich

Dr.-Ing. Marco Bergmann
Civil engineer, HRA Ingenieurgesellschaft Bochum

Dedication

In loving memory of my father,

M. ZOGU (1954-2023)

Acknowledgements

To everyone who provided support in any way in the work described in this dissertation, I would like to express my deepest gratitude.

The most profound acknowledgement belongs to Prof. Dr.-Ing. Markus Schäfer, for his unwavering guidance, understanding, and trust. He served as an excellent academic supervisor and a well-respected mentor to me over the past four years, his guidance has been crucial to my advancement as a professional. This research would not be possible without his vision and support. Additionally, I would like to express my gratitude also to the CET members, Prof. Dr. Giovanni Muciaccia and Prof. Dr. Stefan Maas for their highly valuable suggestions and guidance. I also want to thank my friends and colleges, who were all very supportive.

Last but not least, I want to express my deepest gratitude to my mother for her unwavering support and encouragement throughout my long period away from home while pursuing my Ph.D. and to my beloved father, who I lost a few months before completing this dissertation, and who is the reason I began it in the first place. This achievement is a tribute to you.

Luxembourg, February 2024   Pëllumb ZOGU

Abstract

The focus of this study is the safety and reliability assessment for the design of composite columns in accordance with the general method with the overall safety factor γ_0 based on the strain-limited N-M interaction diagram, as this method is not yet explicitly included in the EN 1994-1-1 but it is in discussion to be considered in the second generation of Eurocode 4. This dissertation employs the Stochastic Finite Element Method (SFEM), which combines the standard Finite Element Method (FEM) procedure with the probability theory to solve stochastic problems and evaluate the reliability and safety. The semi-probabilistic approach, which is also known as the Level II method or First Order Reliability Method (FORM) in Eurocode 0 EN 1990, is used to further develop Eurocodes, while in this study, is implemented to validate the safety and reliability of the general method with the overall safety factor γ_0 determined by the strain-limited N-M interaction diagram for composite columns. To conduct nonlinear Stochastic Finite Element Analysis (FEA), Monte Carlo Simulation (MCS) or sampling technique such as Latin Hypercube Sampling (LHS) should be used. In this study, Latin Hypercube Sampling (LHS) is used to generate random variables resulting from statistical distribution of the geometry and material parameters of the composite columns in steel and concrete. The concept of safety and the approved safety levels in Eurocode 0 and Eurocode 4 have been thoroughly discussed.

The parametric nonlinear SFEM analysis results demonstrate that, the overall safety factor γ_0 based on the strain-limited N-M interaction diagram within the general method attain the safety level as required by Eurocode 0 (reliability index β=3.04), which corresponds to a probability of failure of 0.1% quantile for a normal building at the ultimate limit state with a reference period of 50 years.

Additionally, sensitivity analyses are carried out implementing the Sobol's indices method in order to determine the extent to which each random variable affects the resistance of the composite columns in steel and concrete under compression load.

Table of Contents

Notations

Notation used in this work are based on Eurocodes and *fib* Model Code [1].

Composite column a composite member subjected mainly to compression or compression and bending [2].

Composite member a structural member with components of concrete and of structural or cold-formed steel, interconnected by shear connection so as to limit the longitudinal slip between concrete and steel [2].

Member imperfections refers to geometrical and structural imperfections [3].

Overall (safety) factor refers to a factor used to deal with the uncertainties related to geometry, material, and the model.

Plastic resistance refers to resistance at a cross-section level, based on rectangular stress block [3].

Reliability refers to the ability of a structure or a structural member to perform its intended function satisfactorily (from the viewpoint of the stakeholder) for its intended life under specified environmental and operating conditions [1].

Safety refers to the ability of a structure or structural element to ensure that no harm would come to the users and the people in the vicinity of the structure under any (combination of) expected actions [1].

Strain-limited refers to non-linear resistance at a cross-section level [3].

Symbols

Symbols related to the stability of steel and composite columns

A	Cross-section area
A_a	Cross-section area of the structural steel section
A_c	Cross-section area of the concrete part
A_V	Shear area the structural steel section
A_s	Cross-section area of the reinforcement
E	Elastic modulus
E_a	Modulus of elasticity of structural steel
E_{cm}	Secant modulus of elasticity of concrete
$E_{c,eff}$	Effective modulus of elasticity for concrete
E_s	Design value of modulus of elasticity of reinforcing steel
$(EI)_{eff}$	Effective flexural stiffness for calculation of relative slenderness
$(EI)_{eff,II}$	Effective flexural stiffness for use in second-order analysis
e_0	Equivalent bow imperfection
f_{cd}	Design value of compressive strength of concrete
f_{cm}	Mean value of compressive strength of concrete
f_{ctm}	Mean value of tensile strength of concrete
f_{sd}	Design value of yield strength of reinforcement
f_{sm}	Mean value of yield strength of reinforcement
f_u	Ultimate strength
f_y	Nominal value of the yield strength of structural steel
f_{yd}	Design value of the yield strength of structural steel
f_{ym}	Mean value of the yield strength of structural steel
I	Second moment of area
I_a	Second moment of area of structural steel section
I_c	Second moment of area of concrete section
I_s	Second moment of area of steel reinforcement
K	Factor related to buckling mode
K_0	Reduction factor for the flexural stiffness of composite columns

$K_{c,II}$	Correction factor for concrete stiffness of composite columns
K_e	Correction factor for concrete stiffness of composite columns
L	Length of the composite column
L_e	Effective length of the composite columns
M_I	First-order bending moment
M_{II}	Second order bending moment
$M_e(x)$	External bending moment at the distance x
$M_{int}(x)$	Internal bending moment at the distance x
M_{Ed}	Design bending moment
$M_{y,Ed}$	Design bending moment applied to the composite column about the y-y axis
$M_{z,Ed}$	Design bending moment applied to the composite column about the z-z axis
$M_{pl,Rd}$	Design value of plastic resistance moment of the composite column
$M_{pl,Rm}$	Mean value of plastic resistance moment of the composite column
$M_{pl,a,Rd}$	Design value of the plastic resistance moment of structural steel section
$M_{pl,y,Rd}$	Design resistance moment of the composite column about the y-y axis
$M_{pl,z,Rd}$	Design resistance moment of the composite column about the z-z axis
N_{cr}	Elastic critical load
N_{Ed}	Design value of the compressive normal force
$N_{G,Ed}$	Design value of the compressive normal force that is permanent
$N_{b,Rd}$	Desing value of the buckling resistance of the composite columns
$N_{pl,Rd}$	Design value of plastic resistance of the composite columns
$N_{pl,Rk}$	Characteristic value of plastic resistance of the composite columns
$N_{pl,Rm}$	Mean value of plastic resistance of the composite columns
R_d	Design resistance from global GMNIA
R_m^{GMNIA}	Mean resistance from global GMNIA
$R_{pl,d}$	Load vector calculated from plastic N-M interaction diagram based on design values
$R_{pl,m}$	Load vector calculated from plastic N-M interaction diagram based on mean values
$V_{a,Ed}$	Design value of the shear force acting on the structural steel section
$V_{pl,Rd}$	Desing value of the plastic resistance of the composite column to vertical shear
$V_{pl,a,Rd}$	Desing value of the plastic resistance of the structural steel section to vertical shear
w_0	Initial geometric imperfection
w_m	Maximum displacement at the midspan of the column calculated from global GMNIA

α	Imperfection factor
α_M	Shape factor
α_c	Reduction factor for concrete accounting from long-term effects.
β	The equivalent moment factor
γ_0	Overall safety factor for the general method
γ_{M1}	Partial factor for structural steel
δ	Steel contribution
ε_{c1}	Compressive strain in the concrete at the peak stress
ε_{cu1}	Ultimate compressive strain in the concrete
λ	Slenderness ratio
$\bar{\lambda}$	Relative slenderness
λ_1	Reference slenderness
μ_d	Factor related to design for compression and uniaxial bending
$\mu_{d,y}$	Factor related to design for compression and uniaxial bending about y-y axis
$\mu_{d,z}$	Factor related to design for compression and uniaxial bending about z-z axis
ρ	Parameter related to reduced design bending resistance accounting for vertical shear
ρ_s	Reinforcement ratio
σ_{cr}	Critical elastic stresses
σ_R	Residual stresses on steel profile
σ_{max}	Maximum stresses
$\varphi_{t,eff}$	Effective creep coefficient
$\varphi_t(t, t_0)$	Creep coefficient
ϕ	Intermediate factor
χ	Reduction factor for flexural buckling

Symbols related to the stochastic finite element method

α_E	First Order Reliability Method (FORM) factor related for effects of actions
α_R	First Order Reliability Method (FORM) factor for resistance
β	Reliability index
γ_R	Global safety factor
γ_{Rd}	Model uncertainty factor
μ	Mean value
μ_E	Mean values for action effects
μ_g	Mean value of the limit state function
μ_R	Mean values for resistance
ρ_{RS}	Correlation coefficient between resistance and action effect
σ	Standard deviation
σ_E	Standard deviation for action effect
σ_g	Standard deviation of the limit state function
σ_R	Standard deviation for resistance
$\Phi(-\beta)$	Cumulative distributive function of Gaussian distribution
E	Action effect
E_d	Design action effect
N	Total number of simulations for Monte Carlo Simulation
N_f	Total number of failed simulations for Monte Carlo Simulation
P_f	Probability of failure
R	Resistance
R_d	Design resistance
S_i	Main Sobol index
S_{ij}	Total Sobol index
V	Coefficient of Variation
V_R	Coefficient of Variation for resistance

Abbreviations

CC	Consequence classes
CDF	Cumulative Distributive Function
CDP	Concrete Damage Plasticity
CEC	Concrete Encased Composite Column
CFSB	Concrete Filled Steel Box Column
CFST	Concrete Filled Steel Tube Column
ECCS	European Convention for Constructional Steelwork
ECOV	Estimation of Coefficient of Variation
FEA	Finite Element Analysis
FEM	Finite Element Method
FORM	First Order Reliability Method
GMNIA	Geometric and Material Nonlinear Analysis with Imperfections
JCSS	Joint Committee on Structural Safety
LBA	Linear Buckling Analysis
LHS	Latin Hypercube Sampling
MCS	Monte Carlo Simulation
NLA	Nonlinear Analysis
PCEC	Partial Concrete Encased Composite Column
PDF	Probability Density Function
RC	Reliability classes
SFEA	Stochastic Finite Element Analysis
SFEM	Stochastic Finite Element Method
SORM	Second Order Reliability Method

Chapter 1

Introduction

In the field of civil and structural engineering, a column refers to a compression structural member that is typically loaded in compression or compression and bending [2]. A composite column made of steel and concrete is a compression member created by combining these two main construction materials, which are commonly used in buildings, bridges, and other civil engineering structures. Steel is known for high tensile strength and high ductility, making it an excellent complement to concrete, which has low tensile strength, low ductility, and high compressive strength, and providing advantages for fire design.

The first composite columns made of steel and concrete were developed in the United States in the 20th century [4]. Initially, wet low-strength concrete was used to protect steel columns from fire in high-rise buildings [4]. However, it was later discovered that by changing the quality of the concrete and adding reinforcement bars, the columns could be designed as composite members. At first, it was believed that concrete only increased the column resistance to compression and stability. However, it was later demonstrated that both steel and concrete resist compression forces and bending by interacting together through bonding, friction, or mechanical interlock [4]. Compared to steel and reinforced concrete columns, composite columns offer higher resistance and greater ductility with relatively small cross-section dimensions. Based on the interaction between steel and concrete or steel and reinforced concrete, composite columns are classified into four types:

- Concrete Encased Composite Columns (CEC)
- Partial Concrete Encased Composite Columns (PCEC)
- Concrete Filled Steel Tube (CFST)
- Concrete Filled Steel Tube (CFST) with inner steel profile or massive steel core

Figure 1.1 displays different types of composite columns. In the case of CEC and CFST columns with I-section or massive inner steel core, the steel inside concrete is well protected from fire.

In the case of CFST columns, the inner part can be with or without additional steel profile depending on resistance demand. CEC columns are characterized by the highest load-bearing capacity, fire resistance, and the most favourable solution in terms of material cost among composite columns, making them the most commonly used composite columns in high-rise buildings.

(CEC)   **(PCEC)**   **(CFST)**
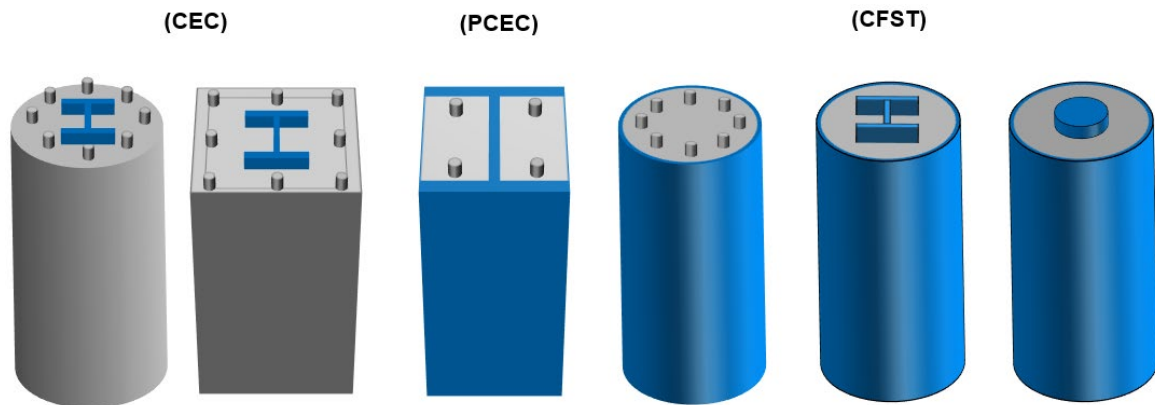
Figure 1.1 Different types of Composite Columns

In Europe, the design of composite columns made of steel and concrete is based on Eurocode 4 EN 1994-1-1 [2], and for evaluating the resistance to buckling two methods exists:

– The simplified methods,
– The general method.

When the resistance of a structural elements like the composite columns in steel and concrete is evaluated, there are a lot of uncertainties involved, and these uncertainties are primarily associated with the material parameters, the geometry, and the model that characterizes the behaviour of the structure. Due to randomness involved in these parameters, probabilistic analyses are required to assess the safety and reliability of structural elements e.g., composite columns. Currently, the structural elements are designed using a method known as partial factor design, as described by Eurocode 0 EN 1990 [5], for a particular reliability level and safety format that covers a wide variety of design situations. This approach assumes a linear limit state function, and is applied on the cross-section level, while the effects on the global level are not considered. To consider global effects, a non-linear finite element analysis on global level is required. However, the global non-linear finite element analysis cannot be used

in combination with partial factor design method [6] as the assumption of linear limit state function might be incorrect. As a consequence, in this work a reliability assessment of the general method with the overall (safety factor) based on strain-limited N-M interaction diagram for composite columns in steel and concrete is performed using the Stochastic Finite Element Method (SFEM), which combines the non-linear finite element analysis (NFEA) with reliability methods. To generate random variables from variation in geometry and material parameters, Latin Hypercube Sampling (LHS) is used. The statistical distribution of the main parameters related to resistance are based on recommendations of the Joint Committee on Structural Safety (JCSS) Model Code Part 3: Material properties [7], prEN1992-1-1 [8], and prEN 1993-1-1 [9]. In addition, the Stochastic Finite Element Method (SFEM) is used to conduct also sensitivity analysis based on Sobol's indices method [10], to understand the influence of each random variable on the overall resistance of the composite columns under compressive load. The considered composite columns for reliability assessment and sensitivity analyses are presented in Figure 1.1.

In Eurocode 0 EN 1990 [5], this approach is referred as semi-probabilistic method and it is used for further development of the Eurocodes, while in this study is employed for further develop of the general method with the overall (safety) factor γ_0 based on strain-limited N-M interaction.

1.1 Motivation

The number of high-rise buildings, bridges, and other types of structures requiring greater ductility and resistance at relatively small cross-sectional dimensions has led to an increase in the use of composite columns made of steel and concrete in recent decades.

In Europe, the Eurocode 4 EN 1994-1-1 [2] is the guideline for the design of composite columns in steel and concrete. In current version of EN 1994-1-1 [2] only a brief paragraph is dedicated to the verification of the composite columns according to general method, while the design process is not sufficiently explained. However, in the new version prEN1994-1-1 [3] more details are presented. This lack of information and complexity of this method makes

the general method not yet well-established and commonly used in everyday engineering practice.

One of the open discussions about the general method was related to the calculation of the overall (safety) factor γ_0 based on non-linear (strain-limited) N-M interaction diagram, whether this should be incorporated in the general method or plastic resistance should always be the reference. Until now, a limited number of studies are conducted on this topic, whether the overall (safety) factor γ_0 based on strain-limited N-M interaction diagram is reliable and attain the safety level required by Eurocode 0 EN 1990 [5].

All of this served as the motivation to investigate the reliability and safety of the general method with the overall (safety) factor γ_0 based on strain-limited N-M interaction curve using semi-probabilistic analyses such as Stochastic Finite Element Method as one of the methods used for further development of Eurocodes.

1.2 Objectives

The present dissertation aims to investigate the stability problem and the design of composite columns made of steel and concrete using the general method provided by EN 1994-1-1 [2] and prEN1994-1-1 [3]. As previously stated, the verification of composite columns against buckling according to the general method is not straightforward procedure but rather complex, due to the fact that, this method contains two parts; non-linear finite element analysis on global level so-called Geometric and Material Nonlinear Analysis with Imperfections (GMNIA), and non-linear N-M interaction diagram to determine the overall (safety) factor γ_0 on the cross-section level.

The first objective of this study is to find experimental test study conducted on composite columns in steel and concrete, as well as a thorough review of the literature in order to identify important observations that other researchers have made on the application of the general method.

The second objective is to investigate the effect of geometric imperfections and residual stresses on steel and composite columns through development of Finite Element (FE) models

to conduct non-linear finite element analyses (GMNIA) and benchmark the FE with experimental test results from online literature. Furthermore, a comparison between the buckling resistance according to EN 1994-1-1 [2] the simplified method (European buckling curves) and the general method with the overall (safety) factor γ_0 based on plastic and strain-limited N-M interaction is conducted.

The third objective consist of in-depth investigation of the theory behind the safety concept and reliability assessment of the structures provided in Eurocode 0 EN 1990 [5], *fib* Model Code [1] and review of the literature that other researchers have made in this area.

The fourth objective is to assess the safety and reliability of the general method with the overall (safety factor) based on strain-limited N-M interaction diagram for composite columns in steel and concrete using the Stochastic Finite Element Method (SFEM).

The fifth objective is to conduct sensitivity analysis to determine the impact of each random variable including material properties, cross-sectional geometry, geometric imperfections as well residual stresses on composite columns made of steel and concrete subjected to compression force.

1.3 Dissertation structure

The flowchart displayed in Figure 1.2 is used to present the structure of this dissertation. The structure is composed of two supporting parts, the theoretical framework, and the results. The supporting part I, consisting of symbols, notations, and abbreviation used in the thesis, while in the supporting part II, the list of tables, the list of figures and the bibliography are included. The state of the art related to stability problem, safety and reliability analysis for composite columns are discussed in the theoretical frameworks. Additionally, this section includes the software and methodology used in this study. The findings of this work are presented in the results section and involve the following:

- The effect of initial geometric and structural imperfections,
- The application of the general method for composite columns in steel and concrete,
- Safety and reliability assessment of composite columns using SFEM,

− Sensitivity analysis for composite columns using SFEM.

Supporting part I

Symbols	Notations	Abbreviations

Theoretical framework

Introduction

State of the Art

Stability Problem

Safety & Reliability

Euler Buckling
Buckling of Real Columns
European Buckling Curves
Geometric and Structural Imperfections
Design of Composite Columns
- Cross-section resistance
- The simplified methods
- The general method

Basic Concept of Safety and Reliability
Safety Format in EN 1990
- Limit states and reliability methods
- Reliability index β
Safety Format in *fib* Model Code
- Probabilistic analysis
- Global safety factor

Methodology

Finite Element Method

Stochastic Finite Element Method

GMNIA in ABAQUS

GMNIA in OpenSees

Benchmarking ABAQUS with experimental tests

Benchmarking OpenSees with ABAQUS

Stochastic Finite Element Analysis
Sampling Method
- Monte Carlo Simulation
- Latin Hypercube Sampling
Sensitivity Analysis

Results

The effect of initial imperfections – benchmark cases

Steel Columns

Composite Columns

CEC Columns

PCEC Columns

CFST Columns

Application of the general method for composite columns in accordance with prEN1994-1-1

Safety & Reliability Assessment of Composite Columns using Stochastic Finite Element Method

Reliability Analysis

Sensitivity Analysis

Summary and Conclusions

Supporting part II

List of Tables

List of Figures

Bibliography

Figure 1.2 Structure of the thesis

Chapter 2

State of the art

In this chapter the state of the art is given to present the evidence and findings from previous studies on the scientific topics relevant to this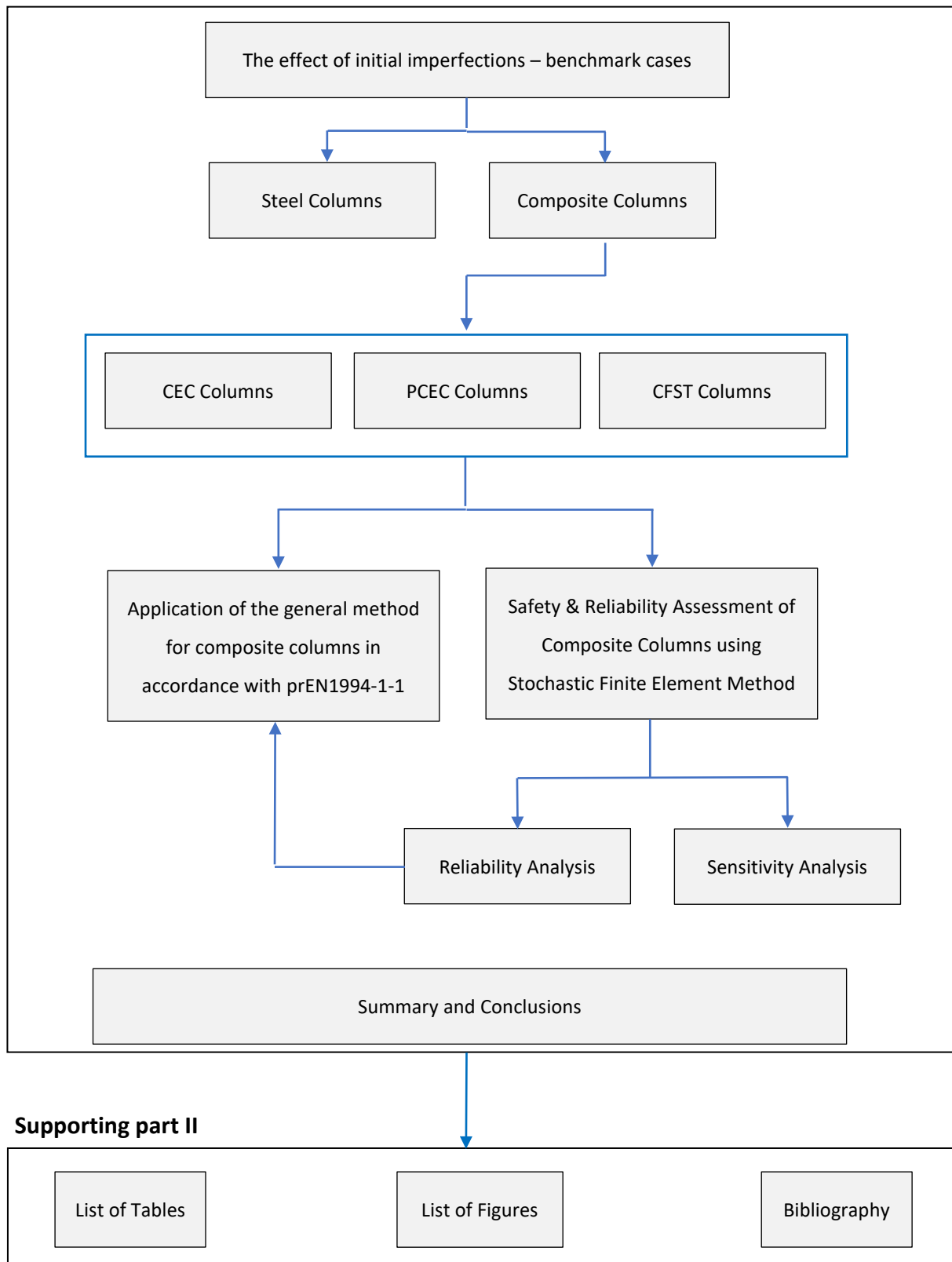 dissertation. The main topics of interest are related to the stability problem for compressive members, the effect of initial geometric and structural imperfections on steel and composite columns, design of composite columns according to EN 1994-1-1 [2], and the basic concept about the probabilistic analysis. The background details for each of these aspects are provided in chronological order.

2.1 Stability problem

2.1.1 Euler buckling

During the 18th century, Leonhard Euler, a Swiss mathematician, solved a differential equation to determine the maximum axial load on a perfectly straight and simply supported column. Figure 2.1 shows an illustration of such a column with ideal conditions.
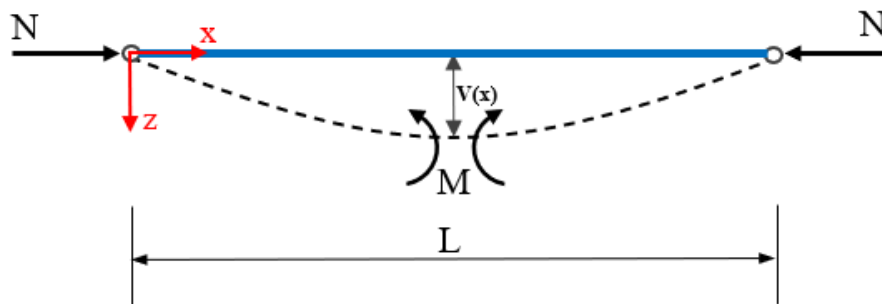

Figure 2.1 Euler's column

This solution is referred to as the elastic critical load or Euler's critical load [11]. Euler's [11] assumptions for deriving the critical load are based on ideal conditions for the column, including:

– the material is isotropic and homogeneous,

– the column is perfect, with no geometric imperfections or initial stress,

- an axial compression load is applied at the centre of the column,

- the cross-section is uniform throughout the length of the column,

- the length of the column is much larger than the cross-section dimensions,

- the column has ideal pin joints boundary conditions with no moment restrains,

- the self-weight of the column is neglected.

Euler [11] stated that, a straight column will reach the instability state and deflect laterally (buckle) when the axial load acting on it reaches the critical load $N = N_{cr}$, and the first buckling mode will follow a half-sinusoidal wave for a double-pinned column as it is illustrated with a dashed line in Figure 2.1.

Concerning Figure 2.1, the external bending moment at e distance *x* to the principal axis is expressed as:

$$M_e(x) = N_{cr} \cdot v(\mathrm{x}) \tag{2.1}$$

Following the Euler-Bernoulli beam theory that the member deformation is small, the internal bending moment is simply the second derivative of the deflection as:

$$M_{int}(x) = -EI \cdot \frac{d^2y}{dx^2} \tag{2.2}$$

To reach the equilibrium, the internal bending moment $M_{int}(x)$ must be equal to the external bending moment $M_e(x)$:

$$M_e(x) = M_{int}(x) \Rightarrow N_{cr} \cdot v(\mathrm{x}) = -EI \cdot \frac{d^2y}{dx^2} \tag{2.3}$$

Rearranging the differential Equation (2.3) we get:

$$\frac{d^2y}{dx^2} + \frac{N_{cr}}{EI} \cdot v(x) = 0 \tag{2.4}$$

This can be written as:

$$v'' + k^2 \cdot v(x) = 0 \quad with \quad k^2 = \frac{N_{cr}}{EI} \tag{2.5}$$

Equation (2.5) represents a classical homogeneous second-order differential equation with general solution given as:

$$v(x) = A \cdot sin(kx) + B \cdot cos\,(kx) \tag{2.6}$$

$$v'(x) = Ak \cdot cos(kx) - Bk \cdot sin\,(kx) \tag{2.7}$$

$$v''(x) = -Ak^2 \cdot sin(kx) - Bk^2 \cdot cos\,(kx) \tag{2.8}$$

The constants A and B can be found using the boundary condition in the general solution. For a double-pinned column, the boundary conditions are as follows:

$$v(0) = 0 \Rightarrow A \cdot sin(0) + B \cdot cos\,s(0) = 0 \Rightarrow B = 0 \tag{2.9}$$

$$v(l) = 0 \rightarrow A \cdot sin(kl) = 0 \tag{2.10}$$

The Equation (2.10) can be satisfied in the cases:

- $A = 0$ (Trivial solution)
- $kl = 0$ (No load in the structure)
- $kl = n\pi$ (Non-trivial solution for buckling to occur)

then,

$$k^2 = \frac{N_{cr}}{EI} = \frac{n^2 \cdot \pi^2}{L^2} \tag{2.11}$$

The first buckling mode occurs when the $n = 1$, and the Euler's critical load for pinned-pinned columns can be expressed as:

$$N_{cr} = \frac{\pi^2 \cdot EI}{L_e{}^2} \tag{2.12}$$

In Equation (2.12) the length L is replaced with L_e which represents the effective length, which for two sides pinned supported column is the same as the column's length, $L_e = L$. The effective length L_e depends on the boundary conditions of the column and can be described as $L_e = K \cdot L$, where K is the factor related to buckling mode and some of the cases are presented in Figure 2.2. Euler's buckling load or critical load give in Equation (2.12) is the maximum load that a column can withstand without buckling elastically, assuming the column is ideal and free of any imperfections. This critical load depends on two main parameters: the stiffness of the column, which can be expressed as EI, and the buckling length L_e, which is determined by the boundary condition.

$$K=0.5 \qquad K=0.7 \qquad K=1.0 \qquad K=2.0$$
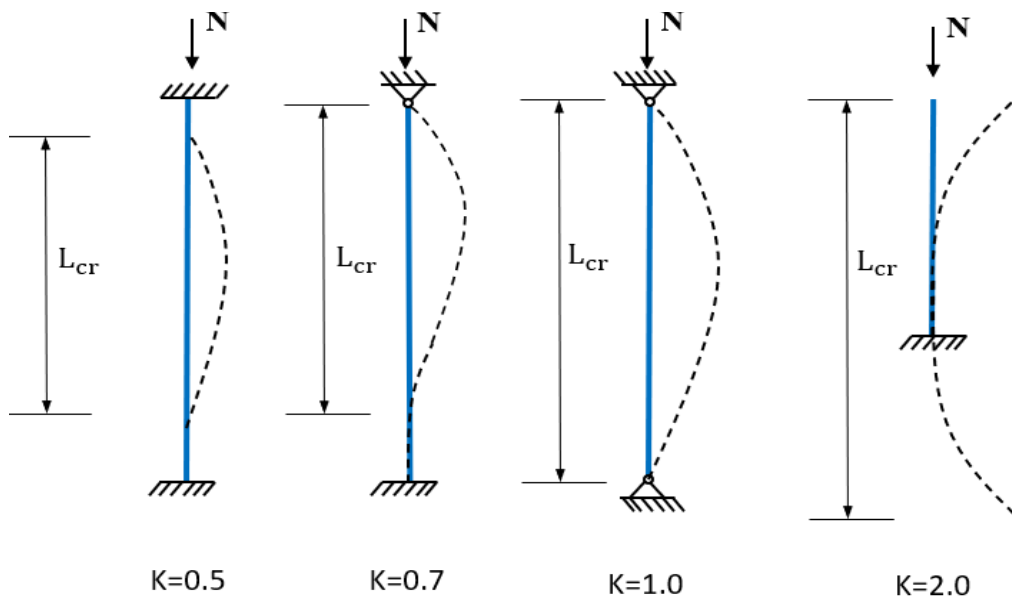
Figure 2.2 Theoretical effective length for compressive members (adopted from [12])

On the other hand, the critical buckling load can be expressed also in terms of stresses as:

$$\sigma_{cr} = \frac{N_{cr}}{A} = \frac{\pi^2 \cdot EI}{A \cdot L_e{}^2} \tag{2.13}$$

By introducing the radius of gyration, $i = \sqrt{\dfrac{I}{A}}$, the critical stresses can be rewritten as:

$$\sigma_{cr} = \frac{\pi^2 \cdot E}{\left(\frac{L_e}{i}\right)^2} \quad (2.14)$$

This new parameter (L_e / i) is called slenderness of the column λ, and therefore the final expression for critical stress is:

$$\sigma_{cr} = \frac{\pi^2 \cdot E}{\lambda^2} \quad (2.15)$$

Moreover, considering that materials are characterized by certain yield stress and assuming the critical stress equal to yield stress, $\sigma_{cr} = f_y$, a new parameter is obtained called reference slenderness λ_1, which represents the "border" between the Euler buckling curve and yield stress, as it is presented in Figure 2.3 (a).

$$\lambda_1 = \pi \sqrt{\frac{E}{f_y}} \quad (2.16)$$

The relation between critical stresses and slenderness can be presented in non-dimensional form as it is shown in Figure 2.3 (b), by introducing the relative slenderness $\bar{\lambda}$, and the reduction factor regarding buckling χ, by using Equation (2.17) and Equation (2.18).

$$\bar{\lambda} = \frac{\lambda}{\lambda_1} = \sqrt{\frac{N_y}{N_{cr}}} \quad (2.17)$$

$$\chi = \frac{\sigma_{max}}{f_y} \quad (2.18)$$
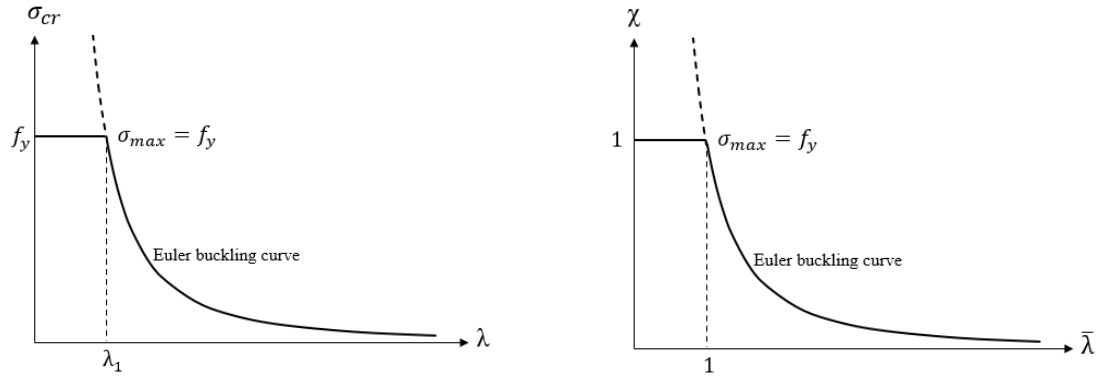
(a) *Relationship between critical buckling stress σ_{cr} and slenderness λ*

(b) *Relationship between reduction factor χ and non-dimensional slenderness $\bar{\lambda}$*

Figure 2.3 Euler buckling curve (adopted from [13]*)*

2.1.2 Buckling of real columns

The above discussion pertains to Euler's theory on the critical load or Eulerian buckling load. However, the theory is based on the assumption of an ideal column or perfect conditions, which is far from reality. Real-life columns and beams behave differently due to geometric and structural imperfections, material nonlinearity (yielding), the load not always being applied in the centre, and non-ideal boundary conditions. Geometric imperfections are referred to as initial crookedness, while structural imperfections are residual stresses present in steel and composite columns from the fabrication process and also unequal distribution of yield stress over the section, as shown in Figure 2.4.
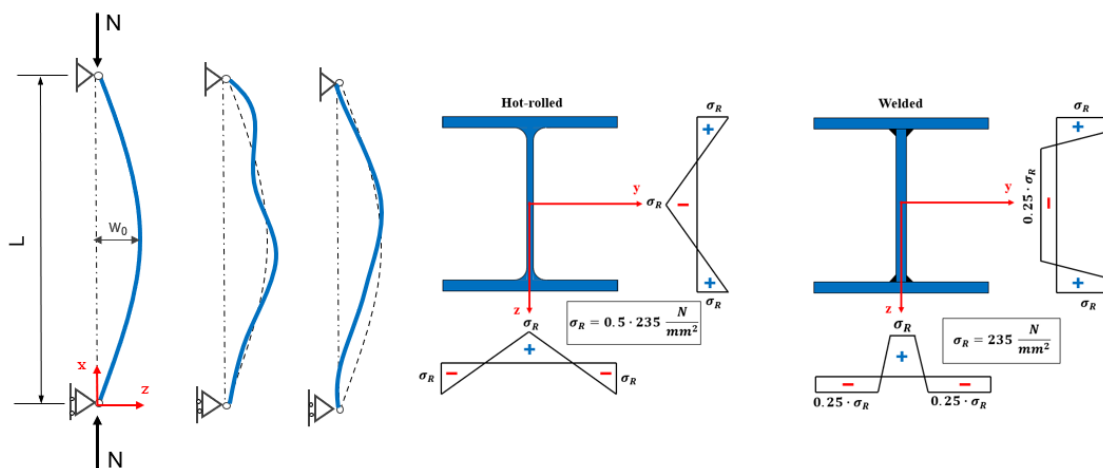

Figure 2.4 Out-of-straightness idealized (w_0), measured, and residual stresses of steel columns [14]

With reference to Figure 2.5, the resistance of the real columns under compression forces is always lower than the Eulerian buckling load, and the columns can never reach the critical load due to the presence of geometric and structural imperfections. As it is reported in [15], these imperfections have a higher impact on columns with intermediate slenderness λ. This is because the difference between the Eulerian buckling curve and the design curves presented in Figure 2.5 is larger for intermediate slenderness, compared to columns with short and high slenderness. The reason for this is that for short columns, initial imperfections are not relevant as resistance is governed by yielding and not buckling, while for columns with high slenderness, the load-bearing capacity is close to the critical load, and the initial imperfections are not decisive. More details on the geometric and structural imperfections and their influence on steel and composite columns in steel and concrete will be presented in Chapter 2.2.
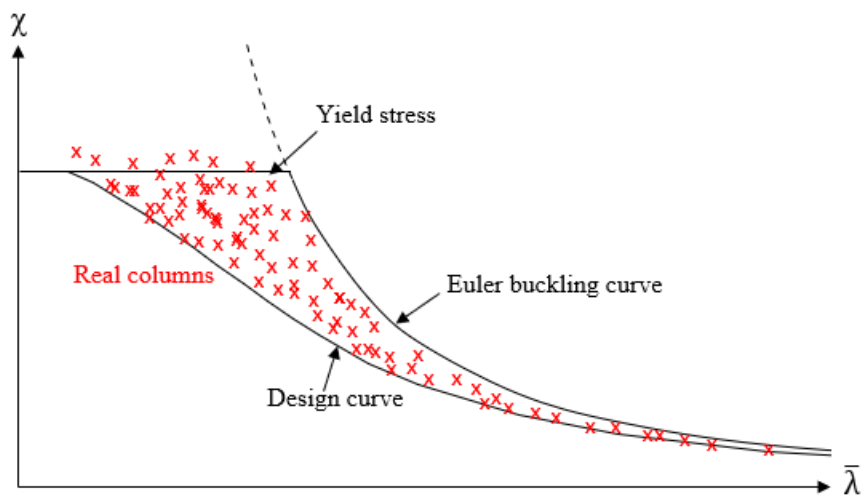

Figure 2.5 Real columns compared to Euler buckling curve and design curve (adopted from [13]*)*

2.1.3   European buckling curves

Eurocode 3 EN 1993-1-1 [16] and Eurocode 4 EN 1994-1-1 [2] provide methods for determining the buckling resistance of the columns, one of which is based on so-called European buckling curves. These curves were developed by The European Convention for Constructional Steelwork (ECCS) [14] based on comprehensive campaign of experimental tests, theoretical studies, numerical studies as well as probabilistic investigation between

1960 and 1970 [17]. All experimental tests were conducted on mild steel profile IPE 160 – S235, while the theoretical background and numerical (deterministic) study was derived from the previous studies carried out by Sfinitesco [18] and Beer & Schulz's [19]. In addition, the probabilistic investigation based on Monte Carlo Simulation were conducted by Bjorhovde [20] and Strating & Vos [21] regarding the reliability of failure. A key issue concerned the European buckling curves was related to the initial bow imperfection. Based on Strating & Vos [21] probabilistic analysis, the bow imperfection for steel columns follows a normal distribution with mean value $m = 0.00085L = L/1176$ and that mean with two standard deviation $m + 2s = 0.00125L = L/800$, while Bjorhovde [20] used mean value of $L/1470$ [17]. Later on, an equivalent bow imperfection and a plateau for relative slenderness lower than $\lambda_0 = 0.2$ was introduced based on so-called "Ayrton-Perry" approach [17] which is present also today in the current European buckling curves. The aim was to establish a single design rule for the buckling resistance of steel columns in Europe. As a result, five different buckling curves named (a_0, a, b, c, d) were developed, which were later adopted in Eurocodes and are still used today for buckling resistance of steel and composite columns. More details about the history of the development of the European buckling curves can be found in [17], [22].According to EN 1993-1-1 [16], for the verification of members subjected to compressive force, the following equation must be satisfied:

$$\frac{N_{Ed}}{N_{b,Rd}} \leq 1 \tag{2.19}$$

In structural engineering, the design compressive load is denoted as N_{Ed}, while the design buckling resistance is denoted as $N_{b,Rd}$. According to EN 1993-1-1 [16], steel cross-sections are categorized into four classes. Cross-sections in class 1 to class 3 are affected by global buckling, whereas the cross-sections in class 4 are affected by local buckling. For the purpose of this study, only the global buckling of the columns is investigated, and local buckling is not considered in this study. Therefore, the buckling resistance for cross-sections in class 1 to class 3 is determined using Equation (2.20).

$$N_{b,Rd} = \frac{\chi \cdot A \cdot f_y}{\gamma_{M1}} \qquad (2.20)$$

The area of the cross-section is denoted by A, the yield stress of the steel is denoted by f_y, the reduction factor is denoted by χ, and the partial safety factor for buckling members is denoted by γ_{M1}. The reduction factor χ can be determined analytically or directly from the European buckling curves. Analytically, it can be calculated using the expression provided in [16].

$$\chi = \frac{1}{\phi + \sqrt{\phi^2 - \bar{\lambda}^2}} \quad but \ \chi \leq 1 \qquad (2.21)$$

where, ϕ is known as the intermediates factor and is calculated as:

$$\phi = 0.5 \cdot [1 + \alpha \cdot (\bar{\lambda} - 0.2) + \bar{\lambda}^2] \qquad (2.22)$$

where, α is the imperfection factor, and non-dimensional slenderness, denoted as $\bar{\lambda}$ is determined by the geometrical and mechanical properties of a member. This parameter dependents on the member's class, and for cross-section in classes 1, 2, and 3 is calculated using Equation (2.23).

$$\bar{\lambda} = \sqrt{\frac{A \cdot f_y}{N_{cr}}} = \sqrt{\frac{N_{pl,Rk}}{N_{cr}}} \qquad (2.23)$$

Eurocode 3 EN 1993-1-1 [16] provides five different buckling curves for calculating the buckling resistance, as shown in Figure 2.6. Depending on the steel cross-section's properties (height, width, thickness) and yield stress, the appropriate buckling curve, and its corresponding imperfection factor α, should be selected (refer to Figure 2.7).
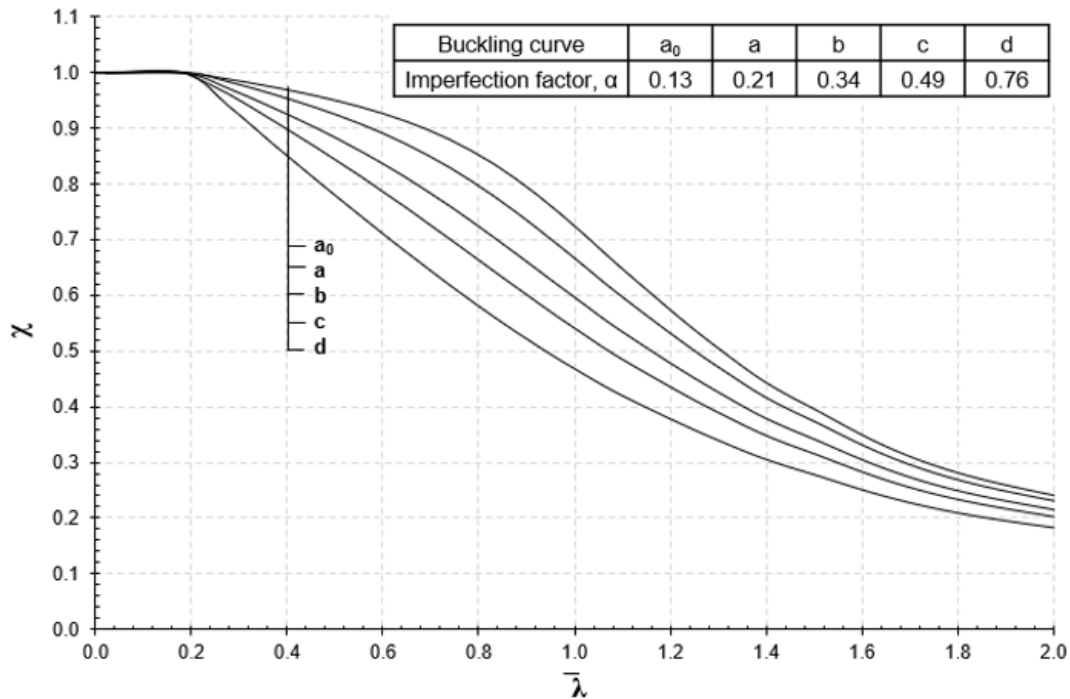
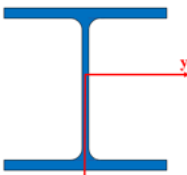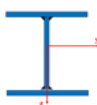*Figure 2.6 European buckling curves according to EN-1993-1-1* [16]

Cross section			Limits	Buckling about axis	Buckling curve S 235 S 275 S 355 S 420	S 460
Rolled sections	h/b > 1.2	$t_f \leq 40$ mm		y-y	a	a_0
				z-z	b	a_0
		40 mm $< t_f \leq 100$ mm		y-y	b	a
				z-z	c	a
	h/b ≤ 1.2	$t_f \leq 100$ mm		y-y	b	a
				z-z	c	a
		$t_f > 100$ mm		y-y	d	c
				z-z	d	c
Welded I-sections			tf ≤ 40 mm	y-y	b	b
				z-z	c	c
			tf > 40 mm	y-y	c	c
				z-z	d	d

Figure 2.7 Determination of buckling curves depending on properties of the cross-section

2.2 Geometric and structural imperfections

In this chapter, the effect of initial imperfections on compressive members e.g., (steel columns, and composite columns in steel and concrete) subjected to buckling will be discussed and investigated. First, an overview of the phenomenon is presented, then the

results of the benchmark cases on steel and composite columns, providing the readers with information about the impact of the initial imperfections. As mentioned above in the discussion about the real column behaviour, the initial imperfections are always present in the real columns, and based on their nature, the initial imperfections are divided into two categories:

− Initial geometric imperfections,
− Structural (mechanical) imperfections referred to as residual stresses.

2.2.1 Initial geometric imperfections

Initial geometric imperfections usually refer to global imperfections which include the initial out of straightness (not perfectly straight column along the longitudinal direction), out of plumbness (deviation of boundary conditions), and the cross-section imperfections which refers to the local deviation of the geometry from nominal dimensions as presented in Figure 2.8. The effect of geometric imperfections is essentially inevitable. For stability analysis of isolated compressive members e.g., (steel columns, composite columns in steel and concrete) the resistance is highly influenced by the out-of-straightness (bow imperfection), while the out-of-plumbness (sway imperfection) and cross-sectional imperfection are in general less relevant. In this study, only the out-of-straightness imperfection is examined because the composite columns are analysed as isolated members. Nonetheless, the sway imperfection holds significance for the examination of the frame system, as its orientation and magnitude are equally important.
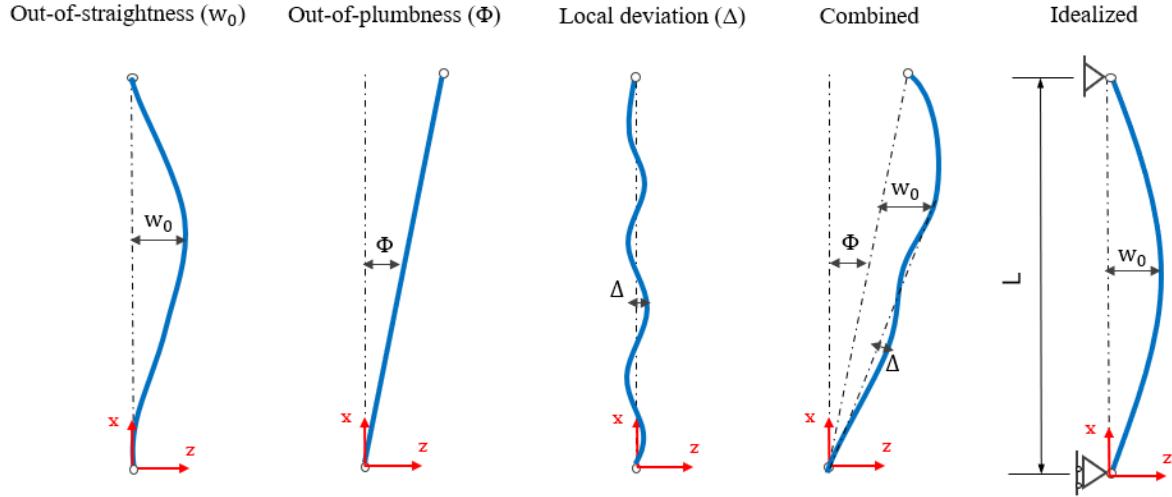
Figure 2.8 Initial geometric imperfections presented in steel and composite columns (adopted from [23]*)*

With reference to Figure 2.9, the initial bow imperfection in a member subjected to compressive centric loading along the longitudinal direction leads to a second-order moment which impacts the load-bearing capacity of the column.
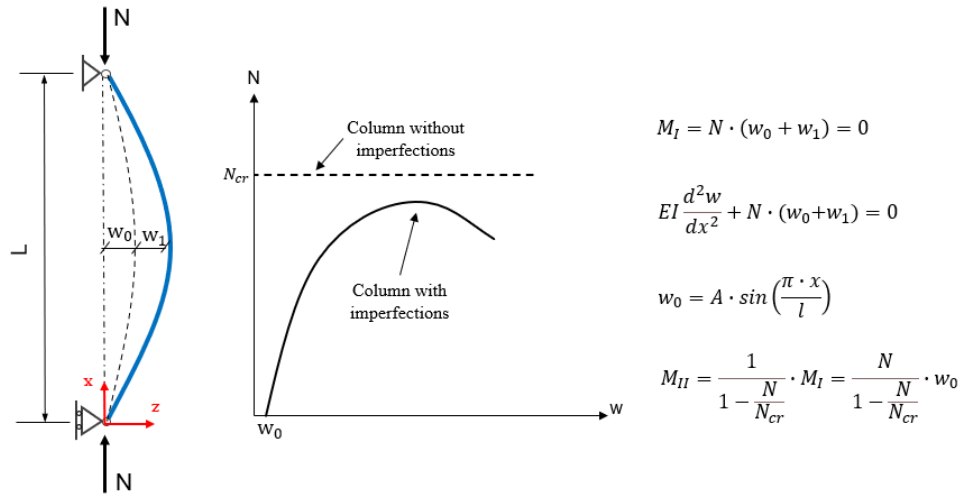

$$M_I = N \cdot (w_0 + w_1) = 0$$

$$EI \frac{d^2w}{dx^2} + N \cdot (w_0 + w_1) = 0$$

$$w_0 = A \cdot sin\left(\frac{\pi \cdot x}{l}\right)$$

$$M_{II} = \frac{1}{1 - \frac{N}{N_{cr}}} \cdot M_I = \frac{N}{1 - \frac{N}{N_{cr}}} \cdot w_0$$

Figure 2.9 Initial bow imperfection in a member subjected to compression load

According to prEN 1993-1-14 [24], when performing FE analysis for steel columns subjected to buckling, the initial geometric imperfection, and residual stresses should be taken into account directly with geometric imperfection $w_0 = L/1000$, or in a simplified form as equivalent initial bow imperfection by considering the deformed shape of the column using half-sinusoidal wave which covers the effect of both, the geometric imperfection and residual

stresses. In this case, the values are given as a function of European buckling curves (a_0, a, b, c, d) varying between $e_0 = L/350$ and $e_0 = L/150$ for elastic analysis and between $e_0 = L/350$ and $e_0 = L/100$ for plastic analysis as it is presented in Table 2.1.

Table 2.1 Equivalent bow imperfection (adopted from [24])

Buckling curve	Equivalent bow imperfection	
	Elastic	Plastic
a0	L/350	L/300
a	L/300	L/250
b	L/250	L/200
c	L/200	L/150
d	L/150	L/100

The same approach of equivalent bow imperfection is adopted also in Eurocode 4 [2], for the design of composite columns as the equivalent bow imperfections presented in Table 2.1 can be used for simplified methods as well as the general method. However, for the general method, the equivalent bow imperfection leads to conservative results, and rather as explained in the Chapter 2.6, the geometric imperfections and residual stresses should be taken into account separately. In this study, the initial geometric imperfection and residual stresses are always considered separately and not with equivalent initial bow imperfection.

Nevertheless, the magnitude of the geometric imperfection for composite columns is still under discussion and review by CEN/TC250/SC4WG as in the current Eurocode 4 EN 1994-1-1 [2] no information is provided, while often in literature [6], [25] a magnitude of $w_0 = L/1000$ is proposed. However, in case of composite columns there are several factors which might affects the magnitude and the shape of the geometrical imperfection, such as installation tolerance, non-straightness of the concrete due to formwork and casting, non-accurate positioning of reinforcement bars, different bow imperfection of the concrete, steel profile or steel tubes. All these parameters require tremendous effort to measure the imperfections of the composite column once the concrete is casted. Therefore, a numerical calibration is required. A more recent study [26] followed a similar approach by calibrating numerically the geometric imperfection for slender Concrete Encased Composite (CEC) columns and proposing a value of $w_0 = L/660$ for CEC columns.

2.2.2 Residual stresses

Residual stresses sometimes referred to as structural imperfections are just as important as geometric imperfections. These stresses arise during the manufacturing process of the steel section, more specifically during the rolling process e.g., hot-rolling or cold-rolling of the steel section, as some parts of the cross-section cool down faster which results in non-uniform residual stresses in the cross-section [27]. In the case of a member subjected to axial force such as columns, they tend to reduce the load bearing capacity. By definition, the residual stresses are self-balanced stresses [27] which are presented before any external load is applied in the section, and they act in the longitudinal direction of the cross-section. With reference to Figure 2.10, the side of the flanges, and middle part of the web tend to cool down faster compared to web-flanges intersections, and on these parts (black part Figure 2.10), compressive stresses are created, while to satisfy the equilibrium between stresses, on the other parts of the section (intersections between web and flanges) tensile stresses are created.
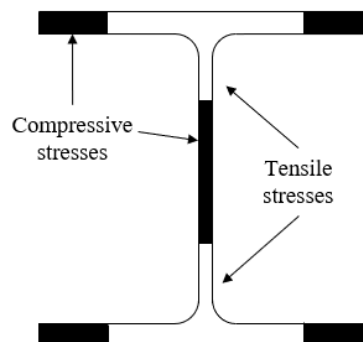

Figure 2.10 Residual stresses on hot-rolled section

To better understand how residual stresses impact the columns subjected to a compressive force (e.g., buckling), in Figure 2.11 the stress-strain curve of the steel sample under compression force is presented.
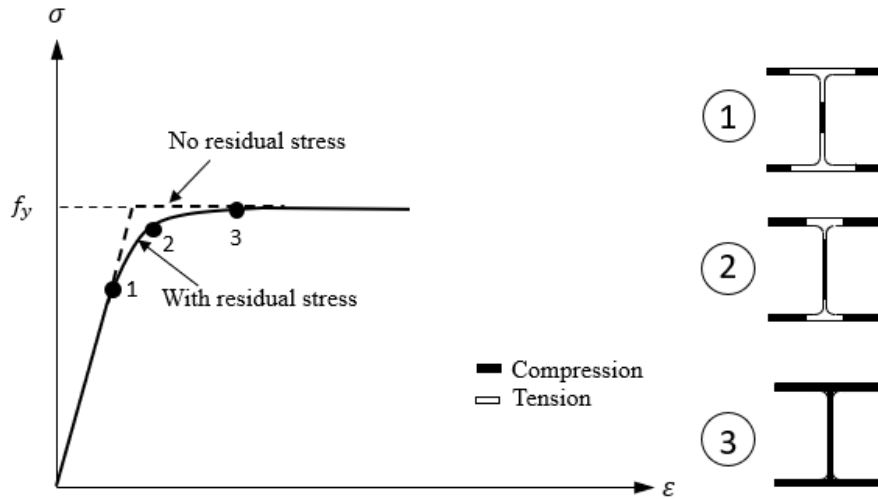
Figure 2.11 Impact of the residual stresses on column subjected to compression force (adopted from [28])

According to Figure 2.11, in the flanges, the yielding starts from the sides and continues toward the centre, while in the web, the yielding starts from the centre and continues toward the intersections between the web and flanges. As the residual stresses are presented in the section before any external load is applied, parts of the cross-section which are subjected to initial compressive residual stresses (edges of the flanges and the centre of the web) tend to yield faster, and with the load progressively increasing also the initial tensile residual stresses yield. This can be better understood also from Figure 2.12 where it is shown the stress propagation (the sum of the initial residual stresses (σ_R) and the stresses from the external load (σ_N)) until the full yield is reached for the steel flanges of the hot-rolled section with idealized triangular residual stress distribution and neglecting the web.
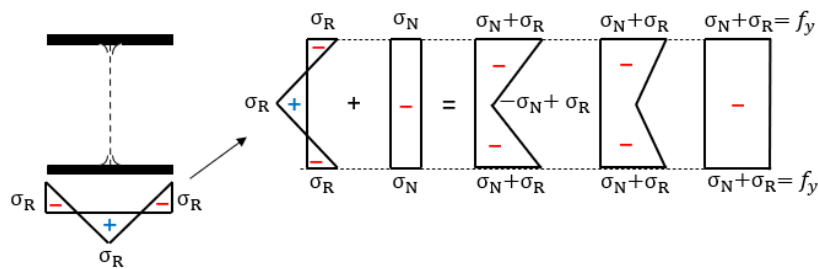

Figure 2.12 Initial residual stresses effect on hot-rolled section (adopted from [15])

(ECCS) publication No. 33 [29] provided the first information regarding the distribution and the magnitude of the initial residual stresses. In this publication, an extensive experimental

program was carried out on full-scale steel columns subjected to buckling, for developing of the so-called European Buckling curves. The magnitude of the residual stresses reported in this study is related to yield stress $f_y = 235 \, N/mm^2$ as all bucking tests were carried out on columns with mild steel S235. Figure 2.13 shows the magnitude and the shape residuals stresses for different types of steel sections recommended by [29].
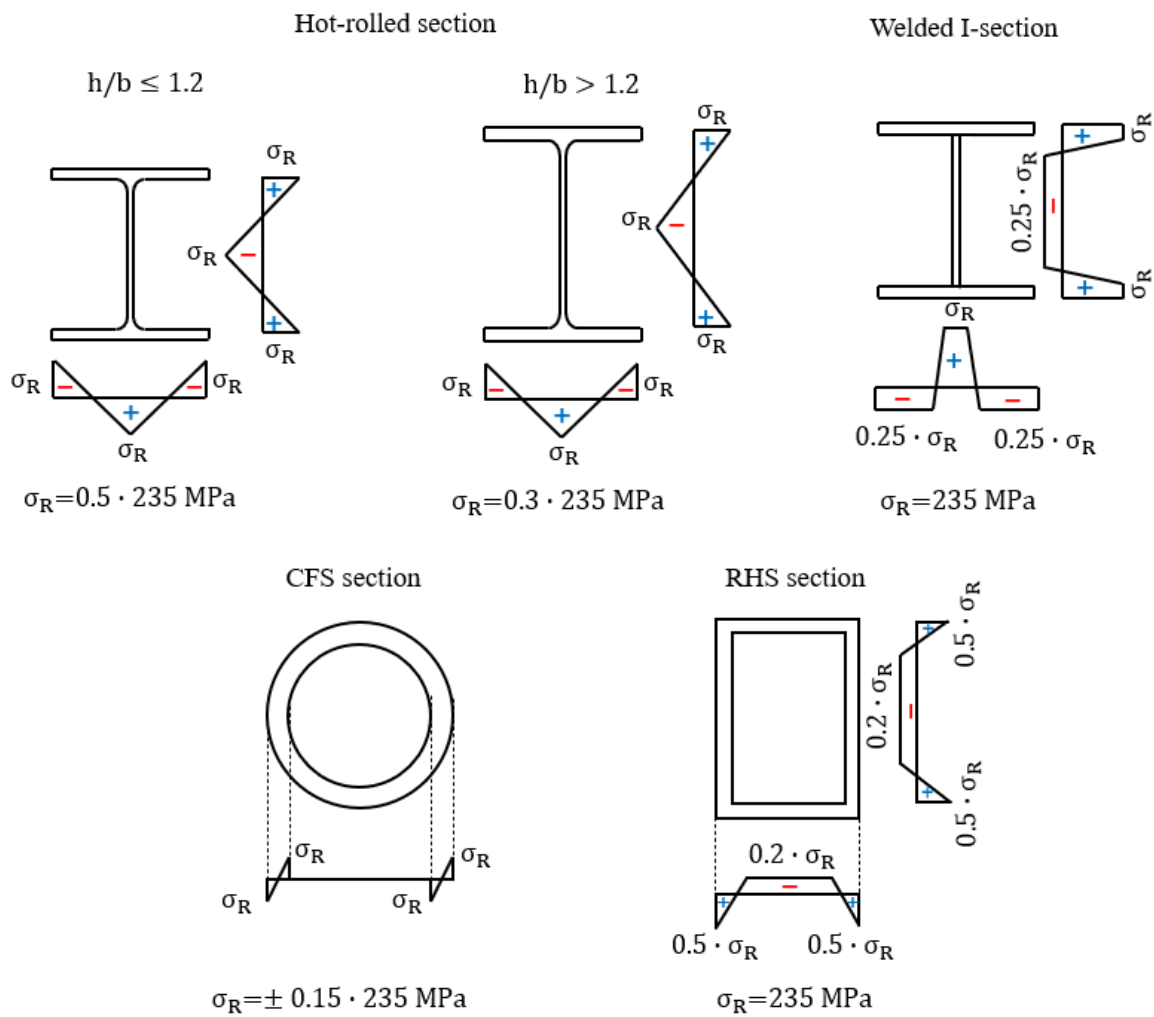

Figure 2.13 Residual stresses for steel section according to ECCS No. 33 [29]

However, in the new draft of Eurocode 3, prEN 1993-1-14 [24] the same distribution is reported for steel sections, while regarding the magnitude of the stresses, for hot-rolled section and RHS section, the stresses are based on steel grade S235 as in ECCS publication [29], while for welded sections and CFS section, the residual stresses may be taken based on

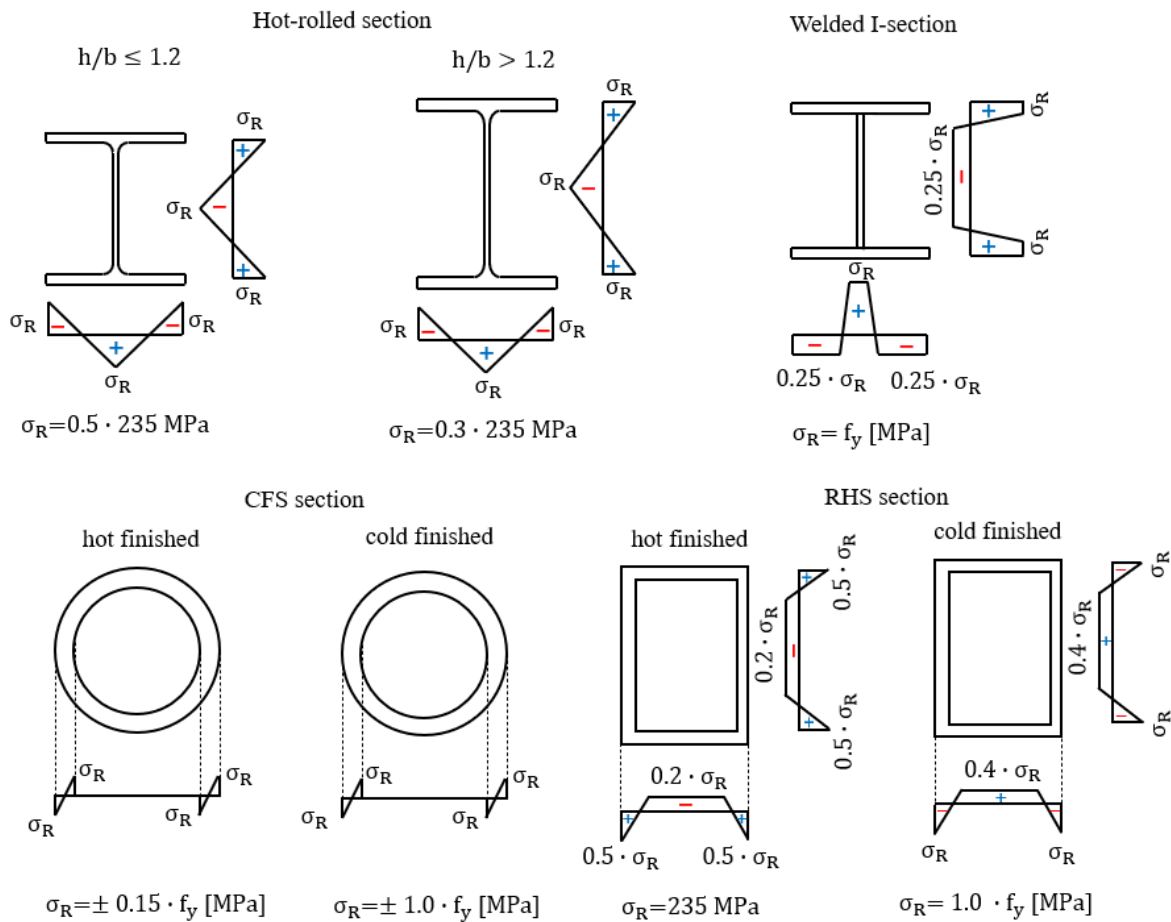yield strength of the considered material varying between S235 and S700 as it is presented in Figure 2.14.

Figure 2.14 Residual stresses for steel sections according to prEN1993-1-1 [24]

Regarding the residual stresses distribution and magnitude of the stresses in the case of massive round steel cores, such as the one used for composite columns (CFST) with a massive inner steel core, neither ECCS [29] nor Eurocodes provide any information. Up to now, only a few investigations have been conducted on the distribution of residual stresses on a massive steel cores, and most of the studies are based on the recommendation from Lippes [30]. Figure 2.15 shows the distribution and the magnitude of residual stresses reported in [30], in the case of composite columns with massive steel core.
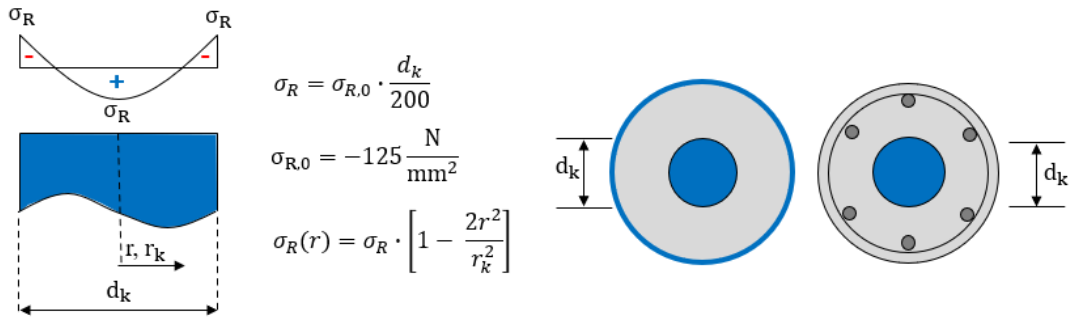
CFST with massive inner steel core

Figure 2.15 Residual stresses in massive steel core (adopted from [30])

2.3 Composite columns in accordance with EN 1994-1-1

2.3.1 Cross-section resistance

According to EN 1994-1-1 [2], the plastic resistance of the composite column cross-section subjected to only compression force is simply the sum of the plastic resistance of its components; steel, concrete and reinforcements as:

$$N_{pl,Rd} = A_a \cdot f_{yd} + A_c \cdot \alpha_c f_{cd} + A_s \cdot f_{sd} \tag{2.24}$$

Equation (2.24) includes the factor α_c which reduces the strength of concrete accounting for long-term loading effects. For CEC and PCEC columns, the value of α_c is 0.85, while for CFST columns, it is equal to 1.0. When a column is subjected to compression force and bending moment, the resistance of the cross-section is calculated by developing the N-M interaction diagram based on the rectangular stress block in accordance with EN 1994-1-1 [2] as it is presented in Figure 2.16. Moreover, If the shear force on the steel section $V_{a,Ed}$ is higher than 50% of the design shear resistance $V_{pl,a,Rd}$ of steel section [2], the influence of the shear force should be taken into account [2]. This is considered by reducing the design steel strength $(1 - \rho)f_{yd}$ in the shear area A_V as presented in Figure 2.16.
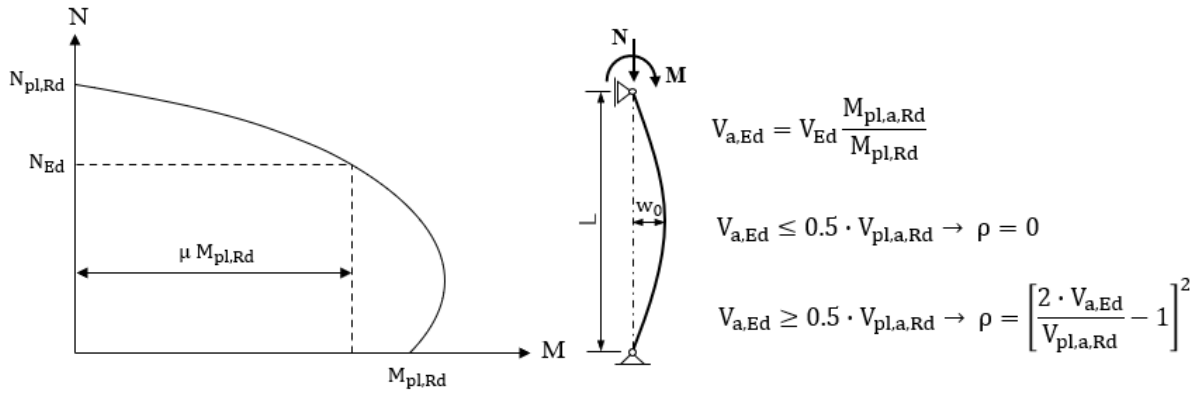
$$V_{a,Ed} = V_{Ed} \frac{M_{pl,a,Rd}}{M_{pl,Rd}}$$

$$V_{a,Ed} \leq 0.5 \cdot V_{pl,a,Rd} \rightarrow \rho = 0$$

$$V_{a,Ed} \geq 0.5 \cdot V_{pl,a,Rd} \rightarrow \rho = \left[\frac{2 \cdot V_{a,Ed}}{V_{pl,a,Rd}} - 1\right]^2$$

Figure 2.16 N-M interaction diagram for combined compression and bending adopted from [2]

2.4 Structural stability resistance

The resistance of a composite column to compression force, with or without eccentricity, is influenced by several parameters, but the main one is slenderness (λ), which is typically related to the length of column. Short columns experience cross-section capacity-driven resistance as the ultimate limit strain is reached before instability occurs. However, as column length increases, stability checks against buckling become more important.

Eurocode 4 EN 1994-1-1 [2] provides two methods for verifying the structural stability of composite columns in steel and concrete against buckling:

- The simplified methods,
- The general method.

Several parameters must be considered to select the verification method for structural stability. The simplified methods can be used for specific types of composite columns with certain limitations, mainly related to cross-section geometry, loading type, and material grade. On the other hand, the general method can be applied to any type of composite column, but it is more complex, and it is based on geometric and material nonlinear analysis with imperfections (GMNIA). Figure 2.17 provides a schematic representation of these two methods and the design approaches that should be followed.
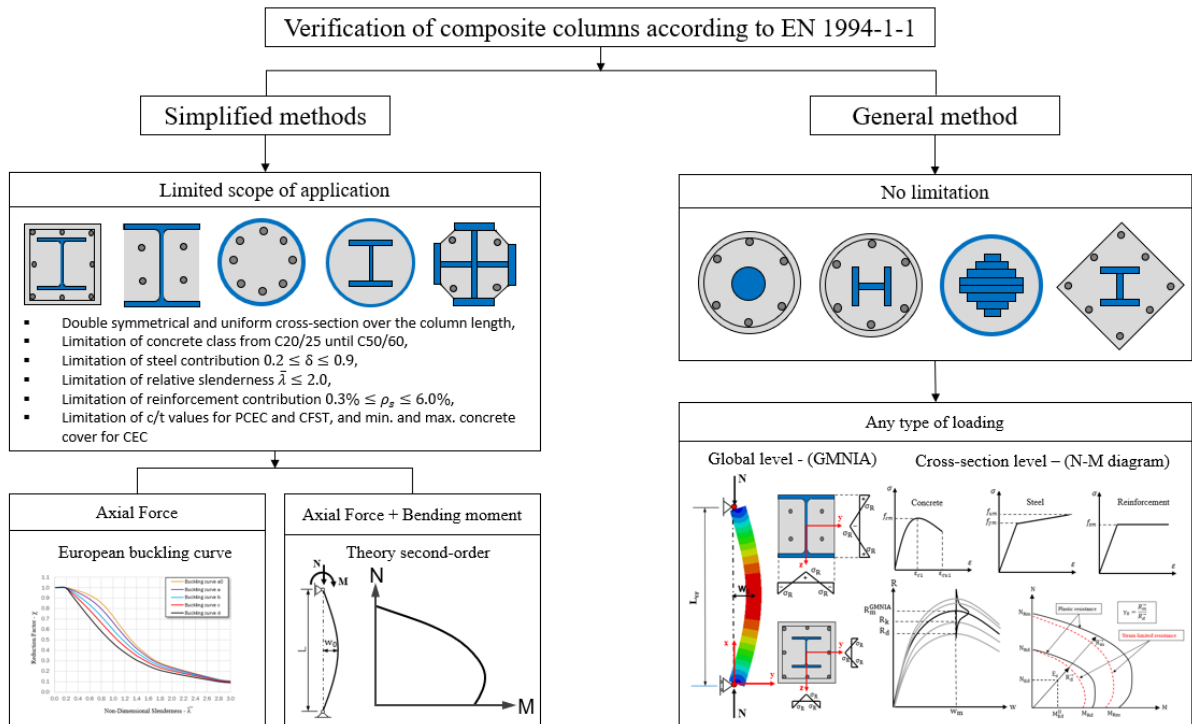
Figure 2.17 Design methods for composite columns according to EN 1994-1-1 [2]

2.5 Simplified methods

With simplified methods the structural stability and design verification of composite columns can be performed analytically without the use of a computer, making the simplified methods the most commonly used in everyday design practice. Depending on the type of loading (such as compression force or compression force with bending moment), the verification should be based on either the European buckling curve for centric loading or the theory of second order with equivalent initial imperfection for eccentric loading, as shown in Figure 2.17. To be eligible for verification according to the simplified methods, composite columns must satisfy certain conditions related to the geometry and the material parameters, as presented in [31] [32]:

− They must be double symmetric with uniform cross-section along the column length,

− the concrete class should be from C20/25 up to C50/60 (normal strength),

− the steel contribution should be between $0.2 \leq \delta \leq 0.9$,

− the reinforcement contribution should be between $0.3\% \leq \rho_s \leq 6.0\%$,

- the non-dimensional slenderness should be limited to $\bar{\lambda} \leq 2.0$,
- limitation of c/t values and respecting the min. and max cover for CEC columns.

Typical cross-sections of composite columns suitable for design according to simplified methods are shown in Figure 2.18.
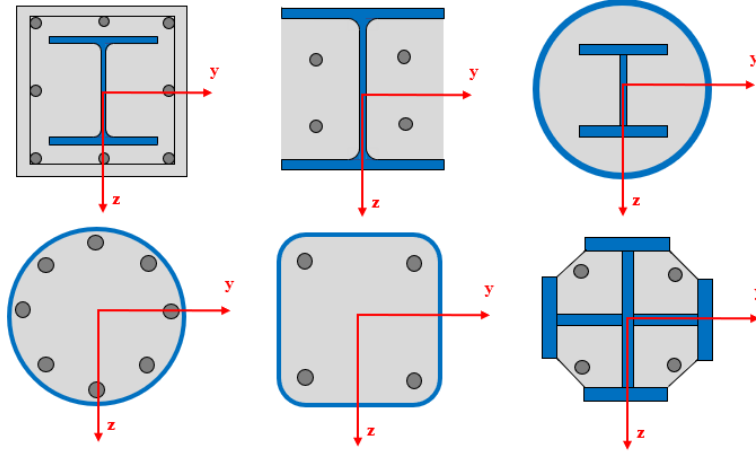

Figure 2.18 Double symmetric cross-section eligible for simplified methods

2.5.1 Simplified method for centric loading using European buckling curve

Based on background documents [33] reported also in Eurocode 3 EN 1993-1-1 [16], the design of composite columns for centric loading is determined by using European buckling curves presented in Chapter 2.1.3. According to EN 1994-1-1 [2] and [33], the following equation should be satisfied to verify members subjected to compressive force:

$$\frac{N_{Ed}}{\chi \cdot N_{pl,Rd}} \leq 1 \tag{2.25}$$

N_{Ed} represents the design compressive load and $N_{pl,Rd}$ represents the plastic resistance of the cross-section as per Equation (2.24). The reduction factor χ is associated with the relevant buckling mode [16], and its value depends on the relative slenderness $\bar{\lambda}$. This value can be calculated analytically using the expression provided in EN-1993-1-1 [16] as:

$$\chi = \frac{1}{\phi + \sqrt{\phi^2 - \bar{\lambda}^2}} \quad but \; \chi \leq 1 \tag{2.26}$$

where, ф is known as intermediate factor calculated as:

$$\phi = 0.5 \cdot [1 + \alpha \cdot (\bar{\lambda} - 0.2) + \bar{\lambda}^2] \tag{2.27}$$

where α is the imperfection factor according to Figure 2.6. In order to determine if a column is suitable for analysis using the simplified method (European buckling curves), the relative slenderness must be verified using the following expression:

$$\bar{\lambda} = \sqrt{\frac{N_{pl,Rk}}{N_{cr}}} \leq 2.0 \tag{2.28}$$

To determine the critical buckling load, N_{cr}, the following expression is used:

$$N_{cr} = \frac{(EI)_{eff} \times \pi^2}{L_e^2} \tag{2.29}$$

where, the flexural stiffness is calculated using the following expression:

$$(EI)_{eff} = E_a \cdot I_a + E_s \cdot I_s + K_e \cdot E_{c,eff} \cdot I_c \tag{2.30}$$

In the Equation (2.30), to account for the effect of cracking in concrete, a correction factor of $K_e = 0.6$ is used. To consider the long-term effect (creep) on concrete, the modulus of elasticity of concrete should be replaced with the effective elastic modulus of concrete as:

$$E_{c,eff} = \frac{E_{cm}}{1 + \left(\frac{N_{G,Ed}}{N_{Ed}}\right) \times \varphi_t(t, t_0)} \tag{2.31}$$

According to EN 1992-1-1 [34], $\varphi_t(t, t_0)$ is the creep coefficient. However with reference to [32], for concrete filled hollow sections (CFST), an effective creep coefficient should be used, as:

$$\varphi_{t,eff} = 0.25 \cdot \varphi_t(t, t_0) \tag{2.32}$$

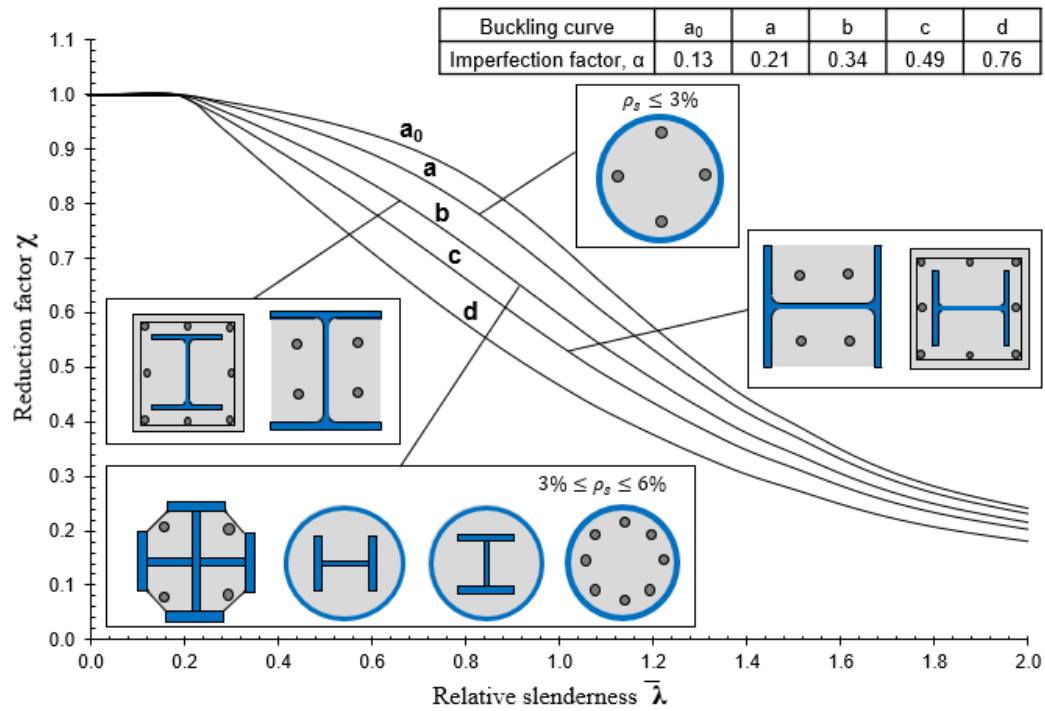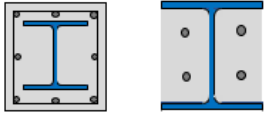Figure 2.19 show the classification of the composite columns according to the simplified method EN 1994-1-1 [2].
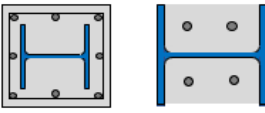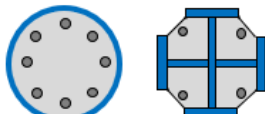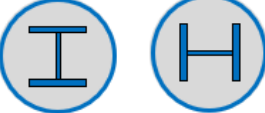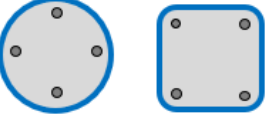

Figure 2.19 European buckling curves for composite columns (adopted from [35])

According to Figure 2.19, CEC and PCEC columns are classified into *buckling curve c* for buckling about the weak axis, while into *buckling curve b* for buckling about the strong axis. On the other hand, the CFST columns with or without steel profile and with the reinforcement ration between $3\% \leq \rho_s \leq 6\%$ are classified into *buckling curve b* regardless the strong or weak axis, and in case when the reinforcement ration is lower than 3% ($\rho_s \leq 3\%$), the CFST columns are classified into *buckling curve a* as it is presented also in Table 2.2.

Table 2.2 Equivalent geometrical imperfections for composite columns as function of buckling curves

Composite column cross-section	Buckling curve	Equivalent geometrical imperfections
	b	$\dfrac{L}{200}$
	c	$\dfrac{L}{150}$
3% ≤ ρ_s ≤ 6%	b	$\dfrac{L}{200}$
	b	$\dfrac{L}{200}$
ρ_s ≤ 3%	a	$\dfrac{L}{300}$

2.5.2 Simplified method based on the theory of second order with equivalent imperfection

The simplified method that uses second order theory with equivalent imperfection can be utilized for both centric and eccentric compression loads, as well as centric loads with bending moments. This method is based on second order linear elastic analysis [2], and plastic N-M interaction diagrams on the cross-section level, as presented in Chapter 2.3.1. To determine the internal forces according to second order theory, an effective flexural stiffness is introduced:

$$(EI)_{eff,II} = K_0 \cdot (E_a \cdot I_a + E_s \cdot I_s + K_{c,II} \cdot E_{cm} \cdot I_c) \tag{2.33}$$

In the Equation (2.33), the reduction factor for the total flexural stiffness is denoted K_0 is equal to $K_0 = 0.9$. Meanwhile, the correction factor for concrete stiffness is represented by $K_{c,II} = 0.5$ as per EN 1994-1-1 [2]. The long-term effect should be considered similarly to the European buckling curves, where the elastic modulus of concrete E_{cm} is replaced by the effective elastic modulus $E_{c,eff}$ as given in Equation (2.31). On the other hand, the column imperfections, including geometrical and structural imperfections are considered by the equivalent initial bow imperfection presented in Table 2.2. Since the method is based on second order analysis, the maximum moment should be calculated either by exact or simplified solution to account for the second order effect.
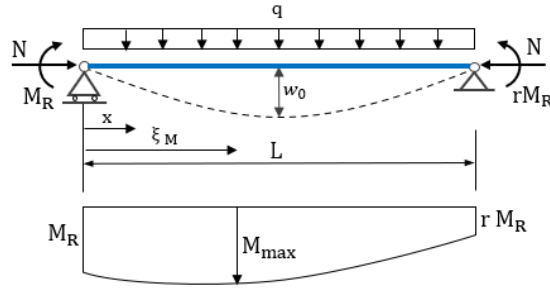

Figure 2.20 Bending moment including second order effects (adopted from [32])

Based on Figure 2.20, the exact solution for the maximum bending moment at point ξ_M, including second-order effects, is given according to [32] as:

$$M_{max} = [0.5 \cdot M_R \cdot (1 + r) + M_0] \cdot \frac{\sqrt{1 + c^2}}{\cos(0.5\varepsilon)} - M_0 \tag{2.34}$$

where,

$$M_0 = (q \cdot L^2 + 8 \cdot N \cdot w_0) \frac{1}{\varepsilon^2} \tag{2.35}$$

and the c and ε factors are computed in the following manner:

$$c = \frac{M_R \cdot (r-1)}{M_R \cdot (1+r) + 2M_0} \cdot \frac{1}{\tan(0.5\varepsilon)} \tag{2.36}$$

$$\varepsilon = L \cdot \sqrt{\frac{N_{Ed}}{(EI)_{eff,II}}} \tag{2.37}$$

According to EN 1994-1-1 [2], the second order effect is taken into account by multiplying the first order bending moment, M_{Ed}^I by a factor k given as:

$$k = \frac{\beta}{1 - N_{Ed}/N_{cr,eff}} \tag{2.38}$$

where, $N_{cr,eff}$ is the critical load for effective stiffness and β is the equivalent moment factor from Table 6.4 in EN 1994-1-1 [2]. In accordance with [33] and EN 1994-1-1 [2], for centric loading the design is according to Equation (2.25), while for the members that are subjected to combined compression force and bending moment the following expression should be satisfied:

$$\frac{M_{Ed}}{M_{pl,N,Rd}} = \frac{M_{Ed}}{\mu_d \cdot M_{pl,Rd}} \leq \alpha_M \tag{2.39}$$

The maximum bending moment in a member is denoted by M_{Ed}. The plastic moment resistance is represented by $M_{pl,Rd}$ and μ_d is the coefficient defined in the N-M interaction diagram for the relevant axis, and α_M is the shape factor that takes into account the difference between the plastic and strain limited cross-section resistance to compression and bending, as presented in Figure 2.21 [36]. According to [2], the value of the shape factor is 0.9 for steel grades S235 and S355, and 0.8 for S420 and S460.
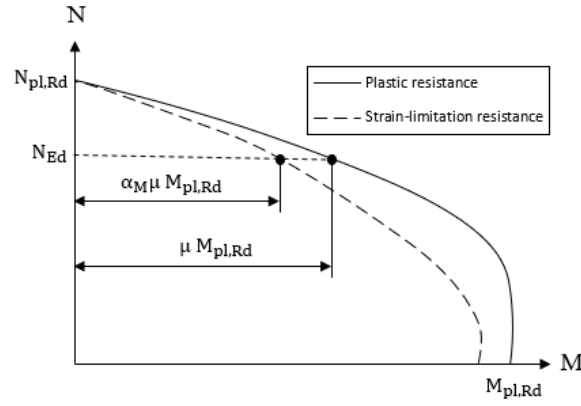
Figure 2.21 N-M interaction diagram using plastic and strain-limitation resistance

In case of biaxial bending moment with compression force, the values for μ_d should be calculated separately for each axis (μ_{dy}, μ_{dz}), as shown in Figure 2.22, and the following expressions should be satisfied:

$$\frac{M_{y,Ed}}{\mu_{dy} \cdot M_{pl,y,Rd}} \leq \alpha_M \quad , \qquad \frac{M_{z,Ed}}{\mu_{dz} \cdot M_{pl,z,Rd}} \leq \alpha_M \tag{2.40}$$

$$\frac{M_{y,Ed}}{\mu_{dy} \cdot M_{pl,y,Rd}} + \frac{M_{z,Ed}}{\mu_{dz} \cdot M_{pl,z,Rd}} \leq 1.0 \tag{2.41}$$
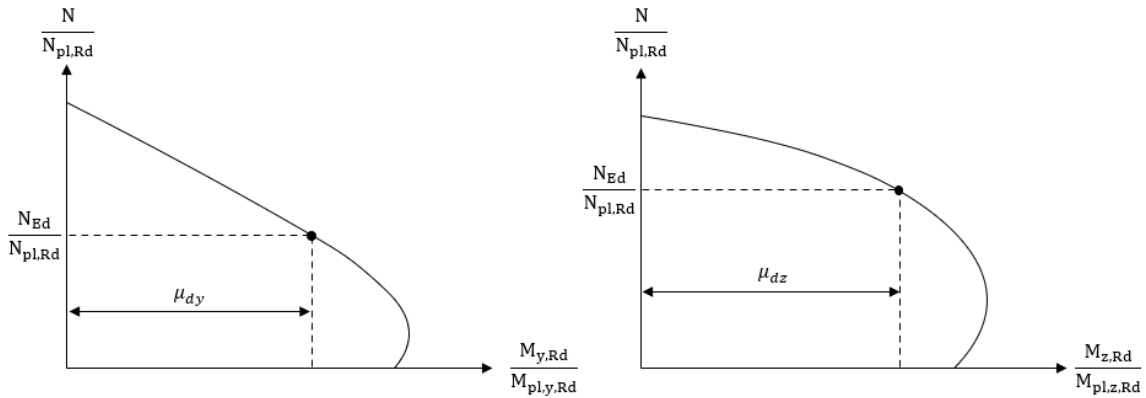

Figure 2.22 Determination of μ_d factor in N-M interaction curves about the weak (z-z) and strong axis (y-y)

2.6 The general method

In the previous discussion about the resistance of structural members, it is highlighted that simplified methods are preferred over the general method since they can be calculated

analytically (by hand calculation) without the need for a computer's software. However, the simplified methods have limitations, as mentioned before. In practice, many composite columns used in buildings and bridges exceed these limitations, especially when the concrete is not of normal strength, such as C20/25 up to C50/60 and when the steel or reinforcement ratio is inadequate. Moreover, non-uniform cross-sections over the length of the column can also be problematic. In such cases, the verification of structural stability should be performed using the general method according to EN 1994-1-1 [2].

The term "general" indicates that this method can be used for any type of composite column regardless the cross-section geometry, material parameters, loading type or boundary conditions. The general method is a sophisticated method which requires tremendous computation time and effort, since it is based on non-linear finite element analysis so-called Geometric and Material Nonlinear Analysis with Imperfections (GMNIA), taking into account all kind of nonlinearities related to material and geometry, present in the composite column members such as: geometric imperfection, residual stresses, local buckling, cracking of concrete, steel yielding, as well as long-term effects on concrete. Thus, with general method it is re-created (modelled) the real column behaviour in the structure. Nevertheless, due to its complexity, the general method is not yet well-established in engineering practice, but also in the current Eurocode 4: EN 1994-1-1 [2], as no sufficient information are provided for the design procedure, while in the new version prEN1994-1-1 [3], more information are presented on the application of the general method [31], which will also be discussed in this dissertation.

Based on [31], the general method comprises two parts. The first part involves global analysis based on Geometric and Material Nonlinear Analysis with Imperfections (GMNIA) and the second part involves determining the overall (safety) factor γ_0 from the N-M interaction diagram based on plastic or strain-limited resistance on the cross-section level. Figure 2.23 shows the procedure for applying the general method according to prEN 1994-1-1 [3].
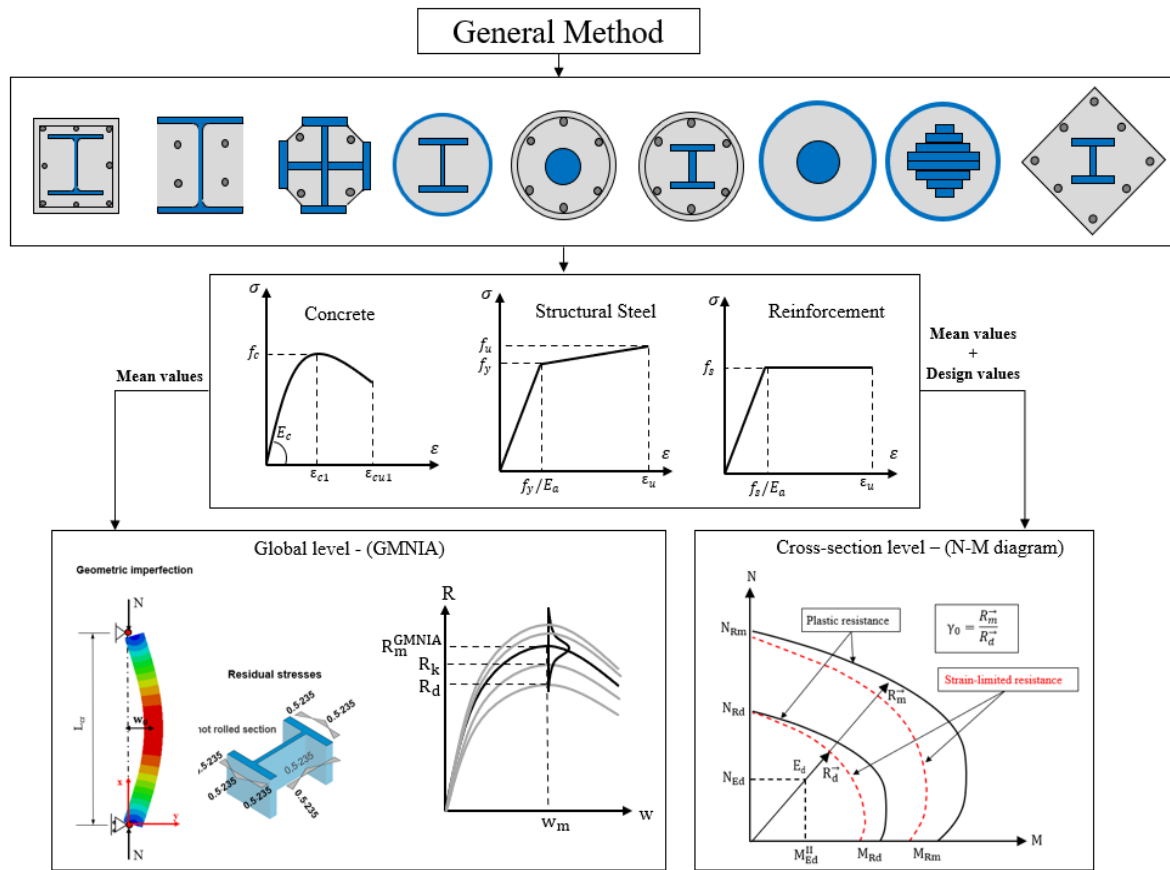
Figure 2.23 A schematic presentation of the general method

2.6.1 Global analysis (GMNIA)

On global level, the incremental non-linear finite element analysis (GMNIA) must be performed, taking into account initial geometric imperfection, residual stresses on the steel section, and non-linear material stress-strain curves based on the mean values for concrete, steel, and reinforcement bars as per prEN1992-1-1 [37] and prEN1993-1-1 [9]. For the initial geometric imperfection, the value $w_0 = L/1000$ reported in [38], [39], [32], and [36] is used in this study. This imperfection was originally measured and reported for steel members (IPE160 – S235 mild steel) when ECCS buckling curves were being developed [22]. Later, this value was also adopted for composite columns. However, the experimental test data performed on CEC columns reported in [26], the average initial geometrical imperfection (out-of-straightness) in 9 test series is around $L/660$. In the latest version of prEN 1994-1-1 [3] it is recommended that the geometric imperfection should be $L/400$ (similar to reinforced

concrete columns) unless the National Annex gives a different value. Nonetheless, it is worth mentioning that this part is still under investigation if the imperfection value $L/1000$ can be applied to all kinds of composite columns.

When it comes to steel profiles, residual stresses can develop during the manufacturing process. According to ECCS [29], hot-rolled and welded profiles should adhere to certain standards, while massive steel cores should follow guidelines set out in [30] (as shown in Figure 2.24). Nevertheless, for the sake of simplicity, according to Eurocode 4 EN 1994-1-1 Clause 6.7.2 [2] it is possible to use the equivalent initial bow imperfection (as presented in Table 2.2) as a substitute for geometrical imperfection and residual stresses in the general method.
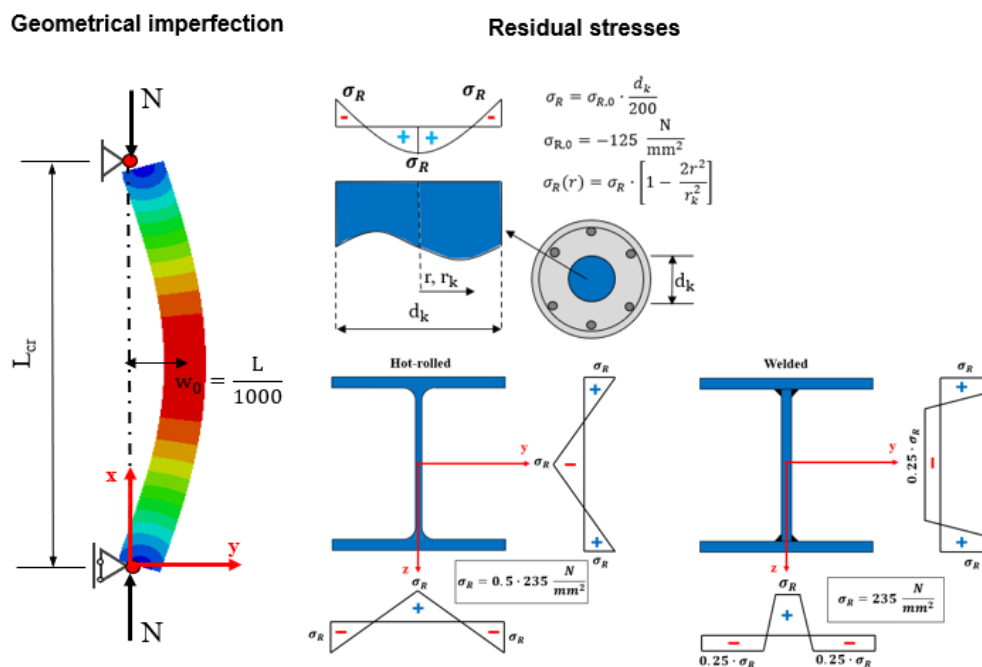

Figure 2.24 Geometrical imperfection and residual stresses according to [24] *and* [30]

In the global GMNIA, the material stress-strain curves are based on mean values. Therefore, the obtained resistance R_m and corresponding displacement w_m represent the average load-bearing capacity and displacement of the columns, as illustrated in Figure 2.25.
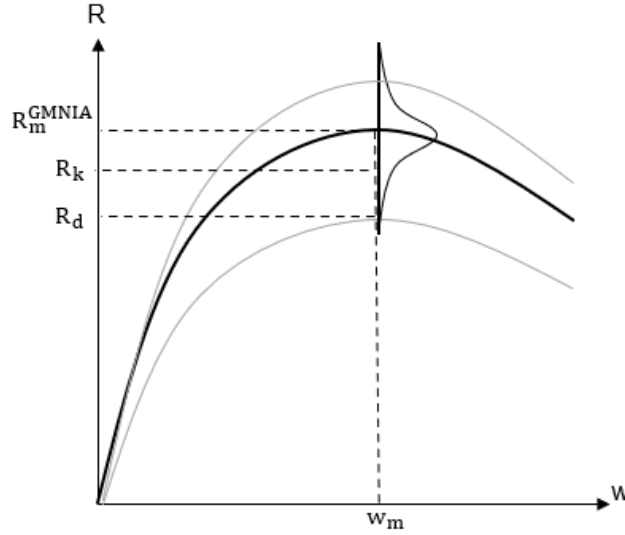
Figure 2.25 Geometric and Material Nonlinear Analysis with Imperfections (GMNIA)

Next, we calculate the design resistance as:

$$R_d = \frac{R_m^{GMNIA}}{\gamma_0} \tag{2.42}$$

where, γ_0 is the overall (safety) factor obtained from N-M interaction diagram, based on a plastic or strain-limited resistance at the cross-section level. The upcoming sub-chapter will provide detail explanation regarding the calculation of the overall (safety) factor γ_0.

2.6.2   The overall (safety) factor γ_0 based on plastic N-M interaction diagram

With reference to Figure 2.26, the overall (safety) factor γ_0 is calculated from the N-M interaction diagram based on plastic or strain-limited resistance [31] as:

$$\gamma_0 = \frac{R_{pl,m}}{R_{pl,d}} \tag{2.43}$$

where, $R_{pl,m}$ is the resistance vector in N-M interaction diagram (blue line Figure 2.26) based on mean material strength for concrete f_{cm}, steel profile f_{ym}, and reinforcement bars f_{sm}. The mean compressive strength of concrete is given in prEN 1992-1-1, Table 5.1 and Table A.1 [37], while for reinforcement bars the mean strength is given in prEN 1992-1-1, 5.2.4: Figure 5.2, curve 2, where the f_{sk} should be replaced with f_{sm} which is given in Table A.1 [37], and

for structural steel is given in prEN 1993-1-1, Clause 7.4.3(3) where f_{yk} should be replaced with f_{ym} which is given in prEN1993-1-14, Clause 5.3.2. On the other hand, $R_{pl,d}$ is the resistance vector in N-M interaction diagram (red line Figure 2.26) based on design values for concrete f_{cd}, steel profile f_{yd} and reinforcement bars f_{sd}. The design values are obtained using partial safety factor $\gamma_c = 1.5$ for concrete according to [34], $\gamma_{M1} = 1.0$ recommended value for structural steel according to [16], and $\gamma_s = 1.15$ for reinforcement bars according to [34]. For concrete, the coefficient that takes into account the long-term effects on compressive strength (α_{cc}) should also be considered. The relevant design compressive strength for concrete stress block is $0.85 \cdot f_{ck}$ with $f_{cd} = f_{ck}/1.5$ for Concrete Encased Composite (CEC) columns and Partial Concrete Encased (PCEC) columns, and $1.0 \cdot f_{ck}$ for CFST columns according to [34].
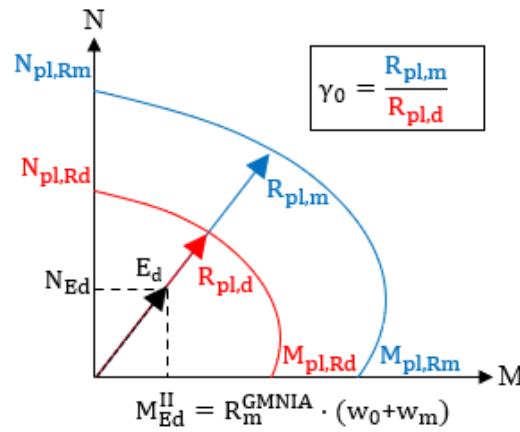

Figure 2.26 Determination of the overall safety factor γ_0 for general method

The direction of vectors $R_{pl,d}$ and $R_{pl,m}$, is affected by the compression force N_{Ed} and second-order moment M_{Ed}^{II}. If the external actions are unknown, then the mean resistance R_m^{GMNIA} calculated from global GMNIA and the corresponding second-order moment M_x^{II} presented in Equation (2.44) may be used.

$$M_x^{II} = R_m^{GMNIA} \cdot (w_{0,x} + w_{m,x}) \qquad (2.44)$$

Where, $w_{m,x}$ is the maximum displacement at the midspan of the column calculated from global GMNIA, and $w_{0,x}$ is the initial geometric imperfection. Additionally, the overall (safety)

factor can be calculated by developing the N-M interaction diagram based on strain-limited resistance.

2.6.3 The overall (safety) factor γ_0 based on strain-limited N-M interaction diagram

The term "strain-limited" indicates that the calculation according to this method is based on limitation of the strain for the considered materials. Originally the "strain limited design" is used for reinforced concrete members with design guidelines provided by Eurocode 2 EN 1992-1-1 [34], which later on is extended also to Eurocode 4 EN 1994-1-1 [2] by incorporation also structural steel in strain limit. The idea behind the strain-limited design is to establish strain limits at the cross-section's critical fibers and calculate the equilibrium between the external and internal forces, regardless of the computation method used —FEM analysis, numerical methods, or analytical calculation [40]. The fundamental point of the strain-limited design is the selection of proper material constitutive laws.

Figure 2.27 depicts the stress-strain material constitutive laws used for concrete, steel, and reinforcement bars to calculate the overall (safety) factor γ_0 based on strain-limited N-M interaction diagram from composite columns in steel and concrete.
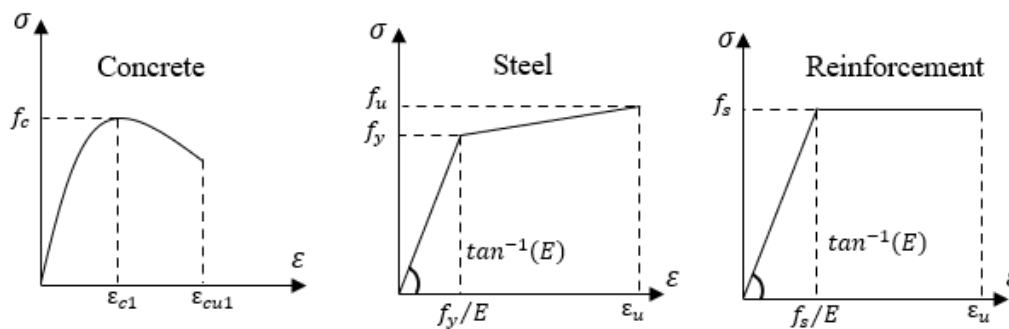

Figure 2.27 Material constitutive law for strain-limited

The concrete is defined using non-linear strain-strain relationship with the strain ε_{c1} at peak stresses and ultimate compressive strain ε_{cu1} according to Eurocode 2 EN 1992-1-1, Table 3.1 [12]. In [12] the strain ε_{c1} is given as a function of the mean compressive strength f_{cm} but limited to maximum 2.8 ‰, while the ultimate compressive strain ε_{cu1} is limited to 3.5 ‰ for concrete class between C12/15 up to C50/60, while for high strength concrete, the value is

reduced to 2.8 ‰. However, the draft version of the next generation of prEN1992-1-1 [37] suggest to use the ultimate strain $\varepsilon_{cu1} = 3.5$ ‰ for all classes of concrete. With reference to Figure 2.28, both, the non-linear and parabola-rectangle stress-strain curve can be used when the design resistance vector R_d is calculated, but the f_{cm} and E_{cm} should be substituted with f_{cd} and E_{cd} respectively, with $E_{cd} = E_{cm}/\gamma_{cE}$ in accordance with EN 1992-1-1 [12]. In [12] the design compressive strength is defined as $f_{cd} = \alpha_{cc} \cdot f_{ck}/1.5$, while in Eurocode 4 EN 1994-1-1 [2] and also in this work, the f_{cd} is defined as $f_{cd} = f_{ck}/1.5$ with $0.85 \cdot f_{ck}$ for CEC and PCEC columns and $1.0 \cdot f_{ck}$ for CFST columns. It is important to notice that in the new draft version of code prEN 1992-1-1 [37], the f_{cd} is defined as $f_{cd} = \eta_{cc} \cdot k_{tc} \cdot f_{ck}/1.5$ with $\eta_{cc} = (40/f_{ck})^{1/3} \leq 1$, and $k_{tc} = 1.0$ for reference time loading $t_{ref} \leq 28$ days, and $k_{tc} = 0.85$ for reference time $t_{ref} \leq 56$ days, while in prEN1994-1-1 [3], $\eta_{cc} = (40/f_{ck})^{\frac{1}{3}} \leq 0.85$ for CEC and PCEC columns, and $\eta_{cc} = (40/f_{ck})^{\frac{1}{3}} \leq 1.00$ for CFST columns. When dealing with a non-linear (strain-limited) N-M interaction curve, it is necessary to apply the design resistance specified in prEN 1992-1-1[37].
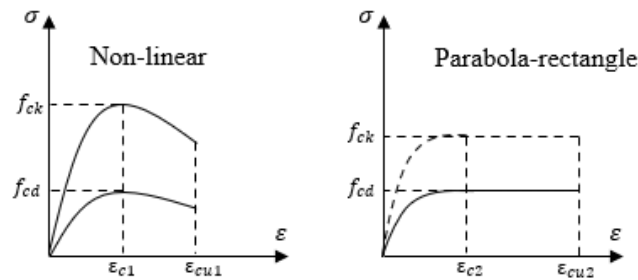

Figure 2.28 Concrete stress-strain curve for calculation of the design resistance vector R_d according to [12]

For reinforcement bars the bilinear stress-strain material law without strain hardening as it is shown in Figure 2.27 according to EN 1992-1-1 [12] is used with the strain limited to 5% for reinforcement bars class B, while for the structural steel, the bilinear stress-strain material law with strain hardening according to prEN 1993-1-14 [24] is used. With reference to Figure 2.29, the procedure to calculate the overall (safety) factor γ_0 from the N-M interaction diagram is the same as it is previously explained in sub-chapter 2.6.2 for plastic resistance.
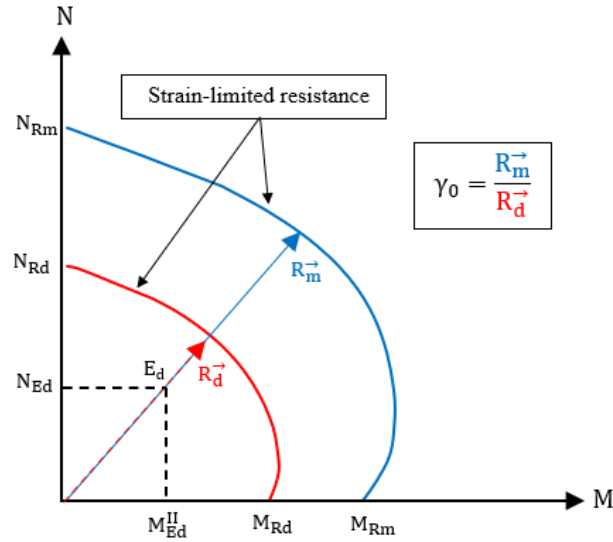
Figure 2.29 Overall (safety) factor based on strain-limited N-M interaction diagram

This study demonstrates that, in comparison to plastic resistance the calculation of the overall (safety) factor γ_0 based on nonlinear (strain-limited) N-M interaction diagram provides fewer conservative results for all considered composite columns under compression axial load. This is because, when the N-M interaction diagram based on mean material resistance is developed for calculation of the vector $R_{pl,m}$, the yielding of the steel profile and reinforcement bars under compression in not reached due to strain limitation of the concrete [41]. As a result this leads to smaller values of γ_0 calculated based on strain-limited resistance since for the calculation of the overall (safety) factor γ_0 is important the ratio between the vectors $R_{pl,m}$ and $R_{pl,d}$ as it is shown in Figure 2.26. This can also be explained with reference to Figure 2.21 where the shape factor $'\alpha_M'$ which is defined as the ratio between the strain-limited and plastic cross-section resistance to compression and bending $\alpha_M = M_{sl,Rd}/M_{pl,Rd}$, and the value of the shape factor is 0.9 for steel grades S235 and S355, and 0.8 for S420 and S460. So, in any case the N-M interaction diagram based on strain limitation is below the plastic resistance.

Regarding the calculation of N-M interaction diagram, the software SL.com [42] developed by Dr. Zhang in research group of composite structure Department of Engineering at University of Luxembourg is used for developing the N-M interaction diagram on cross-section level

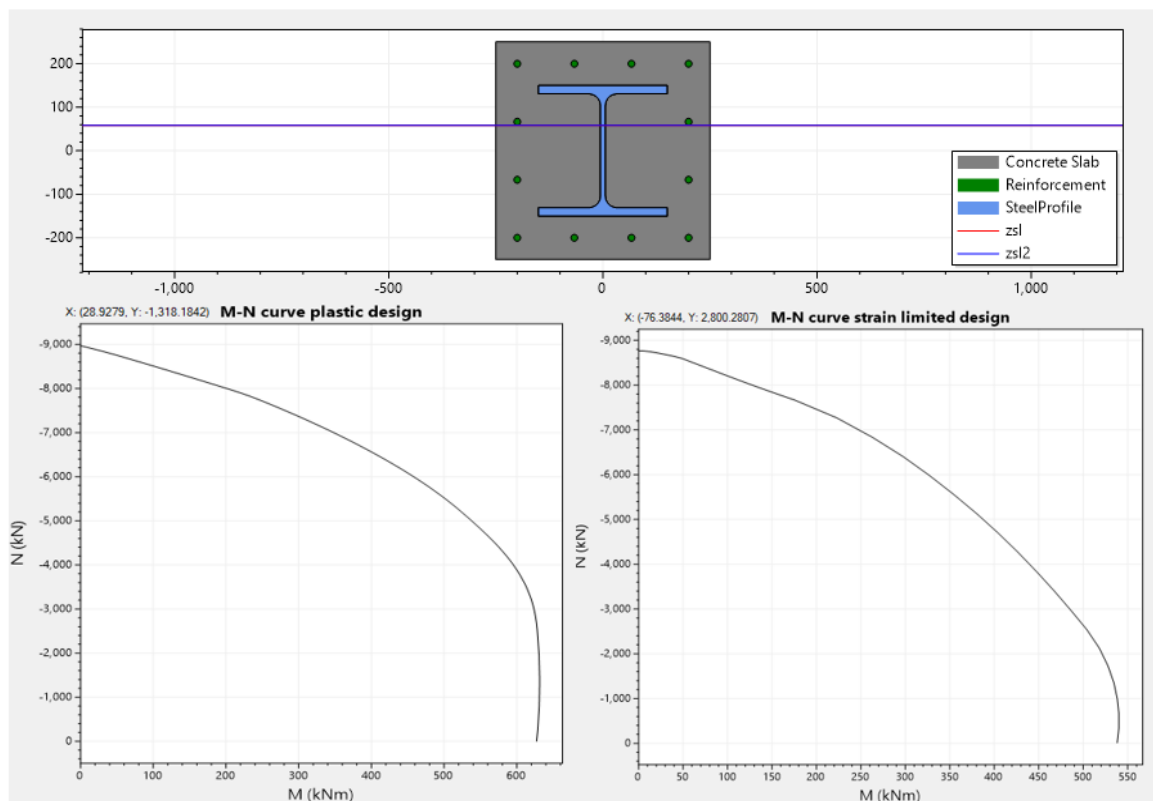based on plastic and strain-limited resistance. Figure 2.30 show the results provided by the software SL.com [42].

Figure 2.30 Calculation of N-M interaction diagram in SL.com

2.7 Safety and reliability of the structures

In this sub-chapter, the basic concept regarding the safety and reliability of the structures and structural elements in particular composite columns in steel and concrete will be discussed in detail. Because the structures are related to humans' lives, the safety of the structure (level of risk) is at the core of the Eurocodes series. However, this concept is widely used but briefly explained, which makes it more difficult to understand and apply. In general, at the core of the reliability and safety of the structures is the theory of probability and statistics. In Europe, the risk levels related to the safety and reliability of the structure are provided in Eurocode 0 EN 1990 [5].

At the beginning of this chapter, the main concept related to reliability and safety will be presented, followed by detailed information on reliability analysis for composite columns in steel and concrete using non-linear analysis.

2.7.1 Uncertainties

In general, in the most common probabilistic literature [43] the uncertainties are categorized into two groups, named objective and subjective uncertainty, or in some literature are referred to as *aleatory* and *epistemic* uncertainty respectively [43]. The first, *aleatory* is randomness by nature as the name is derived from the Latin language, meaning "rolling the dice" and cannot be eliminated, so, aleatory is outside our control. The second one, *epistemic* is described as a lack of knowledge or data about a process, and this type of uncertainty can be improved by collecting more data or improving the model. However, in the civil engineering area because of the complexity of the structures a high aleatory and epistemic uncertainties are always present. For instance, the aleatory uncertainty can be the wind load or earthquake which by nature are uncertain and unpredictable, while epistemic uncertainty is usually related to the material which has been used, geometry of the structure, theoretical model, inaccurate measurement, errors in design and execution etc. Being characterized by all these uncertainties, the complete secure structure or structural element does not exist, and to know the safety level of the structure, engineers may use probabilistic methods such as Monte Carlo simulation to evaluate the level of risk and provide design solution able to endure these uncertainties.

Nevertheless, when dealing with the calculation of the resistance of structural elements rather than the whole structure, such as composite columns in steel and concrete using non-linear analysis (NLA), the main uncertainties can be simplified into three categories: the uncertainties related to material parameters, the geometry and the model adopted to describe the structural behaviour, as it is presented in Figure 2.31.

Regarding material uncertainty, the steel and reinforcement have relatively small variation, whereas the majority of the material uncertainty is in concrete [44]. According to [7], the coefficient of variation of steel yield stress is around 7%, while the coefficient of variation of

concrete compressive strength is generally estimated 15%. On the other hand, the geometry uncertainties are related to the deviation from nominal (actual) geometry, while model uncertainty is the difference between the model in Finite Element Analysis (FEA) and the actual response of the structure.
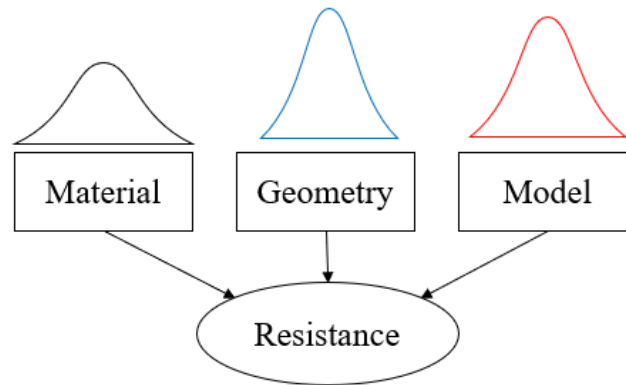

Figure 2.31 Uncertainties related to the resistance of structural elements

Mathematically, the uncertainties are represented using *The Probability Density Function (PDF)* as shown in Figure 2.32, where the centre and the tails of the distribution have the highest and the least probable regions, respectively.
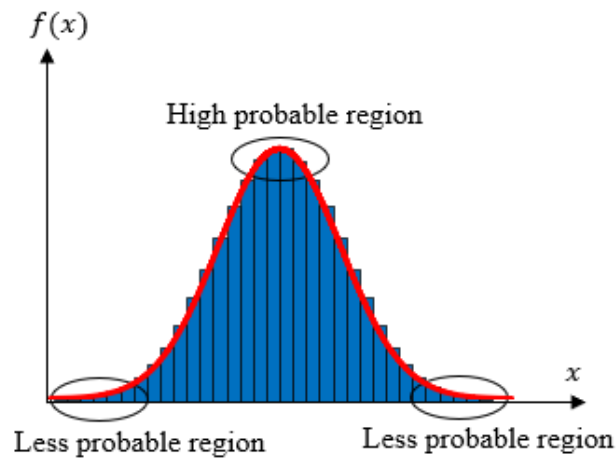
Figure 2.32 Probability Density Function of the uncertainties (Adopted from [43]*)*

2.7.2 Probability density function (PDF) and cumulative distribution function (CDF)

In general, random variables can be categorized as discrete random variables and continuous random variables. The discrete random variable has certain (finite) number of values, while

the continuous random variable has infinite number of values. These random variables can be expressed mathematically using functions called *Probability Density Function (PDF)* and *Cumulative Distributive Function (CDF).* PDF is usually denoted with $f_x(x)$, while the CDF is denoted with uppercase letters $F_X(x)$. The probability density function expresses the odds that a random variable will be within certain values, while the CDF is simply the integral of PDF, so the relation between the PDF and CDF is simply the derivative and the integral of each other. Figure 2.33 shows the *Probability Density Function (PDF)* and the associated Cumulative *Distributive Function (CDF)*.
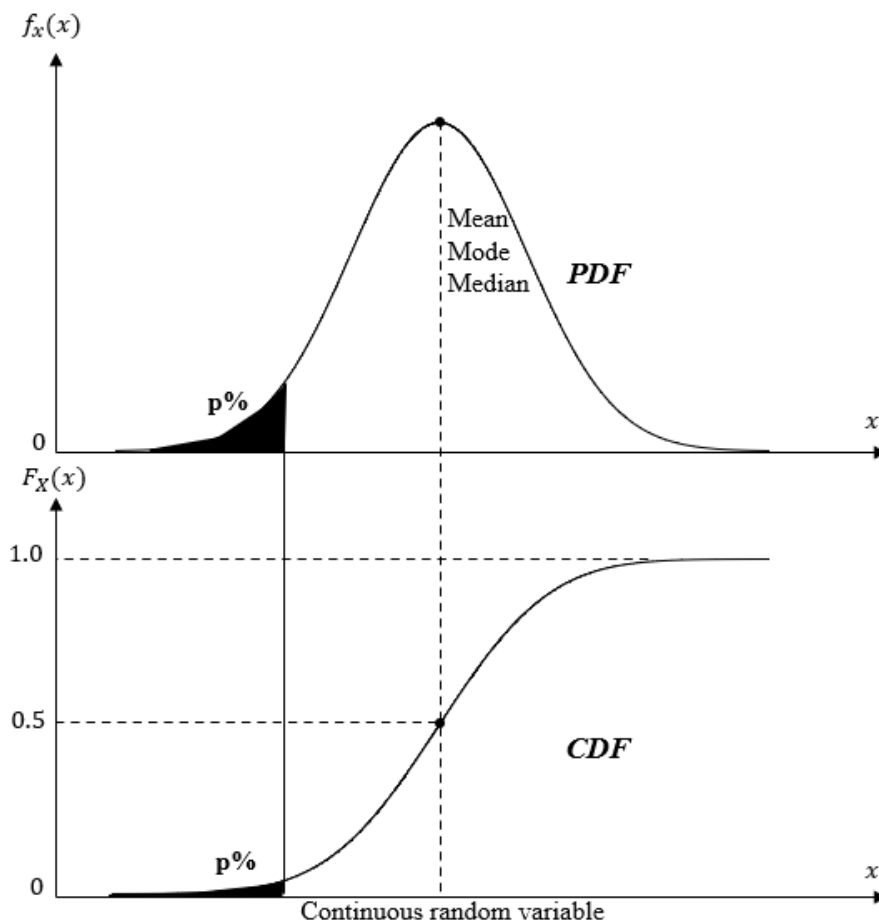

Figure 2.33 Probability Density Function (PDF) and associated Cumulative Distributive Function (CDF)

2.7.3 Safety

The next fundamental concept after uncertainties which is important in probabilistic analysis is the safety concept. The aim of the safety is to ensure that the resistance R, is always greater

than the action effect (load) E. In Eurocode 0 EN 1990 [5], the safety concept is addressed through general requirements necessary for the structure and structural elements to provide safety of the people's life. As it was stated before, a completely safe structure cannot be achieved, and when engineers refer to the term of a safe structure usually means that a low-risk level is present. This "low risk" is achieved through design codes which provide information on design situation, testing and quality control.

For instance, on the resistance side, to provide safety about the material used in the structure, the safety factors are used to reduce the resistance from mean to design value, while on the other hand, on the loading side, an increase from mean to design load is done by a safety factor, and if both the resistance and loading side are expressed in terms of Probability Density Function (PDF) the reduction/increase will be from high to less probable region as it is shown Figure 2.34. The intersection between the tails of the Probability Density Function (PDF) of the load and resistance represents the design region. This transition from mean to design values is done with the help of the so-called reliability index β, which will be explained in detail in Chapter 2.8.
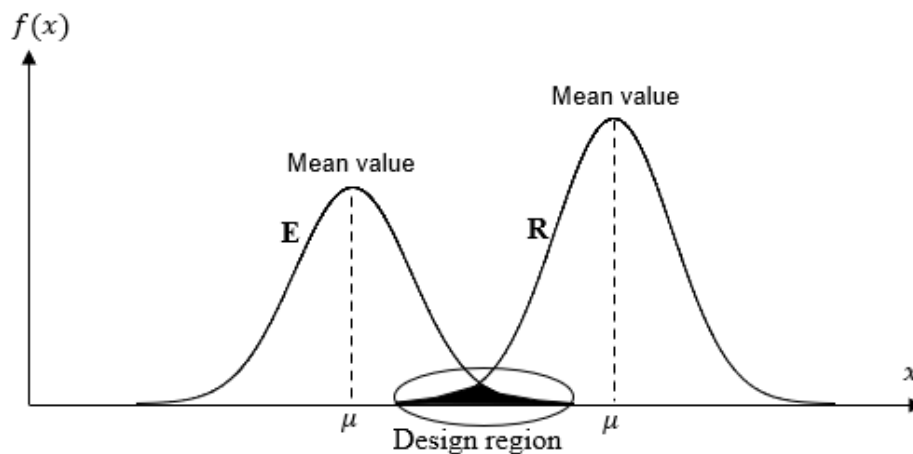

Figure 2.34 PDF of the load E and resistance R from mean to design point (adopted from [45]*)*

2.7.4   Reliability

Contrary to how usually the term reliability is used and simplified, in the structural engineering field the term reliability is simply, the probability that the structure will fulfil its requirements for a defined time and not fail under certain conditions. However, in Eurocode

0 [5] there is no clear definition of reliability, and rather it refers to safety and serviceability that the structure needs to attain for a certain period referred to as durability. In mathematical terms, the reliability problem is determined through the so-called *limit state function g(x)* and expressed using the *limit state equation* $g(x) = R - E = 0$. The *x* represents the random variable, while the *R* and *E* are the resistance and action effect respectively. The failure is defined when $g(x) < 0$ (failure domain), and $g(x) > 0$ (safety domain), and expressed in terms of probability of failure P_f as:

$$P_f = \int_{g(x)} f_x(x)dx = P[g(x) \leq 0] = P[R - E \leq 0] \tag{2.45}$$

The main purpose of reliability methods is to solve Equation (2.45), and the Joint Committee of Structural Safety (JCSS) [46] gives three levels of reliability analysis for evaluation of the Equation (2.45):

- Level III methods using Monte Carlo Simulation or numerical integration to solve the probability of failure. This method is the most accurate since each random variable is expressed using the probability density function (PDF).
- Level II methods using First Order Reliability Method (FORM) or Second Order Reliability Method (SORM) to solve the probability of failure.
- Level I methods by using partial safety factors. This method is semi-probabilistic since the integral of the probability of failure is not solved, but instead, it is checked if safety is achieved. In this method for each variable the "design values" are used $E_d \leq R_d$ instead of a probability density function, and these values are based on the reliability index β. Nevertheless, because of its simplicity, this method is mostly used in everyday practice design.

2.8 Reliability and safety format in Eurocode EN 1990

2.8.1 Limit states and reliability methods

As it is formulated in Eurocode 0 EN 1990 [5], a limit state is a condition (state) over which the structure or part of the structure no longer meets the required criteria which are

essentially for the use of the structure [5]. The limit states are distinguished into the *ultimate limit states* and *serviceability limit states*. The ultimate limit states deal with the safety of the people and the overall structure, and this condition can be exceeded from loss of the structure equilibrium, instability fatigue or other phenomenon. While, serviceability limit states are related to the normal functioning of the structure, in particular the deformations of the structure, the comfort of the users, the appearance of the structure (visual aspect) etc. In general, the ultimate limit states are more important and "dangerous" which means that a lower probability of occurrence is tolerated in these states. This can be observed also in Table 2.3, (adopted from Eurocode 0 [5]) where the minimum required reliability index β at ultimate limit states is higher compared to serviceability limit states.

Table 2.3 Minimum values of β for a reliability class RC2 (adopted from Eurocode 0 [5]*)*

Limit states	1 year	50 years
Ultimate limit states	4.7	3.8
Serviceability limit states	2.9	1.5

With reference to Table 2.4, in Eurocode 0 EN 1990 [5] it is presented the table with five categories for design working life in years for the building based on the purpose of the building.

Table 2.4 Design working life for buildings (adopted from Eurocode 0 [5]*)*

Design working life category	Working life (years)	Examples
1	10	Temporary structures
2	10-24	Replaceable structural parts
3	15-30	Agricultural and similar structures
4	50	Building structure and other common structures
5	100	Monumental building structures (bridges, churches)

Moreover, the structural buildings are classified according to consequence classes (CC) and reliability classes (RC) which are linked with a certain level of reliability index β. Consequence class (CC3) represent high consequence for human life loss, CC2 represent medium consequence and CC1 has low consequence. In general, CC3 are the public buildings where the number of people inside is large, CC2 are the residential buildings (common buildings), and CC1 are agricultural and similar buildings. Table 2.5 presents the correlation between consequence classes (reliability classes) and minimum reliability index β for different reference period at the ultimate limit state. As it is shown in Table 2.5, for a normal building with a reference period of 50 years the minimum reliability index β should be 3.8.

Table 2.5 Reliability index β for ultimate limit state (adopted from Eurocode 0 [5])

Consequence class (CC)	Reliability class (RS)	Minimum value for β	
		1 year reference	50 years reference
CC3	RS3	5.2	4.3
CC2	RS2	4.7	3.8
CC1	RS1	4.2	3.3

On the other hand, regarding the reliability methods, in Eurocode 0 [5], similar to JCSS [46], there are three levels for reliability methods, which are subdivided into two main categories named; probabilistic methods and deterministic methods as shown in Figure 2.35. Probabilistic methods can be sub-divided into fully probabilistic and semi-probabilistic. A fully probabilistic approach takes into account randomness in both the resistance and the load, whereas a semi-probabilistic approach only takes into account randomness in the resistance or the load. In this work, the load is defined as deterministic, and randomness is only taken into consideration on the resistance part.
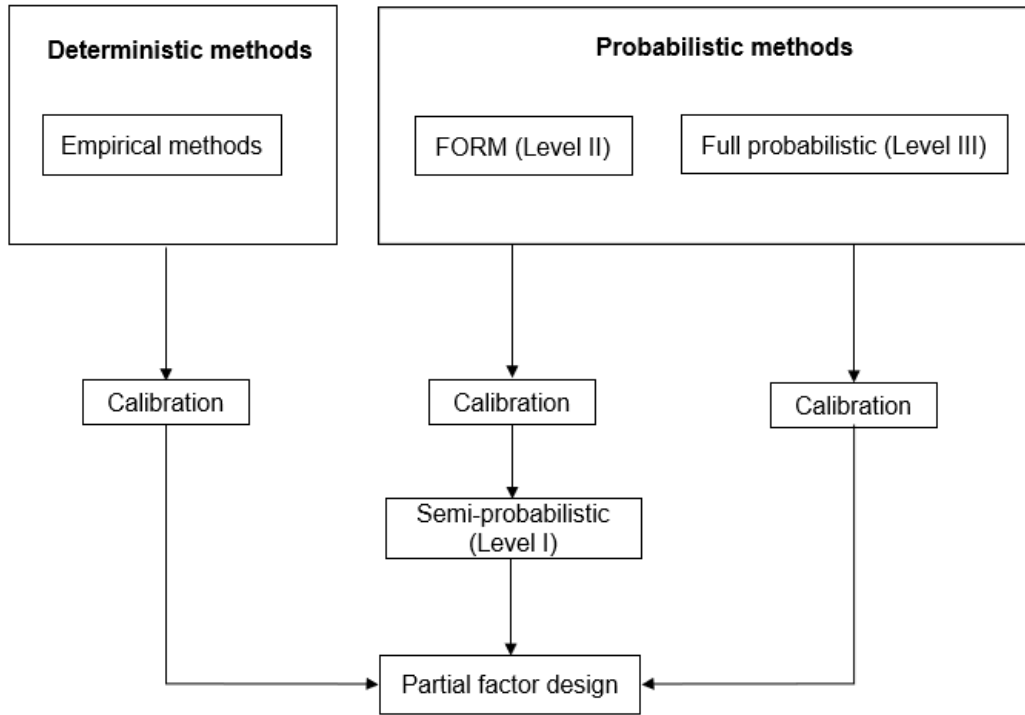
Figure 2.35 Reliability methods (adopted from Eurocode 0 [5])

2.8.2 Reliability index β

The derivation of reliability index β is based on [43]. As stated in sub-chapter 2.7.4 the limit state function $g(x) = R(x) - E(x)$, where with the x is expressed the random variable vector. The structure is safe when the resistance R is greater than the action effect E meaning that $g(x) > 0$, and when $g(x) < 0$ the structure is unsafe. Being so, the probability of failure is defined as:

$$P_f = \int_{g(x)} f_x(x)dx = P[g(x) \leq 0] = P[R(x) - E(x) \leq 0] \qquad (2.46)$$

Considering that both, the resistance R, and action effect E are related to uncertainties and are defined as random variables, the probability density function (PDF) is described using a normal (Gaussian) distribution as:

$$f_g(g) = \frac{1}{\sigma_g \cdot \sqrt{2\pi}} \exp\left[-\frac{1}{2} \cdot \left(\frac{g - \mu_g}{\sigma_g}\right)^2\right] \qquad (2.47)$$

where, μ_g, and σ_g are the mean and the standard deviation of the limit state function $g(x)$ with the mean defined as:

$$\mu_g = \mu_R - \mu_E \qquad (2.48)$$

where, μ_R and μ_E are the mean values for the resistance and the action effect respectively, while the standard deviation of $g(x)$ is defined as:

$$\sigma_g = \sqrt{\sigma_R^2 + \sigma_E^2 - 2\rho_{RS}\sigma_R\sigma_E} \qquad (2.49)$$

where, σ_R and σ_E are the standard deviation of the resistance and the action effect, while ρ_{RS} is the correlation coefficient between the resistance and the action effect. Then, the reliability index (safety index) β is determined as:

$$\beta = \frac{\mu_g}{\sigma_g} = \frac{\mu_R - \mu_E}{\sqrt{\sigma_R^2 + \sigma_E^2 - 2\rho_{RS}\sigma_R\sigma_E}} \qquad (2.50)$$

For the cases when the resistance and action effect are uncorrelated ($\rho_{RS} = 0$), the safety index is defined as:

$$\beta = \frac{\mu_R - \mu_E}{\sqrt{\sigma_R^2 + \sigma_E^2}} \qquad (2.51)$$

Graphically, the reliability index β represents the distance from the mean value μ_g to the limit state function $g(x) = 0$ as shown in Figure 2.36, where the shaded area represents the probability of failure, so that $\mu_g - \beta\sigma_g = 0$. Now, by substituting Equation (2.47) in Equation (2.46) we get:

$$P_f = \int_{-\infty}^{0} f_g(g)dg = \int_{-\infty}^{0} \frac{1}{\sigma_g \cdot \sqrt{2\pi}} \exp\left[-\frac{1}{2}\cdot\left(\frac{g - \mu_g}{\sigma_g}\right)^2 dg\right] \qquad (2.52)$$

Having a limit state function equal to zero $g(x) = 0$, and substituting the safety index β in the equation we get:

$$P_f = \int_{-\infty}^{0} \frac{1}{\sigma_g \cdot \sqrt{2\pi}} \exp\left[-\frac{1}{2} \cdot \left(\frac{0 - \mu_g}{\sigma_g}\right)^2 dg\right] \tag{2.53}$$

$$P_f = \int_{-\infty}^{0} \frac{1}{\sigma_g \cdot \sqrt{2\pi}} \exp\left[-\frac{1}{2} \cdot \beta^2 dg\right] \tag{2.54}$$

$$P_f = 1 - \Phi(\beta) = \Phi(-\beta) \tag{2.55}$$

Rearranging the Equation (2.53), we get the Equation (2.55) where $\Phi(-\beta)$ is called the Cumulative Distributive Function (CDF) of the Gaussian distribution and is used to express the correlation between the probability of failure P_f and reliability index β, and this correlation is given in Table 2.6. Moreover, in case the probability of failure is known, the reliability index β can be calculated using the Inverse Cumulative Distributive Function of the Gaussian distribution using Equation (2.56).

$$\beta = -\Phi^{-1}(P_f) \tag{2.56}$$

Table 2.6 Correlation between reliability index β and probability of failure P_f

P_f	10^{-1}	10^{-2}	10^{-3}	10^{-4}	10^{-5}	10^{-6}	10^{-7}
β	1.28	2.32	3.09	3.72	4.27	4.75	5.20
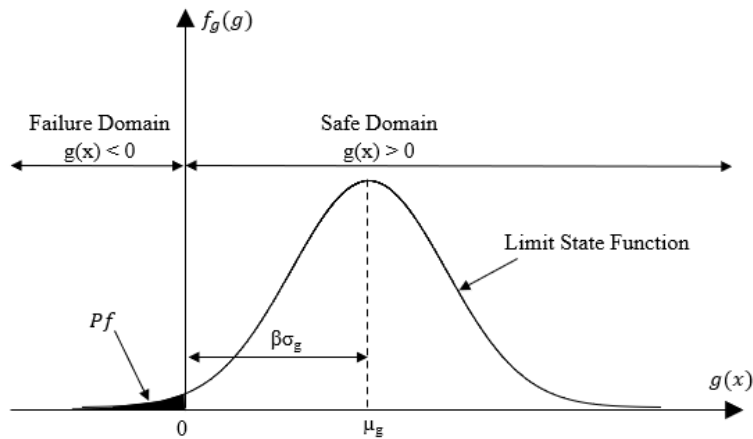
Figure 2.36 Reliability index β (adopted from [43]*)*

In terms of design, the reliability index β depicts the distance from the mean to design values of the resistance and action effect. This can be presented also in a two-dimensional form as it is shown in Figure 2.37, where α_E and α_R are so-called First Order Reliability Method (FORM) sensitivity factors and may be taken as $\alpha_E = -0.7$, and $\alpha_R = 0.8$ according to Eurocode 0 EN 1990 [5].
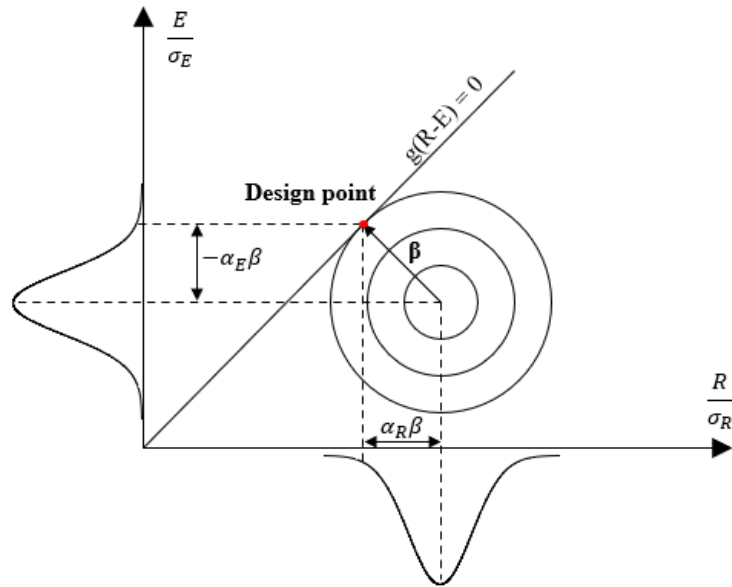
Figure 2.37 Design point and reliability index β (adopted from Eurocode 0 [5])

The design values for action effect E and resistance R considering the FORM sensitivity factor are defined as:

$$P(E > E_d) = \Phi(+\alpha_E \beta) \tag{2.57}$$

$$P(R > R_d) = \Phi(-\alpha_R \beta) \tag{2.58}$$

More details about the determination of the FORM sensitivity factors can be found in [5]. In other words, if we considered only the resistance side for a normal building with a reference period of 50 years at the ultimate limit state with consequence class (CC2) and reliability class (RS2), the minimum reliability index β will be:

$$\beta = \alpha_R \cdot \beta_{50years} = 0.8 \cdot 3.8 = 3.04 \tag{2.59}$$

Which according to Table 2.6, corresponds to the probability of failure $P_f \approx 10^{-3}$ or 0.1% quantile. Nevertheless, depending on what kind of distribution function is used e.g., Gaussian distribution, log-normal distribution, the design value should be calculated according to Table 2.7 adopted from [5], where μ, σ, V are the mean (μ), the standard deviation (σ), and the coefficient of variation (V).

Table 2.7 Design values for normal and lognormal distribution (Adopted from Eurocode 0 [5])

Distribution	Design values
Normal	$\mu - \alpha\beta\sigma$
Log-normal	$\mu \cdot exp(-\alpha\beta V), \quad V = {}^{\sigma}/_{\mu} < 0.2$

2.9 Safety Format in *fib* Model Code

2.9.1 Probabilistic analysis

Similar to what JCSS [46] refers to as the Level III method, also in *fib* Model Code [1] the probabilistic method is the most sophisticated and reliable method for assessment of the structure safety. However, due to complexity and time consuming this method is applied only in special cases and for special structures. Briefly explained according to *fib* Model Code [1], to perform probabilistic analysis, three steps are required:

− First step is to create a non-linear finite element model to describe the resistance of the structure or structural element and to perform deterministic non-linear finite element analysis.

− The second step is to transform the non-linear deterministic model into a probabilistic one, by considering the input parameters such as material properties, geometry of the cross-section, the model etc. as a random variable. These random variables are defined with mean and standard deviation using normal or log-normal distribution.

− The third step is to perform a probabilistic analysis of the resistance, by using either numerical method such as Monte Carlo Simulation (MCS) or more a sophisticated method such as the Latin Hypercube Sampling (LHS). From this analysis we obtain the

distribution function of the resistance (either normal or log-normal) which is described by mean (μ), standard deviation (σ) and skewness (κ).

Then, after getting the resistance R from probabilistic analysis, assuming that resistance follows a normal distribution, the design value is obtained as:

$$R_d = \frac{R(\alpha_R \beta)}{\gamma_{Rd}}$$

(2.60)

where, R is the resistance from probabilistic non-linear analysis, α_R is the FORM sensitivity factor, β is the reliability index and γ_{Rd} the model uncertainty factor. Similar to Eurocode 0 [5], for a normal building with a reference period of 50 years at ultimate limit state with consequence class (CC2) and reliability class (RS2) the value of the reliability index is $\alpha_R \beta = 0.8 \cdot 3.8 = 3.04$. The model uncertainty factor $\gamma_{Rd} = 1.0$ for case of no uncertainty, $\gamma_{Rd} = 1.06$ for low uncertainty and $\gamma_{Rd} = 1.10$ for high uncertainty according to *fib* Model Code [1].

On the other hand, in the case when the resistance R is described with log-normal distribution, the design resistance is calculated as:

$$R_d = \frac{\mu_R \cdot [exp(-\alpha_R \beta V_R)]}{\gamma_{Rd}}$$

(2.61)

where, μ_R and V_R are the mean and coefficient of variation obtained from probabilistic non-linear analysis. Moreover, it is worth mentioning that, in the structural engineering field, the uncertainties related to material parameters are described using log-normal distribution, while the uncertainties related to geometry are described using a normal distribution.

2.9.2 Global safety factor

To account for all uncertainties related to the material parameters, the geometry of the cross-section and the model, a global safety factor γ_R is presented in the form of a coefficient. According to the *fib* Model Code [1], this coefficient is simply the ratio between the mean and the design values:

$$\gamma_R = \frac{R_m}{R_d} = exp(\alpha_R \beta V_R) \tag{2.62}$$

where, R_m is the resistance obtained from non-linear analysis using mean values for material properties and nominal values for geometry, while the design value R_d is obtained as:

$$R_d = R_m \cdot exp(-\alpha_R \beta V_R) \tag{2.63}$$

where $\alpha_R \beta = 0.8 \cdot 3.08 = 3.04$, while V_R is the coefficient of variation of the resistance obtained from probabilistic analysis. As the procedure to obtain the coefficient of variation requires probabilistic analysis, a simple procedure and less time-consuming was introduced by Červenka [47], [48], called "Estimation of Coefficient of Variation (ECOV)". The basic assumption of this method is that the resistance is described by log-normal distribution as it is usually accepted in structural engineering. However, to get the coefficient of variation, the resistance of the structure needs to be calculated using non-linear (NLA) with mean and characteristic value for material parameters e.g., concrete and steel and then the coefficient of variation (COV) is calculated using the following equation:

$$V_R \leq \frac{1}{1.65} ln\left(\frac{R_m^{NLA}}{R_k^{NLA}}\right) \tag{2.64}$$

where, R_m^{NLA} and R_k^{NLA}, are the resistance from non-linear analysis using mean and characteristic values for material parameters respectively.

2.10 Chapter summary

In this chapter a literature review is presented to discuss the concepts and findings of previously conducted study related to the stability problem of composite columns in steel and concrete. The literature review produced a set of information regarding the stability problem for compressive members, the design of composite columns in steel and concrete according to EN 1994-1-1 [2] in particular the general method with the overall (safety) factor γ_0 based on strain-limited N-M interaction diagram, the basic concept of the safety and reliability of

the structures and structural elements, and the safety format according to EN 1990 [5] and *fib* Model Code [1].

Section 2.1, discusses the stability problem for members that are subject to compressive force and provides the differential equation's solution to determine the Eulerian buckling load. In Section 2.2, the effects of initial imperfections on compressive members e.g., (steel columns, and composite columns in steel and concrete) subjected to buckling are discussed and investigated. Section 2.3 discusses the design of composite columns according EN 1994-1-1 [2], including the simplified methods presented in Section 2.5 and the general method in presented in Section 2.6.

Section 2.7 discusses the basic concept related to probabilistic analysis, such as uncertainties, probability density function (PDF), reliability index β and safety, while the Section 2.8 and Section 2.9 provide more information regarding the reliability and safety format according to EN 1990 [5] and *fib* Model Code [1].

Chapter 3

Methodology

After the review of the literature in the chapter 2 regarding the fundamental concepts of the stability problem, the impact of geometric and material imperfections, the design of composite column, and the basic concept about probabilistic analysis, the next chapter provides an explanation of the methodology and software used in this study. In this dissertation, non-linear analysis and probabilistic analysis are employed to investigate the design of composite columns using the general method with the overall (safety) factor γ_0 based on strain-limited N-M interaction diagram, and to evaluate the safety and reliability of this method. Non-linear analysis are conducted using finite element method (FEM) in ABAQUS/CAE [49] and Open System for Earthquake Engineering Simulation (OpenSees) [50] software, while the probabilistic analysis and sensitivity analysis are performed using Stochastic Finite Element Method (SFEM) in OpenSees [50] and The Quantified Uncertainty with Optimization For The Finite Element Method (QuoFEM) software [51]. While, to calculate the N-M interaction diagram based on plastic and strain-limited resistance the software SL.com [42] is used.

3.1 Finite element method (FEM)

The Finite Element Method (FEM) has proven to be a useful and effective approach to solving engineering problems constrained by boundary conditions, first introduced in aircraft industry in the USA and Europe [52]. One of the most common applications of FEM is Finite Element Analysis (FEA), which is used to find an approximate numerical solution to mathematical problems characterized by differential equations. FEA is a powerful tool for validating analytical results and is often chosen over experimental testing due to the cost and the ability to investigate multiple cases through simulation.

In the civil engineering field, a finite element model consists of various structural elements such as beams, columns, plates, cables, and bars, each characterized by different materials

with unique mechanical properties such as concrete, steel, and timber. The FE-model is composed of nodes and elements, with all elements in the model connected to each other at nodes. A node is essentially a point in the graphical display of the model characterized by multiple degrees of freedom. In a 3-dimensional model (3D), a node has six degrees of freedom, and in a 2-dimensional model (2D), it has three degrees of freedom, as shown in Figure 3.1. These degrees of freedom are horizontal movement, vertical movement, and rotations.
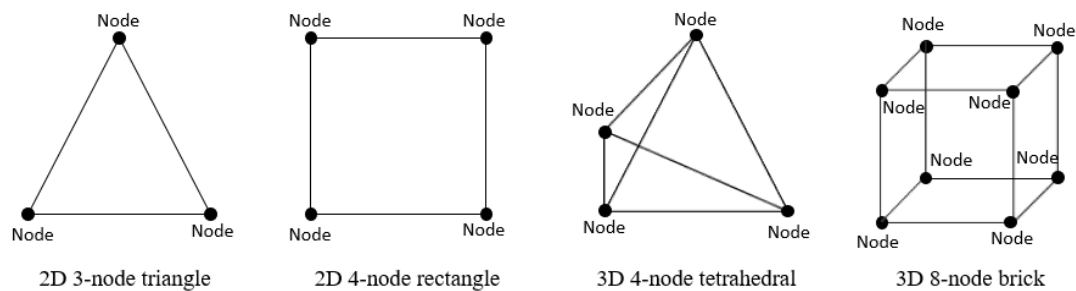
Figure 3.1 2D and 3D FEM element types

A finite element model is constructed by assembling several small elements in a mesh to create a discretized mathematical model that represents the structure in a simplified form. In a standard FE commercial software such as ABAQUS/CAE [49] there is a wide variety of one-dimensional (1D), two-dimensional (2D), or three-dimensional (3D) elements that can be utilized. Figure 3.2. shows some of the most commonly used elements.
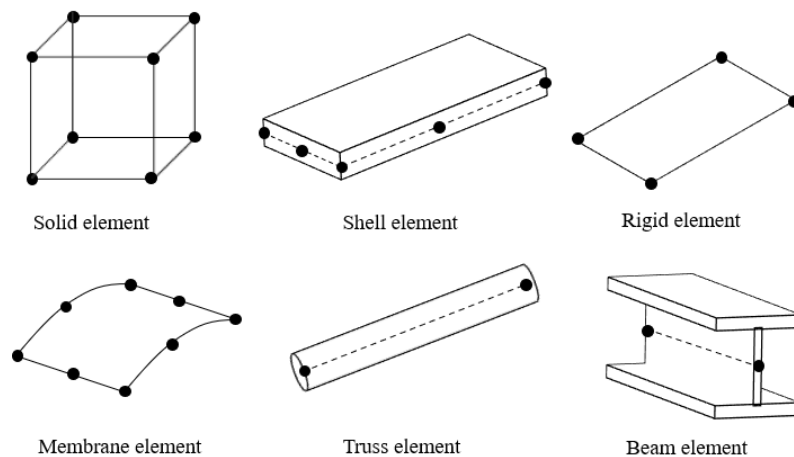
Figure 3.2 Standard elements in ABAQUS [49]

To create a finite element model, a standard procedure needs to be followed. First, the geometry and material parameters are defined. Then, the boundary conditions and load are assigned for the entire model. Finally, the mesh type and size are generated according to the structure's geometry. However, the analysis quality depends on several factors among which the most important ones being the quality of meshing, the simplification of the geometry during modelling, and the numerical solution for approximating the analysis. The combination of elements depends on the structure being modelled. For instance, composite columns in steel and concrete use 3D solid elements to model the concrete, 2D shell elements to model the steel profile, and 1D truss elements to model the reinforcement bars.

In structural engineering, the solution of finite element analysis is found by satisfying the compatibility equation in all nodes of the system.

$$[K] \cdot [u] = [F] \tag{3.1}$$

In linear analysis, the external load and structural response have a linear relationship, which is simplified by assuming that the stiffness of the structure remains linear. This means that the material used in the structure behaves elastically. The stiffness and displacement matrices are represented by K and u respectively, while the force matrix is represented by F. However, real-world structural engineering problems are usually characterized by high levels of nonlinearity, mainly due to the material parameters, geometry of the cross-section, and the contact between structural elements. In non-linear analysis, the solution is strictly related to load increments and to satisfy the compatibility equation, external loads must be applied in small steps called increments in order to satisfy Equation (3.1). Thus, a procedure of adjustment will be carried out to the stiffness matrix in order to meet the new incremental load. This process is continued until a solution is obtained or the model is unable to converge to a solution. Although non-linear analysis is a powerful tool, it has certain drawbacks as well. Compared to linear analysis, non-linear analysis will take much more time and effort due to its complexity. In this study non-linear finite element analyses called Geometric and Material Nonlinear Analysis with Imperfections (GMNIA) are conducted to evaluate the resistance of composite columns in steel and concrete.

3.2 Stochastic finite element method (SFEM)

As the name indicates, the Stochastic Finite Element Method (SFEM) is an extension of the Finite Element Method (FEM) which combines the deterministic FEM procedure with probability theory to solve stochastic problems including structural safety and reliability analysis [43].

In SFEM, material parameters, and the geometry of the section are defined as random variables, while the FEM is used to calculate the equilibrium and boundary conditions. FEM solves Hook's law (linear elasticity) where the stiffness matrix K multiplied by the displacement matrix u will be equal to the load matrix F.

$$[K] \cdot [u] = [F] \qquad (3.2)$$

With SFEM, the stiffness matrix K is divided into two parts: the deterministic part K_0 and the uncertain part K_1 [43], then from the Hook's law we get:

$$[(K_0 + K_1)] \cdot [u] = [F] \qquad (3.3)$$

To conduct Stochastic Finite Element Method (SFEM) analysis using Monte Carlo Simulation (MCS) or Latin Hypercube Sampling (LHS), it is necessary to perform thousands of simulations with tremendous computational time and effort. Due to that, the standard 3D finite element software such as ABAQUS/CAE [49] is not suitable for these kinds of analyses. To overcome this issue, in this study, the SFEM analyses were carried out using open-source software OpenSeesPy [50] and QuoFEM [51]. OpenSeesPy [50] is a Python module of OpenSees [53] software which is a free finite element software mostly used for earthquake engineering. As reported in [54], OpenSees [53] is suitable for SFEM. In this software it is possible to perform different kinds of deterministic analysis including non-linear static and dynamic analysis, earthquake simulation, sensitivity analysis etc., with Tcl and Python scripting language. On the other hand, QuoFEM [51] is a recently developed software able to be combined with Python scripts of the OpenSeesPy [50] to perform reliability analysis (Monte Carlo, Latin Hypercube Sampling), sensitivity analysis (Sobol indices), parameter estimation etc.

3.2.1 Stochastic finite element analysis (SFEA)

OpenSees [53] is used to create a deterministic model for the calculation of non-linear analysis (GMNIA) for composite columns subjected to concentrated load. From the deterministic model, with the help of QuoFEM software [51], the model is transformed into a probabilistic one by considering material parameters, and the geometry of the cross-section as a random variable (defined by normal or log-normal distribution) to perform reliability analysis and sensitivity analysis (Sobol indices [10]). Figure 3.3 shows schematically the procedure to transfer the deterministic model into a probabilistic one to perform reliability and sensitivity analysis for composite columns in steel and concrete.
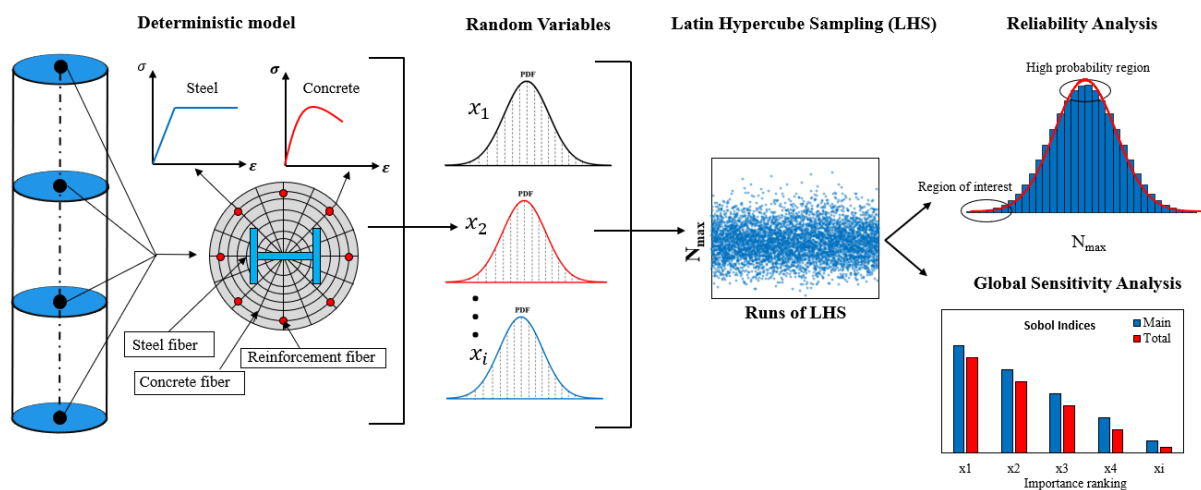
Figure 3.3 Stochastic Finite Element Analysis (SFEA) for composite columns in steel and concrete

3.3 Sampling Methods

3.3.1 Monte Carlo Simulation (MCS)

As the name indicates, the Monte Carlo Simulation (MCS) is named after casino games such as slots, dice, and roulettes where randomness is present [43]. MCS is considered one of the most powerful, reliable, and easier-to-understand sampling methods. The basic idea of this method is to generate random sampling for a set of random variables. Due to advances in computer tools and the availability of powerful computers, besides casino games, this method finds application in other fields including structural engineering. The core of this method is in

the generation of random numbers with a specific probability distribution, usually a Cumulative Distributive Function (CDF) with random numbers between 0 and 1. To explain the computation procedure of MCS, let's consider the design of composite columns in steel and concrete and the evaluation of the safety (probability of failure).

The following steps outline the process:

- Determine the random variable which influences the behaviour of the column e.g., concrete compressive strength, yield strength of steel, geometry of the cross-section,
- Select the probability density function to describe the random variables, e.g., normal, or log-normal distribution,
- Generate random samples, usually the higher the number of samples the more accurate the outcome,
- Analyse and evaluate the results e.g., the probability of failure and level of safety,
- Repeat and refine the model until desired results are obtained.

Mathematically this can be written as:

$$P_f = \frac{N_f}{N} = \frac{\sum_i^N I(g(x))}{N} \tag{3.4}$$

where, N is the total number of simulations and N_f is the number of failed simulations (*limit state function $g(x) < 0$*), as the main idea of this method is to solve the integral (Equation (2.46)) presented in Section 2.8.2. Schematically the Monte Carlo Simulation (MCS) is presented in Figure 3.4.
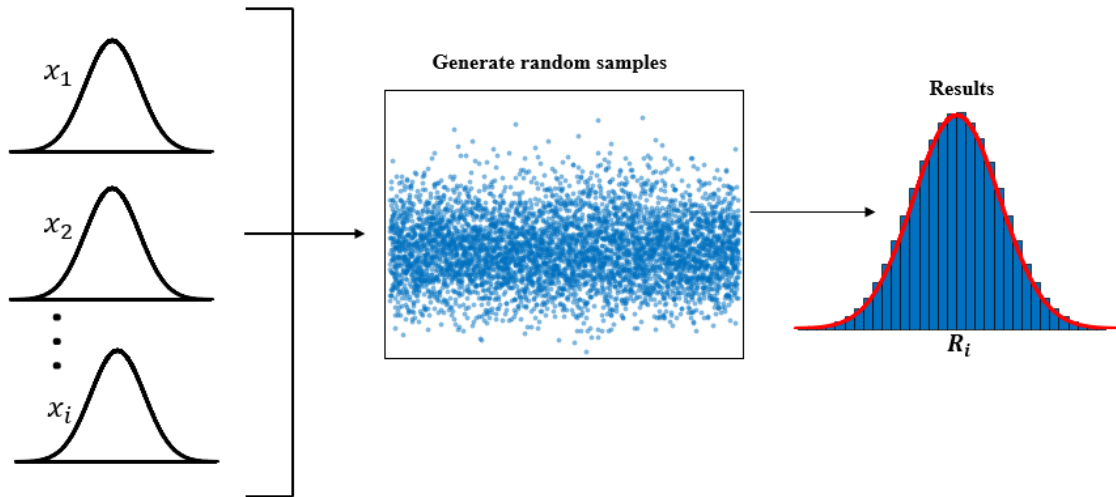
Figure 3.4 Monte Carlo Simulation (MCS) schematically presented

However, when Monte Carlo Simulation (MCS) is used, to get accurate and reliable results a very large number of samplings need to be generated (usually $>10^5$) and this implies that a huge effort and computational time is required. According to following studies [55] [56],[57] and [58], the minimum number of simulations is defined as:

$$v_{p_f} = \frac{1}{\sqrt{N \cdot P_f}}$$

(3.5)

where N is the number of simulations, v_{p_f} is the variation coefficient and P_f is the probability of failure. For instance, if the variation coefficient is 10% (which is acceptable in structural engineering) and the probability of failure $P_f = 10^{-3}$ ($\beta = 3.04$), the minimum acceptable number of simulations is $N \geq 10^5$. Because of this, new techniques are developed such as important sampling method, split sampling, or Latin Hypercube Sampling (LHS) [43].

3.3.2 Latin hypercube sampling (LHS)

In the previous discussion about the Monte Carlo Simulation (MCS), it is highlighted that this sampling method requires a large number of simulations and computational effort. Moreover, in [59] it is emphasized that due to time demanding, MCS is not suitable for nonlinear finite element analysis. To overcome the convergence problem and computational

time of the Monte Carlo Simulation (MCS), a more sophisticated method is introduced, called Latin Hypercube Sampling (LHS). This sampling method was first introduced by McKay, et. al [60] and it is also known as "Stratified Sampling Technique" [43]. The core concept of LHS is to use fewer samples for the same accuracy of the results, and this is done by dividing the probability density function (PDF) of the random variables into equal intervals, and then selecting randomly a sample from each interval as it is presented in Figure 3.5.
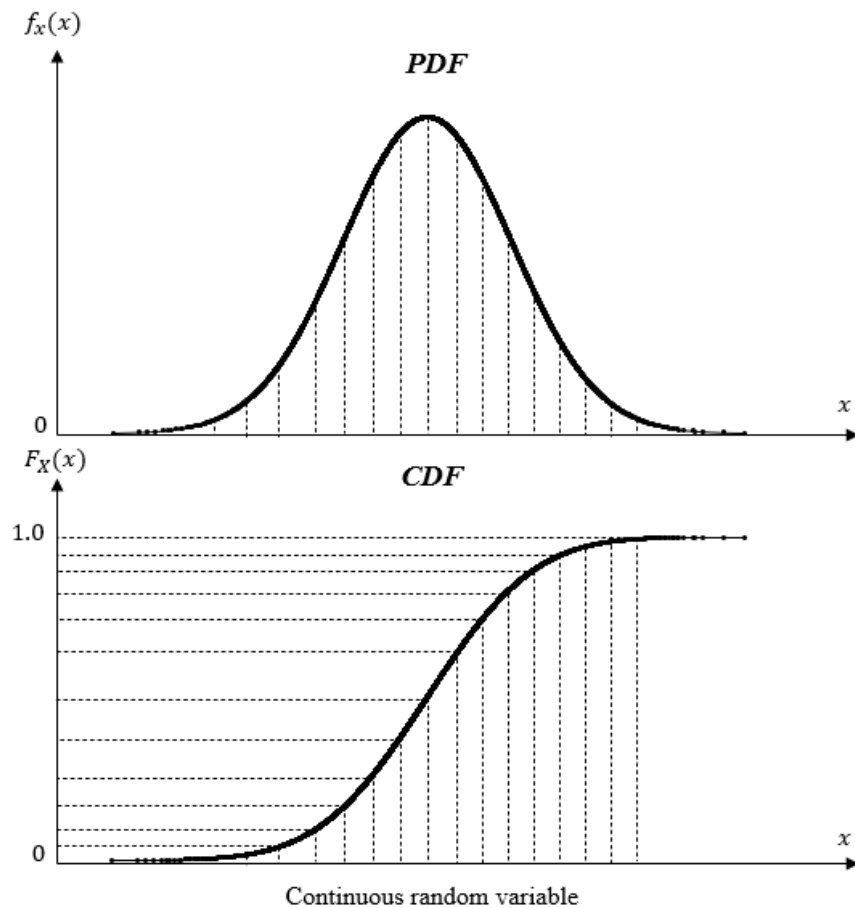
Figure 3.5 Basic concept of Latin Hypercube Sampling (LHS) (adapted from [61]*)*

As can be observed from Figure 3.5, from each column and a row of the random variables, at least one point is selected, which means that the probability density function is well represented. On the contrary, in Monte Carlo Simulation (MC) the samples are completely random without considering the previously generated sample, which implies that for a low number of samples, the most selected point would be around the mean value, while the values around the tails of the normal distribution may not be well represented. Because of

that, to get accurate and reliable results from MCS we need to generate a very large number of simulations, while with LHS this can be achieved with a much smaller number of samples. Figure 3.6 shows the difference between the simulation with Latin Hypercube Sampling (LHS) and Monte Carlo Simulation (MCS) with only 4 samples. In the case of MCS, three out of four simulations are selected around the high probable region (mean values) while the tails of the normal distribution are not well represented. On the other hand, by using LHS the normal distribution is well represented even with a small number of simulations as can be observed in Figure 3.6.
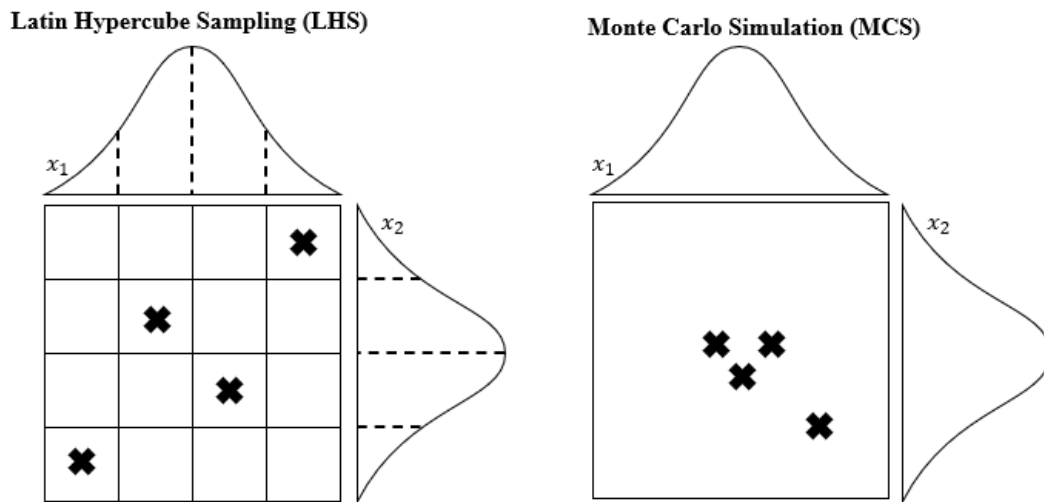
Figure 3.6 Comparison of Latin Hypercube Sampling (LHS) and Monte Simulation (MCS)

3.3.3 Convergence of MCS and LHS

Having concluded in the previous discussion that the LHS is more representative than MCS, now let's analyse the convergence rate of these two sampling methods. For each method the convergence rate with be evaluated considering a simple example of a PCEC column with a length of $3\,m$ as the one shown in Figure 6.6. For both sampling methods the number of sample size is increased up to 10000 simulations. With reference to the Figure 3.7, the dashed black line is used as a reference value and represents the true mean resistance of PCEC column calculated using deterministic approach (non-linear finite element analysis). The red line corresponds to Latin Hypercube Sampling (LHS), while the blue line corresponds to Monte Carlo Simulation (MCS).

As expected, the results of convergence study indicate that, the LHS is more efficient as the values are very close to the true mean value when the sample size is greater than 1000. On the other hand, in case of Monte Carlo Simulation, the results oscillate around the true mean value and when the sample size is greater than 5000, the results are very close to the true mean value as well as the LHS. Thus, the LHS is utilized in this study to produce random samples for the Stochastic Finite Element Method (SFEM) with a sample size equal to 2000 simulations.
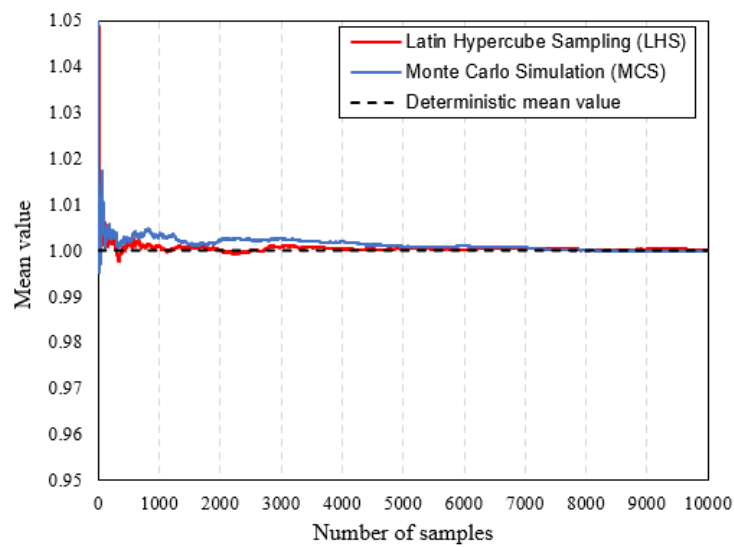
Figure 3.7 Mean resistance convergence rate in MCS and LHS

3.4 Sensitivity Analysis

When performing reliability analysis, it is important to know how much each input random variable influences the behaviour of the system or the quantity of interest. In the case of composite columns, it is important to know which parameters (random variable) such as concrete compressive strength, steel yielding, geometry of the cross-section etc., impact more the overall resistance of the column. One way to do it, is by performing sensitivity analysis.

One of the most known and easy-to-understand types of sensitivity analysis is the so-called Sobol indices [10]. The name comes from Russian mathematician Ilya M. Sobol. Similar to reliability analysis also for sensitivity analysis to generate samples, either Monte Carlo or Latin

Hypercube Sampling (LHS) can be used. Considering that when performing reliability analysis for composite columns there is more than one random variable, it is important to know how much each random variable influences the overall resistance of the column but also the interaction effect with other random variables.

Sobol indices sensitivity analysis can be *first-order Sobol index* and *second-order Sobol index* [10]. *First-order Sobol* also referred to as the *Main Sobol index* [62], measures the sensitivity of each random variable without considering the interaction with other random variables and is defined as:

$$S_i = \frac{Var_{xi}[E_x[y|x_i]]}{Var[y]}, \quad i = 1,..,d \tag{3.6}$$

Where, this equation can be understood intuitively, as the numerator is related to the input random variable while the denominator is related to the output variable (quantity of interest). The value of S_i varies from zero to one, with zero indicating that the random variable has no impact on the quantity of interest and vice versa. In cases when $E_x[y|x_i]$ is almost constant the variance operator $Var_{xi}[E_x[y|x_i]]$ is near zero, so the y is not sensitive to the change of x_i, and S_i approaches to zero. On the other hand, when one random variable x_i drops or increases (not constant) $E_x[y|x_i]$, the variance operator is large, so the y is sensitive to the change x_i, and S_i is approached to one [63]. It should be mentioned that the variance decomposition shown above is derived under the premise that the input variables are independent [64]. Figure 3.8 illustrates how the expression works, a positive/negative strong correlation between y and x_i as the increase/decrease of the x_i also induces an increase/decrease of the y, while on the other side, it is presented the case when there is no correlation between y and x_i.
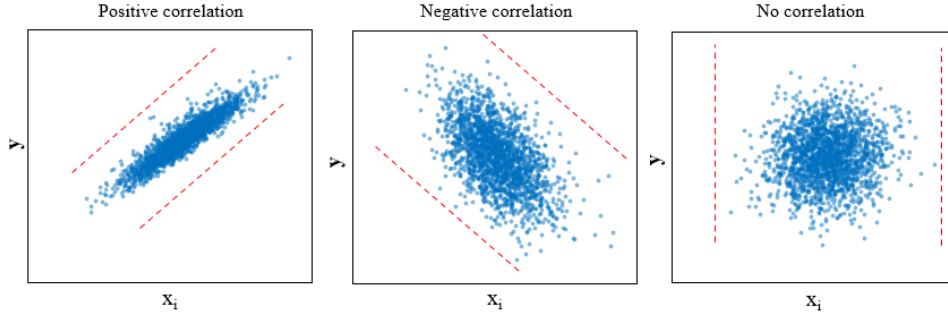
Figure 3.8 Sensitivity analysis using Sobol indices

On the other hand, *the second-order Sobol index* referred to as the *Total Sobol index* [62] account also for the interaction between random variables and is defined as:

$$S_{ij} = \frac{Var_{xi,xj}[E_{xi,xj}[y|x_i, x_j]]}{Var[y]} - S_i - S_j, \qquad i,j = 1, \dots, d \qquad (3.7)$$

In case all the random variables are uncorrelated and independent from each other we get:

$$\sum_{i=1}^{d} S_i + \sum_{i<j}^{d} S_{ij} + \cdots + S_{12..d} = 1 \qquad (3.8)$$

In this study, the Sobol indices sensitivity analysis is used to determine the impact of each random variable such as the geometry of the cross-section, the material parameters, the geometric imperfections, residual stresses for composite columns in steel and concrete subjected to compression force.
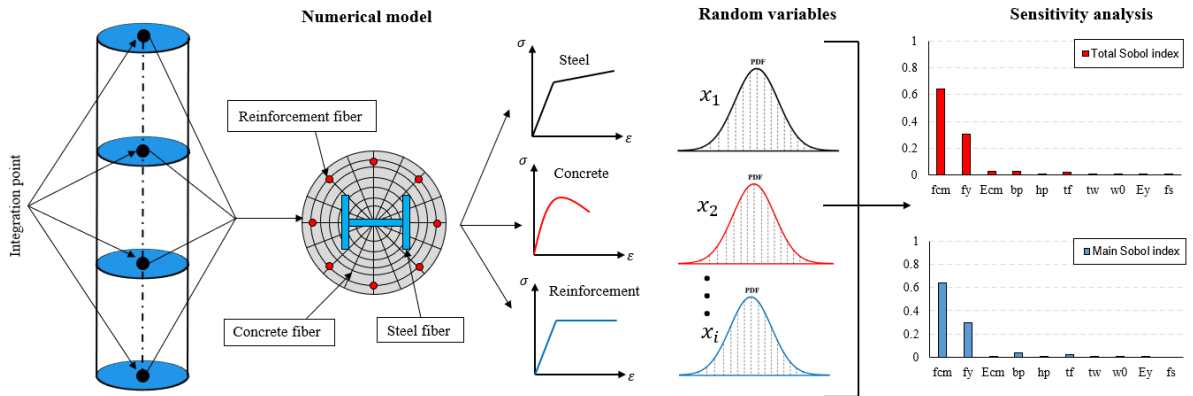
Figure 3.9 Concept of Sobol's indices sensitivity analysis

3.5 GMNIA for composite column in ABAQUS

This sub-chapter explains the modelling procedure for performing Geometric and Material Nonlinear Analysis with Imperfections (GMNIA) for composite columns according to the general method. An example is provided, with details regarding the material modelling, boundary conditions, meshing, and assumptions used for initial imperfection and residual stresses etc. GMNIA is necessary to evaluate the resistance of composite columns according to the general method, which is the core of this study.

3.5.1 Model description and assumption

The composite column considered in this example is a Concrete Encased Composite (CEC) column. Material, geometry, and boundary conditions of the composite column are summarized in Figure 3.10.
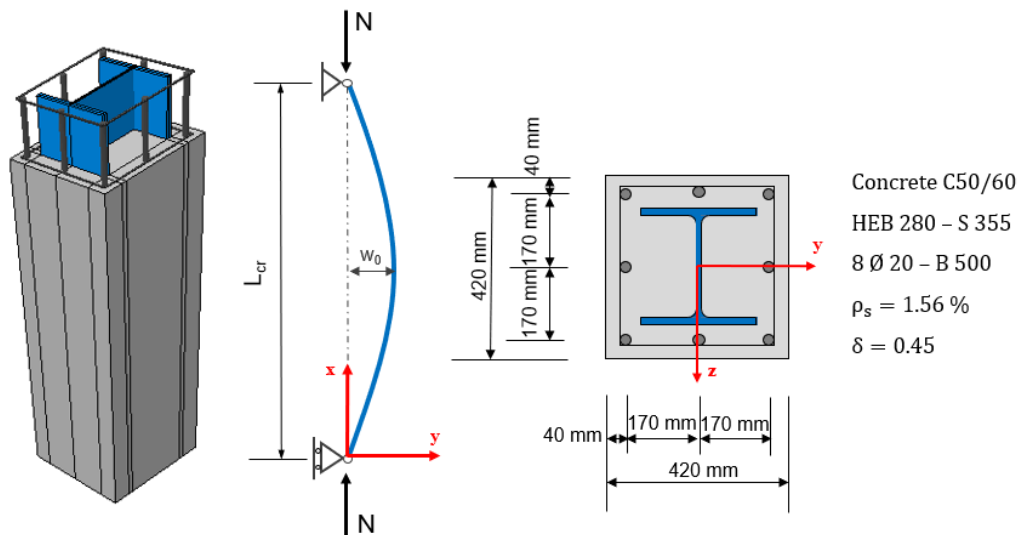
Figure 3.10 Considered steel and composite columns for GMNIA analysis in ABAQUS

3.5.2 Material model for structural steel

The stress-strain constitutive law for structural steel outlined in prEN 1993-1-14 [24] provides four different options depending on the required level of accuracy and analysis type. For this study, elastic-plastic with strain hardening, as presented in Figure 3.11 is used for design by GMNIA. In ABAQUS [49], the elastic part is described by Young's modulus E and Poisson's

ratio ν. For the considered structural steel, the elastic modulus is set to $E_a = 210\,000\ N/mm^2$ and Poisson's ratio is set to $\nu = 0.3$. The plastic part is defined by the yield stress, and according to the general method for GMNIA, the mean values should be used. For steel profile HEB 280 – S355, the mean value according to prEN 1993-1-1 [9], Table E.1 should be used.
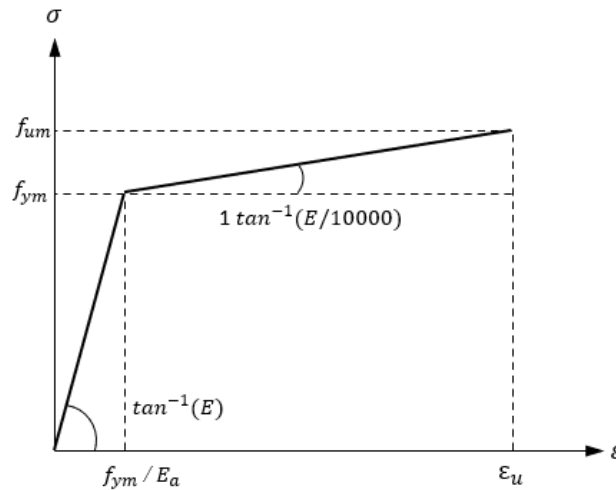
Figure 3.11 Stress-strain relationship for structural steel according to [24]

3.5.3 Material model for reinforcement

Reinforcement bars in construction projects are subjected to varying levels of stress and strain. To model the behaviour of these bars, the material model used is the linear elastic-perfectly plastic without strain hardening, as prescribed by prEN 1992-1-1 [37]. The elastic part of this model is defined by the elastic modulus $E_s = 200\,000\ N/mm^2$ and Poisson's ratio $\nu = 0.3$. Meanwhile, the plastic part of the model is defined by using the mean value for reinforcement bars, specifically the B500 type according to prEN 1992-1-1, Table A.1 [37]. For a better understanding of the material model, Figure 3.12, shows the stress-strain material law used for reinforcement bars in the ABAQUS software.
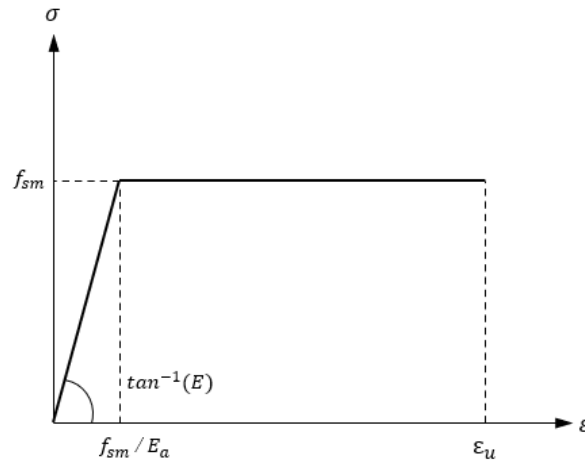
Figure 3.12 Stress-strain material law for reinforcement bars according to [37]

3.5.4 Material model for concrete

In the analysis of composite columns made of steel and concrete, selecting the appropriate material model for concrete is a critical factor that affects the accuracy and quality of the FEA results. If experimental test results are not available, the non-linear stress-strain material law of concrete based on prEN 1992-1-1 [37] can be used as a reference, as shown in Figure 3.13. This non-linear curve is based on the mean strength of concrete (f_{cm}) with a strain limitation of 3.5 ‰, and the formulas required to derive the curve are presented in Figure 3.13.
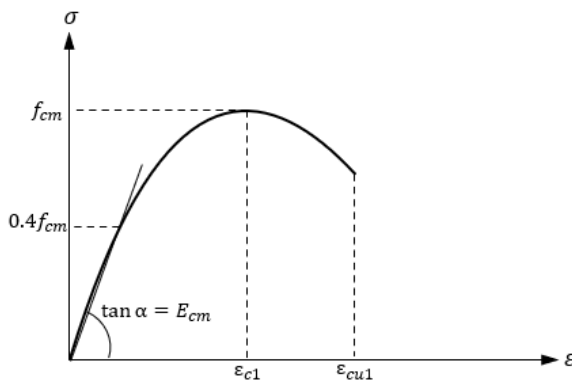
$$\frac{\sigma_c}{f_{cm}} = \frac{k\eta - \eta^2}{1 + (k-2)\eta} \qquad k = \frac{1.05 E_{cm} \cdot |\varepsilon_{c1}|}{f_{cm}} \qquad \eta = \frac{\varepsilon_c}{\varepsilon_{c1}}$$

$$E_{cm} = 9500 \left(\frac{f_{cm}}{10}\right)^{1/3} \qquad f_{cm} = f_{ck} + 8$$

$$\varepsilon_{c1}(‰) = 0.7 \cdot f_{cm}^{1/3} \leq 2.8 ‰$$

$$\varepsilon_{cu1}(‰) = 2.8 + 14 \cdot (1 - f_{cm}/108)^4 \leq 3.5 ‰$$

σ_c = Compressive stress in concrete

ε_c = Compressive strain in the concrete

ε_{c1} = Compressive strain in the concrete at the peak stress

Figure 3.13 Stress-strain curve of concrete (Adopted from [37])

Compared to steel profiles and reinforcement bars, defining the material model for concrete in ABAQUS [49] is not a straightforward process. Concrete is a quasi-brittle material, and the

compressive strength is different from the tensile strength. To model concrete in ABAQUS [49], the "Concrete Damage Plasticity" (CDP) material model is used [49]. In this model, the compressive and tensile strengths of concrete are modelled separately, and few parameters need to be defined to describe the plastic part, while the elastic part is defined by elastic modulus of concrete set equal to $E_{cm} = 36773\ N/mm^2$ and Poisson's ratio $v = 0.2$. For compressive strength of the plastic part the inputs parameters are summarized in Table 3.1. The dilation angle (Ψ) describes the behaviour of concrete under varying stresses, ranging from 25° for brittle behaviour to 40° for ductile behaviour, with the default value being 36° [49]. The eccentricity (ε) defines the ratio between tensile and compressive strength, which for concrete is 0.1 [49], as the tensile strength is approximately ten times lower than the compressive strength. The ratio between the bi-axial strength and un-axial strength is represented by fb0/fc0, with a default value of 1.16 for concrete [49]. The shape parameter (κ) is related to failure surface, with a value ranging from 0.5 to 1. A value of 0.5 corresponds to the Drucker-Prager model, while a value of 1.0 corresponds to the Rankine formulation [49]. The default value adopted in ABAQUS is 2/3. Finally, the viscosity (μ) is related to the behaviour of the concrete after peak resistance, which is related to its post-failure behaviour. The default value for viscosity is 0 [49].

Table 3.1 Inputs parameters for CDP model

Ψ	ε	fb0/fc0	κ	μ
36	0.1	1.16	0.667	0

On the other hand, the concrete tensile strength can be determined by defining its corresponding fracture energy G_f. In the Eurocode 2 EN 1992-1-1 [34], the fracture energy G_f is not specified. Therefore, the tensile strength is defined according to the *fib* Model Code [1] which is illustrated in Figure 3.14.

The figure shows a graph with Tensile Stress [MPa] on the y-axis and Crack opening w [mm] on the x-axis, with points f_{ctm} and $0.2 f_{ctm}$ marked, G_f = area under stress-crack, $w_1 = G_f / f_{ctm}$ and $w_c = 5 \cdot G_f / f_{ctm}$.

$$G_f = 73 \cdot f_{cm}^{0.18}$$

$$f_{ctm} = 0.3 \cdot f_{ck}^{2/3} \qquad \text{for concrete grade} \leq \text{C50}$$

$$f_{ctm} = 2.12 \cdot \ln(1 + 0.1 \cdot f_{cm}) \qquad \text{for concrete grade} > \text{C50}$$
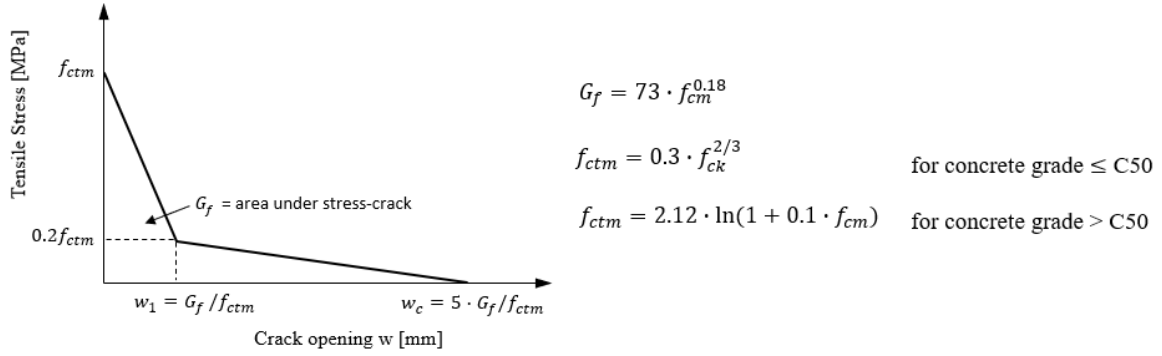
Figure 3.14 CDP model, tensile strength of concrete

3.5.5 Geometry, meshing and element type

In the previous discussion related to FEM, it was emphasized that meshing quality and the simplification of the geometry are crucial factors for accurate FEA results. Concrete is modelled using a solid element (C38DR) with an approximate mesh size of 30 mm, whereas steel profiles are modelled using shell elements (S4R) with the same mesh size. However, steel profiles can also be modelled using solid elements, as the results are practically identical, with only computational time changing. Longitudinal reinforcement bars and stirrups are modelled using 2-node linear beam element (B31) available in ABAQUS [49]. In this study, composite columns of different lengths were investigated, ranging from 1 meter to 15 meters, which significantly increased the element number and computational time. To address this, symmetry was used in modelling, where only half of the composite columns were modelled. Figure 3.15 shows the finite element mesh and element type for the considered CEC column. The selection of the element type and mesh size was an iterative procedure, as the accuracy of the model developed in ABAQUS [49] was benchmarked with experimental test results available from online literature presented in Chapter 4.
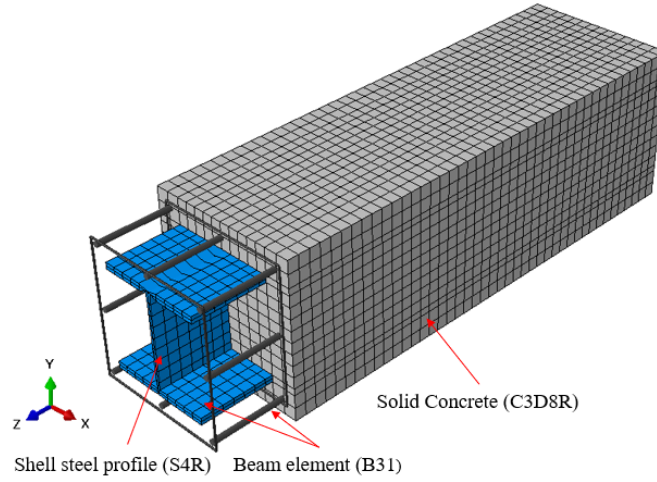
Figure 3.15 CEC column geometry, mesh, and element type

3.5.6 Boundary conditions and interaction

To replicate the theoretical behaviour of a simple supported column, kinematic coupling constrains were used to select boundary conditions. Reference points RP-1 and RP-2 were created at the centre of the cross-section at both ends, as shown in Figure 3.16. The external load is applied at RP-1, where the displacement along the x-axis and y-axis, as well as the rotation about the z-axis ($U_x = U_y = R_z = 0$) are constrained. At RP-2, which corresponds to the midspan of the column due to symmetry in modelling, the displacement along the z-axis is constrained, and the two rotations about the x-axis and y-axis ($U_z = R_x = R_y = 0$).

On the other hand, to define the contact between the concrete and steel profile, the general contact is used available in [49], with the normal behaviour defined as "hard contact", while for the tangential behaviour, "penalty friction" is selected with a friction coefficient $\mu = 0.5$, as recommended by EN 1994-1-1 [2]. The interaction between the concrete and the reinforcement bars/stirrups is defined by embedding reinforcement bars and stirrups into concrete [65].
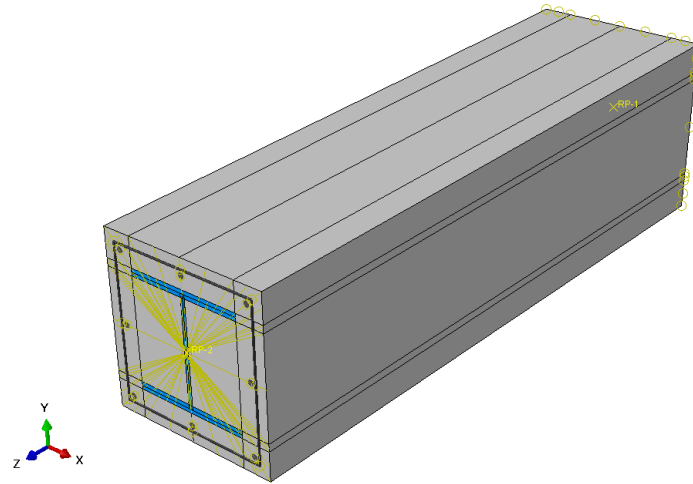
Figure 3.16 Boundary conditions using kinematic coupling constrains

3.5.7 Geometric and material imperfections and solution strategy

To consider the initial geometric imperfection (out-of-straightness) in the composite column, a linear buckling analysis (LBA) is run to get the Eulerian buckling loads (critical load N_{cr}) and the corresponding buckling modes, then the magnitude and the shape of the buckling modes are used for GMNIA model. This is done by editing the Python script of the GMNIA model and by adding these lines:

*IMPERFECTION, FILE= (*LBA), STEP=1
*1, *(e_0/L)

In the (*LBA) should be inserted the name of the LBA file, while in the second row (*1, *(e_0/L)) the required mode shape and the magnitude of the initial geometrical imperfection is inserted. The magnitude of the initial geometric imperfection is L/1000 as it was discussed in Chapter 2.6.

On the other hand, the residual stresses are considered in the model using the initial stress condition [66] available in the predefined field option in a model tree in ABAQUS [49]. Constant stresses are assumed along the numerical model's height [66]. To apply the initial stresses in the model, sets of elements are created along the flanges and the web of the steel profile as presented in Figure 3.17, and the average value of initial stresses was applied in every element. The magnitude and the shape of the residual stresses presented in Figure 3.17 are for hot-rolled and welded sections according to ECCS [29].

Regarding the solution strategy, dynamic explicit is selected to perform the analysis as the GMNIA model is characterised by nonlinearities related to the material, the geometry, as well as and the contact between different types of elements (solid, shell, beam), making the standard static analysis challenging to carry out. In general, dynamic explicit is used for dynamic analysis, but can also be used for quasi-static analysis if the smooth amplitude is used [67] to limit the oscillation and the inertia force is kept small enough so it remains insignificant. In this study, the load was applied using a smooth amplitude displacement at a rate of 10 mm/s and due to the large size of the model, the mass scaling factor was set to 10 to improve the simulation time. The selection of the displacement rate and the mass scaling factor was an iterative procedure, and the accuracy of the selected values were benchmarked with experimental test results available from online literature presented in Chapter 4.
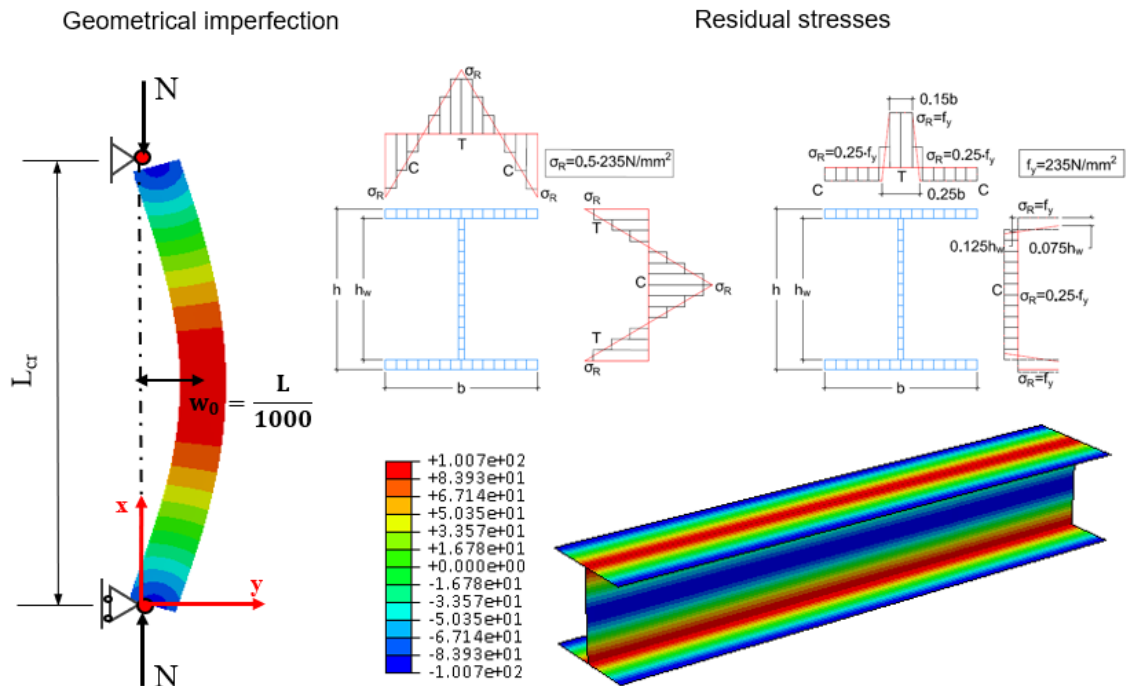
Figure 3.17 Initial geometrical imperfection and residual stresses in ABAQUS

More details about the effect of geometric imperfection and the residual stresses in steel and composite columns are presented in Chapter 2.2.

3.6 GMNIA for composite column in OpenSees

3.6.1 Model description and assumption

Composite columns in steel and concrete under compressive force are characterized by high non-linearities, and these non-linearities are usually related to the material parameter, the geometry, and the contact between elements. Like in most standard finite element software, the modelling procedure starts with creating nodes, elements, and constraints (boundary condition). To create non-linear analysis in OpenSees [53] the modelling is based on so-called distributed plasticity (fibre method) which allows the plasticity to be spread, so the yielding can occur at any part of the element [68] as it is shown in Figure 3.18.
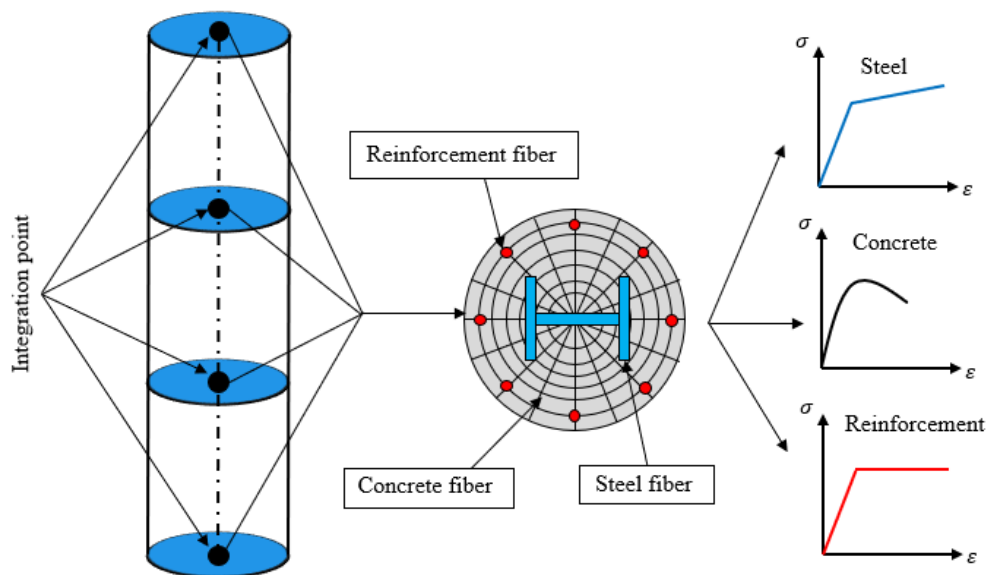
Figure 3.18 Distributed plasticity model for composite columns in steel and concrete

To use the fiber method for composite column the following assumptions are made:

- Section remains plane after deformation (Bernoulli-Euler assumption),
- non-linear stress-strain material law for reinforced concrete and steel,
- full interaction between the steel and concrete,
- the geometric imperfection and residual stresses are considered,
- the confinement effect in concrete is considered,
- the tensile strength is considered for concrete.

3.6.2 Material model for steel and concrete

Regarding the materials, there are several material models in OpenSees [53] library. For structural steel and reinforcement bars, the uniaxial Giuffre-Menegotto-Pinto stress-strain material with isotropic strain hardening is used [53]. The material is defined by providing, the initial elastic modulus E, the yield strength f_y and the strain hardening ratio b as it is shown in Figure 3.19 (left side).

For concrete, two material models are used, the normal uniaxial Popovics concrete material with tensile strength, and the confined concrete for the concrete inside the stirrups cage [53]. Normal concrete is defined by providing the initial elastic modulus E_s, the concrete compressive strength at 28 days f_c, the concrete tensile strength at 28 days f_t, the concrete strain at maximum strength ε_c, and the concrete strain at ultimate strength ε_{cu}, while for confined concrete additional parameters related to (confined effect) are defined. More details can be found about modelling of the materials can be found in [53].
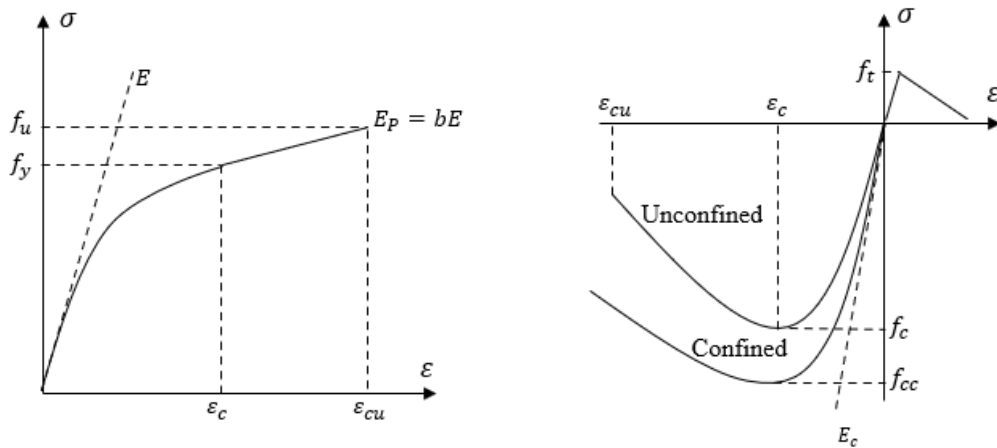
Figure 3.19 Stress-strain material law for steel (left side) and concrete (right side) in OpenSees

3.6.3 Geometrical imperfection and residual stresses

Geometric imperfection is considered by "shifting" the nodes from the original position following the half-sinusoidal shape with maximum amplitude at the mid-length [69] as shown in Figure 3.20, while, the residual stress on the steel profile was considered using the initial stress condition command available in OpenSees [53], applying average stresses along the

normal direction on the of plane of web and flanges similar as in ABAQUS [49]. Constant stresses are assumed along the numerical model.
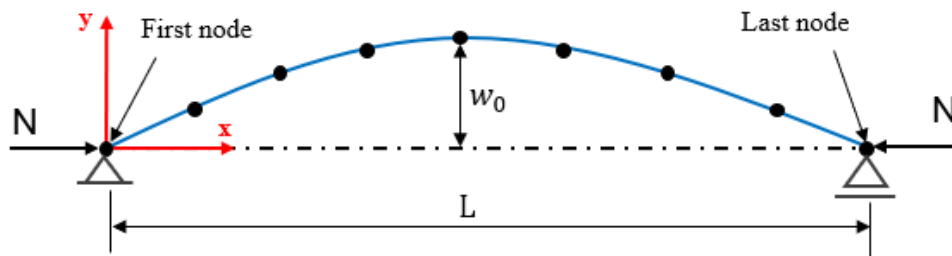
Figure 3.20 Initial bow imperfection (adopted from [69]*)*

3.7 Chapter summary

The methodology and software employed in this dissertation are addressed in this chapter. Regarding the methodology, the theoretical background related to the Finite Element Method (FEM), the Stochastic Finite Element Method, sampling methods and sensitivity analysis are provided.

General information about Finite Element Method (FEM), Stochastic Finite Element Method (SFEM) and the software used to perform these types of analysis for composite columns in steel and concrete are presented Section 3.1 and Section 3.2, following with Section 3.3 dedicated to sampling methods where two sampling methods called Monte Carlo Simulation (MCS) and Latin Hypercube Sampling (LHS) are presented and discussed. Sensitivity analysis is covered in Section 3.4 where the Sobol's indices method [10] is given and its implementation for composite columns is thoroughly explained. In Section 3.5 and Section 3.6 are presented a detailed explanation of the modelling process for executing geometric and material nonlinear analysis with imperfections (GMNIA) for composite columns in ABAQUS/CAE [49] and OpenSees [53].

Chapter 4

Benchmarking of the FEA with experimental test results

In this sub-chapter, the results of Finite Element Analysis (FEA) are benchmarked with experimental test results from existing online literature. To check the reliability of the FEA in ABAQUS [49], experimental test results performed in different types of composite columns from different sources are considered. Based on the composite column type, three groups of experimental test data are used for benchmarking. The first group is comprised of Concrete Encased Composite (CEC) columns tested at Ruhr-Universität Bochum reported in [26] and reinforced concrete columns with massive steel core tested in Slovak University of Technology, Slovakia reported in [70] and [71]. The second group is comprised of Concrete Filled Steel Tubes (CFST) columns tested at the University of Technology Göteborg, Sweden reported in [72], and Concrete Filled Steel Box (CFSB) columns tested by [73] and reported in [74]. The third group is comprised of Concrete Filled Steel Tubes (CFST) with inner steel core tested at Bergische Universität Wuppertal reported in [30].

4.1 Concrete encased composite (CEC) columns

The experimental campaign was funded by ArcelorMittal, carried out at Ruhr-Universität Bochum in collaboration with the University of Luxembourg and the University of Kaiserslautern, while the experiments results were presented by T. Bogdan et.al [26]. In total, nine concrete-encased composite columns were tested, from which five had circular cross-sections and four with rectangular cross-sections as presented in Figure 4.1. All composite columns were composed of high-strength concrete with compressive strength varying between C50 and C100. The steel profile was HEB 160 with yield strength of $f_y = 523\ MPa.$ The column length was $L_{eff} = 6.340\ m$ for all the specimens [26]. The columns were subjected to initial geometric imperfection, and eccentricity in both directions (y-y) and

(z-z), as it is shown in Figure 4.1. More details about the eccentricity in two directions and initial geometrical imperfection are presented in [26]. Table 4.1 and

Table 4.2 summarize the configuration details of the circular and rectangular specimens. The testing procedure was based on EN 1994-1-1 [2], and all the columns were oriented to buckle around the strong axis (y-y) except specimen A1.1 which buckle about the weak axis [26]. Moreover, in [26] it is reported that the numerical analysis is conducted in ABAQUS, and the concrete is modelled using the CDP model with a modification of the strains limit in order to capture the correct post-peak behaviour of the experimental results, and the model is calibrated here using the same stress-strain curve that is presented in [26].
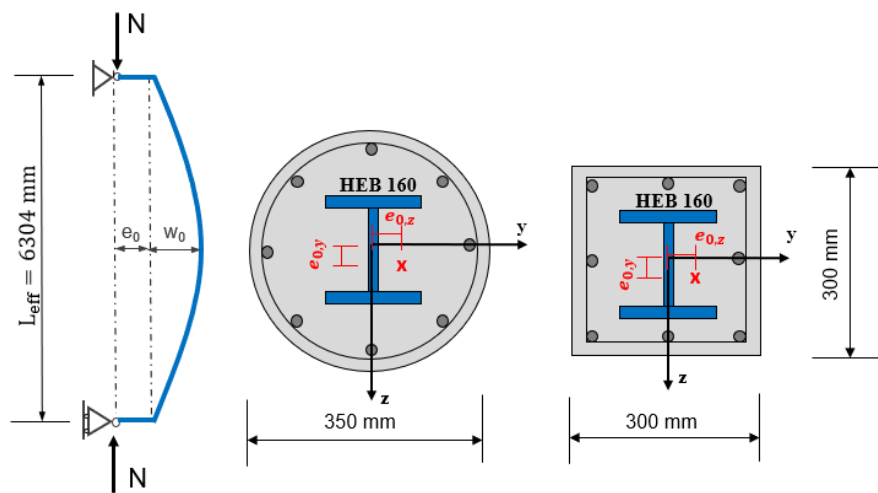
Figure 4.1 Considered composite columns (adopted from [26]*)*

Table 4.1 Circular CEC columns (adopted from [26]*)*

Specimen	Steel profile		Concrete		Long. rebars	Trans. rebars
	HEB 160		Ø 350 mm		-	-
	E_s	f_y	E_{cm}	f_{cyl}	Diameter	Diameter
	[N/mm^2]	[N/mm^2]	[N/mm^2]	[N/mm^2]	[mm]	[mm]
A1.1			36229	90.9	8 Ø 16	Ø 10 / 75
A1.2			37008	86.3	8 Ø 16	Ø 10 / 75
A1.3	210 000	523	35115	88.0	8 Ø 16	Ø 10 / 75
A1.4			33477	59.5	8 Ø 20	Ø 8 / 100
A1.5			36296	98.9	12 Ø 20	Ø 8 / 100

Table 4.2 Rectangular CEC columns (adopted from [26])

Specimen	Steel profile		Concrete		Long. rebars	Trans. rebars
	HEB 160		300 x 300 mm		-	-
	E_s	f_y	E_{cm}	f_{cyl}	Diameter	Diameter
	[N/mm^2]	[N/mm^2]	[N/mm^2]	[N/mm^2]	[mm]	[mm]
B1.1			36986	91.4	8 Ø 16	Ø 10 / 75
B1.2			34550	89.1	8 Ø 16	Ø 10 / 75
B1.3	210 000	523	38171	105.3	8 Ø 20	Ø 8 / 100
B1.4			35161	94.8	12 Ø 20	Ø 8 / 100

Figure 4.2 shows the comparison between FEA in ABAQUS and the experimental test results in terms of the load-displacement curve for two columns, A1.1 (circular) and B1.1 (rectangular), while Table 4.3 presents the results summary of all tested columns and the corresponding FE analyses.

The load-displacement curves of columns A1.1 and B1.1 show a good agreement between experimental results and FEA in both ascending and descending branches, as the behaviour of the composite columns was replicated in a correct way in ABAQUS model developed here. However, according to results presented in Table 4.3, the numerical models are able to correctly predict the maximum resistance as the difference between FEA and experimental results is less than 3% in all considered columns, while in terms of maximum displacement at the midspan, the difference exceeds 10% in some cases. This can be due to the complexity of the geometric imperfection that may result by different bow imperfection of steel, concrete and reinforcement, offset of steel profile and reinforcement tolerance. All these data cannot be measured for a CEC column and is simplified by taking on uniformed bow imperfection. Nevertheless, the FEA presented in [26] showed a similar difference in terms of maximum displacement at the midspan.
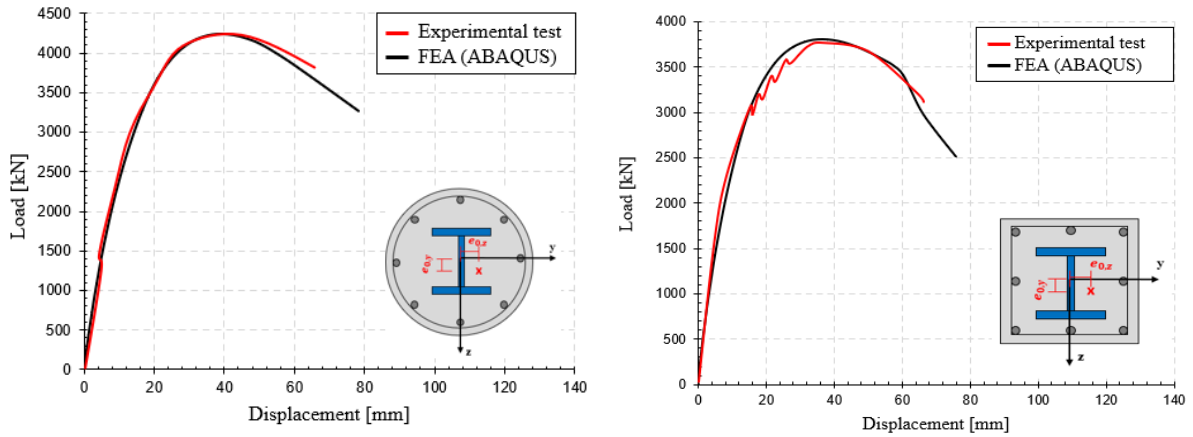
Figure 4.2 Load-displacement curve for A1.1 and B1.1 CEC columns

Table 4.3 Comparison of maximum force and displacement

| Specimen | Exp. Results | | FEA results | | Ratio |
| | N_{max} | w_{Nmax} | N_{max} | w_{Nmax} | N_{max} |
	[kN]	[mm]	[kN]	[mm]	[%]
A1.1	4224	40	4246	40	99%
A1.2	3669	59	3575	45	103%
A1.3	3395	68	3389	54	100%
A1.4	2979	58	3012	71	99%
A1.5	3665	73	3690	86	99%
B1.1	3721	37	3804	37	98%
B1.2	4341	23	4451	28	98%
B1.3	5529	33	5698	44	97%
B1.4	4689	50	4702	45	100%

Regarding the reinforced concrete columns with massive inner core, the authors J. Frólo and Š. Gramblicka tested six composite columns at the Slovak University of Technology reported in [70] and [71]. Three columns were simply supported with the length $L = 3000\ mm$ and three with $L = 3850\ mm$. In all considered cases, the composite columns were subjected to compressive force with initial eccentricity $e_0 = 20\ mm$ as presented in Figure 4.3. Moreover, also the initial bow imperfection was measured before testing as it is shown in Table 4.4. The concrete used in the experimental campaign was high-strength concrete with $f_{cyl} = 63.9\ N/mm^2$, while the massive inner steel cores had yield strength of $f_{y,core} =$

327.3 N/mm^2, and the reinforcement bars had yield strength of $f_{y,s} = 548.7 \; N/mm^2$. The geometry of the cross-section and the boundary conditions are presented in Figure 4.3.
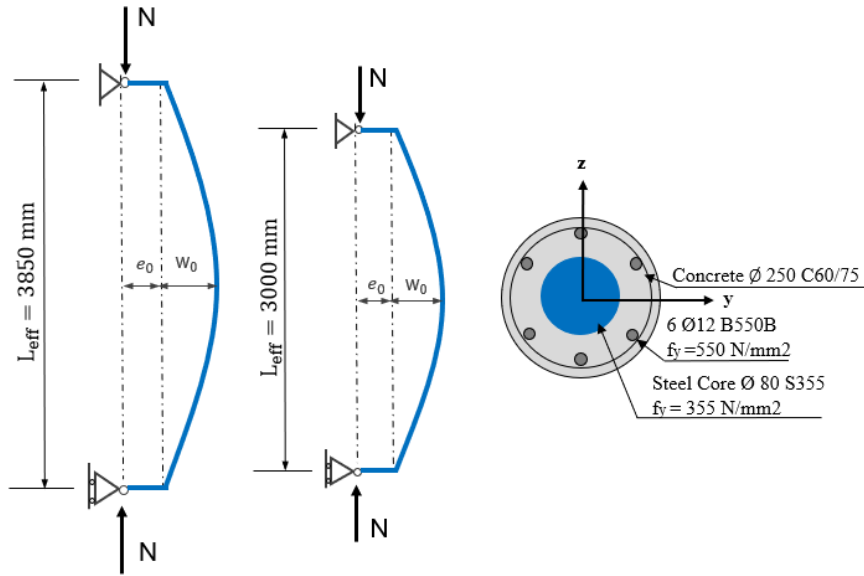
Figure 4.3 Cross-section geometry and boundary conditions

Table 4.4 Measured initial imperfection and eccentricity (adopted from [70])

Series	Length	Imperfection	Eccentricity
	L [m]	w_0 [mm]	e_0 [mm]
S1.1	3.85	1.09	20
S1.2	3.85	0.15	20
S1.3	3.85	2.51	20
S2.2	3.00	1.04	20
S2.3	3.00	0.99	20

Table 4.5 presents the ultimate loads obtained by testing and FEA in ABAQUS. As the results indicate, there is a good agreement between ultimate loads obtained by experimental campagna and finite element analysis, except for specimen S1.2 where the difference is 5%. However, this difference can be due to difficulty to measure the initial bow imperfection of concrete and steel core during experimental testing, as the difference between the maximum load recorded of specimen S1.1 and S1.2 is less than 1% while the reported measured imperfection in S1.2 is much smaller compared to S1.1.

Table 4.5 Comparison between ultimate load from experimental tests and FEA

Series	Length	Imp.	Ecc.	Test results	FEA	Test / FEA
	L [m]	w_0 [mm]	e_0 [mm]	N_{max} [kN]	N_{max} [kN]	[-]
S1.1	3.85	1.09	20	1829	1855	0.99
S1.2	3.85	0.15	20	1811	1899	0.95
S1.3	3.85	2.51	20	1777	1789	0.99
S2.2	3.00	1.04	20	2294	2324	0.99
S2.3	3.00	0.99	20	2292	2327	0.98

Figure 4.4 shows the load-displacement curve of the column S2.3 from the test campaign reported in [70] and [71], and the recalculation with FEA in ABAQUS in this study. As the results indicate, there is a good agreement between test results and Finite Element Analysis.
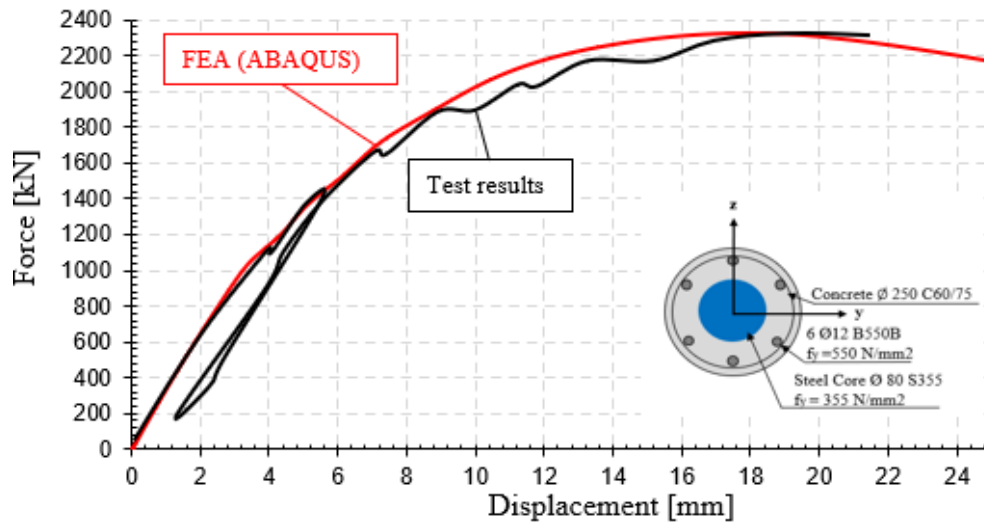
Figure 4.4 Load-displacement curve (adopted from [70]*)*

4.2 Concrete filled steel tube (CFST) and filled box (CFSB) column

In the second group, the FE analyses are benchmarked with Concrete Filled Steel Tube (CFST) reported in [72] and Concrete Filled Steel Box (CFBS) reported in [74] and [75].

In [72] eleven columns are reported, of which, nine were CFST columns while 2 were without concrete. All the tested columns were hinged at both ends to replicate the simple supported boundary conditions with a length of 2500 mm and subjected to compressive force with load eccentricity of $e_0 = 10 \ mm$, which was applied on concrete section (three specimens), steel

section (three specimens) and on the entire section (three specimens) as it is presented in Figure 4.5.
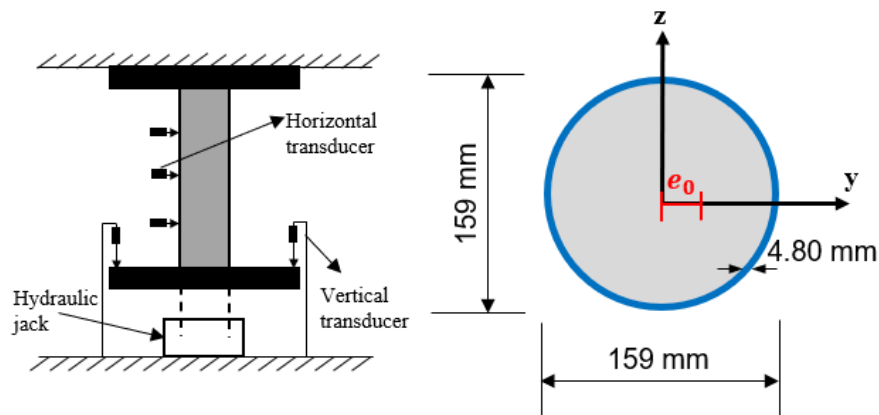
Figure 4.5 Geometry and test setup (adopted from [75]*)*

To validate the FEA analysis, only the CFST columns with compressive force applied on the entire section were investigated. Table 4.6 presents the material parameters for concrete and steel used in the testing campaign reported in [72].

Table 4.6 Concrete and steel material properties (adopted from [75]*)*

$f_{c,cube}$	$f_{c,cyl}$	E_0	E_c	G_F	f_y	f_u	E_a	ε_{sh}	ε_{au}
[MPa]	[MPa]	[GPa]	[GPa]	[N/m]	[MPa]	[MPa]	[GPa]	[‰]	[‰]
79.4	64.5	39.5	38.5	157	433	568	206	29	136

Table 4.7 presents the comparison of maximum load resistance obtained from the test and FE analysis while Figure 4.6 shows the load-displacement curve obtained from the testing campaign and FE analyses presented in [72] and FEA analyses performed in this study.
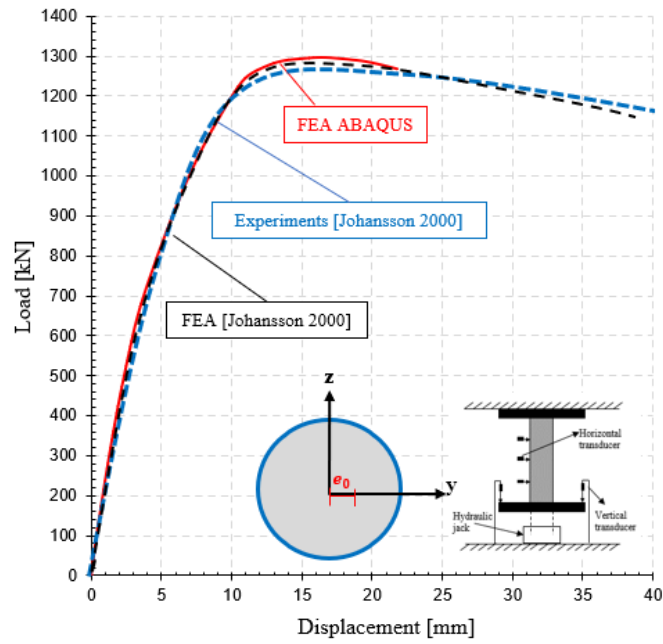
Figure 4.6 Comparison of load-displacement curve for CFST column

The dashed blue line represents the mean value from three experimental testing results, the dashed black line represents the results from FEA reported in [72] and the red line represents the results from FEA conducted in this study. The results indicated that there is a good agreement between FEA and the testing results with a difference between test and FE of 5%, while the difference between FE analyses was less than 1%. Moreover, the load-displacement curve in FEA fits almost perfectly in both, the ascending and descending branch.

Table 4.7 Comparison of maximum load resistance obtained from testing and FE analysis

Load application	P_{max} [kN]		P_{max} [kN]	Ratio	Ratio
	Test	FEA	ABAQUS	ABAQUS/TEST	FEA/ABAQUS
Entire	1230	1290	1295	1.05	1.00

Regarding the concrete-filled steel box CFBS columns, the experimental campaign was conducted by Bridge [73] and reported in [75]. Eight simply supported composite columns subjected to eccentric compressive force were tested. Figure 4.7 shows the geometry and the material properties used for one of the test specimens called (SHC-1) adopted from [75].
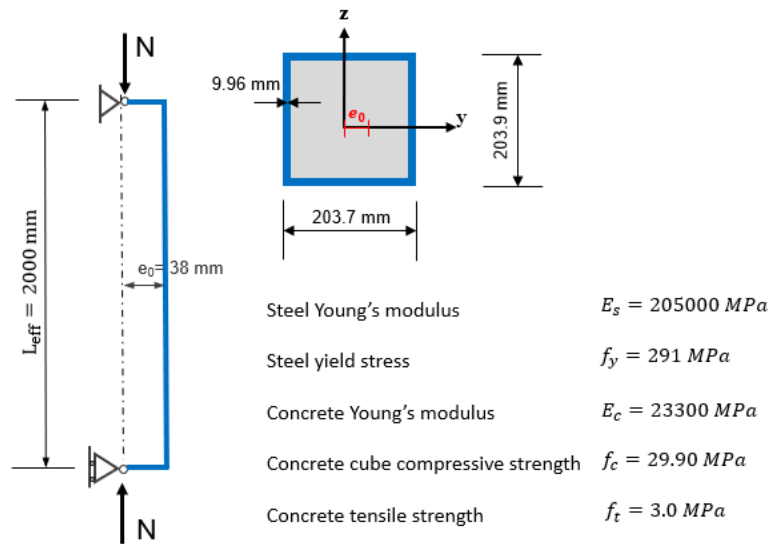
Figure 4.7 Concrete fillet steel box (CFSB) tested by Bridge (1976) (adopted from[75])

Figure 4.8 shows the comparison between the load-displacement curve obtained from the experimental campaign for one specimen and FEA in ABAQUS. The result shows that the FEA model in ABAQUS correctly predicts the behaviour of the concrete-filled steel box, in both ascending and descending branches.
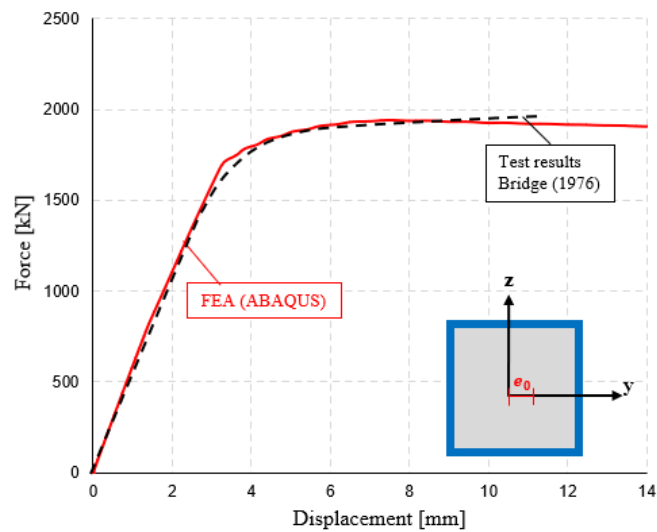
Figure 4.8 Comparison of load-displacement curve for CFSB column

4.3 CFST columns with inner steel core

In the third group, the FEA is benchmarked with Concrete Filled Steel Tubes (CFST) with inner steel core tested at Bergische Universität Wuppertal reported in [30]. As reported in [30], twelve columns were tested, from which six were CFST with an inner massive steel core. The composite columns were simply supported and subjected to eccentric compressive force. The effective length of all considered columns was the same $L_{eff} = 3792\ mm$. The geometry and material properties are presented in Table 4.8 and Figure 4.9 adopted from [30]. Regarding the residual stresses in massive steel core, in [30] it is reported the approximate value of residual stresses that are determined using time-dependent temperature simulation. In this study the residual stresses as well as geometric imperfections are considered in FE analysis as presented in sub-chapter 3.5.7

Table 4.8 Material parameters for steel and concrete

Test	Core [N/mm²] f_y	Tube [N/mm²] f_y	Concrete [N/mm²] f_{cyl}
C2	411	447	95
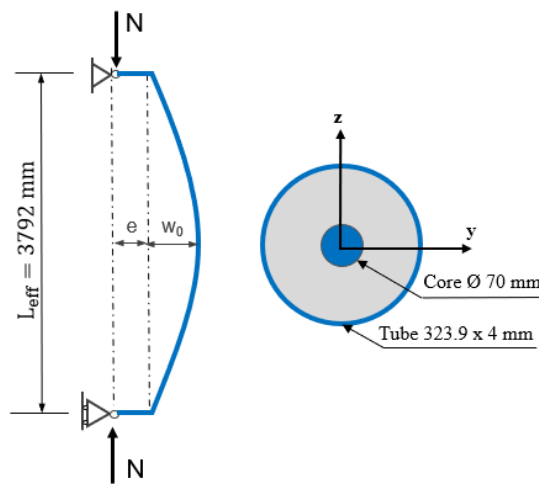
Figure 4.9 Cross-section geometry and boundary conditions

Table 4.9 presents the results summary of all tested columns and the corresponding FE analyses, while Figure 4.10 shows the load-displacement curve of experimental testing and

the recalculation with FEA in ABAQUS. Experimental results are shown with dashed lines while the FEA analyses with continuous lines. As the results indicate, there is a good agreement between test results and FEA in the ascending branches until the maximum resistances are reached. However, in FEA once the maximum resistance is reached, a drop in resistance is observed, contrary to experimental testing results, and this can be due to the assumption adopted for the CDP model. Nevertheless, the post-buckling behaviour of the composite columns is not investigated in this study but rather the ultimate load and the corresponding displacement.
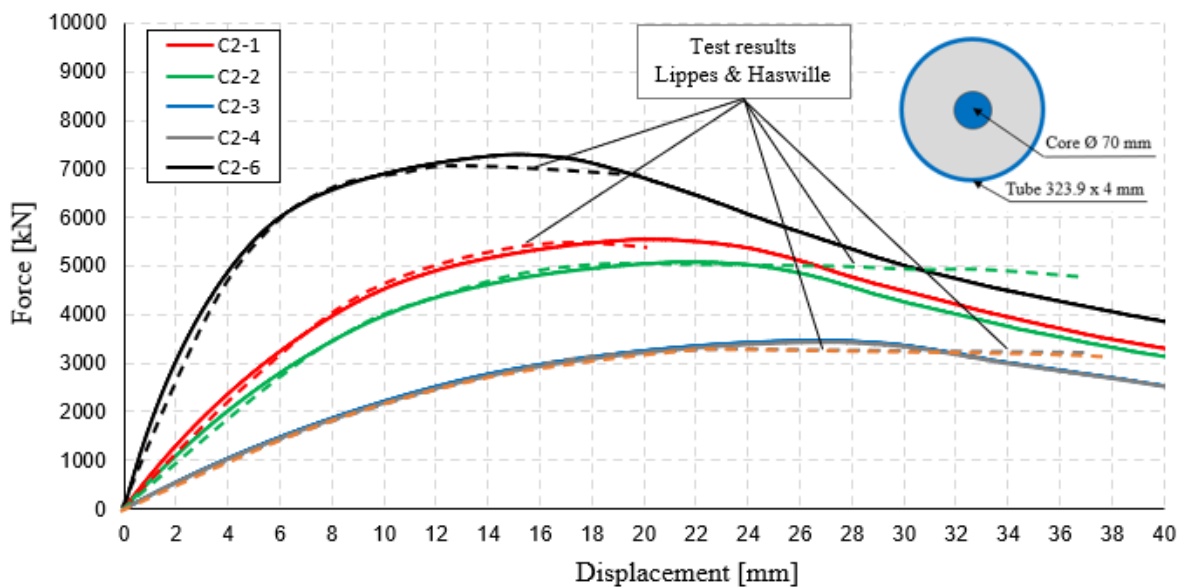
Figure 4.10 Comparison of the load-displacement curve for CFST columns with inner steel core

Table 4.9 Comparison of load-displacement curve for CFST with inner steel core

Test	Experimental tests				ABAQUS			Test / FEA	
	Ecc.	F_u	u_x (Fu)	$e_{x,u}$	F_u	u_x (Fu)	$e_{x,u}$	F_u	$e_{x,u}$
	[mm]	[kN]	[mm]	[mm]	[kN]	[mm]	[mm]	[%]	
C2-1	30	5560	16	46	5544	20	50	100%	92%
C2-2	37	5322	16	53	5077	22	59	105%	91%
C2-3	70	3392	24	94	3469	27	97	98%	96%
C2-4	71	3277	23	94	3431	27	98	96%	96%
C2-6	12	7359	15	27	7291	16	28	101%	95%

Chapter 5

Benchmarking of the OpenSees with ABAQUS

5.1 Benchmark of the results

To ensure that the self-developed model in OpenSeesPy [50] provides reliable numerical calculation, the results from Geometric and Material Non-linear Analysis with Imperfection (GMNIA) in OpenSeesPy [50] model are validated with a 3D model in ABAQUS [49] for different types of composite columns. In the experimental test results presented in Chapter 4, in most of the cases the composite columns were subjected biaxial bending due to load eccentricity in two directions, which could not be taken into consideration in OpenSeesPy [50], since the model only works with eccentricity in one direction. The matter is resolved by calibrating the ABAQUS [49] model with experimental test data, as discussed in Chapter 4, and then, validating the OpenSeesPy [50] model with ABAQUS [49] model.

The considered columns cross-sections are presented in Figure 5.1 named: Concrete Encased Composite (CEC) column, Partial Concrete Encased Composite (PCEC) column and Concrete Filled Steel Tubes (CFST) with inner steel profile and massive steel core. The boundary conditions are selected to simulate an idealized simple supported column. The composite columns are subjected to concentrated axial force inducing flexural buckling about the weak axis (z-z). Initial geometric imperfection is $w_0 = L/1000$, while residual stresses are based on steel grade S235 according to ECCS [29]. Because in this study the composite columns are investigated for different lengths to cover all the relative slenderness between $0.2 \leq \bar{\lambda} \leq 2.0$, the results of GMNIA in OpenSeesPy [50] and ABAQUS [49] are compared in terms of the load-displacement curve for one length and, as a function of columns slenderness presented in non-dimensional form using reduction factor χ and relative slenderness $\bar{\lambda}$. The resistance of the composite columns is calculated according to the general method with the overall (safety) factor γ_0 based on plastic resistance.
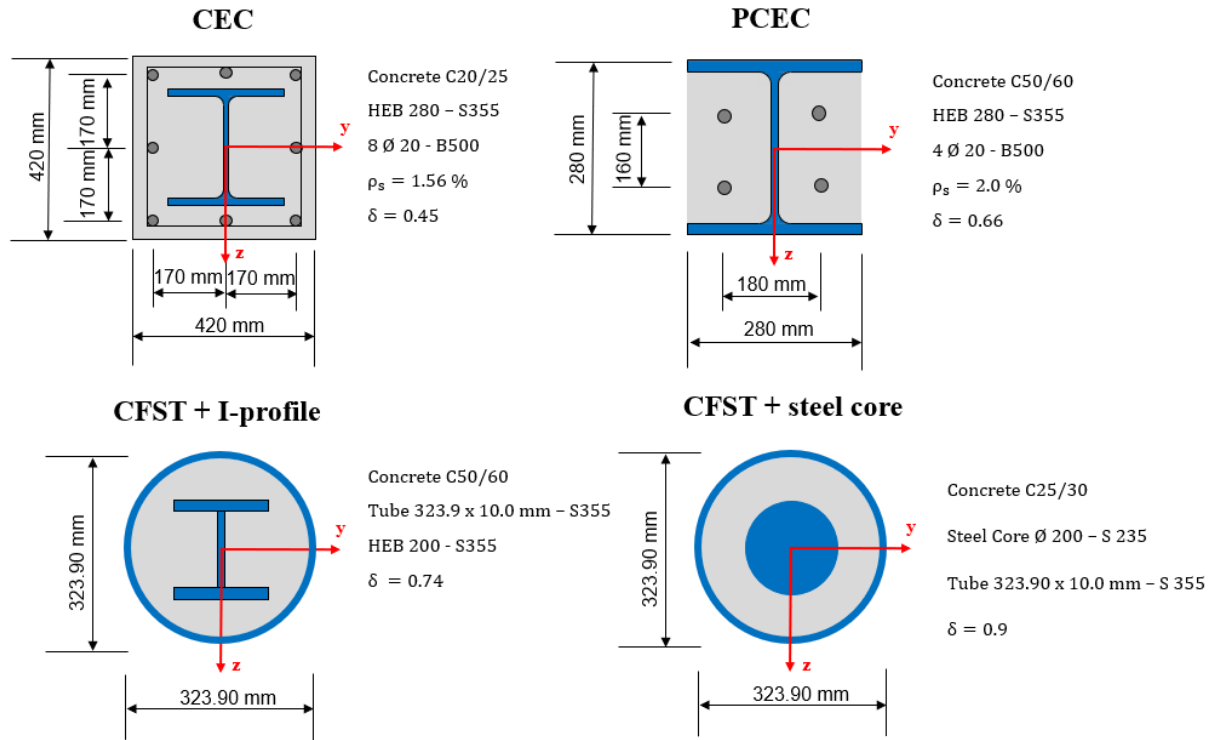
Figure 5.1 Considered columns for benchmarking OpenSeesPy [50] *results with ABAQUS* [49]

Figure 5.2 and Figure 5.3 show the comparison of OpenSeesPy [50] results with ABAQUS [49] for CEC and PCEC columns, while Figure 5.4 and Figure 5.5 show the comparison for CFST columns with inner steel profile and massive steel core.
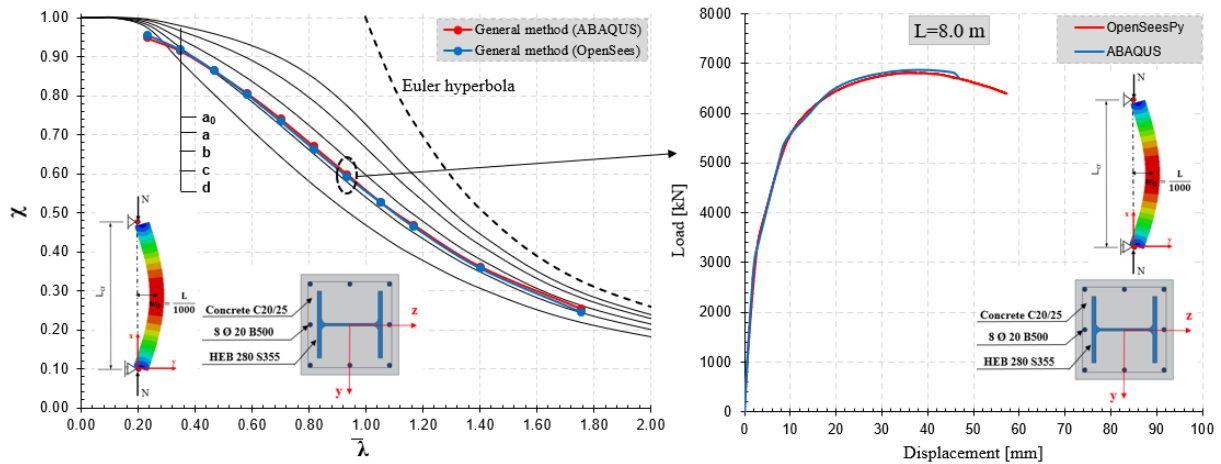
Figure 5.2 Comparison of the results from OpenSeesPy and ABAQUS for CEC column
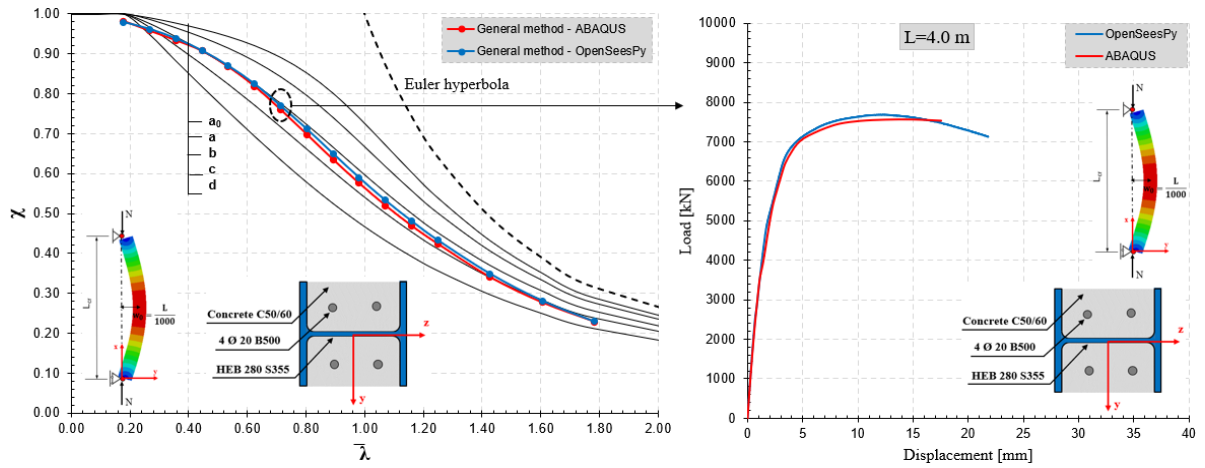
Figure 5.3 Comparison of the results from OpenSeesPy and ABAQUS for PCEC column
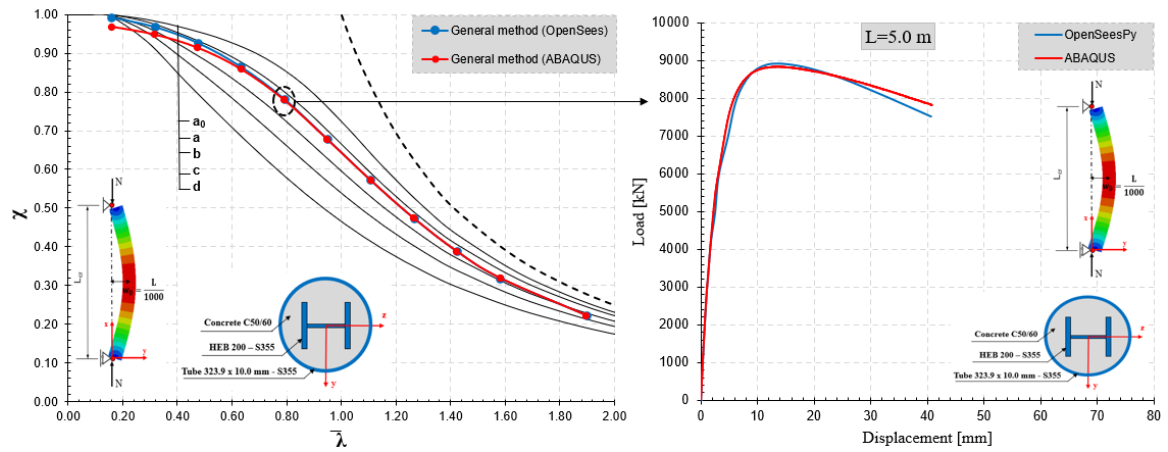
Figure 5.4 Comparison of the results from OpenSeesPy and ABAQUS for CFST column with inner steel profile
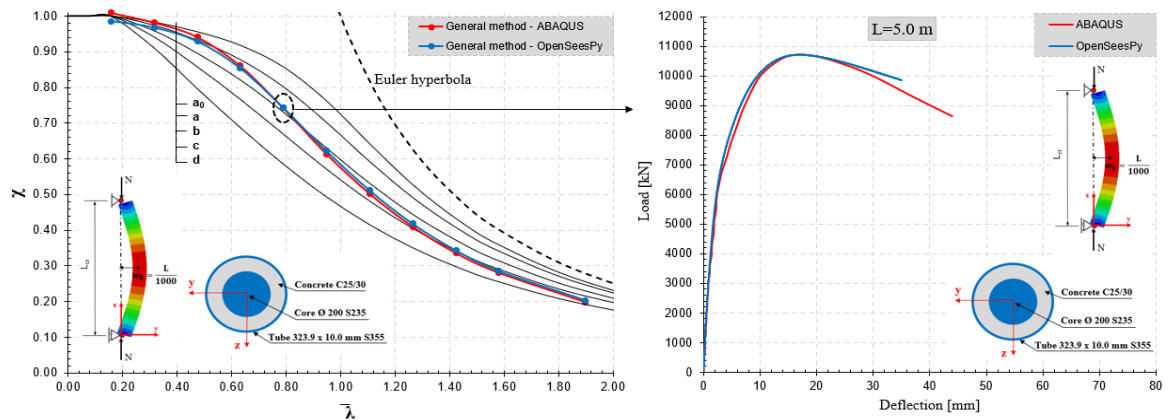
Figure 5.5 Comparison of the results from OpenSeesPy and ABAQUS for CFST column with inner massive steel core

The results from non-linear incremental finite element analysis (GMNIA) show that there is a good agreement between the OpenSeesPy [50] model developed in Python scripting language and the 3D ABAQUS model, as the difference in the resistance is less than 3% in all considered columns. The load-displacement curves presented for different types of composite columns show that the OpenSeesPy [50] model is capable of correctly describe the behaviour of the composite column under concentrated axial force in the ascending branch until the maximum resistance is reached, as well as in the descending branch.

Chapter 6

The effect of initial imperfections – benchmark cases

6.1 Column with steel section

To investigate the influence of initial geometric imperfection and the residual stresses on the stability problem, two steel columns are considered, a hot-rolled HEB 280 steel section with steel class S355, and a welded I-section with steel class S355. Both sections are in class 1 according to EN 1993-1-1 [16], and are subjected to centric compressive axial load, while the boundary conditions are selected to simulate simply supported columns as shown in Figure 6.1. Initial geometric imperfection is $w_0 = L/1000$, while residual stresses are based on steel grade S235 according to ECCS [29] presented in Figure 2.13. The analyses were performed by varying the length of the column to cover all the relative slenderness between $0.2 \leq \bar{\lambda} \leq 3.0$. In this study, the non-linear analyses (GMNIA) are performed in ABAQUS [49] using nominal strength values, and following the modelling procedure presented in Chapter 3.5.
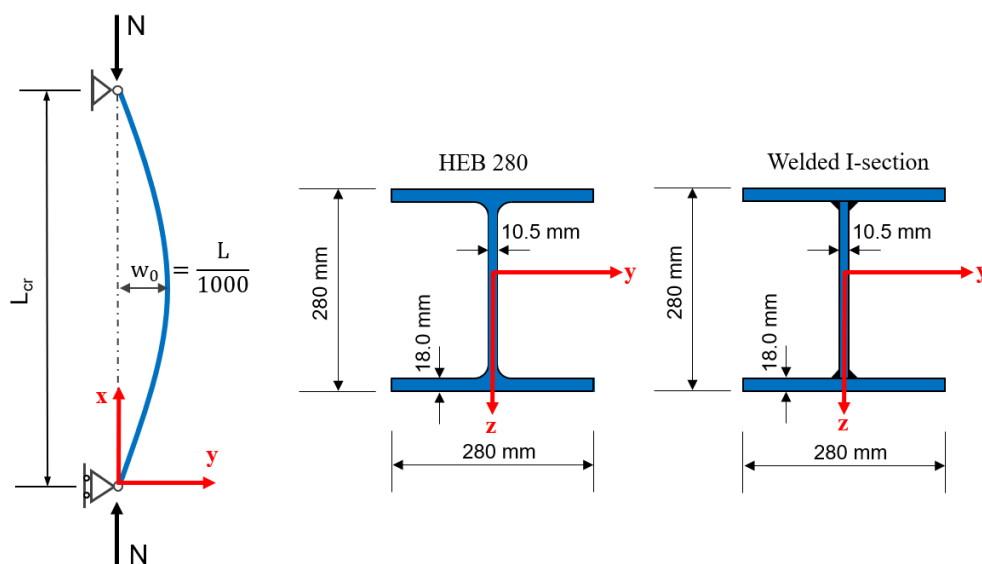
Figure 6.1 Geometry and boundary conditions of steel columns

Figure 6.2 shows the results as a function of columns slenderness presented in non-dimensional form using reduction factor χ and relative slenderness $\bar{\lambda}$ defined according to EN

1993-1-1 [16] for the verification of the members subjected to compressive force and presented also in sub-chapter 2.1.3. The continuous lines show the so-called European buckling curves (a₀, a, b, c, d), the dashed line represents the theoretical critical load or Euler hyperbola, while the results of non-linear finite element analyses with initial imperfections (GMNIA) are shown with blue and red circles. The blue circles show the results of analyses with only initial geometric imperfection $w_0 = L/1000$, while the red circles show the results of analyses with initial geometric imperfection and residual stresses.
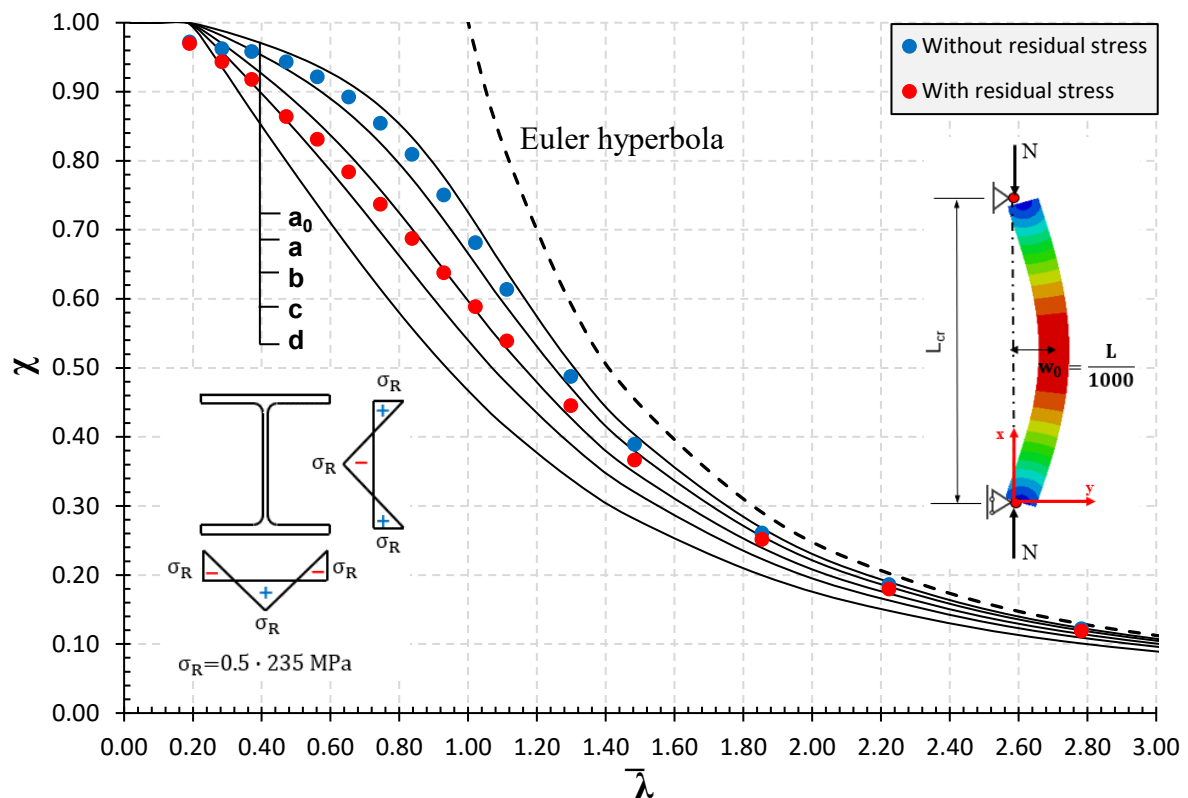
Figure 6.2 Hot-rolled section buckling about weak axis z-z

First, it should be noted that, the resistance of the steel column with $\bar{\lambda} = 0.2$ calculated based on GMNIA does not reach the European buckling curve plateau. As reported in [22], the authors (Young [76] and Dwight [77]) proposed a plateau for slenderness $\bar{\lambda} \leq 0.2$ following the so-called "Ayrton-Perry" formulation as they though that the stocky columns can reach or even exceed the so-called "squash load" due to the effect of strain-hardening [77]. However, as it is reported in [22], but also in the present dissertation, the plateau value

cannot be proven by GMNIA even if the strain-hardening are included in the model, as the values calculated from GMNIA with strain-hardening included in the model are below the plateau.

The results indicate that the effect of the residual stresses on the load-bearing capacity of the steel column subjected to compression load is significant and cannot be neglected. Moreover, the effect of residual stresses is highly correlated with the slenderness of the column, as the effect is more significant for columns with an intermediate slenderness ratio ($0.3 \leq \overline{\lambda} \leq 1.2$) compared to columns with low and very high slenderness. This is understandable since short columns maintain their yield strength regardless the effect of the residual stresses, while very long columns are not influenced by the yielding as the ultimate load resistance is close to the critical buckling load. This can be observed also from the load-displacement curve of the HEB 280 column with a 5-meter length (intermediate slenderness) presented in Figure 6.3. The continuous blue line shows the load-displacement curve when only the initial geometric imperfection is considered, while the continuous red line shows the load-displacement curve with additional residual stresses impact. The results show an approximate 15% reduction of the load-bearing capacity due to residual stresses. Moreover, on the right side of Figure 6.3 are presented the stresses along the longitudinal direction during both analyses with and without residual stresses consideration. The first two figures on top are the stresses without initial residual stresses, while the two bottom ones are when also initial residual stresses are considered. The results of stress propagation show that in the flanges the yielding starts from the sides and is continuous toward the centre, while in the web, the yielding starts from the centre and is continuous toward the intersections between the web and flanges, and the presence of the residual stresses causes premature yielding of the flanges and the web, inducing inelastic buckling of the column.
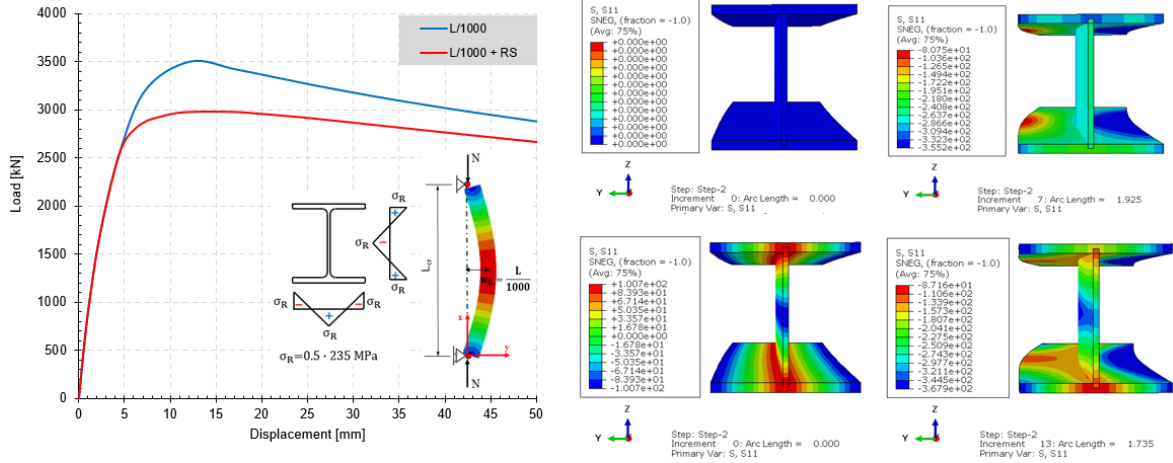
Figure 6.3 Load-displacement and stresses in longitudinal direction (σ_{11}) with initial geometric imperfection and with or without residual stresses for hot-rolled section HEB280

In the same way are presented also the results for welded I-section in Figure 6.4 and Figure 6.5. As in the case of the hot-rolled section, the resistance of the steel column with $\bar{\lambda} = 0.2$ calculated based on GMNIA does not reach the European buckling curve plateau. Regarding the effect of residual stresses, there is a correlation with the slenderness of the column, as the effect is more significant for columns with intermediate slenderness ratio ($0.3 \leq \bar{\lambda} \leq 1.0$) compared to columns with low and very high slenderness. Moreover, in case of the welded section for intermediate slenderness between ($0.4 \leq \bar{\lambda} \leq 0.8$) a greater reduction is observed compared to the hot-rolling section even though the magnitude of the initial residual stresses is the same $\sigma_R = 235 \, MPa$. This is because, for welded sections a larger portion of the web and flanges contains compressive residual stresses [78]. However, as the slenderness is increased, the impact of the residual stresses is similar (slightly lower) with the hot-rolled section as shown from the load-displacement curve of the 5-meter column presented in Figure 6.5, where an approximate 12% reduction of the load-bearing capacity is observed due to residual stresses effect.
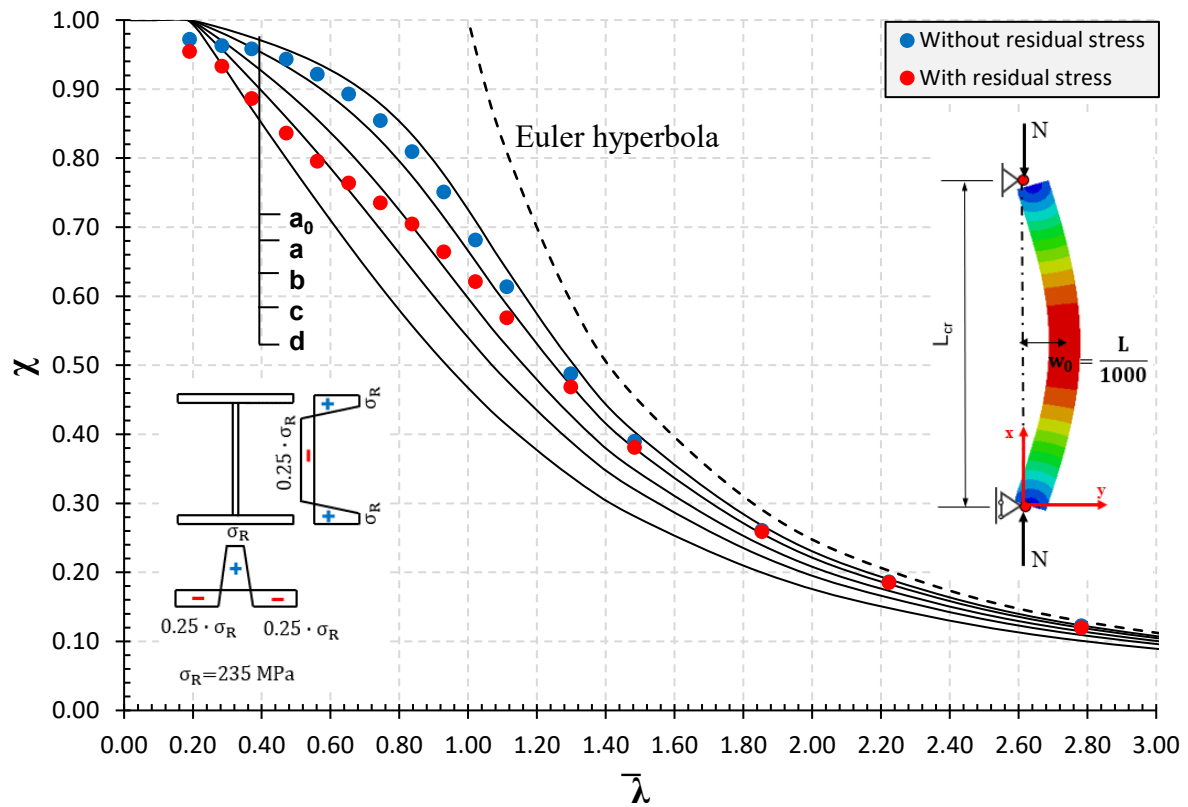
Figure 6.4 Welded section buckling about the weak axis z-z
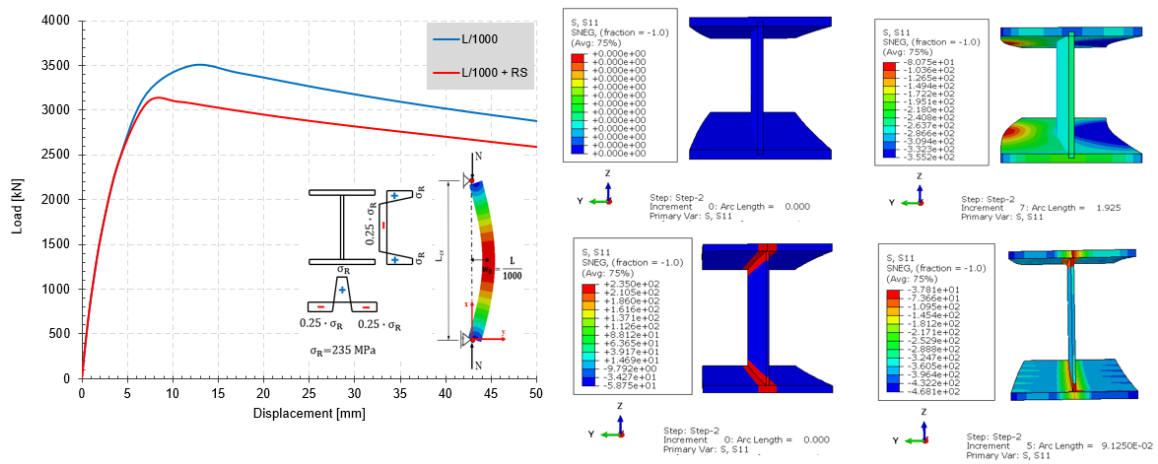
Figure 6.5 Load-displacement and stresses in longitudinal direction (σ_{11}) with initial geometric imperfection and with or without residual stresses for welded I-section

6.2 Partial concrete encased composite column (PCEC)

Figure 6.6 shows the geometry, material parameters, and boundary conditions used to investigate the effect of initial geometric imperfection and residual stresses on Partial Concrete Encased Composite (PCEC) columns. For the sake of simplicity and comparison with steel columns, the same steel profiles HEB 280 and welded I-section are considered also for the PCEC column. The concrete class is C50/60, and the reinforcement bars considered are $\varnothing 20 \ mm$ with yield strength $f_{sk} = 500 \ N/mm^2$. The analyses were performed by varying the length of the column to cover the relative slenderness between $0.2 \leq \bar{\lambda} \leq 2.0$ as it is presented in Table 6.1.
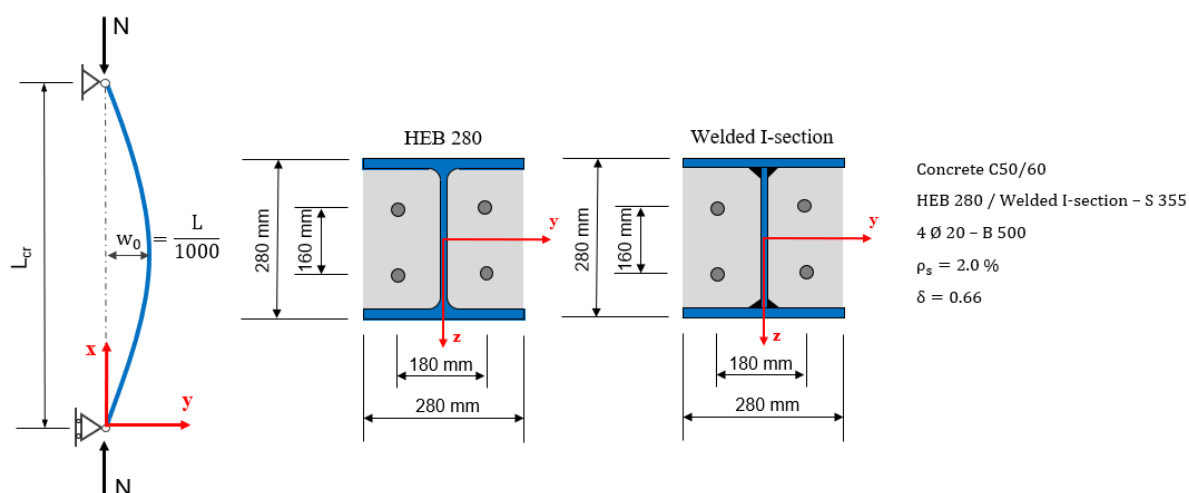
Figure 6.6 Material, geometry, and boundary conditions of PCEC columns

Table 6.1 Considered length for PCEC column

$L \ [m]$	1.0	2.0	3.0	4.0	5.0	6.0	7.0	8.0	9.0	10.0
$\bar{\lambda}_{nom}$	0.18	0.37	0.55	0.73	0.92	1.10	1.29	1.47	1.65	1.84

Figure 6.7 and Figure 6.8 show the results from GMNIA for the Partial Concrete Encased Composite (PCEC) column as a function of column's slenderness presented in non-dimensional form using reduction factor χ and relative slenderness $\bar{\lambda}$, for the verification of the members subjected to compressive force. The reduction factor χ for non-linear finite element analyses with initial imperfection (GMNIA) is calculated as:

$$\chi = \frac{N_{GMNIA}}{N_{pl,Rk}}$$ (6.1)

Where, N_{GMNIA} represents the compressive resistance force obtained from (GMNIA) in ABAQUS and $N_{pl,Rk}$ represents the plastic resistance to compressive force using characteristic values for materials calculated as:

$$N_{pl,Rk} = A_a \cdot f_{yk} + A_c \cdot \alpha_c f_{ck} + A_s \cdot f_{sk}$$ (6.2)

As in the case of steel columns, the results of (GMNIA) are shown with blue and red circles. The blue circles show the results of analyses with only initial geometric imperfection, while the red circles show the results of analyses with initial geometric imperfection and residual stresses. According to the results, the initial residual stresses have an impact on all considered lengths, and similar to steel columns, the effect is more significant and cannot be neglected for columns with intermediate slenderness ratio $0.6 \leq \overline{\lambda} \leq 1.2$ compared to columns with short and high slenderness ratio. Moreover, similar to steel columns, the results indicate that there is a difference between the initial residual stresses of the hot-rolled section and welded section in terms of reduction of the load-bearing capacity of the column, as in the case of welded section a higher reduction is observed for short and intermediate slenderness ratio due to the fact that a larger portion of web and flanges contains compressive residual stresses. Nevertheless, for PCEC columns the reduction of load-bearing capacity due to the presence of residual stresses is lower compared to steel columns, as in all considered lengths the maximum reduction is approximately 10%, and this is understandable since in the case of PCEC columns, the reinforced concrete contributes more on the load-bearing capacity of column compared to steel profile.
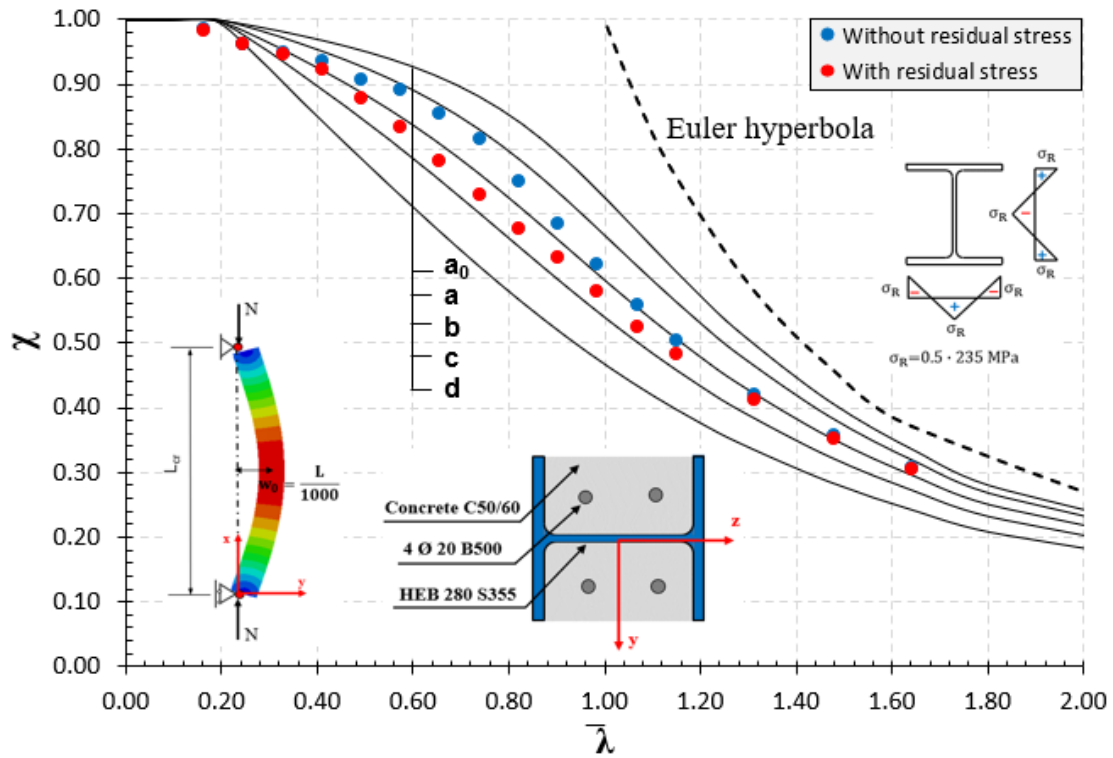
Figure 6.7 PCEC column with hot-rolled section, buckling about the weak axis z-z
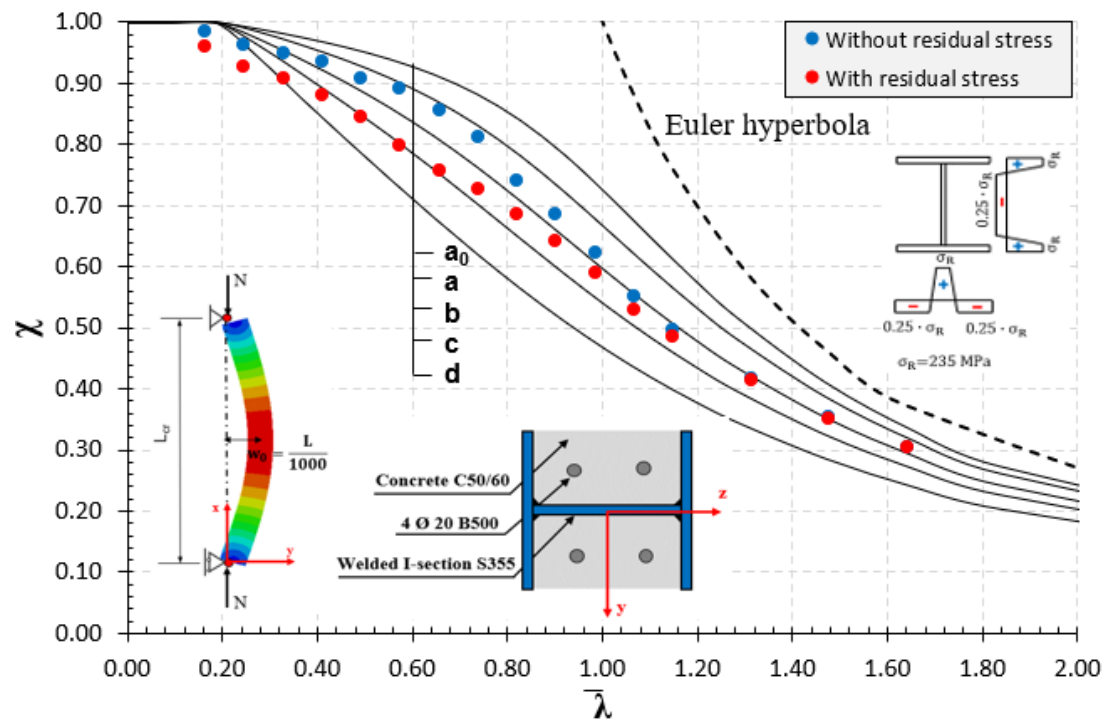
Figure 6.8 PCEC column with welded I-section, buckling about the weak axis z-z

6.3 Concrete encased composite column (CEC)

Figure 6.9 shows the geometry, material parameters, and boundary conditions used to investigate the effect of initial geometric imperfection and residual stresses on Concrete Encased Composite (CEC) columns. For the sake of simplicity and comparison with steel and PCEC columns, the same steel profile HEB 280 hot-rolled is considered also for the CEC column. In the case of CEC column, the initial residual stresses of the welded I-section provide similar results to hot-rolled section, and due to this, in this study, only the results from hot-rolled section are presented. Regarding the materials, for concrete, the class C50/60 is used while the reinforcement bars considered are $\varnothing 20 \, mm$ with yield strength $f_{sk} = 500 \, N/mm^2$. The analyses were performed by varying the length of the column to cover all the relative slenderness between $0.2 \leq \overline{\lambda} \leq 2.0$ as shown in Table 6.2.
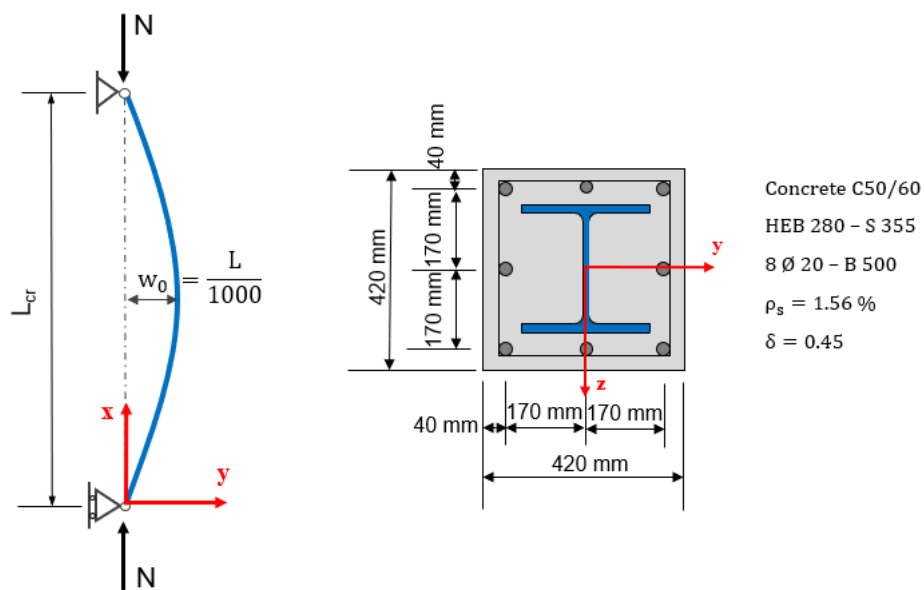
Figure 6.9 Material, geometry, and boundary conditions of PCEC column

Table 6.2 Relative slenderness for CEC column

L [m]	1.0	2.0	3.0	4.0	5.0	6.0	7.0	8.0	9.0	10.0	12.0	15.0
$\overline{\lambda}_{nom}$	0.11	0.23	0.34	0.46	0.57	0.69	0.80	0.92	1.03	1.15	1.38	1.72

Figure 6.10 shows the results from GMNIA for the Concrete Encased Composite (CEC) column as a function of column's slenderness presented in non-dimensional form using reduction factor χ and relative slenderness $\bar{\lambda}$, for the verification of the members subjected to compressive force. As in the previous cases, the reduction factor χ for GMNIA is calculated according to Equation (6.1). The results of non-linear finite element analyses with initial imperfection (GMNIA) are shown with blue and red circles. The blue circles show the results of analyses with only initial geometric imperfection, while the red circles show the results of analyses with initial geometric imperfection and residual stresses. According to results presented in Figure 6.10, in the case of CEC columns, the reduction of load-bearing capacity due to the presence of residual stresses is not significant compared to steel columns and partially encased composite columns, as in all considered lengths the maximum reduction is approximately 3%. This is understandable since in the case of CEC columns, the load-bearing capacity of the composite section is governed by the reinforced concrete section, and the steel profile inside the concrete does not significantly influence the overall behaviour of the column. For CEC columns with high and short slenderness ratios, the effect of residual stresses can be neglected while for columns with intermediate relative slenderness in the range between $0.5 \leq \bar{\lambda} \leq 1.0$ the effect may be taken into account.
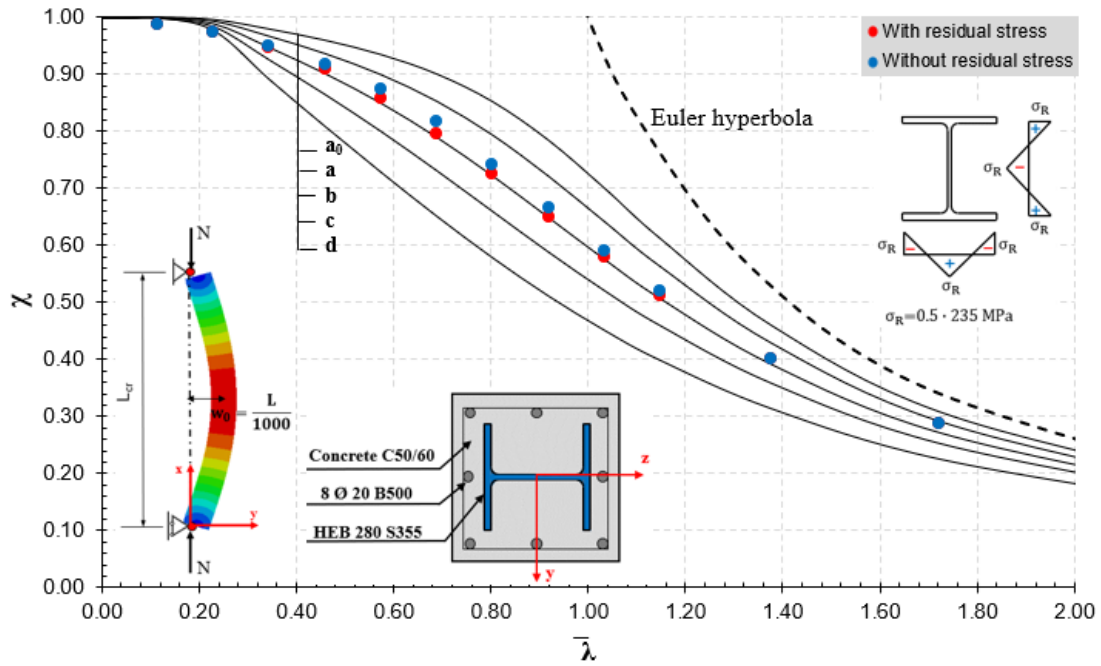
Figure 6.10 CEC column with hot-rolled section, buckling about the weak axis z-z

6.4 Concrete filled steel tube (CFST) with massive steel core column

Figure 6.11 shows the geometry, material parameters, and boundary conditions used to investigate the effect of initial geometric imperfection and residual stresses on the Concrete Filled Steel Tube (CFST) with a massive steel core. The initial residual stresses distribution and magnitude of the stresses in the case of massive round steel cores are based on the recommendation reported in [30] presented in Figure 2.15. The cross-section is composed of a circular tube with an outer diameter of 323.9 mm and thickness of 10 mm with nominal yield strength $f_y = 355\ N/mm^2$, filled with concrete C25/30, and an additional inner massive steel core of diameter $\varnothing 200\ mm$ with nominal yield strength $f_y = 235\ N/mm^2$. The analyses were performed by varying the length of the column to cover the relative slenderness between $0.2 \leq \overline{\lambda} \leq 2.0$ as it shown in Table 6.3.
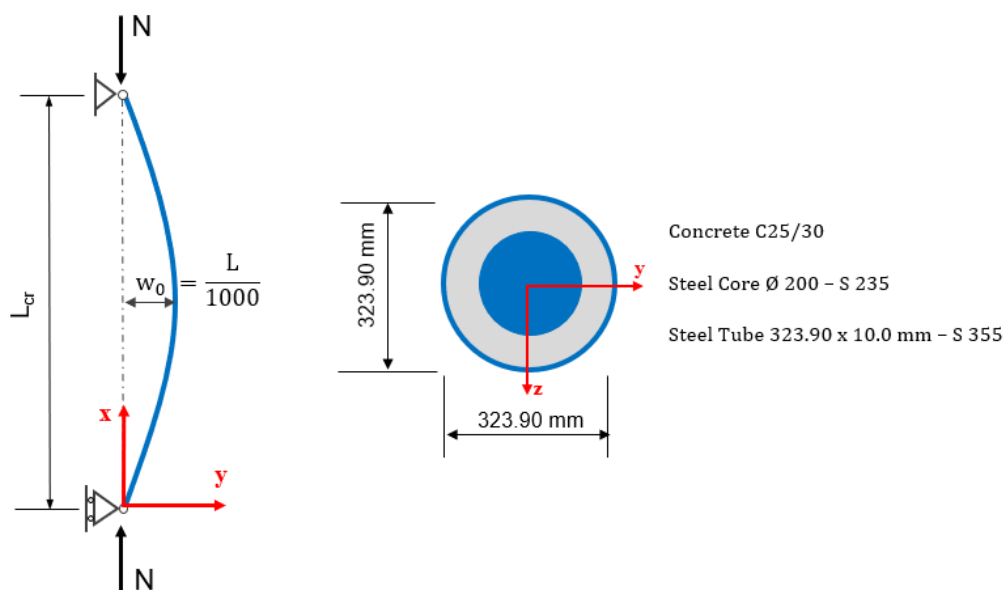
Figure 6.11 Material, geometry, and boundary conditions of CFST with massive steel core column

Table 6.3 Relative slenderness for CFST with massive steel core column

L [m]	1.0	2.0	3.0	4.0	5.0	6.0	7.0	8.0	9.0	10.0	12.0
$\bar{\lambda}_{nom}$	0.16	0.32	0.47	0.63	0.79	0.95	1.11	1.27	1.42	1.58	1.90

Figure 6.12 shows the results from GMNIA for the Concrete Filled Steel Tube (CFST) column with a massive steel core as a function of column's slenderness presented in non-dimensional form using reduction factor χ and relative slenderness $\bar{\lambda}$, for the verification of the members subjected to compressive force. As in the case of steel columns, the results of non-linear finite element analyses with initial imperfections (GMNIA) are shown with blue and red circles. The blue circles show the results of analyses with only initial geometric imperfection, while the red circles show the results of analyses with initial geometric imperfection and residual stresses. According to the results, the initial residual stresses have an impact on all considered lengths, and similar to PCEC columns, the effect is more significant and cannot be neglected for columns with intermediate slenderness ratio $0.6 \leq \bar{\lambda} \leq 1.4$ compared to columns with short and high slenderness ratio. This is understandable because short columns maintain their yield strength regardless of the effect of residual stresses, while very long columns are not influenced by the yielding as the ultimate load resistance is close to the critical buckling load.

The maximum reduction of load-bearing capacity is observed for the column with a 6.0 m length, with an approximate reduction of 10%. However, as it is reported in [30], the influence of the residual stresses on massive steel core is strictly related to the steel grade and diameter of the massive core, since the compressive residual stresses which cause the decrease in load-bearing capacity of the column are present in the surface of the massive steel core [30].
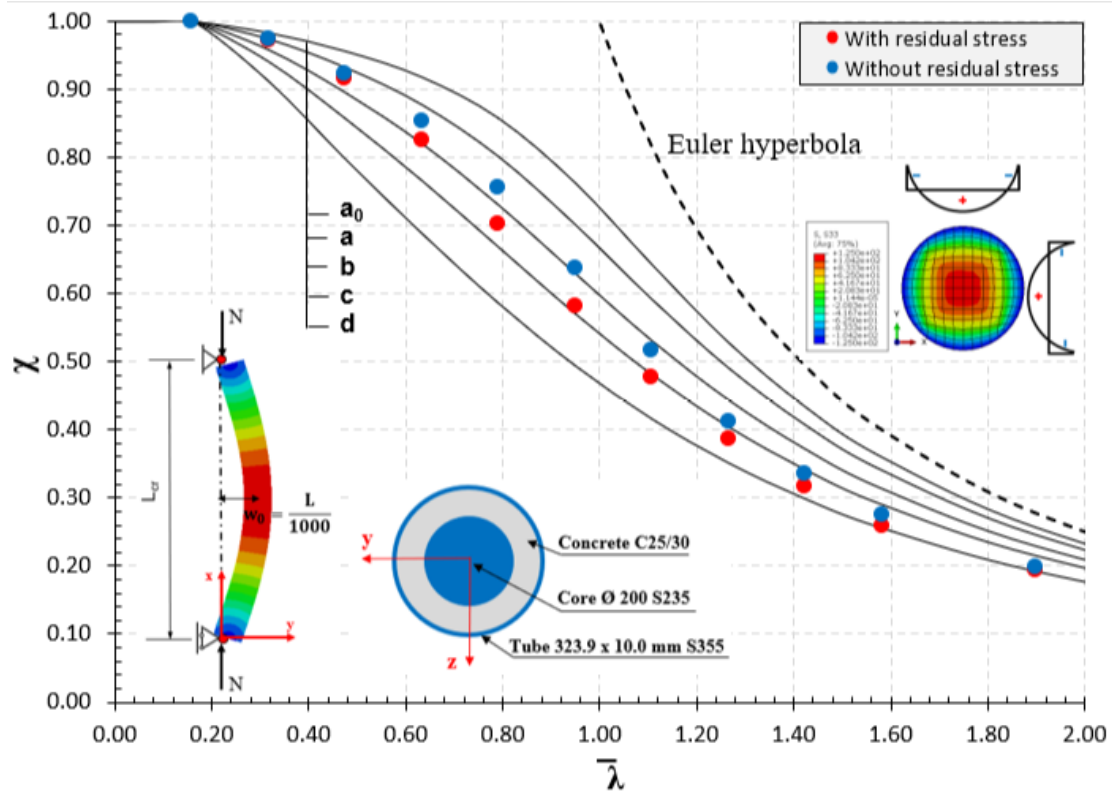
Figure 6.12 CFST with massive steel core column, buckling about the weak axis z-z

6.5 Chapter summary

This chapter addresses the benchmark cases regarding the effect of initial geometric imperfection and residual stresses for steel and composite columns. The examined columns are divided into four groups named: Steel columns, Partial Concrete Encased Composite Column (PCEC), Concrete Encased Composite Column (CEC), and Concrete Filled Steel Tube (CFST). Centric compressive axial load was applied to each column, and the boundary conditions were chosen to resemble simply support columns. The results are presented as a function of columns slenderness in non-dimensional form using reduction factor χ and relative slenderness $\bar{\lambda}$ defined according to EN 1993-1-1 [16]. Additionally, the results are distinguished between scenarios in which residual stresses and initial geometric imperfection are taken into account, as well as scenarios in which only the initial geometric imperfection is considered.

The findings for steel columns show that, residual stresses have a considerable and undesirable impact on flexural buckling of the steel column under compression load for all considered lengths. Furthermore, there is a strong correlation between the effect of residual stresses and the slenderness of the column. This is especially true for columns with an intermediate slenderness ratio $(0.3 \leq \bar{\lambda} \leq 1.2)$, as opposed to those with low or particularly high slenderness. This is reasonable because short columns preserve their yield strength independent of the impact of residual stresses, whereas very long columns are not subject to yielding because their ultimate load resistance is very close to the critical buckling load. Regarding the comparison between welded and hot-rolled section, even though the initial residual stresses have the same magnitude, a larger reduction of the load-bearing capacity is seen in the case of the welded section for intermediate slenderness compared to the hot-rolling section. This is due to the fact that a higher proportion of the web and flanges in welded sections have compressive residual stresses. Also, the results presented in this dissertation demonstrated that, the resistance of the steel column with $\bar{\lambda} \leq 0.2$ calculated based on GMNIA does not reach the European buckling curve plateau, as it is reported also in [22].

For PCEC columns, a smaller reduction in load-bearing capacity due to the initial residual stresses is observed compared to steel columns. This is reasonable because in PCEC columns, reinforced concrete contributes more to the load-bearing capacity of the column. On the other hand, similar to steel columns the findings show that the initial residual stresses affect all lengths with the effect being more pronounced for columns with an intermediate slenderness ratio. Furthermore, as with steel columns, the results show that the initial residual stresses of the hot-rolled and welded sections differ in terms of how much the load-bearing capacity of the column is reduced with welded section having a higher impact.

In the case of CEC columns, the load-bearing capacity reduction caused by residual stresses is not as great in case of steel and PCEC columns in all considered lengths. The effect of residual stresses can be neglected for CEC columns with high and short slenderness ratios, but it may have significance for columns with intermediate relative slenderness ratio.

Similar to the PCEC columns, also for CFST columns the impact of the residual stresses on flexural buckling is more significant for columns with intermediate slenderness. However, as it is reported in [30] the influence of the residual stresses on massive steel core is strictly related to the steel grade and diameter of the massive core, as the surface of the massive steel core is responsible for the reduction of the load-bearing capacity.

Chapter 7

Application of the general method for composite columns in steel and concrete

7.1 Scope

In this chapter, the results from different types of composite columns calculated using the general method according to prEN1994-1-1 [3] are presented. All the calculations are performed using finite element analysis software ABAQUS [49] with modelling procedure and solution strategy presented in Chapter 3.5.

The purpose of this chapter is to compare the resistance obtained from the general method with the overall safety factor γ_0 calculated from N-M interaction diagram based on plastic and strain-limited resistance on the cross-section level, with the resistance according to the simplified method (European buckling curves). As it is presented in Chapter 2.6, first, on a global level an incremental non-linear finite element analysis (GMNIA) has to be carried out, taking into account the initial geometric imperfection w_0, residual stresses on steel section, and non-linear material stress-strain curves based on the mean values for concrete, steel and reinforcement bars, then the design resistance is calculated dividing the mean resistance obtained from GMNIA with the overall safety factor γ_0 calculated from N-M interaction diagram based on plastic or strain-limited resistance on the cross-section level.

The considered columns are Concrete Encased Composite (CEC) columns, Partial Concrete Encased Composite (PCEC) columns, Concrete Filled Steel Tubes (CFST) with or without the addition inner steel profile or a massive steel core as shown in Figure 7.1. The results will be presented separately for each composite column type. Moreover, based on the way the overall safety factor γ_0 is calculated, the results of the general method will be separated between plastic and strain-limited N-M interaction diagram.
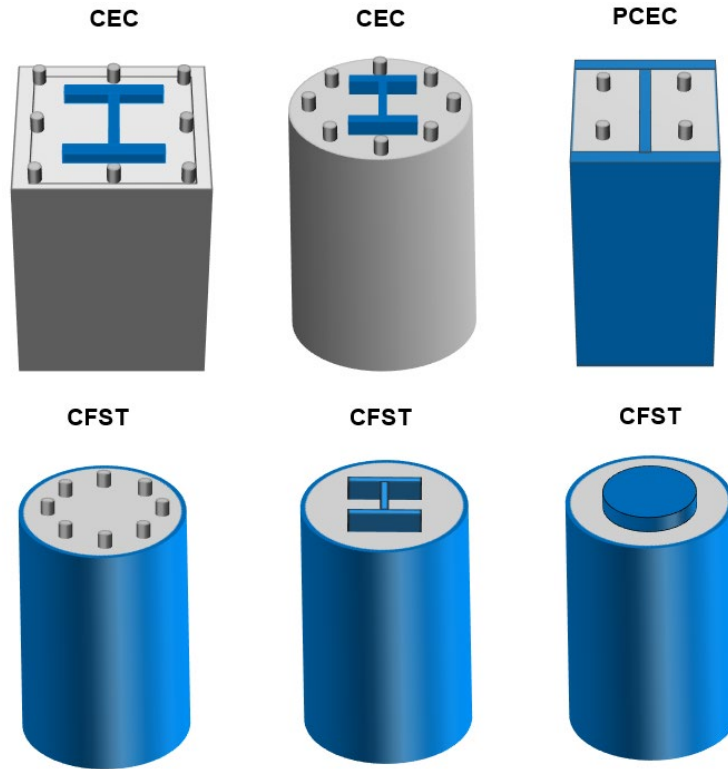
Figure 7.1 Typical composite columns calculated according to general method

7.2 Concrete encased composite column (CEC)

7.2.1 Geometry and boundary conditions

Figure 7.2 shows the geometry, material parameters, and boundary conditions used to investigate Concrete Encased Composite (CEC) columns according to the general method. The rectangular column is composed of steel profile HEB 280 – S355 fully encased in concrete with class C20/25 and eight reinforcement bars $\varnothing$20 mm, while the circular column is composed of steel profile HEM 100 – S355 fully encased in concrete with class C30/37 and six reinforcements bars $\varnothing$12 mm. The boundary conditions are selected to simulate an idealized simple supported column. The composite columns are subjected to concentrated axial force inducing flexural buckling about the weak axis (z-z). The analyses were performed by varying the length of the column to cover the relative slenderness between $0.2 \leq \overline{\lambda} \leq 2.0$.
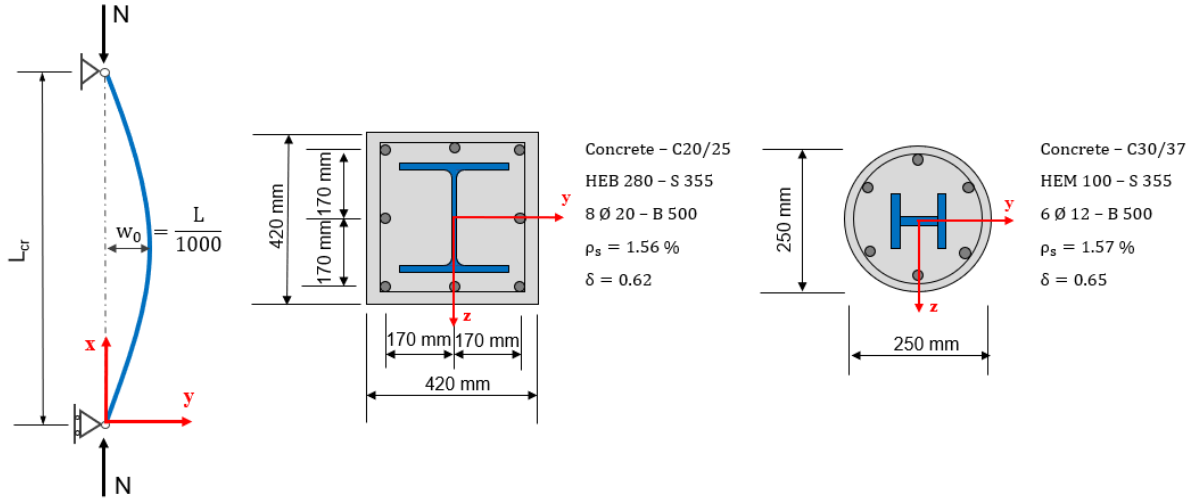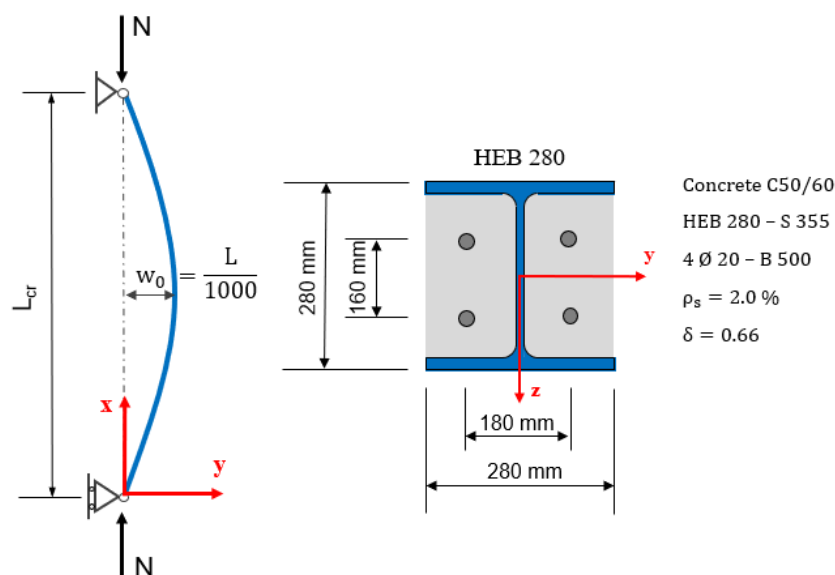
Figure 7.2 Considered CEC columns for application of general method

7.2.2 Results – rectangular CEC column

Figure 7.3 shows the results from incremental non-linear finite element analysis (GMNIA) simulation in ABAQUS for rectangular Concrete Encased Composite (CEC) column as a function of columns slenderness presented in non-dimensional form using reduction factor χ and relative slenderness $\bar{\lambda}$, for the verification of the flexural buckling about the weak axis (z-z). The continuous red and blue lines show the calculation of the resistance according to the general method with the overall safety factor γ_0 based on plastic and strain limited N-M interaction diagram respectively. For buckling about the minor axis (z-z), according to the simplified method (European buckling curves) EN 1994-1-1 [2] this cross-section is classified into *buckling curve c*, and in comparison with the general method a similar classification is observed. However, for short columns (with $0.1 \leq \bar{\lambda} \leq 0.3$) the general method based on plastic resistance N-M interaction diagram is below *buckling curve c* providing more conservative results than the simplified method. Similar to steel columns presented in sub-chapter 6.1, also for CEC columns with the general method based on plastic resistance N-M interaction diagram, the plateau value for slenderness $\bar{\lambda} \leq 0.2$ cannot be proven by GMNIA in case when lower class of concrete are used.
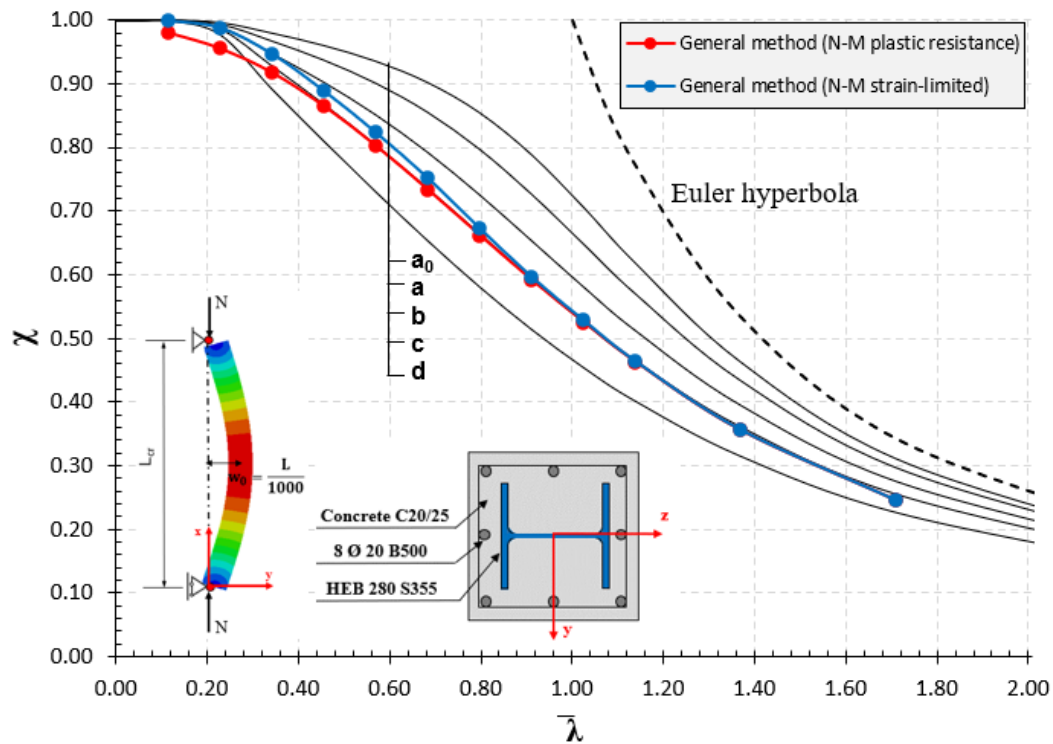
Figure 7.3 Rectangular CEC column according to general method about the weak axis (z-z)

Regarding the classification according to the general method, with reference to Figure 7.4, it can be observed that, in case higher classes of concrete are used the difference between the general method and simplified method becomes greater, with the simplified method providing more conservative results. This is because, the impact of the steel section decreases, and the behaviour of the column is closer to the concrete column. In the above discussion related to the simplified method, it is emphasized that European buckling curves were originally developed for steel columns and later on adopted also for composite columns, and so, in the case when the steel section is dominant (e.g., lower bound of a concrete class is used for composite columns) the two methods provide similar results. This is reported also in background study done by (Hanswille and Bergmann) [79] of the Eurocode 4.
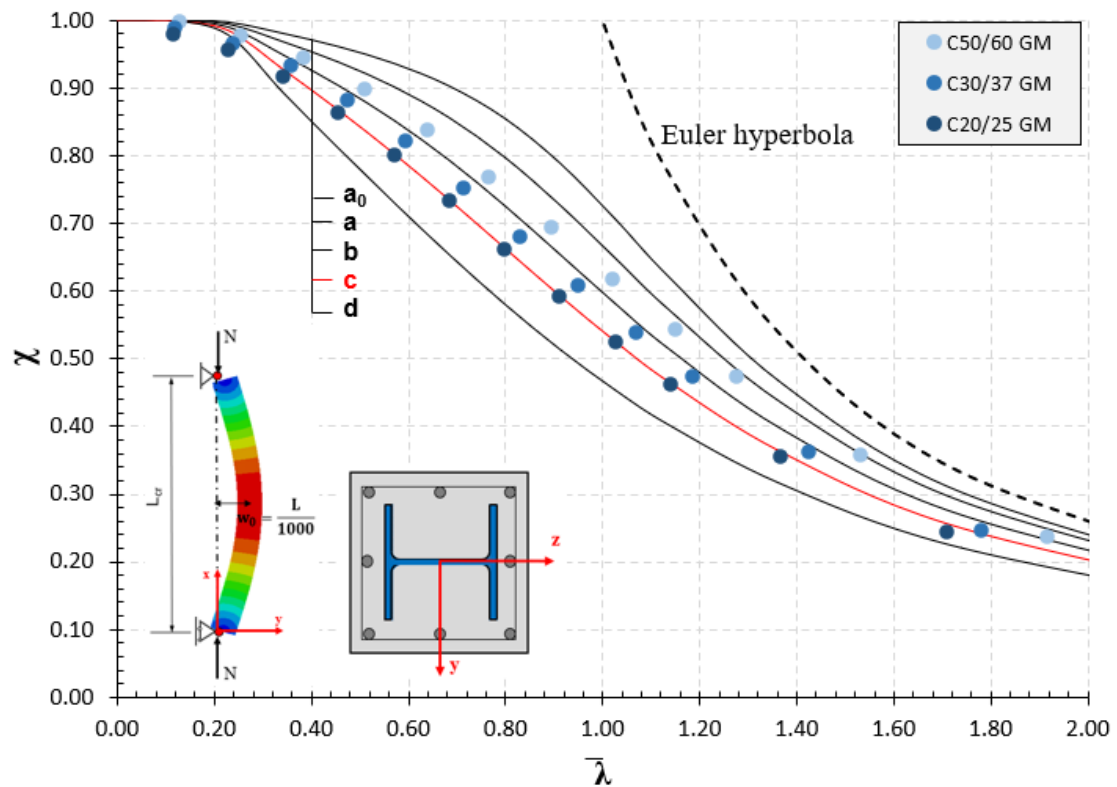
Figure 7.4 Rectangular CEC column according to general method with overall safety factor γ_0 based on plastic N-M interaction about the weak axis (z-z) varying the concrete class

Regarding the calculation of the overall safety factor γ_0, the results show that the N-M interaction diagram based on plastic resistance provides more conservative results compared to strain-limited for columns with a short slenderness ratio with a difference in resistance of around 3%, while for columns with intermediate and long slenderness ratio, the difference is less 1%. This can be observed also in Figure 7.5, where the N-M interaction diagram on the cross-section level using mean and design values based on plastic (continuous lines) and strain-limited (dashed lines) is shown with variation of γ_0 as a function of the as a function of column's length L.
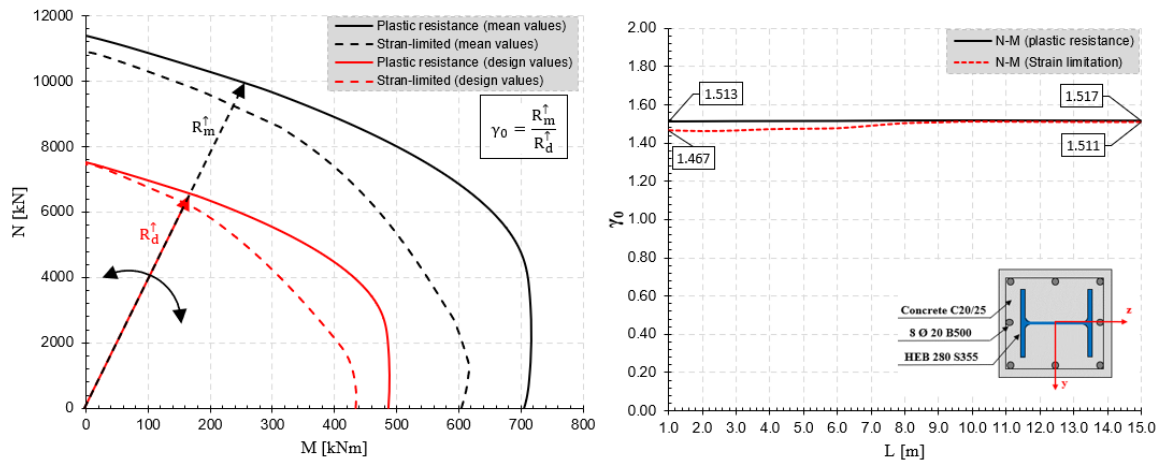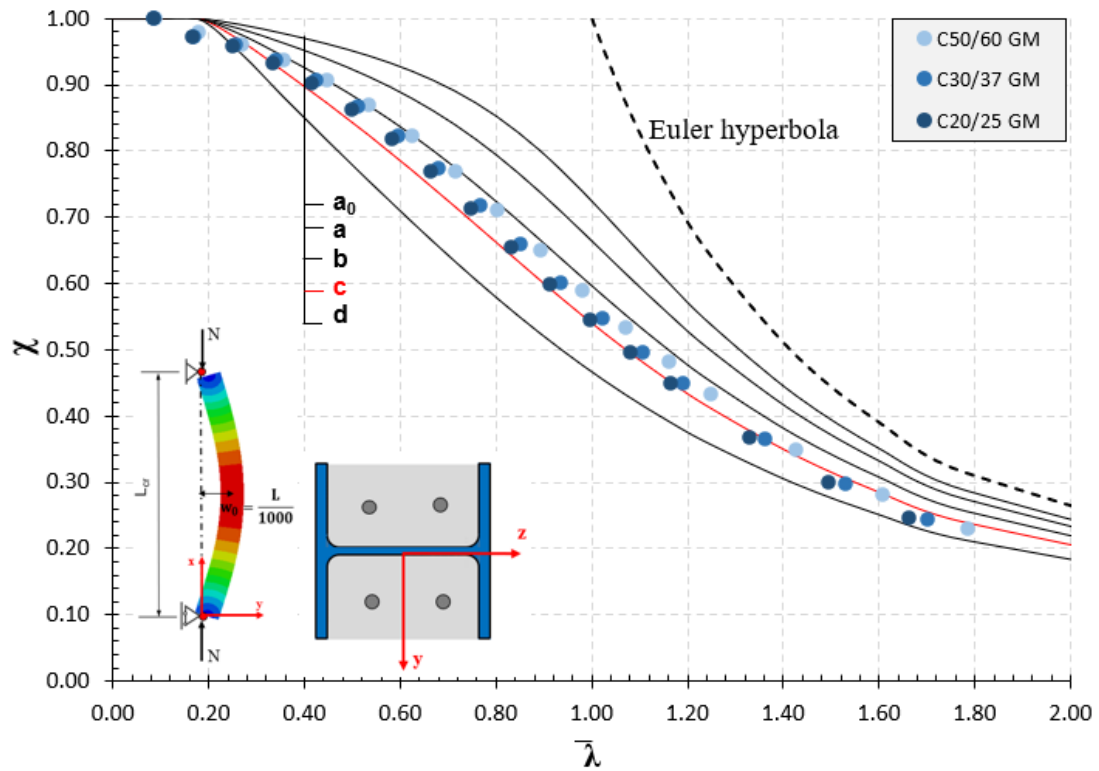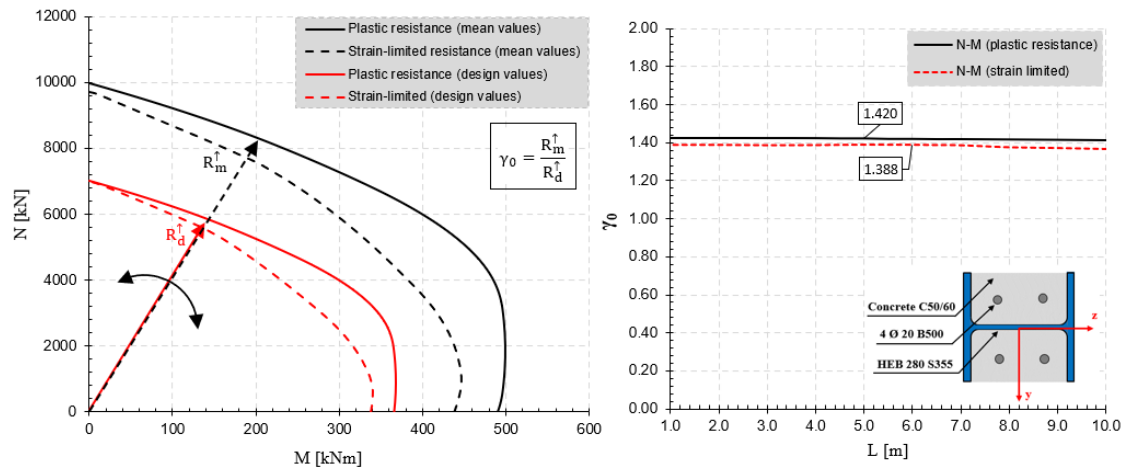
Figure 7.5 The overall safety factor γ_0 for rectangular CEC column based on plastic and strain-limited resistance N-M interaction diagram

7.2.3   Results – circular CEC column

Figure 7.6 shows the results from incremental non-linear finite element analysis (GMNIA) simulation in ABAQUS for the circular Concrete Encased Composite (CEC) column as a function of columns slenderness presented in non-dimensional form using reduction factor χ and relative slenderness $\bar{\lambda}$, for the verification of the flexural buckling about the weak axis (z-z). As in the previous case, the continuous red and blue lines show the calculation of the resistance according to the general method with the overall safety factor γ_0 based on plastic and strain limited N-M interaction diagram respectively. In the current EN 1994-1-1 [2] this cross-section is without any reference regarding the classification into European buckling curves, and so the design according to simplified methods is not possible. However, according to the general method this cross-section can be classified between *buckling curve b* and *buckling curve c* depending on the length of the column. For short and intermediate slenderness ratios, this cross-section is classified into *buckling curve b*, while for slender columns is classified into *buckling curve c*. Regarding the calculation of the overall safety factor γ_0, as in the previous case, the results show that the N-M interaction diagram based on plastic resistance provides more conservative results compared to strain-limited for columns with a short slenderness ratio with a difference in resistance of around 3%, while for columns with intermediate and long slenderness ratio, the difference is less 1%. This can be observed also in Figure 7.7, where the N-M interaction diagram on the cross-section level

using mean and design values based on plastic (continuous lines) and strain-limited (dashed lines) is shown with variation of γ_0 as a function of the as a function of column's length L.
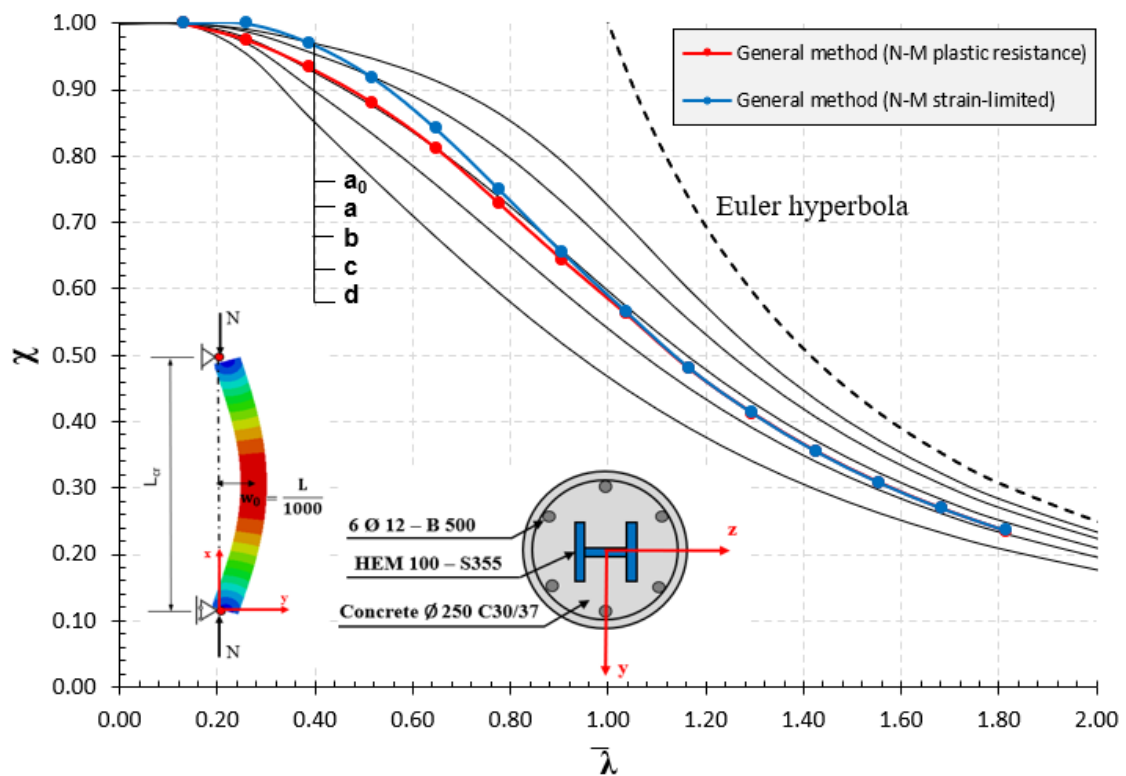
Figure 7.6 Circular CEC column according to general method about the weak axis (z-z)
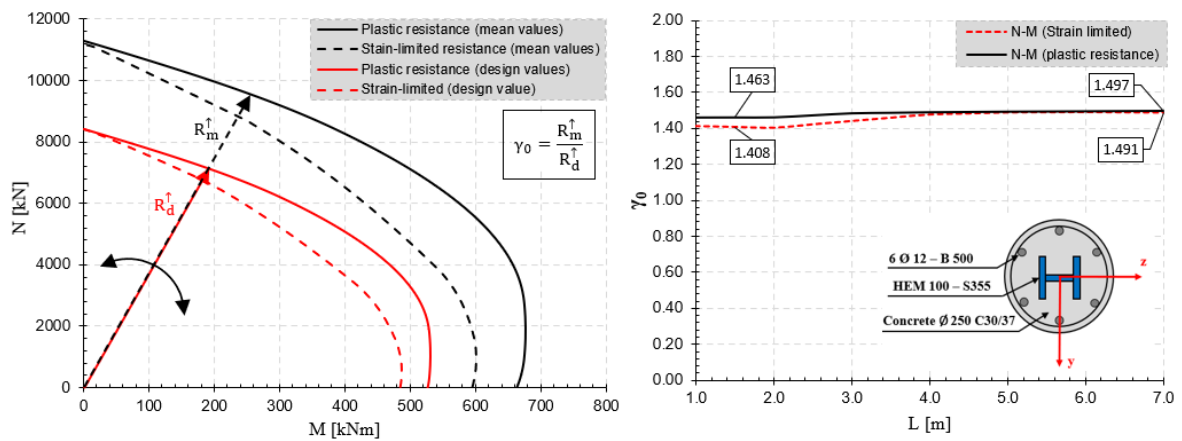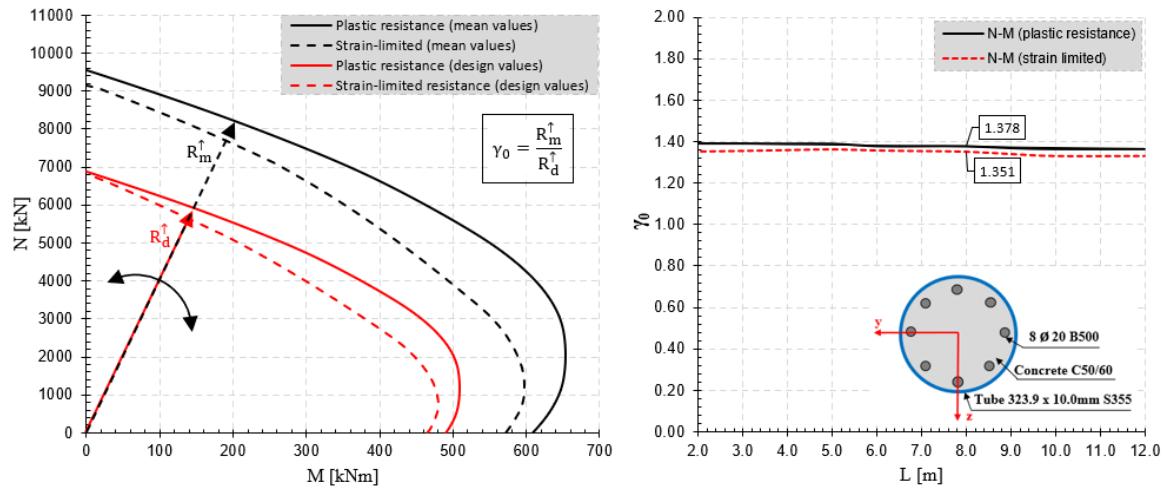

Figure 7.7 The overall safety factor γ_0 for circular CEC column based on plastic and strain-limited resistance N-M interaction diagram

7.3 Partial concrete encased composite column (PCEC)

7.3.1 Geometry and boundary conditions

Figure 7.8 shows the geometry, material parameters, and boundary conditions used to investigate the Partial Concrete Encased Composite (PCEC) column according to the general method. The column is composed of steel profile HEB 280 – S355 partially encased in concrete with class C50/60 and four reinforcement bars $\varnothing$20 mm. The boundary conditions are selected to simulate an idealized simple supported column. As in the previous case, the composite column is subjected to concentrated axial force inducing flexural buckling about the weak axis (z-z). The analyses were performed by varying the length of the column to cover all the relative slenderness between $0.2 \leq \bar{\lambda} \leq 2.0$.

Figure 7.8 Considered PCEC column for application of general method

7.3.2 Results – PCEC column

Figure 7.9 shows the results from incremental non-linear finite element analysis (GMNIA) simulation in ABAQUS [49] for Partial Concrete Encased Composite (PCEC) column as a function of columns slenderness presented in non-dimensional form using reduction factor χ and relative slenderness $\bar{\lambda}$, for the verification of the flexural buckling about the weak axis (z-z). The continuous red and blue lines show the calculation of the resistance according to the

general method with the overall safety factor γ_0 based on plastic and strain limited N-M interaction diagram respectively. For buckling about the minor axis (z-z), according to the simplified method (European buckling curves) EN 1994-1-1 [2] this cross-section is classified into *buckling curve c*, and in comparison with the general method a similar classification is observed as the column is classified between *buckling curve b* and *buckling c* depending on the length of the column. However, for short columns (with $\bar{\lambda} = 0.2 - 0.3$) the general method based on plastic resistance N-M interaction diagram is below *buckling curve c* providing more conservative results than the simplified method.
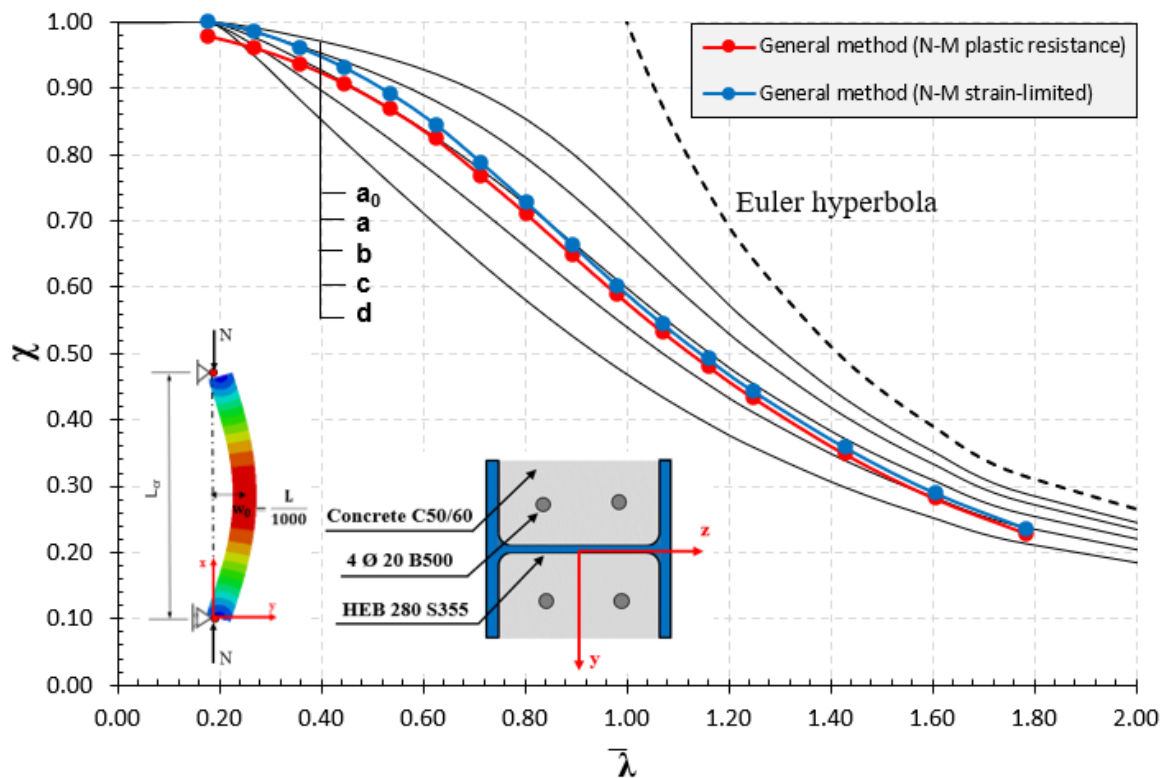
Figure 7.9 PCEC column according to general method about the weak axis (z-z)

Regarding the classification according to the general method, concerning Figure 7.10, it can be observed that similar to the CEC column, in case when higher classes of concrete are used the difference between the general method and the simplified method becomes greater, with the simplified method providing more conservative results. This is because the impact of the steel section decreases, and the behaviour of the column is closer to the concrete column as in the case of the CEC column. Nevertheless, the results show that even by varying the

concrete class from lower bound C20/25 to upper bound C50/60, the column is always classified in between *buckling curve b* and *buckling curve c* which was not the case for the CEC column where the concrete class significantly influenced the resistance of the column. In the case of PCEC columns, the resistance to buckling is more "balanced" between the steel profile and concrete.

Regarding the calculation of the overall safety factor γ_0, the results show that the N-M interaction diagram based on plastic resistance provides more conservative results compared to strain limited resistance for all considered lengths of the column with a difference in resistance of around 3%. Nevertheless, there is not a significantly difference between the two methods and this difference decreases as the column gets longer. This can be observed also in Figure 7.11, where the N-M interaction diagram on the cross-section level using mean and design values based on plastic (continuous lines) and strain-limited (dashed lines) is shown with variation of γ_0 as a function of as a function of column's length L.

Figure 7.10 PCEC column according to general method based on plastic N-M interaction diagram about the weak axis (z-z) varying the concrete class

Figure 7.11 The overall safety factor γ_0 for circular PCEC column based on plastic and strain-limited resistance N-M interaction diagram

7.4 Concrete filled steel tubes column (CFST)

7.4.1 Geometry and boundary conditions

Figure 7.12 shows the geometry, material parameters, and boundary conditions used to investigate Concrete Filled Steel Tubes (CSTS) columns without or with additional steel profile and steel core according to the general method. The circular tube used in three cases has a diameter of 323.9 mm and a thickness of 10 mm. The first column is filled with concrete C50/60 and eight reinforcement bars $\varnothing$20 mm B500, without an inner steel profile or steel core. The second column is filled with concrete C50/60 as well, and with an additional inner steel profile HEB 200 – S355, while the third column is filled with low-class concrete C25/30 and with an additional massive inner steel core $\varnothing$200 mm S235. The boundary conditions are selected to simulate an idealized simple supported column. The composite columns are subjected to concentrated axial force inducing flexural buckling about the weak axis (z-z). The analyses were performed by varying the length of the column to cover all the relative slenderness between $0.2 \leq \overline{\lambda} \leq 2.0$ as in the previous cases.
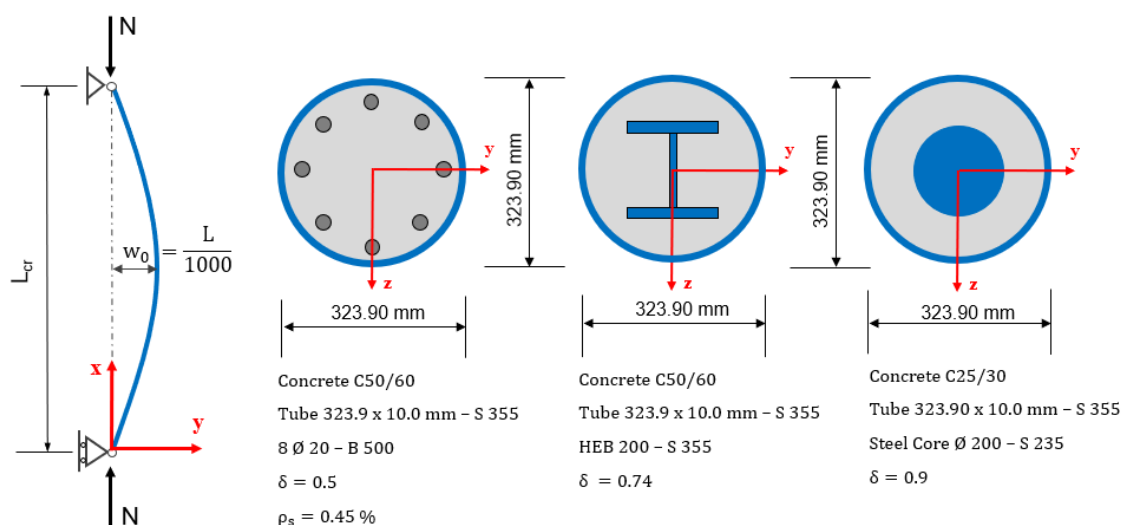
Figure 7.12 Considered CFST columns for application of general method

7.4.2 Results – CFST column

Figure 7.13 shows the results from incremental non-linear finite element analysis (GMNIA) simulation in ABAQUS for Concrete Filled Steel Tube (CFST) column as a function of columns

slenderness presented in non-dimensional form using reduction factor χ and relative slenderness $\bar{\lambda}$, for the verification of the flexural buckling about the weak axis (z-z). The continuous red and blue lines show the calculation of the resistance according to the general method with the overall safety factor γ_0 based on plastic and strain limitation N-M interaction diagram respectively. For buckling about the minor axis (z-z), according to the simplified method (European buckling curves) EN 1994-1-1 [2] this cross-section is classified into *buckling curve a*, and in comparison with the general method, the same classification is observed when the overall safety factor γ_0 is calculated with plastic resistance, while for the case when strain limited resistance is used for the calculation the overall safety factor γ_0, the short columns (with $\bar{\lambda} = 0.2 - 0.4$) are classified into *buckling curve a₀* providing less conservative results.
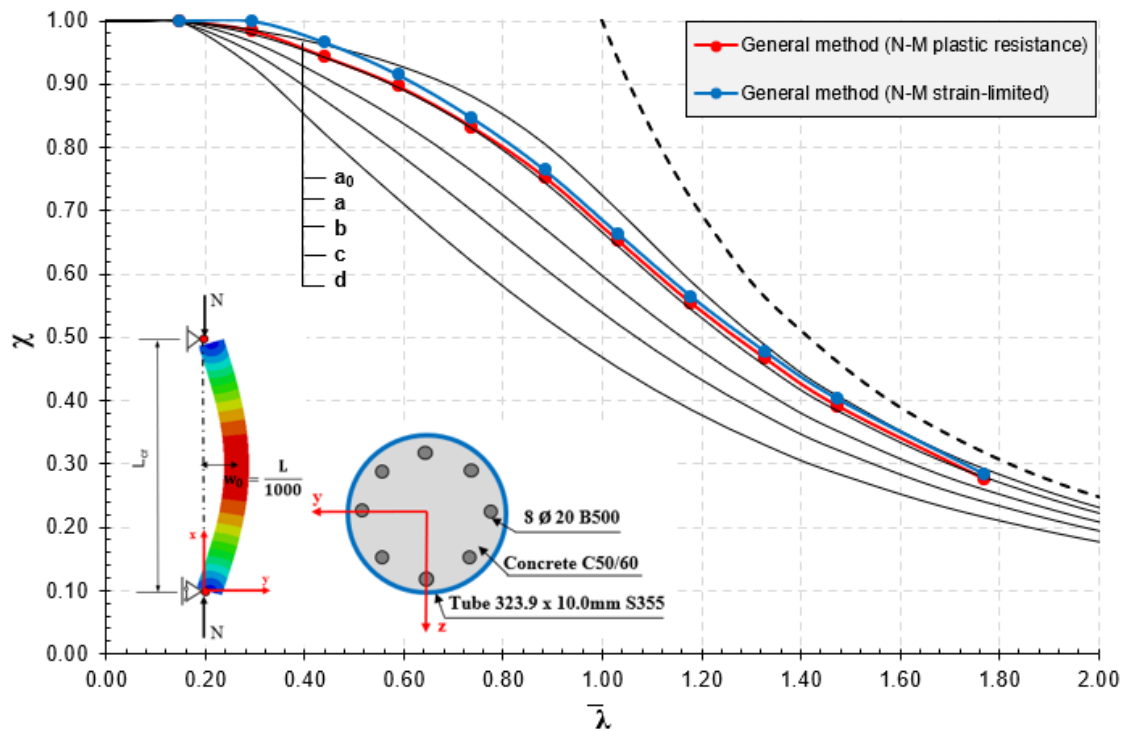
Figure 7.13 CFST column according to general method about the weak axis (z-z)

This can be observed also from the calculation of the overall safety factor γ_0 shown in Figure 7.14. The N-M interaction diagram on the cross-section level using mean and design values based on plastic (continuous lines) and strain-limited (dashed lines) is shown with variation of γ_0 as a function of the column's length L. The results indicate that the N-M interaction

diagram based on plastic resistance provides more conservative results compared to strain limited for columns with a short slenderness ratio with a difference in resistance of around 3%, while for columns with intermediate and long slenderness ratio, the difference is less than 1%.

Figure 7.14 The overall safety factor γ_0 for circular CFST column based on plastic and strain-limited resistance N-M interaction diagram

7.4.3 Results – CFST column with steel profile

Figure 7.15 shows the results from incremental non-linear finite element analysis (GMNIA) simulation in ABAQUS for Concrete Filled Steel Tube (CFST) with additional inner steel profile as a function of columns slenderness presented in non-dimensional form using reduction factor χ and relative slenderness $\bar{\lambda}$, for the verification of the flexural buckling about the weak axis (z-z). Continuous red and blue lines show the calculation of the resistance according to the general method with the overall safety factor γ_0 based on plastic and strain limited N-M interaction diagram respectively. For buckling about the minor axis (z-z), according to the simplified method (European buckling curves) EN 1994-1-1 [2] this cross-section is classified into *buckling curve b*, while according to the general method this cross-section is classified between *buckling curve b* and *buckling curve a* in all considered lengths. However, in the case when the overall safety factor γ_0 is calculated using the strain limited resistance the results are less conservative, and the column is classified into *buckling curve a.* As in previous cases, the difference between the calculation of the overall safety factor γ_0 based on plastic and

strain limitation is small in all considered lengths. This can be observed also in Figure 7.16 where it is shown the calculation of the N-M interaction diagram on the cross-section level using mean and design values based on plastic (continuous lines) and strain-limited (dashed lines) with variation of γ_0 as a function of column's length L. The results indicate that the N-M interaction diagram based on plastic resistance provides more conservative results compared to strain limitation with a difference in resistance of less than 3% in all considered lengths of column.
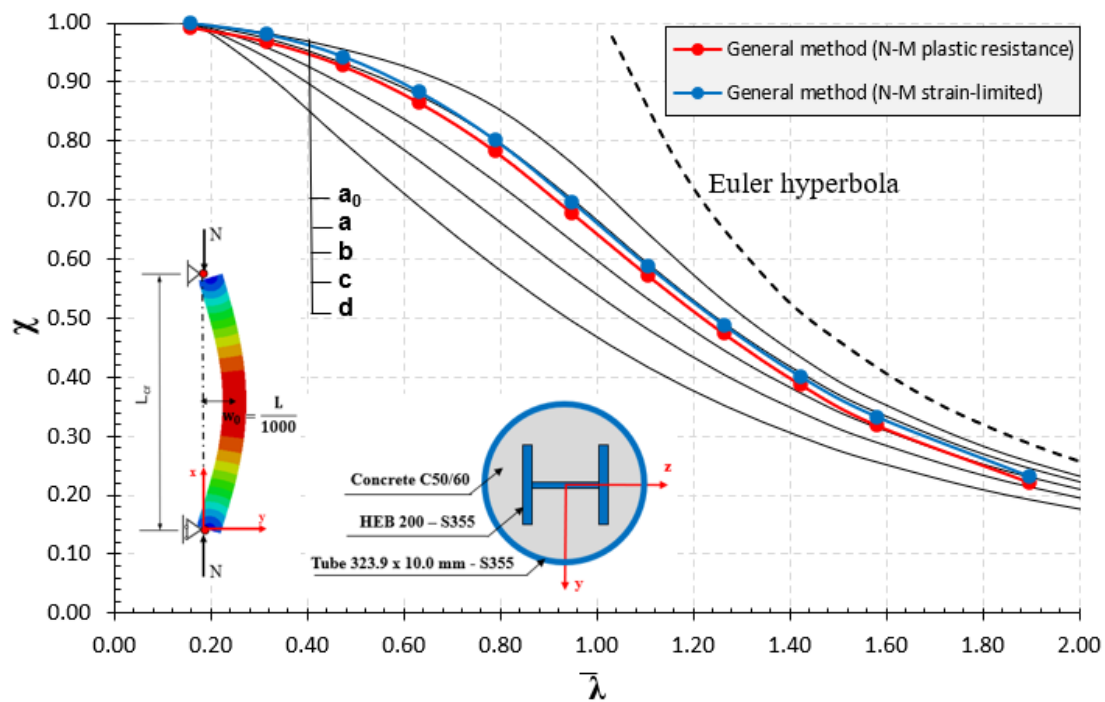
Figure 7.15 CFST with an inner steel profile column according to general method about the weak axis (z-z)
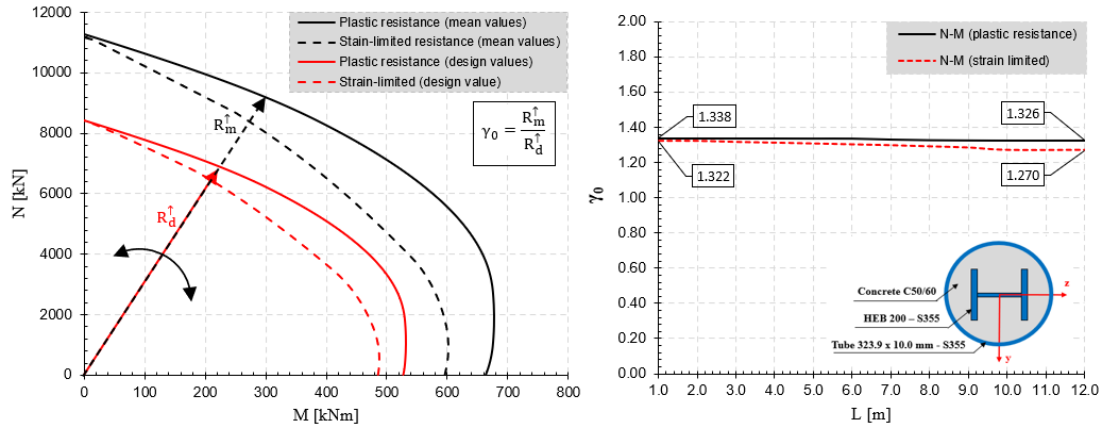
Figure 7.16 The overall safety factor γ_0 for circular CFST with an inner steel profile based on plastic and strain-limited resistance N-M interaction diagram

7.4.4 Results – CFST column with massive steel core

In the same way are presented the results in Figure 7.17 for Concrete Filled Steel Tube (CFST) with an additional massive inner steel core as a function of columns slenderness presented in non-dimensional form using reduction factor χ and relative slenderness $\bar{\lambda}$, for the verification of the flexural buckling about the weak axis (z-z). The continuous red and blue lines show the calculation of the resistance according to the general method with the overall safety factor γ_0 based on plastic and strain limited N-M interaction diagram respectively. In the current EN 1994-1-1 [2] this cross-section is without any reference regarding the classification into European buckling curves, and so the design according to simplified methods is not possible. However, according to the general method this cross-section can be classified between *buckling curve b* and *buckling curve c* depending on the length of the column. For short and intermediate slenderness ratio (with $\bar{\lambda} = 0.2 - 1.0$), this cross-section is classified into *buckling curve b*, while for slender columns is classified into *buckling curve c*.

Figure 7.17 CFST with a massive inner steel core according to general method about the weak axis (z-z)

As in previous cases, the difference between the calculation of the overall safety factor γ_0 based on plastic and strain limitation is small in all considered lengths. This can be observed also in Figure 7.18 where it is shown the calculation of the N-M interaction diagram on the cross-section level using mean and design values based on plastic (continuous lines) and strain-limited (dashed lines) with variation of γ_0 as a function of column's length L. The results indicate that the N-M interaction diagram based on plastic resistance provides more conservative results compared to strain limited resistance with a difference in resistance of less than 2% in all considered lengths of column.
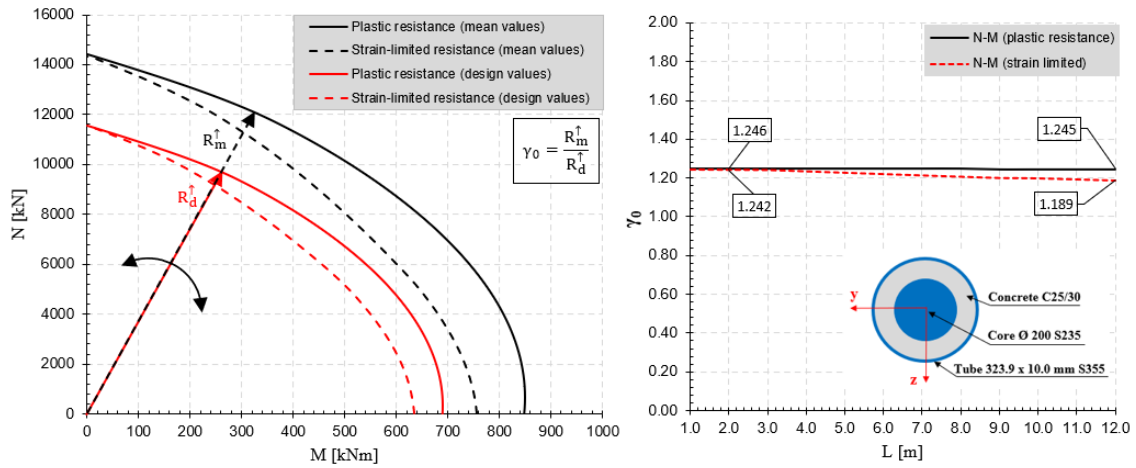
Figure 7.18 The overall safety factor γ_0 for circular CFST with a massive inner core based on plastic and strain-limited resistance N-M interaction diagram

7.5 Chapter summary

This chapter addresses the application of the general method according to prEN1994-1-1 [3] with the overall (safety) factor γ_0 based on plastic and strain-limited N-M interaction diagram. This chapter compares the resistance determined with the simplified method (European buckling curves) against the resistance obtained using the general method. The results are presented as a function of columns slenderness in non-dimensional form using reduction factor χ and relative slenderness $\bar{\lambda}$ defined according to EN 1993-1-1 [16]. The considered columns are Concrete Encased Composite (CEC) columns, Partial Concrete Encased Composite (PCEC) columns, Concrete Filled Steel Tubes (CFST) with or without the addition inner steel profile or a massive steel core as shown in Figure 7.1. The analyses were performed by varying the length of the column to cover the relative slenderness between $0.2 \leq \bar{\lambda} \leq 2.0$. All the computations are carried out using the finite element analysis program ABAQUS [49], with the modelling technique and solution strategy described in Chapter 3.5.

The findings for considered composite columns show that, generally speaking, the simplified method provide more conservative results in comparison with the general method. However, this is not always true as the difference between the general method and the simplified method is strictly related to the concrete class and steel contribution (δ). This can be observed from the results of the CEC column shown in Figure 7.3, when a lower class of

concrete is used the results from the general method are below the simplified method, while in case when high strength concrete is used (see Figure 7.4), consequently the steel contribution is diminished, the difference between two methods increases with the simplified method being more conservative. In those cases, the behaviour of the CEC column is similar to concrete column, while in case when lower class of concrete is used, or the steel contribution is high, the behaviour of the composite column is similar to steel column. This is due to the fact that the European buckling curves (the simplified method) are originally developed for steel columns, and later on adapted to be utilized with composite columns. In Eurocode 4 EN 1994-1-1 [2], the composite columns are classified into buckling curves considering always the lower bound of the concrete class, as it is reported also in background study [79] of the Eurocode 4.

Regarding the calculation of the overall (safety) factor γ_0 for the general method, the outcomes indicate that, in comparison with strain-limited resistance, the N-M interaction diagram based on plastic resistance provides more conservative results for all considered columns. Nevertheless, there is not a significantly difference between the two methods, with the maximum difference of 3%, and this difference decreases as the length of the column grows.

Chapter 8

Safety and reliability assessment of composite columns using SFEM

8.1 Scope

This chapter is dedicated to the safety and reliability assessment of the general method with the overall (safety) factor γ_0 based on strain-limited N-M interaction diagram for the design of composite columns according to prEN1994-1-1 [3], using non-linear Stochastic Finite Element Method (SFEM). This is conducted by comparing the safety level provided by prEN1994-1-1 [3] with 0.1% quantile resistance of reliability analysis which corresponds to the reliability index $\beta = 3.04$ according to Eurocode 0 EN 1990 [5].

As previously mentioned, the European buckling curves were developed originally for steel columns by the European Convention for Constructional Steelwork (ECCS) [14], as a result of a very large campaign of experimental tests (full-scale column tests) with statistical distribution of the main parameters which govern the behaviour of the steel columns. Later on, the authors Bjorhovde [20] and Strating & Vos [21] used the statistical data provided by ECCS tests and applied the Monte Carlo Simulation method to replicate the full-scale tests using numerical (GMNIA) calculation.

In this study, a similar approach to [20], [21] is adapted for the evaluation of the safety and reliability of composite columns, but instead of Monte Carlo Simulation (MCS), a more sophisticated sampling method called Latin Hypercube Sampling (LHS) is used to generate random variables for the statistical distribution of the main geometric and material parameters of the composite columns to perform nonlinear Stochastic Finite Element Analysis. The statistical distribution of the main parameters are based on recommendations of the Joint Committee on Structural Safety (JCSS) Model Code [46], prEN1992-1-1 [8], and prEN 1993-1-1 [9]. Additionally, sensitivity analyses are carried out to determine the extent

to which each random variable affects the resistance of the composite columns. Sensitivity analyses are performed using the Sobol's indices method [10]. The considered columns for reliability and sensitivity analyses are Concrete Encased Composite (CEC) columns, Partial Concrete Encased Composite (PCEC) columns, Concrete Filled Steel Tubes (CFST) with or without the addition inner steel profile or massive steel core, the same as the ones presented in Chapter 7 (Figure 7.1.) for the application of the general method. The results will be presented separately for each column.

8.2 Partial concrete encased composite column (PCEC)

8.2.1 Geometry and boundary conditions of deterministic model

The partial concrete encased composite (PCEC) column model (geometry, materials, and boundary conditions) considered for reliability analysis is presented in Figure 7.8. The cross-section is composed of HEB280 with nominal yield strength $f_y = 355 \ N/mm^2$, partially encased in concrete C50/60 with four longitudinal bars of a diameter Ø20 mm and nominal yield strength $f_y = 500 \ N/mm^2$. The column is simply supported with imperfection (statically determined) and subjected to concentrated axial load. The buckling resistance of the column depends on many parameters (mostly related to geometry and material) and can be described as:

$$N_{b,R} = f \ (L, f_c, f_y, f_s, f_{ct}, E_c, E_s, E_y, w_0, \sigma_{rs}, b_c, h_c, b_p, h_p, t_f, t_w) \tag{8.1}$$

where, L is length of the column, f_c, f_t are the compressive and tensile strength of concrete, f_y is the yield stress of the steel, f_s is the yield stress of the reinforcement bars, E_c, E_s, E_y are the elastic modulus for concrete, steel and reinforcement respectively, w_0 is the geometric imperfection, σ_{rs} is the residual stresses on steel profile, b_c, h_c are the width and height of concrete section, and b_p, h_p, t_f, t_w, are the width and height of the steel profile. To perform non-linear Stochastic Finite Element Analysis (SFEA), the deterministic model is transformed into a probabilistic one by considering the parameters in Equation (8.1) as random variables except the length L, which is kept deterministic. However, the analyses were performed by

varying the length of the column to cover all the column slenderness between $0.2 \leq \overline{\lambda} \leq 2.0$ as it is shown in Table 8.1.

Table 8.1 Length and non-dimensional slenderness of considered (PCEC)

L [m]	1.0	2.0	3.0	4.0	5.0	6.0	7.0	8.0	9.0	10.0
$\overline{\lambda}_{nom}$	0.18	0.37	0.55	0.73	0.92	1.10	1.29	1.47	1.65	1.84

8.2.2 Probability density function of the PCEC column

Table 8.2 presents the list of the parameters considered as random variables that carry the most uncertainties for partial encased composite columns (PCEC) defined by normal and log-normal distribution based on recommendations of Joint Committee on Structural Safety (JCSS) Model Code [46], prEN1992-1-1 [8], and prEN 1993-1-1 [9], while Figure 8.1 presents graphically the probability density function (PDF) of these parameters which influence the resistance of the PCEC column. The mean concrete compressive strength f_{cm}, the corresponding mean elastic modulus of concrete E_{cm} and the mean concrete tensile strength f_{ctm} are calculated according to prEN1992-1-1, Table 5.1 [8]. The mean reinforcement steel strength f_{sm} is calculated according to prEN1992-1-1, Table A.1 [8], while the mean structural steel strength f_{ym}, and the elastic modulus E_y are calculated according to prEN 1993-1-1 Table E.1 [9] and [82]. The mean values for geometric parameters of the structural steel such as the height of the steel profile h_p, the width b_p, thickness of the web t_w, thickness of the flange t_f, are chosen the same as the nominal values according to prEN 1993-1-1 Table E.1 [9] and [81]. Regarding the initial geometric imperfection, the mean value of $L/1000$ is selected, with a 25% coefficient of variation (COV), covering the range between 0 and $L/500$ in the worst cases, while concerning residual stresses, the mean value is chosen the same as the nominal value $\sigma_{rs} = 0.5 \cdot 235\ MPa$ with a 5% coefficient of variation (C0V) in accordance with [21].

Regarding the number of simulations, a series of two thousand (2000) Latin Hypercube Samples (LHS) per each column length were executed. The convergence study presented in

sub-chapter 3.3.3 showed that when the sample size is higher than one thousand simulation, the values obtained are particularly close to the true mean and standard deviation.

In this study, each parameter presented in Table 8.2 is assumed an independent variable, and no correlation between random variables is included in the analyses.

Table 8.2 Summary of random variables for PCEC column

Symbol	Parameter	Mean	COV	Distribution
f_c	Concrete compressive strength	$f_{ck} + 8$	0.15	Log-normal
f_{ct}	Concrete tensile strength	$1.1 \cdot f_{ck}^{1/3}$	0.30	Log-normal
f_y	Steel yield stress	$1.2 \cdot f_{yk}$	0.07	Log-normal
f_s	Reinforcement yield stress	$1.078 \cdot f_{sk}$	0.04	Log-normal
E_c	Concrete elastic modulus	$9500 \cdot f_{cm}^{1/3}$	0.15	Log-normal
E_y	Steel elastic modulus	$E_{y,nom}$	0.03	Log-normal
w_0	Geometrical imperfection	$L/1000$	0.25	Normal
σ_{rs}	Residual stresses	$\sigma_{rs,nom}$	0.05	Normal
h_p	Height of steel profile (concrete)	$h_{p,nom}$	0.009	Normal
b_p	Width of steel profile (concrete)	$b_{p,nom}$	0.009	Normal
t_f	Thickness of the steel flange	$t_{f,nom}$	0.025	Normal
t_w	Thickness of the steel web	$t_{w,nom}$	0.025	Normal
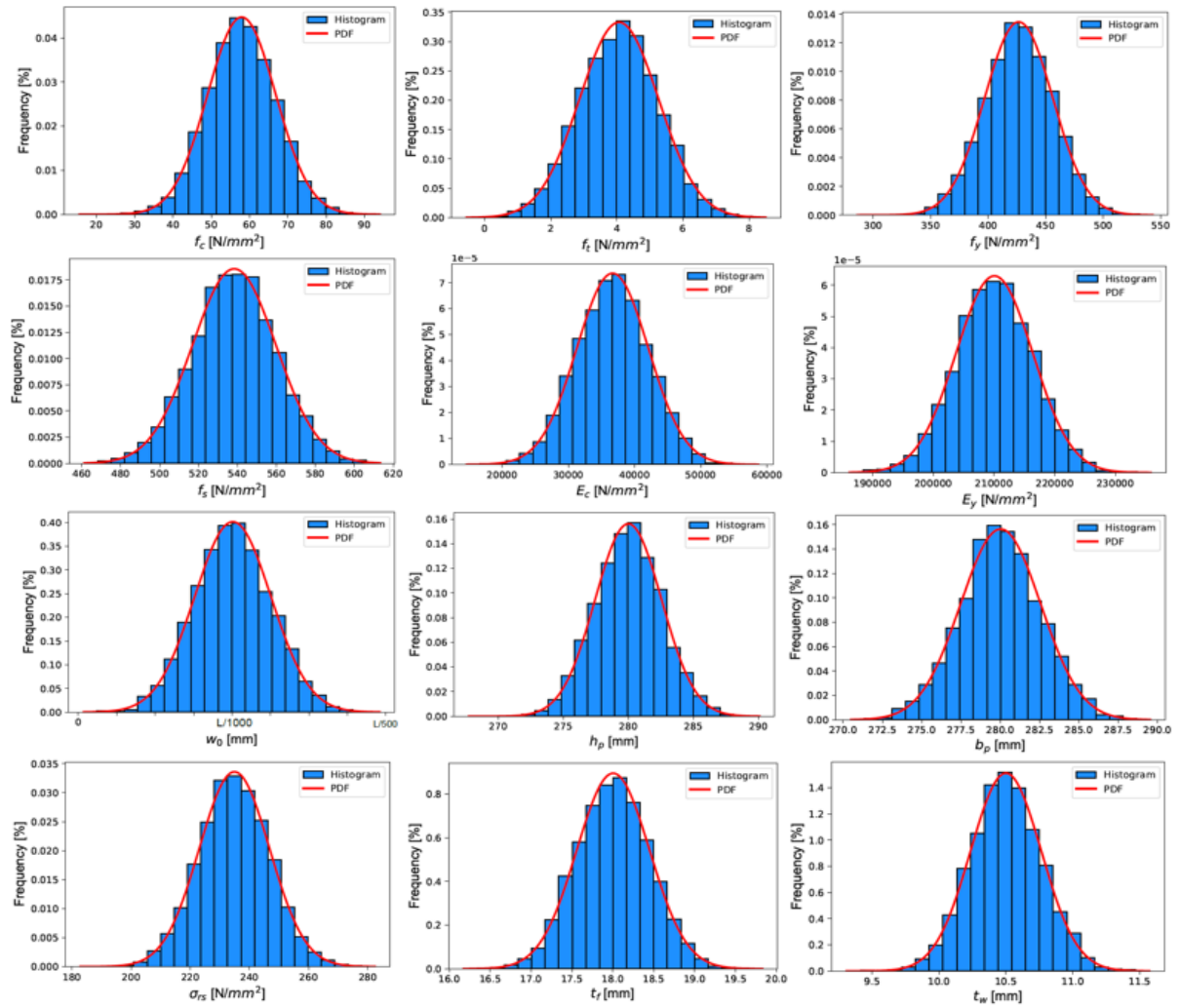
Figure 8.1 Probability Density Function (PDF) for the random variables of PCEC column

8.2.3 Results of reliability analysis for (PCEC)

The purpose of the reliability analysis is to investigate the safety of the general method for the design of composite columns under compressive force according to prEN1994-1-1 [3]. Typically, the buckling resistance of the composite column under compressive load is presented using reduction factor χ and corresponding non-dimensional slenderness $\bar{\lambda}$, which are calculated according to EN 1993-1-1 [16]. On the other hand, from reliability analysis, the results obtained are in the form of Probability Density Function (PDF) defined by the mean μ_R, standard deviation σ_R, and skewness κ as it is presented in Figure 8.2 for PCEC columns with a length of 4 meters. This represents the statistical distribution of the column's resistance.
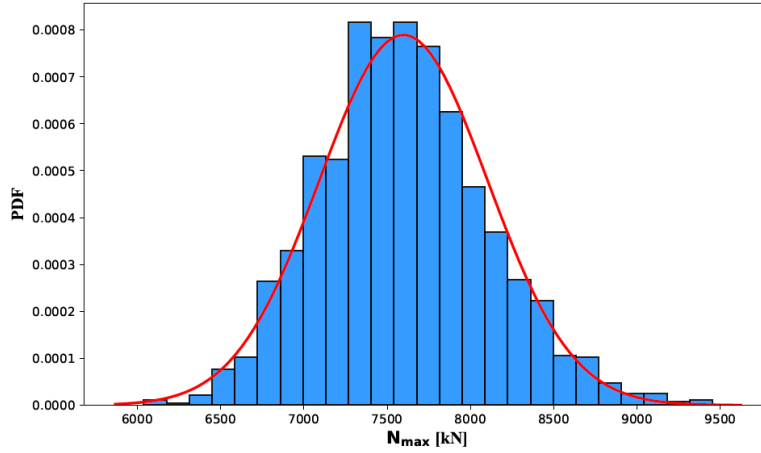
Figure 8.2 Resistance of the 4 m PCEC column described by log-normal distribution

To express the results from SFEA in non-dimensional form, it is necessary to calculate the reduction factor χ as:

$$\chi = \frac{N_{d,SFEM}}{N_{pl,Rd}} \tag{8.2}$$

where, $N_{pl,Rd}$ is the design plastic resistance of composite cross-section calculated according to Equation (2.24), and $N_{d,SFEM}$ is the design resistance from non-linear SFEA as it is described in Chapter 2.9, which for the log-normal distribution function of the column resistance is defined as:

$$N_{d,SFEM} = \frac{\mu_R \cdot [exp(-\alpha_R \beta V_R)]}{\gamma_{Rd}} \tag{8.3}$$

where, μ_R and V_R are the mean and coefficient of variation obtained from non-linear SFEA, $\alpha_R = 0.8$ is FORM sensitivity factor, $\beta = 3.8$ is the reliability index, and $\gamma_{Rd} = 1.06$ is model uncertainty factor assuming a medium model uncertainty according to EN 1992-2 [80] and *fib* Model Code [1], or in case that experimental data are available, this factor can be defined as the ration between experimental results and predicted capacity.

Figure 8.3 shows the results of the non-linear Stochastic Finite Element Analysis (SFEA) and the comparison with the general method (GM) and the simplified method (European buckling

curve) according to [3], using the reduction factor χ and corresponding non-dimensional slenderness $\bar{\lambda}$ about the weak axis (z-z).
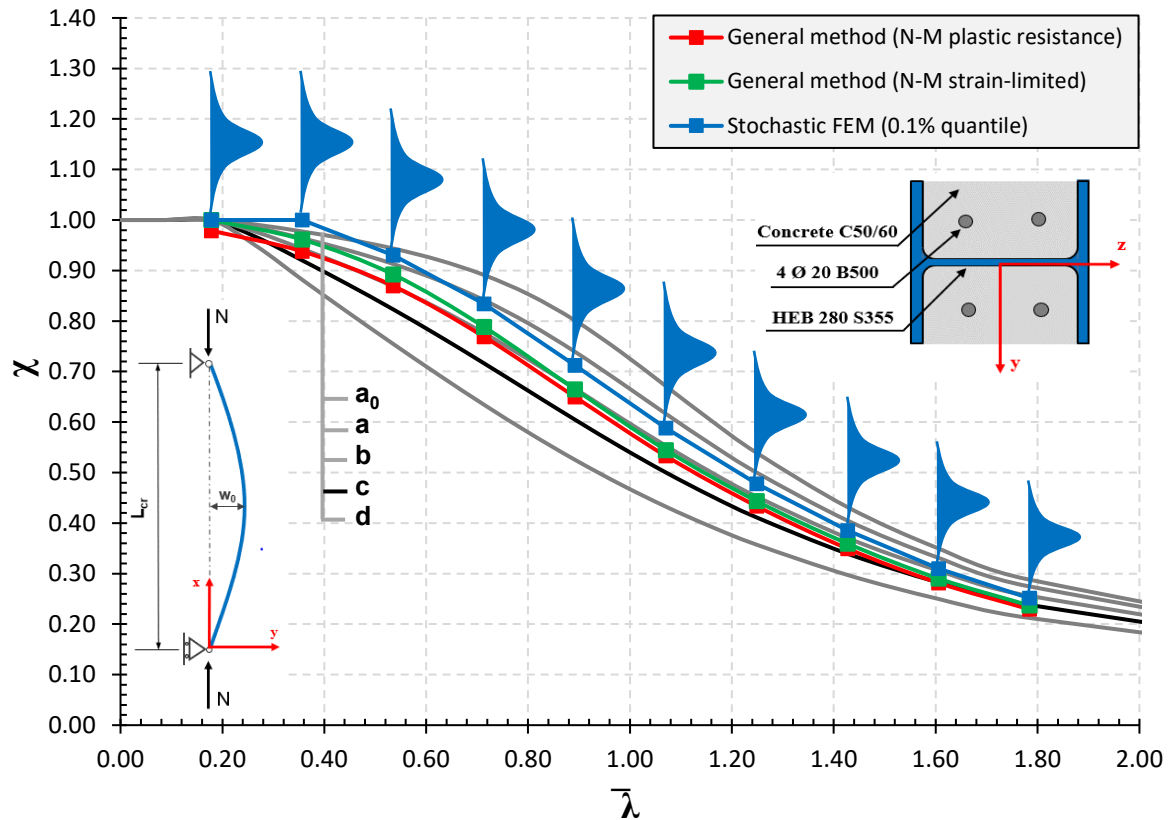
Figure 8.3 Comparison of SFEM with the general and the simplified method for PCEC column

According to the simplified method, for buckling about the weak axis (z-z), the partial concrete composite column is classified in *buckling curve c* (black line in Figure 8.3), while according to the general method this column is classified between *buckling curve b* and *buckling curve c.* On the other hand, according to nonlinear SFEA in all the considered lengths, both, the general method based on plastic and strain-limited N-M interaction diagram, satisfy the safety level required by EN 1990 [5], for a normal building with a reference period of 50 years at ultimate limit state. The results indicate that the resistance follows a log-normal distribution with small positive skewness, and an almost constant reliability level through all considered lengths, with a slightly wider distribution of the resistance for columns with short lengths, indicating that the uncertainties have more impact in stocky columns compare to

slender one. This is due to the fact that, the majority of the material uncertainty in concrete comes from its compressive strength, which is the main factor governing the resistance of the stocky columns which is demonstrated with sensitivity analysis given subsequently. This can be observed also in Figure 8.4 as the safety factor obtained from SFEM analysis is presented together with the overall safety factor γ_0 from the general method.
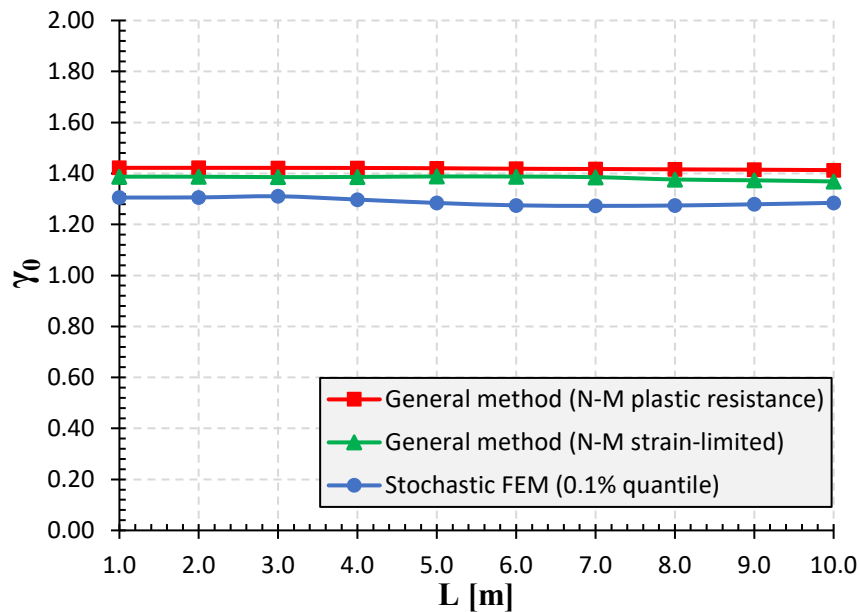
Figure 8.4 Safety factor for PCEC column

The safety level provided by the simplified method as well as the general method according to [3] in comparison with the safety level required by EN 1990 [5] for the PCEC column with $L = 4.0\ m$ is shown also in Figure 8.5 using the probability density function (PDF) of the resistance obtained from SFEM analysis. The results show that, even with the discrepancy between the resistance obtained from the general method and the simplified method, according to probabilistic analysis both methods satisfy the safety level required by Eurocode 0 EN 1990 [5] and are safe to be used for design.
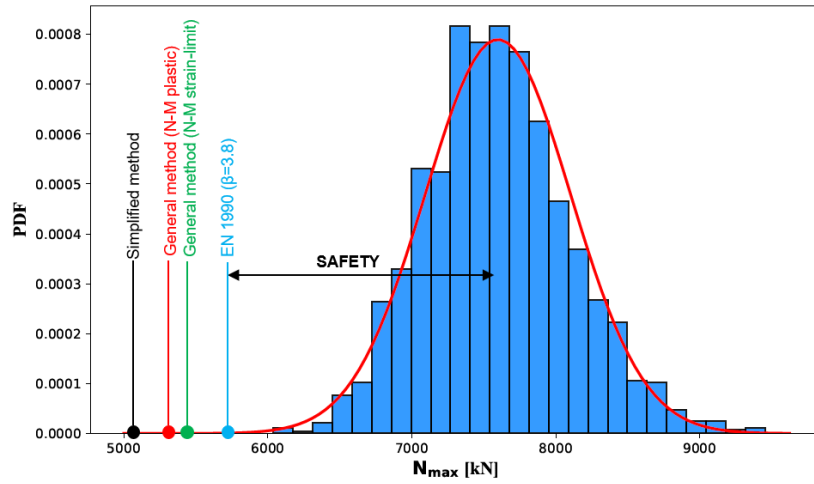
Figure 8.5 Maximum resistance obtained from SFEM for PCEC column with L=4.0 m

Moreover, Figure 8.6 shows the correlation between the maximum load (resistance) and the generated random variables for a 4-meter column. For columns with short and intermediate slenderness ratios as the 4-meter column, the resistance N_{max} of the column is strongly correlated with concrete compressive strength f_{cm} and steel yield stress f_{ym}, as the increase/decrease of the concrete strength or the yield stress of the steel, also increases/decreases the overall resistance of the partial concrete encased composite column.
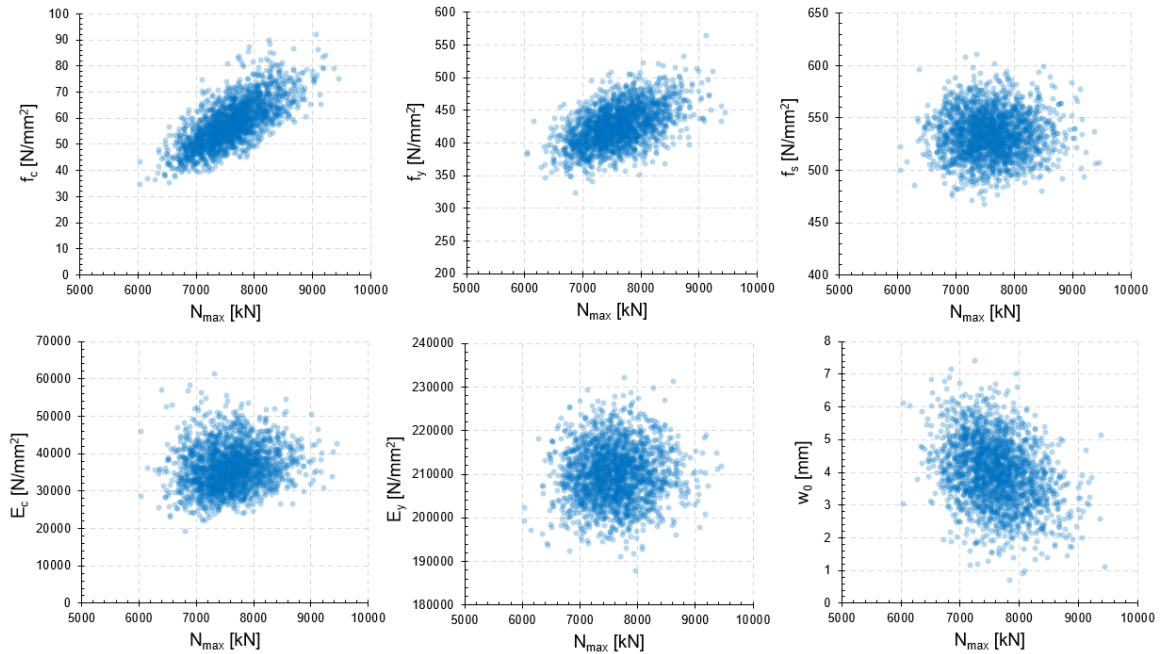
Figure 8.6 Correlation between column resistance and random variables for PCEC column with L=4.0 m

On the other hand, as expected, between the resistance of the column and geometric imperfection w_0, there is a negative correlation as the increase of imperfection reduces the overall resistance of the column as shown in Figure 8.6. While for other parameters such as the height of the steel profile h_p, the width b_p, thickness of the web t_w, and the thickness of the flange t_f, there is no strong correlation with maximum resistance. On the other hand, concerning Figure 8.7 where it is shown the correlation between the maximum load (resistance) and the generated random variables for a 10-meter column, a strong correlation is observed between the resistance N_{max} with the elastic modulus of steel E_s and the elastic modulus of concrete E_c, rather than concrete compressive strength f_{cm} and steel yield stress f_{ym}, as the increase/decrease of one of these parameters increases/decreases also the overall resistance of the column. This is understandable since for columns with a high slenderness ratio the maximum resistance is close to the Eulerian buckling load (critical load), which is strongly related to the elastic modulus of steel and concrete. While, with geometric imperfection w_0, the negative correlation becomes more significant as the length of the column is increased.
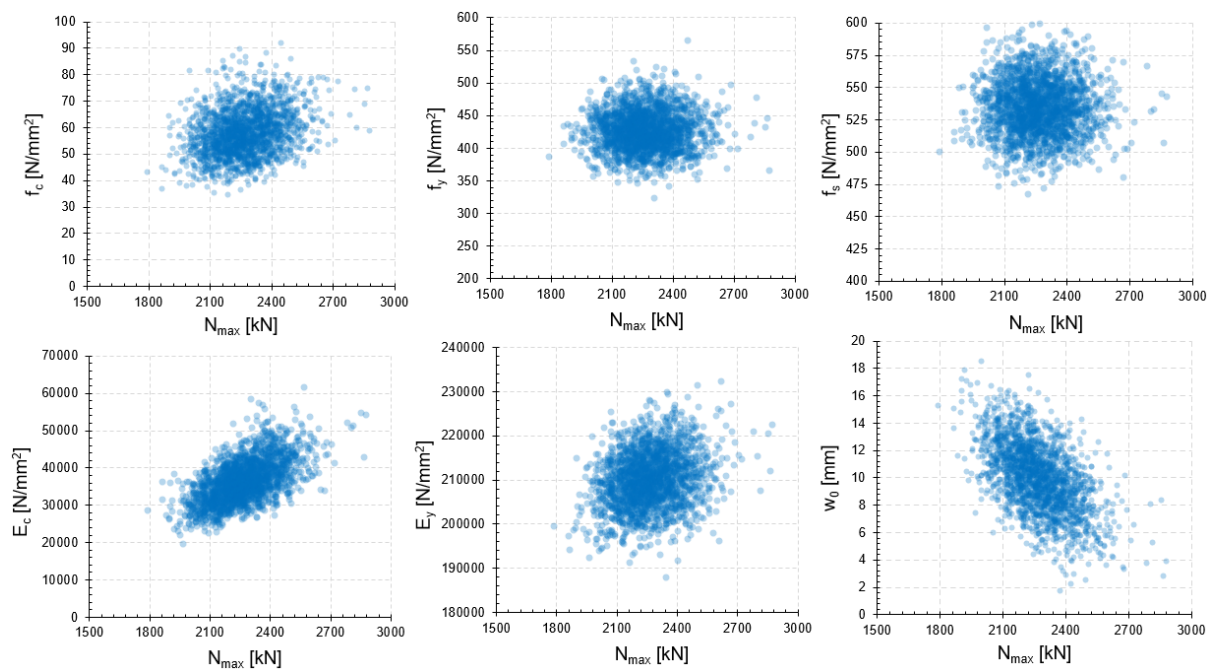
Figure 8.7 Correlation between column resistance and random variables for PCEC column with L=10.0 m

8.2.4 Results of sensitivity analysis for PCEC

As explained in Chapter 3.4, the aim of the sensitivity analysis is to give information on how much each input random variable influences the behaviour of the structural system e.g., (composite columns in steel and concrete under compressive force).

Sensitivity analysis is performed using the Sobol indices method [10], while to generate samples, The Latin Hypercube Sampling (LHS) is used. Similar to reliability analysis, the number of simulations, per each column length is two thousand (2000) Latin Hypercube Samples (LHS). The random variables and their distribution presented in Table 8.2 are used also for the sensitivity analysis.

Figure 8.8 and Figure 8.9 show the results of sensitivity analysis for partial concrete encased (PCEC) columns for different lengths varying from 2 m up to 10 m. For the sake of clarity, the very small values of the sensitivity indices are not depicted. In the x-axis are shown the random variables considered for reliability analysis while in the y-axis are shown *The Main* and *The Total* effect of each random variable on the scale between zero and one hundred percent. *The Main Sobol index* measures the sensitivity of each random variable to the quantity of interest (load-bearing capacity) without considering the interaction with other random variables, while the *Total Sobol index* also considers the interaction between random variables [64].

Based on the initial analysis of the findings, it can be understood that a linear relationship exists between the random variables and the column's length, whereby a linear increase of the column's length causes linear variation in the random variables. The results indicate that, for columns with short and intermediate slenderness ratio, the main parameters which influence the resistance of PCEC columns are concrete compressive strength f_{cm} and steel yield stress f_y. However, as the length of the column is increased the effect of the concrete compressive strength f_{cm}, as well as the steel yield stress f_y is decreased. For columns with a high slenderness ratio (high column length) when the load-carrying capacity is close to the Eulerian buckling load, the overall resistance is more sensitive to the elastic modulus of concrete E_{cm} and geometric imperfection w_0. On the other hand, if we sum up the concrete

parameters f_c and E_c on one side and the steel parameters f_y and E_y on the other, the results of the sensitivity analysis indicate that, on average the concrete accounts for 60% of the load-bearing capacity of the PCEC column under centric load, while the steel contribution is around 20%. Regarding the geometric imperfection, Figure 8.8 and Figure 8.9 show that the increase in the column length also increases the impact of the geometric imperfection varying between 3% to 25%.
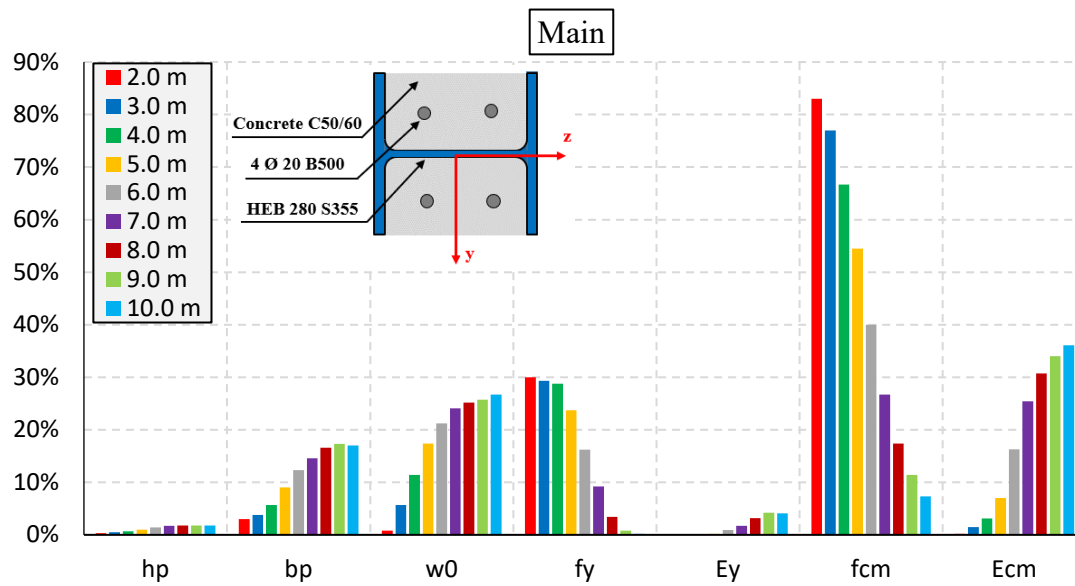
Figure 8.8 Main Sobol index for different lengths of PCEC column
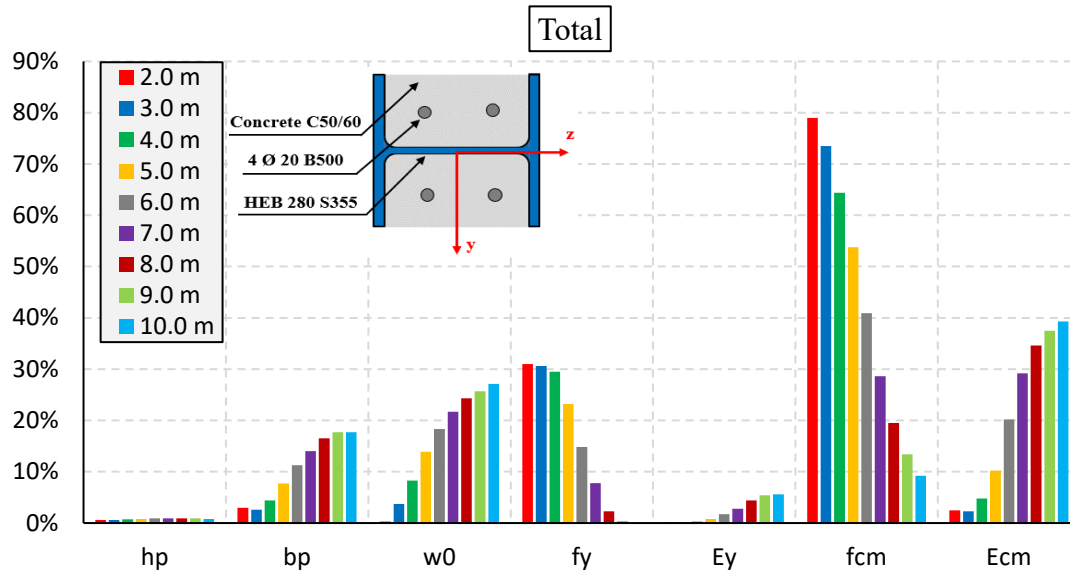
Figure 8.9 Total Sobol index for lengths of PCEC column

8.3 Concrete encased composite column (CEC)

8.3.1 Geometry and boundary conditions of deterministic model

The concrete encased composite (CEC) column model (geometry, material, and boundary conditions) considered for reliability analysis is presented in Figure 7.2. The cross-section is composed of HEB280 with nominal yield strength $f_y = 355 \ N/mm^2$, fully encased in concrete C20/25 with eight longitudinal bars with a diameter of 20 mm and nominal yield strength $f_y = 500 \ N/mm^2$. The column boundary conditions are the same as in the previous case. Similar to the PCEC column, to perform Stochastic Finite Element Analysis, the deterministic model is transformed into a probabilistic one by considering all the geometric and material parameters as random variables except the length L, which is kept deterministic. However, the analyses were performed by varying the length of the column to cover all the column slenderness between $0.2 \leq \overline{\lambda} \leq 2.0$ as it is shown in Table 8.3.

Table 8.3 Length and non-dimensional slenderness of considered (CEC)

L [m]	2.0	3.0	4.0	5.0	6.0	7.0	8.0	9.0	10.0	12.0	15.0
$\overline{\lambda}_{nom}$	0.23	0.35	0.47	0.59	0.70	0.82	0.94	1.05	1.17	1.40	1.76

Probability density function of CEC column Table 8.4 presents the list of the parameters considered as random variables that carry the most uncertainties for the CEC column defined by normal and log-normal distribution based on recommendations of JCSS Model Code [46], prEN1992-1-1 [8], and prEN 1993-1-1 [9], while in Figure 8.10 are presented the probability density function (PDF) of concrete compressive strength f_c, steel yield stress f_y, and elastic modulus of concrete E_c, and steel E_y, as the main random variables which govern the resistance of the CEC column.

Table 8.4 Summary of random variables for CEC column

Symbol	Parameter	Mean	COV	Distribution
f_c	Concrete compressive strength	$f_{ck} + 8$	0.15	Log-normal
f_{ct}	Concrete tensile strength	$0.3 \cdot f_{ck}^{2/3}$	0.30	Log-normal
f_y	Steel yield stress	$1.2 \cdot f_{yk}$	0.07	Log-normal
f_s	Reinforcement yield stress	$1.078 \cdot f_{sk}$	0.04	Log-normal
E_c	Concrete elastic modulus	$9500 \cdot f_{cm}^{1/3}$	0.15	Log-normal
E_y	Steel elastic modulus	$E_{y,nom}$	0.03	Log-normal
w_0	Geometrical imperfection	$L/1000$	0.25	Normal
h_c	Heigh of the concrete	$h_{c,nom}$	0.015	Normal
b_c	Width of the concrete	$b_{c,nom}$	0.015	Normal
h_p	Height of steel profile	$h_{p,nom}$	0.009	Normal
b_p	Width of steel profile	$b_{p,nom}$	0.009	Normal
t_f	Thickness of the steel flange	$t_{f,nom}$	0.025	Normal
t_w	Thickness of the steel web	$t_{w,nom}$	0.025	Normal
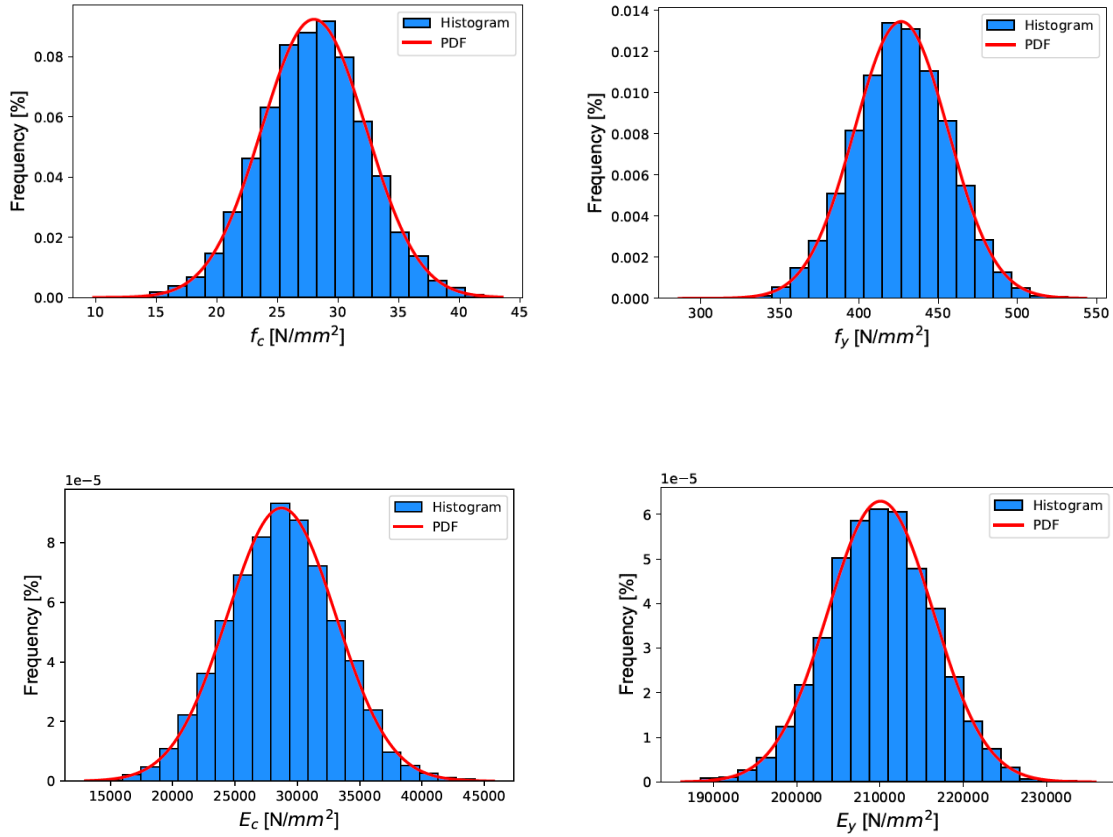
Figure 8.10 Probability Density Function (PDF) for some of the random variables of CEC column

The mean concrete compressive strength f_{cm}, the corresponding mean elastic modulus of concrete E_{cm} and the mean concrete tensile strength f_{ctm} are calculated according to prEN1992-1-1, Table 5.1 [8]. The mean reinforcement steel strength f_{sm} is calculated according to prEN1992-1-1, Table A.1 [8], while the mean structural steel strength, f_{ym} and the elastic modulus E_y are calculated according to prEN 1993-1-1 Table E.1 [9]. The mean values for cross-section parameters of the structural steel and concrete are chosen the same as the nominal values of the deterministic model according to JCSS Model Code [46], and prEN 1993-1-1 [9]. On the other hand, the geometric imperfection w_0 was selected the same as in the case of PCEC column with the mean value of $L/1000$ and 25% coefficient of variation (COV), varying between 0 and $L/500$ in the worst cases. Regarding the number of simulations similar to PCEC column, a series of two thousand (2000) Latin Hypercube Samples (LHS) per each column length were executed.

8.3.2 Results of reliability analysis for CEC column

Figure 8.11 shows the results of the SFEM analysis and the comparison with the general method (GM) and the simplified method according to prEN1994-1-1 [3] using reduction factor χ and corresponding non-dimensional slenderness $\bar{\lambda}$ about the weak axis (z-z). For buckling about the weak axis, according to the simplified method as well as the general method, the CEC column is classified in *buckling curve c* (black line in Figure 8.11)*.* On the other hand, according to probabilistic analysis (SFEM) in all considered lengths, both, the general method based on plastic and strain-limited N-M interaction diagram, satisfy the safety level required by EN 1990 [5] for a normal building with a ref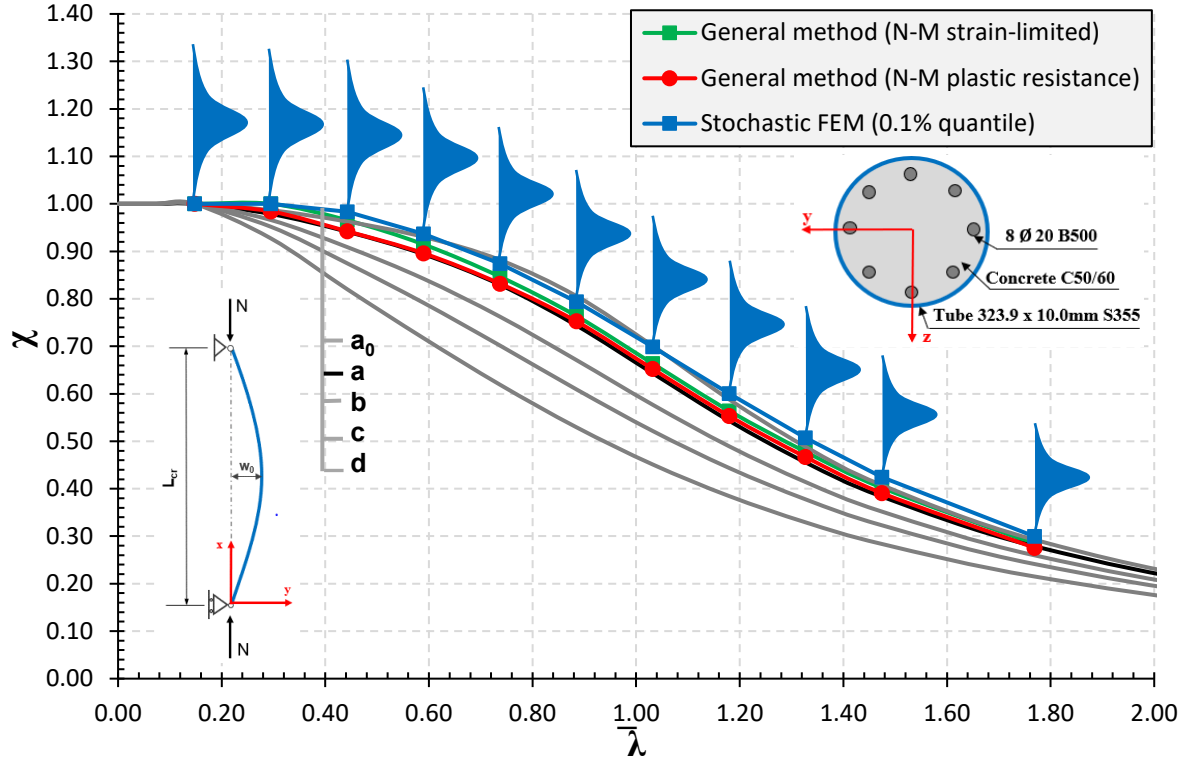erence period of 50 years at ultimate limit state. Moreover, the results indicate that the resistance follows a log-normal distribution with small positive skewness, and non-constant reliability level through considered lengths, with a significantly wider distribution of the resistance for columns with long lengths, indicating that the uncertainties have more impact in slender columns compared to stocky one. This is due to the fact that, the majority of material uncertainty are in concrete compressive strength and elastic modulus of concrete, which are the main parameters governing the resistance of the CEC columns. This can be observed also from Figure 8.12 as the safety factor obtained from SFEM analysis is presented together with the overall safety factor γ_0 from the general method.
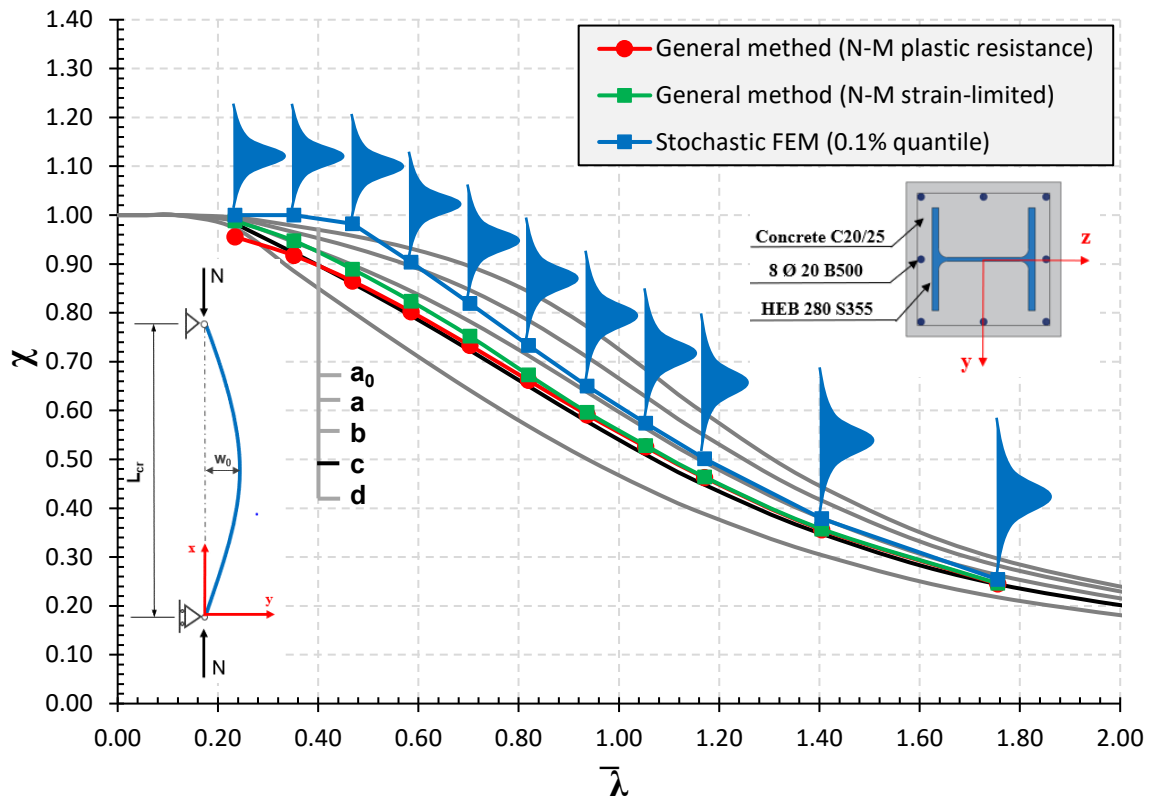
Figure 8.11 Comparison of SFEM with the general and the simplified method for CEC column
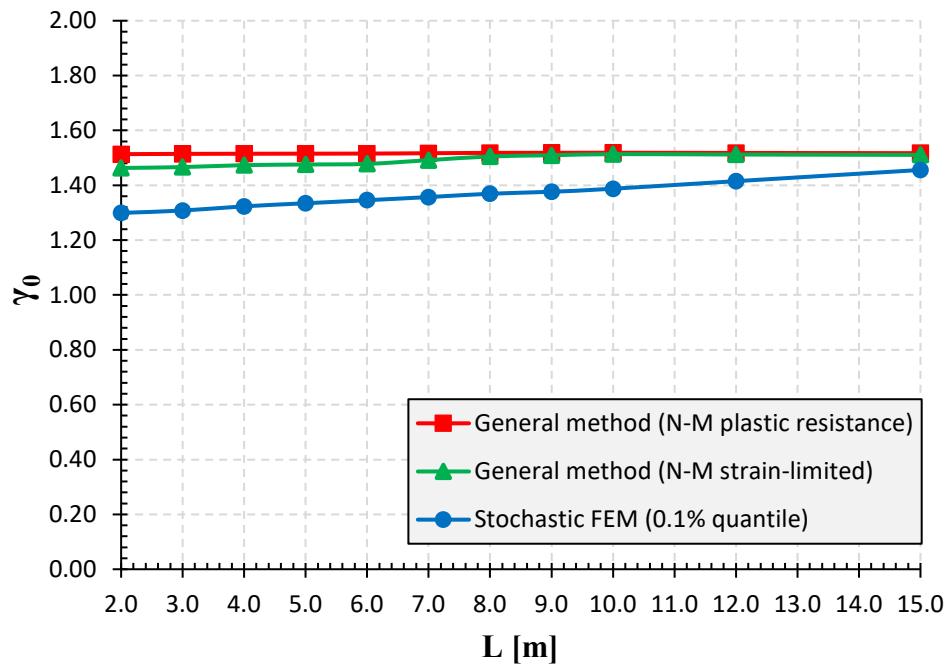
Figure 8.12 Safety factor for CEC column

The safety level provided by the simplified method as well as the general method according to prEN1994-1-1 [3] in comparison with the safety level required by EN 1990 [5] for the CEC column with $L = 4.0\ m$ is shown also in Figure 8.5 using the probability density function (PDF) of the resistance obtained from SFEM analysis. As can be observed, there is a significant gap between the safety level provided by prEN1994-1-1 [3] (the simplified and the general method), and the safety level required by EN 1990 [5] indicating that prEN1994-1-1 [3] provide very conservative results.
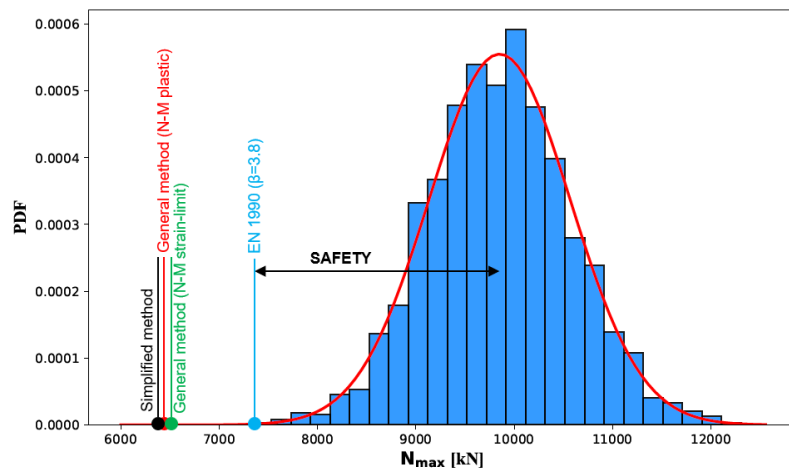
Figure 8.13 Maximum resistance obtained from SFEM for CEC column with L=4.0 m

Moreover, Figure 8.14 shows the correlation between the maximum load and the generated random variables for a CEC column with $L = 4.0\ m$. As can be observed, there is a strong positive correlation between maximum force N_{max} and concrete compressive strength f_{cm}, as the increase of the concrete strength, also increases the overall resistance of the concrete encased composite column. On the other hand, as expected, between the resistance of the column and geometric imperfection w_0 there is a negative correlation as the increase of imperfection reduces the overall resistance of the column. Regarding the other parameters, ther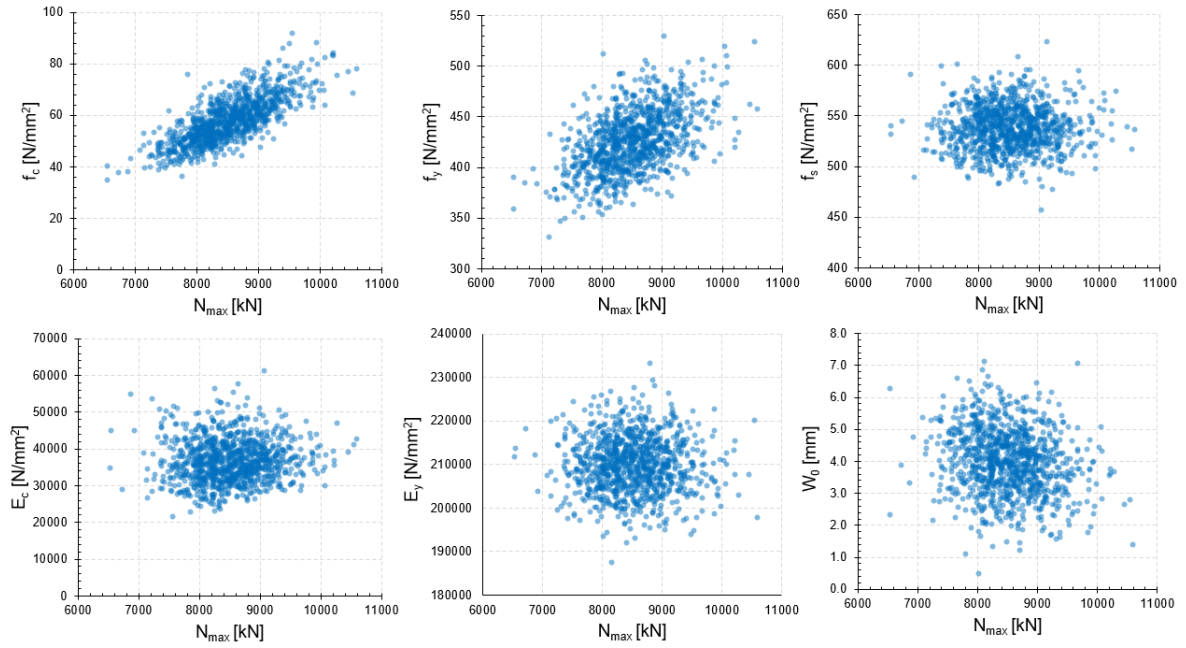e is no strong correlation with the resistance of the column as the concrete compressive strength f_c is the main parameter which governs the load-bearing capacity. Moreover, concerning Figure 8.15 where it is shown the correlation between the maximum load and the generated random variables for a CEC column with $L = 10.0\ m$, the impact of the elastic modulus of concrete E_c becomes important with the increase of the column's length, while

the concrete compressive strength f_{cm} remains the main parameter which governs the load-bearing capacity of the column compared to other random variables.
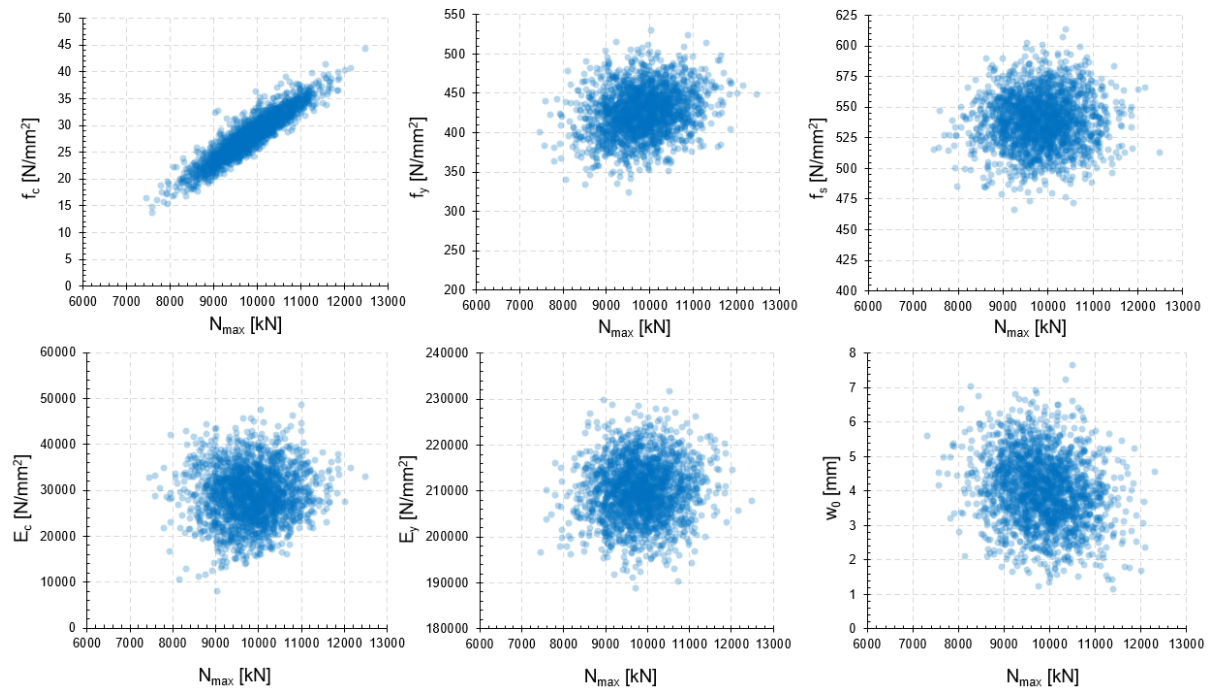
Figure 8.14 Correlation between load-bearing capacity and random variables for CEC column with L = 4.0 m
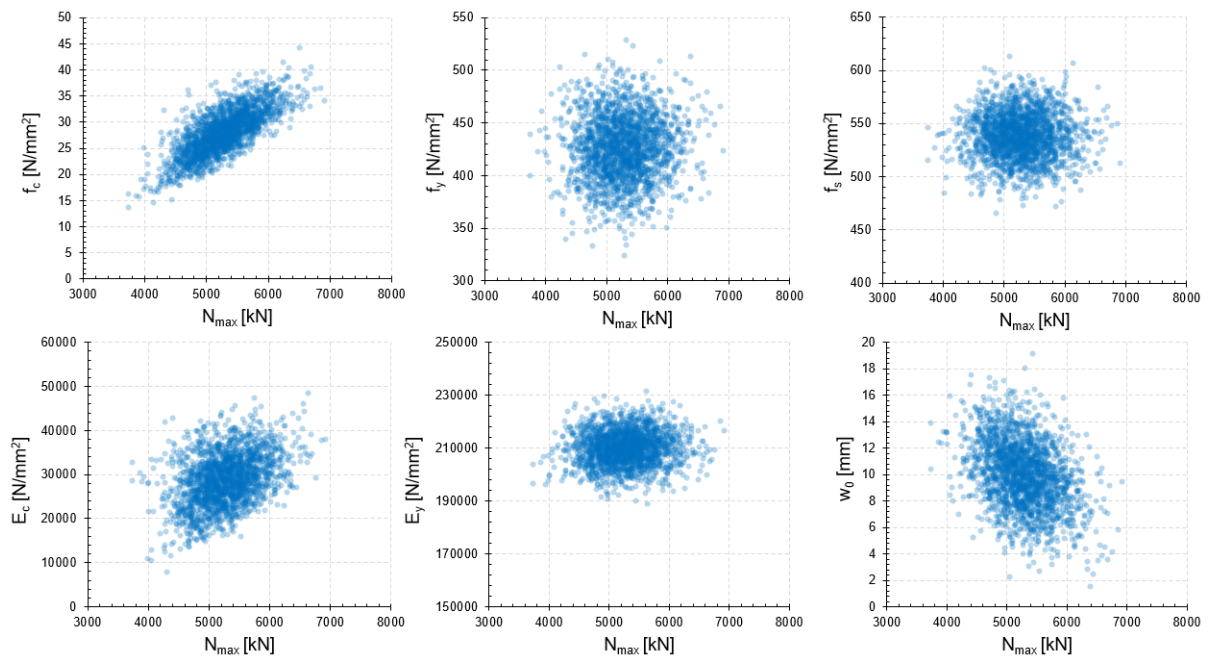
Figure 8.15 Correlation between load-bearing capacity and random variables for CEC column with L =10.0 m

8.3.3   Results of sensitivity analysis for CEC column

Similar to reliability analysis, the number of simulations for sensitivity analysis is 2000 per each column length. The random variables and their distribution presented in Table 8.4 are used also for sensitivity analysis. Figure 8.16 and Figure 8.17 shows the results of sensitivity analysis for concrete encased composite (CEC) column for different lengths varying from 3 m to 10 m. For the sake of clarity, the very small values of the sensitivity indices are not depicted. In the x-axis are shown the random variables considered for reliability analysis while in the y-axis it is shown *The Main effect* and *Total effect* of each random variable on the scale between zero and one hundred percent. *The Main Sobol index* measures the sensitivity of each random variable to the quantity of interest (load-bearing capacity) without considering the interaction with other random variables, while the *Total Sobol index* also considers the interaction between random variables. The results indicate that, for all considered lengths between 3 m and 10 m, the main parameter which governs the resistance (the load carrying capacity) of the CEC column under centric load, is the concrete compressive strength f_{cm}, as the contribution varies between 90% for 3 m column and 60% for 10 m column. Contrary to the PCEC column, the impact of the steel section is less significant compared to concrete for all considered lengths. If we sum up the concrete parameters f_c and E_c on one hand and the steel parameters f_y and E_y on the other, the results of sensitivity analysis indicate that on average the concrete accounts for 90% of the load-bearing capacity of the CEC column under centric load, while the steel contribution is around 3%. On the other hand, regarding the geometric imperfection w_0, Figure 8.16 and Figure 8.17 show that the sensitivity of the geometric imperfection is relatively small compared to f_{cm}. As in previous case, also for CEC columns a linear relationship exists between the random variables and the column's length, whereby a linear increase of the column's length cause linear variation in the random variables.
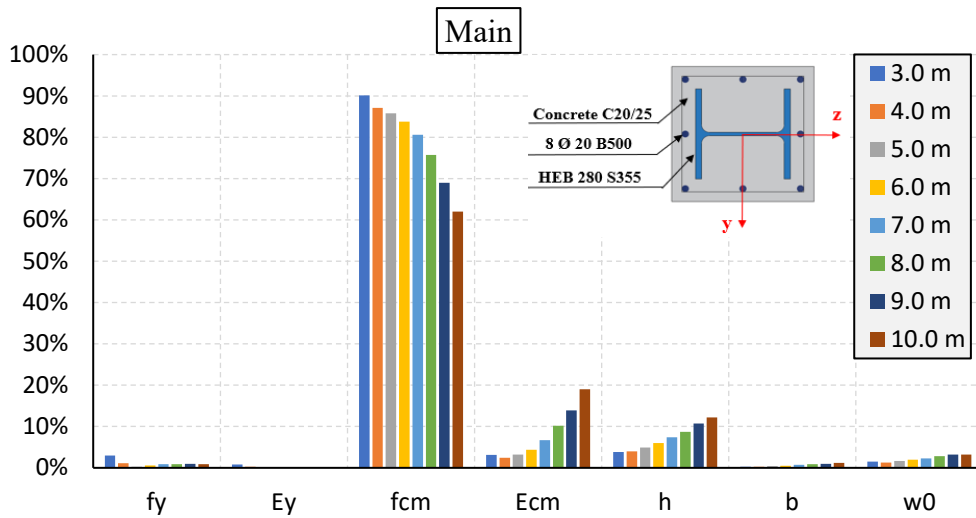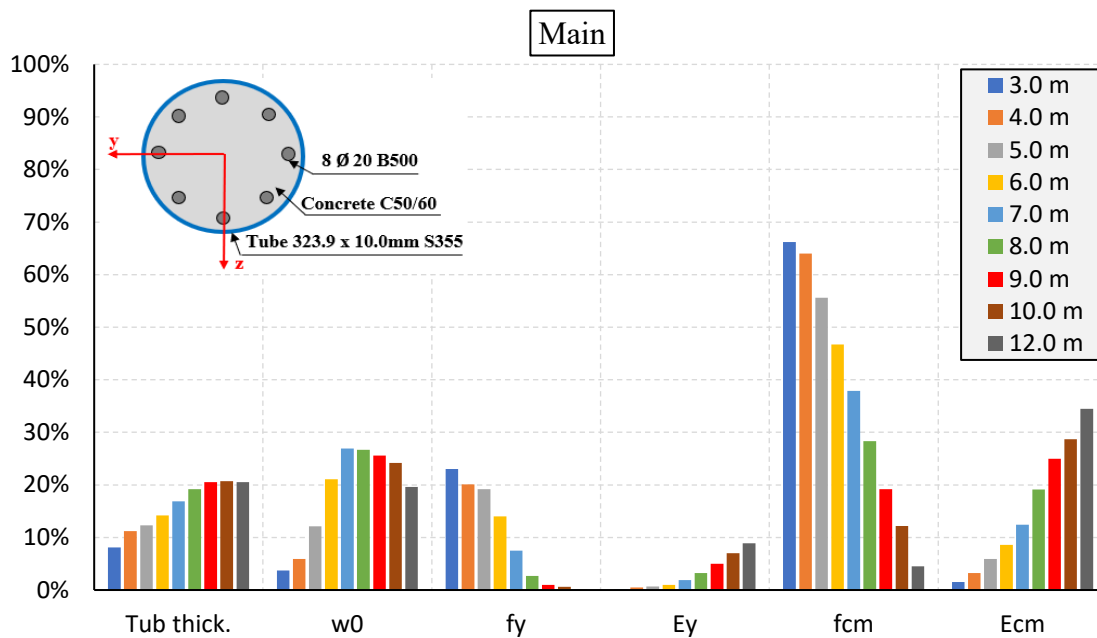
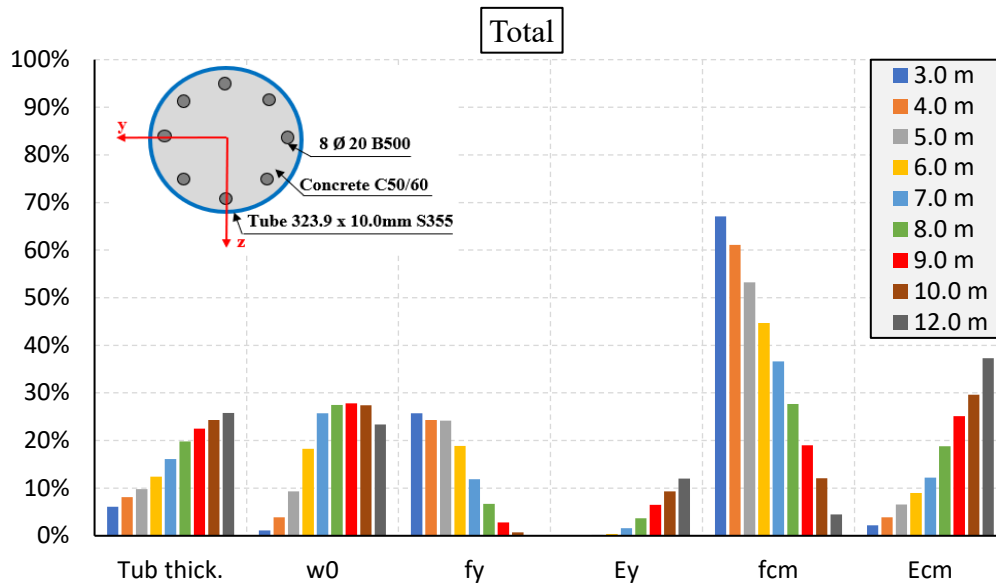*Figure 8.16 Main effect for different lengths of CEC column*
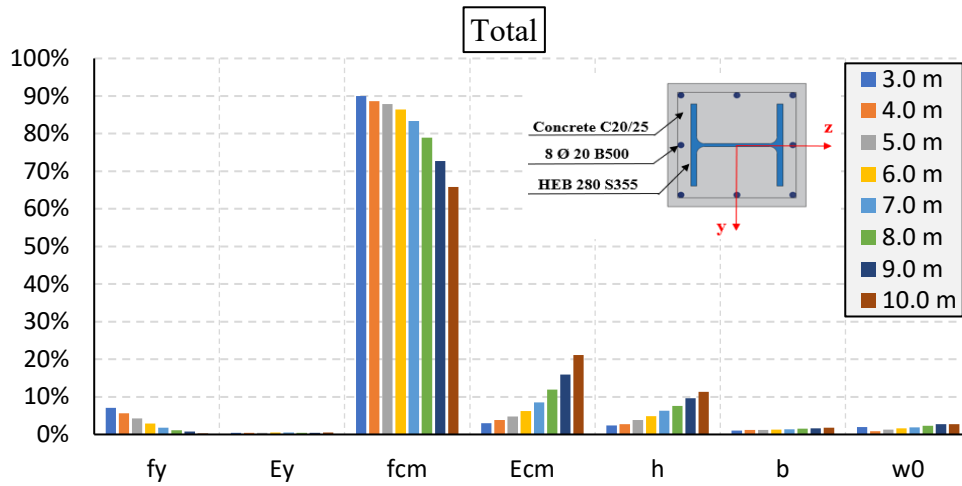
Figure 8.17 Total effect for different lengths of CEC column

8.4 Concrete filled steel tube (CFST)

8.4.1 Geometry and boundary condition of deterministic model

The concrete-filled steel tube (CFST) column model (geometry, material, and boundary conditions) considered for reliability analysis is presented in Figure 7.12. The cross-section is composed circular tube with an outer diameter of $\varnothing 323.9$ mm and thickness of 10 mm with nominal yield strength $f_y = 355 \; N/mm^2$, filled with concrete C50/60, and eight reinforcement bars $\varnothing 20$ mm B500 with nominal yield strength $f_s = 500 \; N/mm^2$. The

column is simply supported with imperfection (statically determined) and subjected to concentrated load. Similar to the previous cases, to perform nonlinear SFEA, the deterministic model is transformed into a probabilistic one by considering all the geometric and material parameters as random variables except the length L, which is kept deterministic. However, the analyses were performed by varying the length of the column to cover the column's slenderness between $0.2 \leq \overline{\lambda} \leq 2.0$ as presented in Table 8.5.

Table 8.5 Length and non-dimensional slenderness of considered (CFST)

L [m]	1.0	2.0	3.0	4.0	5.0	6.0	7.0	8.0	9.0	10.0	12.0
$\overline{\lambda}$	0.15	0.29	0.44	0.59	0.74	0.88	1.03	1.18	1.33	1.47	1.77

8.4.2 Probability density function of CFST column

As in previous cases, Table 8.6 presents the list of the parameters considered as a random variable that carry the most uncertainties for the CFST column defined by normal and log-normal distribution based on recommendations of [46], [8], [9]. Regarding the number of simulations similar to other columns, a series of two thousand (2000) Latin Hypercube Samples (LHS) per each column length were executed.

Table 8.6 Summary of random variables for CFST column

Symbol	Parameter	Mean	COV	Distribution
f_c	Concrete compressive strength	$f_{ck} + 8$	0.15	Log-normal
f_{ct}	Concrete tensile strength	$0.3 \cdot f_{ck}^{2/3}$	0.30	Log-normal
f_s	Reinforcement yield stress	$1.078 \cdot f_{sk}$	0.04	Log-normal
f_y	Tube yield stress	$1.2 \cdot f_{yk}$	0.07	Log-normal
E_c	Concrete elastic modulus	$9500 \cdot f_{cm}^{1/3}$	0.15	Log-normal
E_y	Steel elastic modulus	$E_{y,nom}$	0.03	Log-normal
w_0	Geometrical imperfection	$L/1000$	0.25	Normal
t_{tube}	Thickness of the tube	$t_{tube,nom}$	0.04	Normal
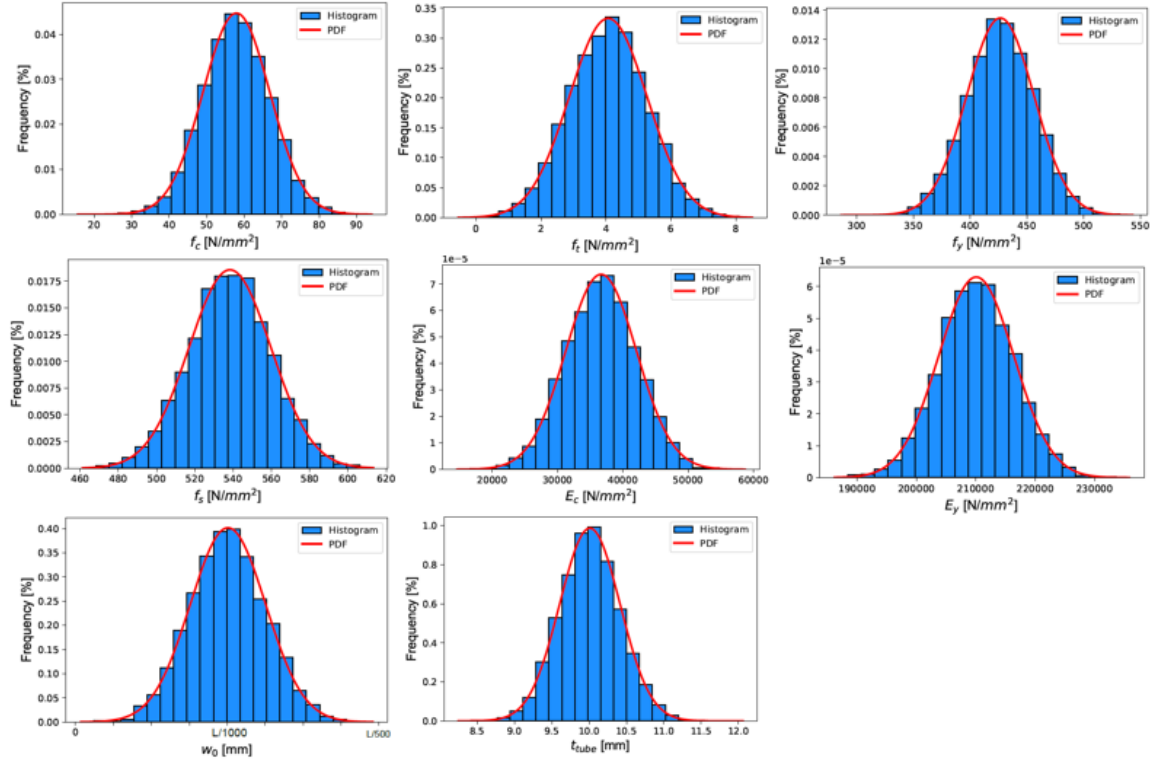
Figure 8.18 Probability Density Function (PDF) for the random variables of CFST column

8.4.3   Results of reliability analysis for CFST column

Figure 8.19 shows the results of the Stochastic Finite Element Method (SFEM) and the comparison with the general method (GM) and the simplified method according to prEN1994-1-1 [3] using reduction factor χ and corresponding non-dimensional slenderness $\bar{\lambda}$ about the weak axis (z-z). For buckling about the weak axis according to the simplified method as well as the general method, the concrete-filled steel tube is classified in *buckling curve a* (black line in Figure 8.19)*. On the other hand, according to SFEM analysis in all considered lengths, both the general method based on plastic and strain-limited N-M interaction diagram, satisfy the safety level required by EN 1990 [5] for a normal building with a reference period of 50 years at ultimate limit state.

Figure 8.19 Comparison of SFEM with the general and the simplified method for CFST column

Moreover, similar to PCEC column, the results indicate that the resistance follows a log-normal distribution with small positive skewness, and a constant reliability level through all considered lengths, with a slightly wider distribution of the resistance for columns with short length, indicating that the uncertainties have more impact in stocky columns compare to slender one. This is due to the fact that, the majority of material uncertainty in concrete comes from concrete compressive strength, which is the primary factor governing the resistance of the stocky columns as it is demonstrated from sensitivity analysis.

Figure 8.20 shows the correlation between the maximum load and the generated random variables for a CFST column with $L = 4.0\ m$. As can be observed, there is a positive correlation between maximum force N_{max} and concrete compressive strength f_{cm}, as the increase of the concrete strength, also increases the overall resistance of the column. On the other hand, as expected, between the resistance of the column and geometric imperfection w_0 there is a negative correlation as the increase of imperfection reduces the overall resistance of the

column. Regarding the other parameters, there is no strong correlation with the resistance of the column.
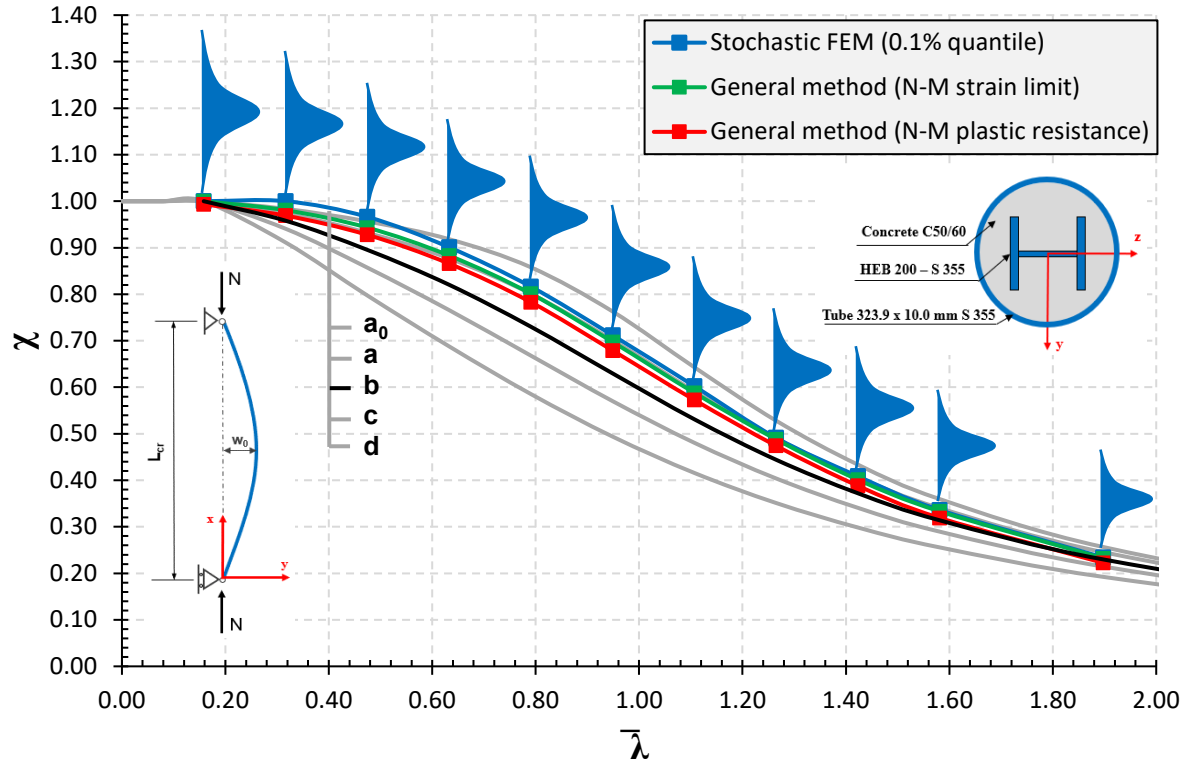

Figure 8.20 Correlation between N_{max} and random variables for CFST column with L = 4.0 m

Concerning Figure 8.21, for slender columns ($L = 10.0\ m$), the resistance N_{max} is strongly correlated with the elastic modulus of concrete E_c, as the increase/decrease of this parameter also increases/decreases the overall resistance of the column. This is understandable since for columns with a high slenderness ratio the maximum resistance is close to the Eulerian buckling load (critical load), which is strongly related to the elastic modulus of concrete. Also, for the CFST slender column ($L = 10.0\ m$), a strong negative correlation is observed between the geometric imperfection w_0 and the resistance N_{max} as the increase of the imperfection induces a reduction of the overall resistance of the column.
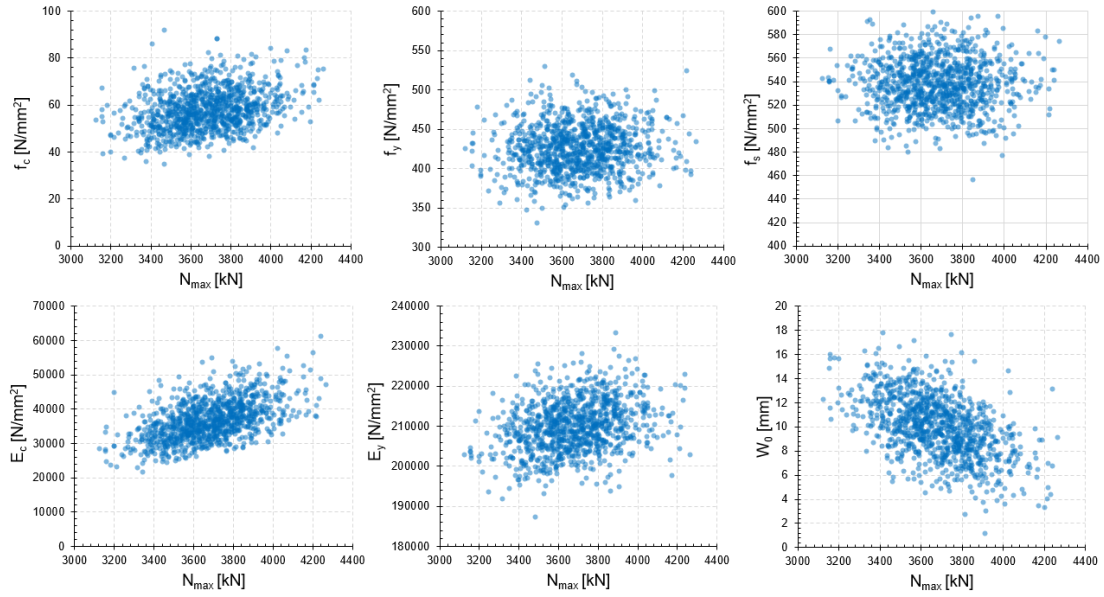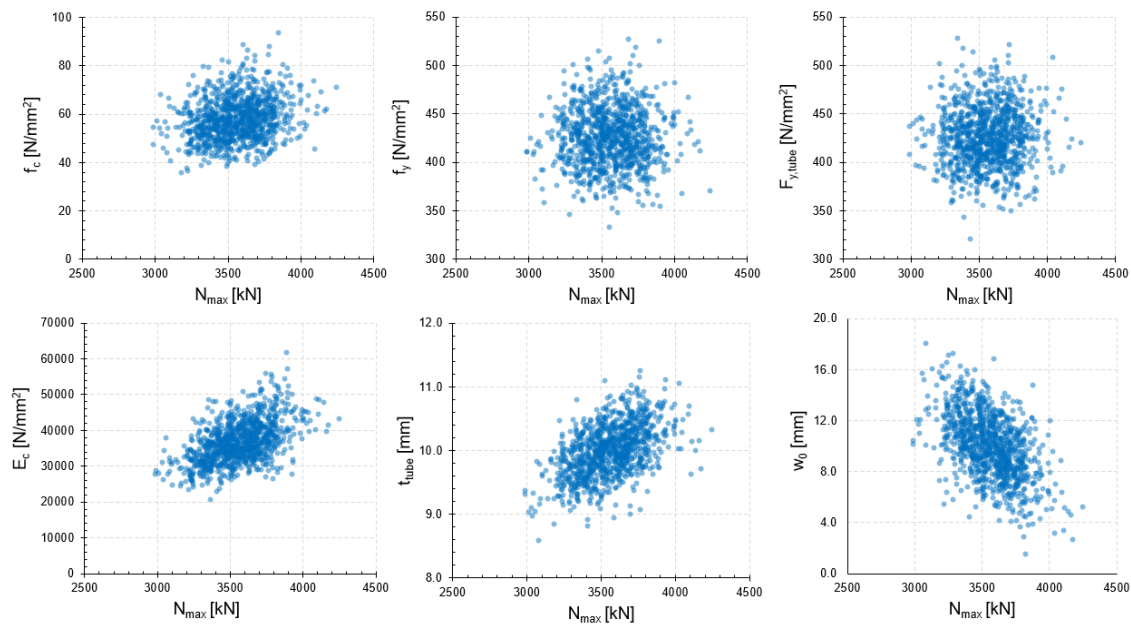
Figure 8.21 Correlation between N_{max} and random variables for CFST column with L = 10.0 m

8.4.4 Results of sensitivity analysis for CFST column

Similar to reliability analysis, the number of simulations, per each column length is two thousand (2000) Latin Hypercube Samples (LHS). The random variables and their distribution presented in Table 8.6 are used also for sensitivity analysis.

Figure 8.22 and Figure 8.23 show the results of sensitivity analysis for the CFST column for different lengths varying from 3 m to 12 m. For the sake of clarity, the very small values of the sensitivity indices are not depicted. In the x-axis are shown the random variables considered for reliability analysis while in the y-axis it is shown *The Main* and *The Total effect* of each random variable on the scale between zero and one hundred percent. *The Main Sobol index* measures the sensitivity of each random variable to the quantity of interest (load-bearing capacity) without considering the interaction with other random variables, while the *Total Sobol index* also considers the interaction between random variables.

The results indicate that, for columns with short and intermediate slenderness, the main parameter which governs the resistance (the load carrying capacity) of the CFST column under centric load, is the concrete compressive strength f_{cm}, as the contribution varies between 65% for 3 m column and 45% for 7 m column, and as the length of the column increases the

resistance becomes more sensitive to the elastic modulus of concrete E_{cm} and tube thickness. On the other hand, also the impact of the geometric imperfection increases with the increase of the column's length as can be observed in Figure 8.22 and Figure 8.23. Moreover, if we sum up the concrete parameters f_c and E_c on one hand and the steel parameters f_y and E_y on the other, the results of sensitivity analysis indicate that on average the concrete accounts for 53% of the load-bearing capacity of the CFST column under centric load, while the steel contribution is around 13%, while the other percentage is attributed to geometric parameters. As in previous case, also for CFST columns, a linear relationship exists between the random variables and the column's length, whereby a linear increase of the column's length cause linear variation in the random variables.

Figure 8.22 Main effect for different lengths of CFST column

Figure 8.23 Total effect for different lengths of CFST column

8.5 Concrete filled steel tube (CFST) with inner I-profile

8.5.1 Geometry and boundary condition of deterministic model

The concrete-filled steel tube (CFST) with an additional inner I-profile column model (geometry, material, and boundary conditions) considered for reliability analysis is presented in Figure 7.12. The cross-section is composed circular tube with an outer diameter of 323.9 mm and thickness of 10 mm with nominal yield strength $f_y = 355\ N/mm^2$, filled with concrete C50/60, and an additional inner steel profile HEB 200 − S355 with nominal yield strength $f_y = 355\ N/mm^2$. The column is simply supported with imperfection (statically determined) and subjected to concentrated load. Similar to the previous cases, to perform nonlinear SFEA, the deterministic model is transformed into a probabilistic one by considering all the geometric and material parameters as random variables except the length L, which is kept deterministic. However, the analyses were performed by varying the length of the column to cover the column's slenderness between $0.2 \leq \overline{\lambda} \leq 2.0$ as shown in Table 8.7.

Table 8.7 Length and non-dimensional slenderness of considered CFST with inner I-profile

L [m]	1.0	2.0	3.0	4.0	5.0	6.0	7.0	8.0	9.0	10.0	12.0
$\bar{\lambda}_{nom}$	0.16	0.32	0.47	0.63	0.79	0.95	1.11	1.26	1.42	1.58	1.90

8.5.2 Probability density function of CFST with inner I-profile column

As in previous cases, Table 8.8 presents the list of the parameters considered as a random variable that carry the most uncertainties for the CFST with an inner I-profile column defined by a normal and log-normal distribution, based on recommendations JCSS Model Code [46], prEN1992-1-1 [8], and prEN 1993-1-1 [9].

Table 8.8 Summary of random variables for CFST column with I-section

Symbol	Parameter	Mean	COV	Distribution
f_c	Concrete compressive strength	$f_{ck} + 8$	0.15	Log-normal
f_{ct}	Concrete tensile strength	$0.3 \cdot f_{ck}^{2/3}$	0.30	Log-normal
$f_{y,p}$	Steel profile yield stress	$1.2 \cdot f_{yk}$	0.07	Log-normal
$f_{y,t}$	Tube yield stress	$1.2 \cdot f_{yk}$	0.07	Log-normal
E_c	Concrete elastic modulus	$9500 \cdot f_{cm}^{1/3}$	0.15	Log-normal
E_y	Steel elastic modulus	$E_{y,nom}$	0.03	Log-normal
w_0	Geometrical imperfection	$L/1000$	0.25	Normal
t_t	Tube thickness	$t_{tube,nom}$	0.04	Normal
h_p	Height of steel profile	$h_{p,nom}$	0.009	Normal
b_p	Width of steel profile	$b_{p,nom}$	0.009	Normal
t_f	Thickness of the steel flange	$t_{f,nom}$	0.025	Normal
t_w	Thickness of the steel web	$t_{w,nom}$	0.025	Normal

8.5.3 Results of reliability analysis for CFST with I-profile column

Figure 8.24 shows the results of the Stochastic Finite Element Method (SFEM) and the comparison with the general method (GM) and the simplified method according to prEN1994-1-1 [3] using reduction factor χ and corresponding non-dimensional slenderness $\bar{\lambda}$ about the weak axis (z-z). For buckling about the weak axis, the concrete-filled steel tube with additional I-profile is classified in *buckling curve b* (black line in Figure 8.19) according to the simplified method, while according to the general method based on plastic and strain-limited N-M interaction diagram, this column is classified between *buckling curve a* and *buckling curve b.* This discrepancy between the simplified method and the general method raises the question regarding the safety of the general method since the results from this method are less conservative. Nevertheless, concerning Figure 8.24, according to probabilistic analysis (SFEM) in all considered lengths, both the general method based on plastic and strain-limited N-M interaction diagram, satisfy the safety level required by EN 1990 [5] for a normal building with a reference period of 50 years at ultimate limit state. However, for very slender columns (e.g., $L = 12.0\ m$) the difference between the SFEM analysis and the general method is very small. Moreover, similar to the CFST column the results indicate that the resistance follows a log-normal distribution with small positive skewness, and a constant reliability level through all considered lengths, with a slightly wider distribution of the resistance for columns with short length (short slenderness ratio), indicating that the uncertainties have more impact in stocky columns compare to slender one.

In addition, Figure 8.25 shows the correlation between the maximum load and the generated random variables for the CFST column with an inner I-profile with $L = 4.0\ m$. As can be observed, there is a positive correlation between maximum force N_{max} and concrete compressive strength f_{cm} and tube yield strength $f_{y,tube}$, as the increase of the concrete strength or the strength of the tube, also increases the overall resistance N_{max} of the column. On the other hand, as expected, between the resistance of the column and geometric imperfection w_0 there is a negative correlation as the increase of imperfection reduces the overall resistance of the column. Regarding the other parameters, there is no strong correlation with the resistance of the column.

Figure 8.24 Comparison of SFEM with the general and the simplified method for CFST column inner I-profile
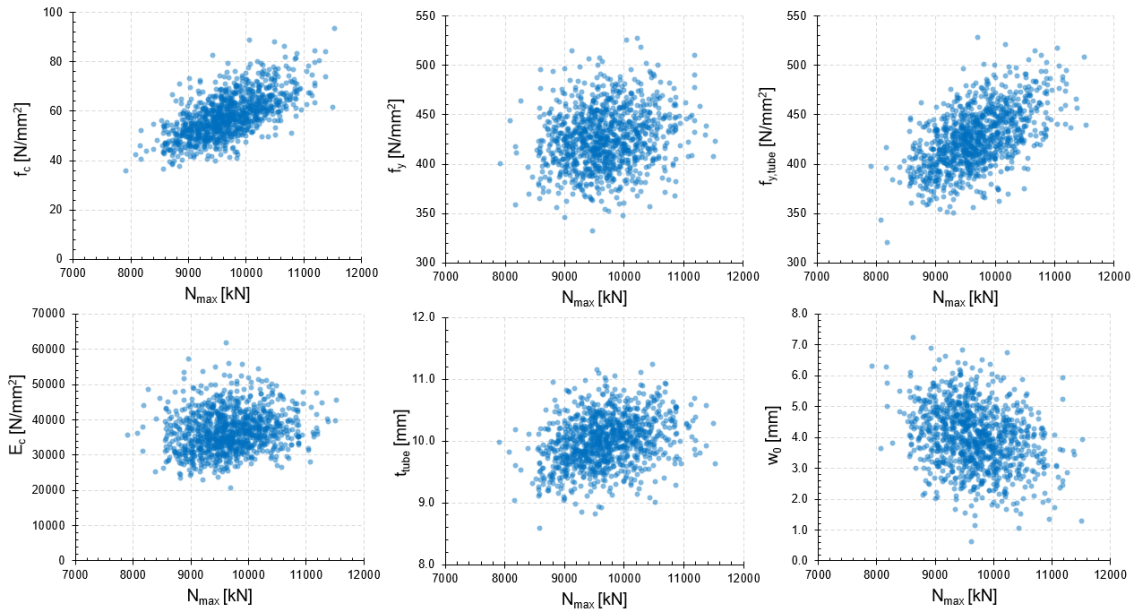
Figure 8.25 Correlation between N_{max} and random variables for CFST column with inner I-profile with L = 4.0 m

Furthermore, with reference to Figure 8.26, for slender columns ($L = 10.0\ m$), the resistance N_{max} is strongly correlated with the elastic modulus of concrete E_c, as the increase/decrease

of this parameter also increases/decreases the overall resistance of the column. This is understandable since for columns with a high slenderness ratio the maximum resistance is close to the Eulerian buckling load (critical load), which is strongly related to the geometry and to the elastic modulus of concrete. Moreover, for the CFST with an additional I-profile slender column ($L = 10.0\ m$), a strong negative correlation is observed between the geometric imperfection w_0 and the resistance N_{max} as the increase of the imperfection induces a reduction of the overall resistance of the column.

Figure 8.26 Correlation between N_{max} and random variables for CFST column with inner I-profile with L = 10.0 m

8.5.4   Results of sensitivity analysis for CFST with I-profile column

Similar to reliability analysis, the number of simulations, per column length is two thousand (2000) Latin Hypercube Samples (LHS). The random variables and their distribution presented in Table 8.8 are used also for sensitivity analysis. Figure 8.27 and Figure 8.28 show the results of sensitivity analysis for the CFST with inner I-profile columns for different lengths varying from 3 m to 10 m. For the sake of clarity, the very small values of the sensitivity indices are not depicted. In the x-axis are shown the random variables considered for reliability analysis while in the y-axis it is shown the main and the total effect of each random variable on the scale between zero and one hundred percent. *The Main Sobol index* measures the sensitivity

of each random variable to the quantity of interest (load-bearing capacity) without considering the interaction with other random variables, while the *Total Sobol index* also considers the interaction between random variables. The results indicate that, for columns with short and intermediate slenderness, the main parameters which govern the resistance (the load carrying capacity) of the CFST with an I-profile column under centric load, are the concrete compressive strength f_{cm}, and tube yield strength $f_{y,tube}$, as the contribution varies between 50% and 20% for compressive strength f_{cm} and 40% to 20% for tube yield strength $f_{y,tube}$. While, as the length of the column increases the resistance becomes more sensitive to elastic modulus of concrete E_{cm} and tube thickness. On the other, also the impact of the geometric imperfection increases with the increase of the column's length as can be observed from Figure 8.27 and Figure 8.28. Moreover, if we sum up the concrete parameters f_c and E_c on one hand and the steel parameters f_y and E_y on the other, the results of sensitivity analysis indicate that on average the concrete accounts for 40% of the load-bearing capacity of the CFST column under centric load, while the steel contribution is around 20%.
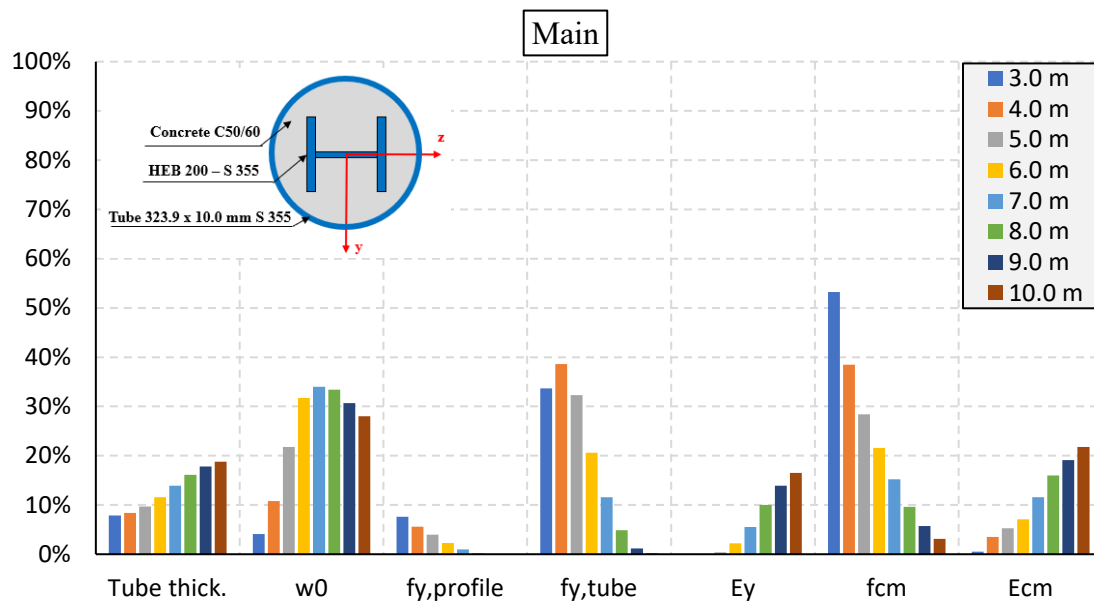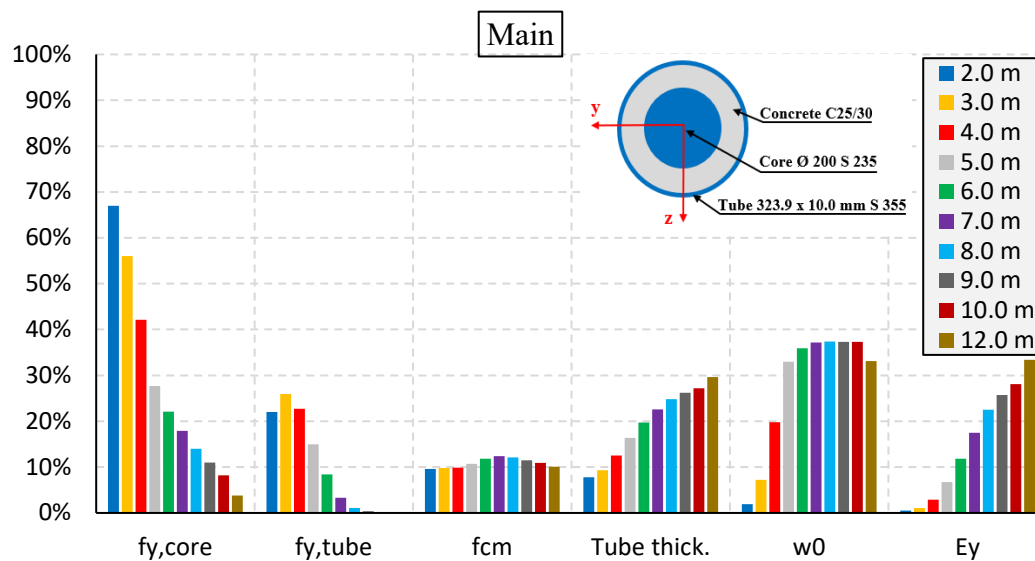

Figure 8.27 Main effect for different lengths of CFST column with inner I-profile
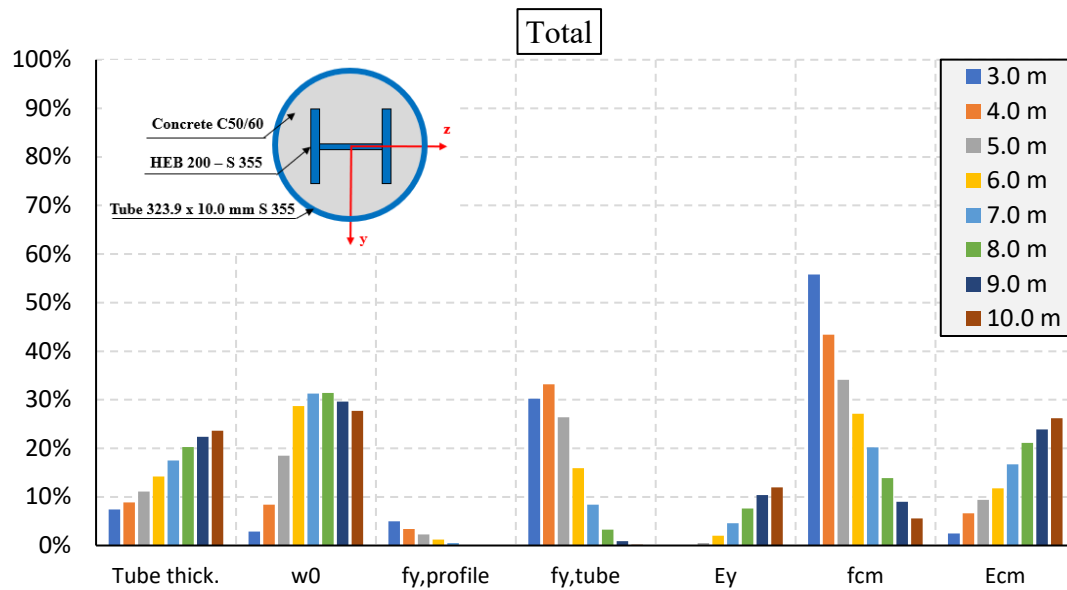
Figure 8.28 Total effect for different lengths of CFST column with inner I-profile

8.6 Concrete filled steel tube (CFST) with massive steel core

8.6.1 Geometry and boundary condition of deterministic model

The concrete-filled steel tube (CFST) with a massive steel core column model (geometry, material, and boundary conditions) considered for reliability analysis is presented in Figure 7.12. The cross-section is composed circular tube with an outer diameter of 323.9 mm and thickness of 10 mm with nominal yield strength $f_y = 355 \ N/mm^2$, filled with concrete C25/30, and an additional massive inner steel core $\varnothing$ 200 mm S235 with nominal yield strength $f_y = 235 \ N/mm^2$. The column is simply supported with imperfection (statically determined) and subjected to concentrated load. Similar to the previous cases, to perform stochastic finite element analysis, the deterministic model is transformed into a probabilistic one by considering all the geometric and material parameters as random variables except the length L, which is kept deterministic. However, the analyses were performed by varying the length of the column to cover the column's slenderness between $0.2 \le \overline{\lambda} \le 2.0$ as presented in Table 8.9.

Table 8.9 Length and non-dimensional slenderness of considered CFST with massive steel core

L [m]	1.0	2.0	3.0	4.0	5.0	6.0	7.0	8.0	9.0	10.0	12.0
$\bar{\lambda}_{nom}$	0.16	0.32	0.47	0.63	0.79	0.95	1.11	1.26	1.42	1.58	1.90

8.6.2 Probability density function of CFST with massive steel core

As in previous cases, Table 8.10 presents the list of the parameters considered as a random variable that carry the most uncertainties for CFST with inner I-profile column defined by normal and log-normal distribution based on recommendations of the Joint Committee on Structural Safety (JCSS) Model Code [46], prEN1992-1-1 [8], and prEN 1993-1-1 [9].

Table 8.10 Summary of random variables for CFST column with massive steel core

Symbol	Parameter	Mean	COV	Distribution
f_c	Concrete compressive strength	$f_{ck} + 8$	0.15	Log-normal
f_{ct}	Concrete tensile strength	$0.3 \cdot f_{ck}^{2/3}$	0.30	Log-normal
$f_{y,p}$	Massive core yield stress	$1.2 \cdot f_{yk}$	0.07	Log-normal
$f_{y,t}$	Tube yield stress	$1.2 \cdot f_{yk}$	0.07	Log-normal
E_c	Concrete elastic modulus	$9500 \cdot f_{cm}^{1/3}$	0.15	Log-normal
E_y	Steel elastic modulus	$E_{y,nom}$	0.03	Log-normal
w_0	Geometrical imperfection	$L/1000$	0.25	Normal
t_t	Tube thickness	$t_{tube,nom}$	0.04	Normal

8.6.3 Results of reliability analysis for CFST with massive steel core

Figure 8.29 shows the results of the Stochastic Finite Element Method (SFEM) and the comparison with the general method (GM) and the simplified method according to prEN1994-1-1 [3] using reduction factor χ and corresponding non-dimensional slenderness $\bar{\lambda}$ about the weak axis (z-z). According to prEN1994-1-1 [3] (simplified method) this cross-section is

without any reference regarding the classification into European buckling curves, while according to the general method this cross-section can be classified between *buckling curve b* and *buckling curve c* depending on the length of the column. For short and intermediate slenderness ratio (with $\overline{\lambda} = 0.2 - 1.0$), this cross-section is classified into *buckling curve b*, while for slender columns is classified into *buckling curve c*. Nevertheless, with reference to Figure 8.29, according to the probabilistic analysis (SFEM) in all considered lengths, the general method based on the plastic and strain-limited N-M interaction diagram, satisfies the safety level required by EN 1990 [5] for a normal building with a reference period of 50 years at ultimate limit state. However, for all considered lengths the difference between the SFEM analysis and the general method based on the plastic and strain-limited N-M interaction diagram is very small, as can be observed in Figure 8.29.
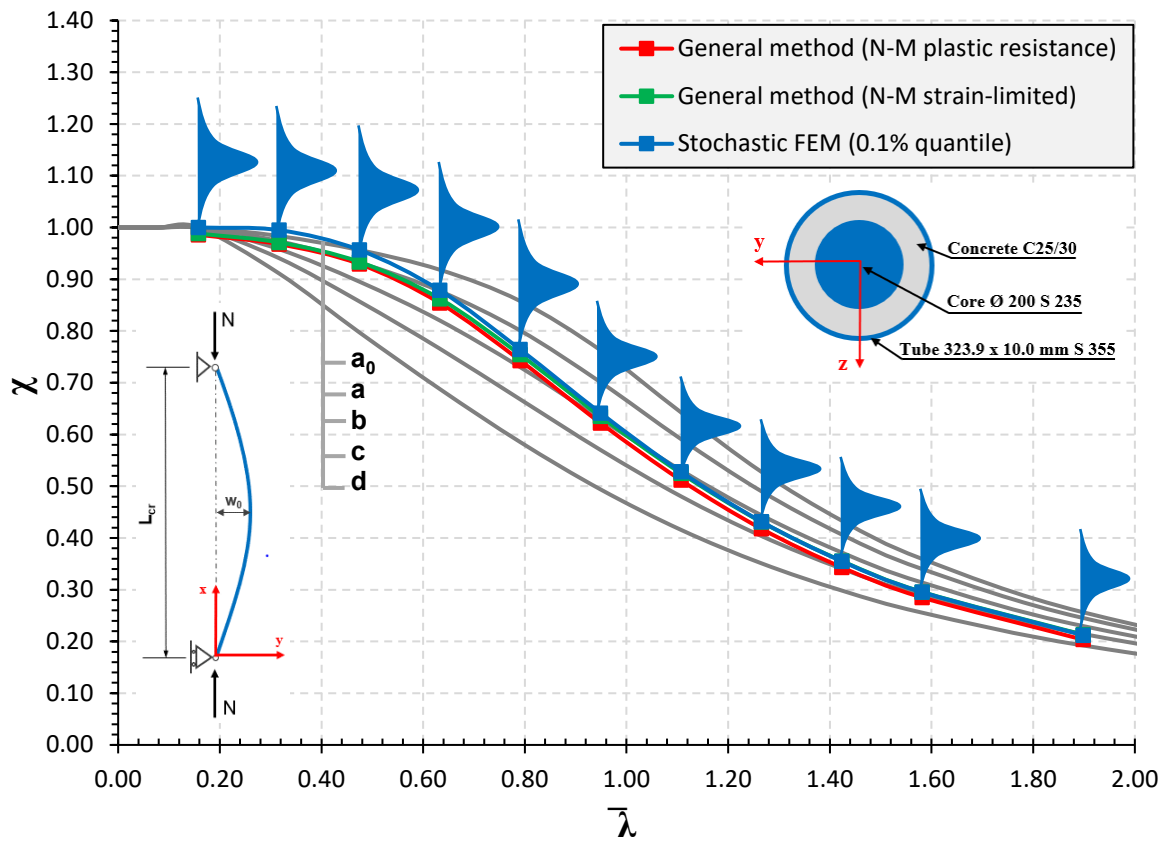
Figure 8.29 Comparison of SFEM with the general and the simplified method for CFST column with massive steel core

Moreover, similar to the CFST column the results indicate that the resistance follows a log-normal distribution with small positive skewness, and a constant reliability level through all considered lengths, with a slightly wider distribution of the resistance for columns with short length (short slenderness ratio), indicating that the uncertainties have more impact in stocky columns compare to slender one. Figure 8.30 shows the correlation between the maximum load and the generated random variables for the CFST column with a massive steel core with $L = 4.0\ m$. The strongest positive correlation is observed between maximum force N_{max} and steel core yield strength $f_{y,core}$, as the increase of the strength of the core, also increases the overall resistance N_{max} of the column. On the other hand, as expected, between the resistance of the column and geometric imperfection w_0 there is a negative correlation as the increase of imperfection reduces the overall resistance of the column. Regarding the other parameters, there is no strong correlation with the resistance of the column.
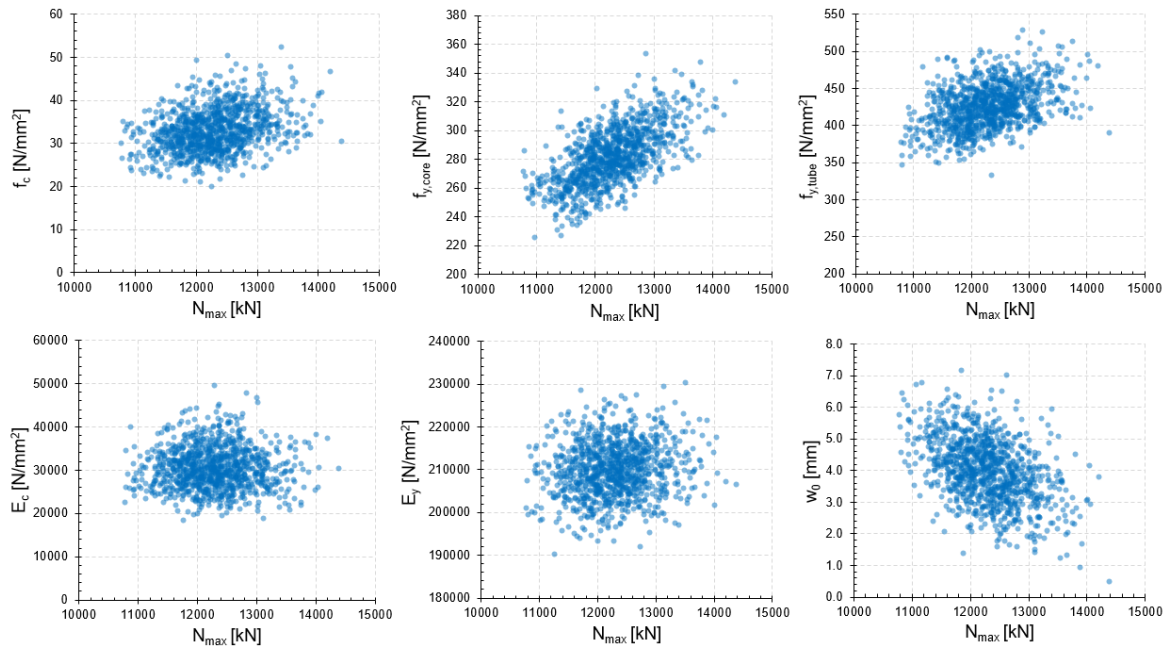
Figure 8.30 Correlation between N_{max} and random variables for CFST column with massive steel core with L = 4.0 m

On the other hand, concerning Figure 8.31, for slender columns ($L = 10.0\ m$), the resistance N_{max} is strongly correlated with the elastic modulus of steel E_y, as the increase/decrease of this parameter also increases/decreases the overall resistance of the column. This is understandable since for columns with a high slenderness ratio the maximum resistance is

close to the Eulerian buckling load (critical load), which is strongly related to the geometry and the elastic modulus. Moreover, for CFST with an additional massive steel core column ($L = 10.0\,m$), a strong negative correlation is observed between the geometric imperfection w_0 and the resistance N_{max} as the increase of the imperfection induces a reduction of the overall resistance of the column.
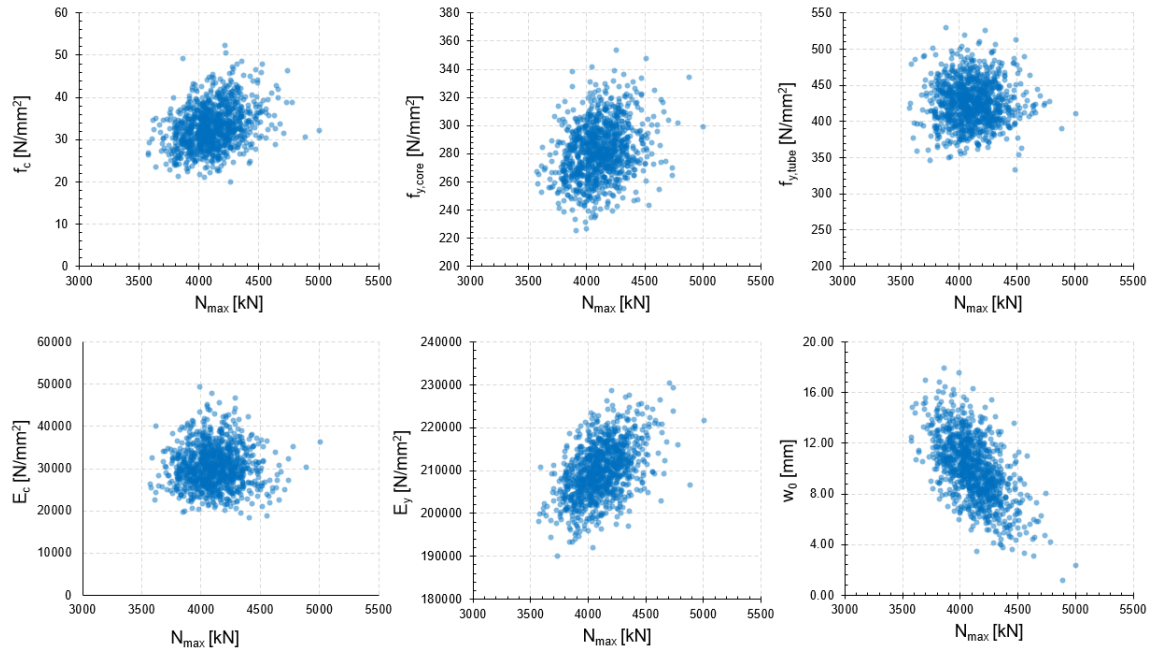
Figure 8.31 Correlation between N_{max} and random variables for CFST column with massive steel core with L = 10.0 m

8.6.4 Results of sensitivity analysis for CFST with massive steel core column

Similar to reliability analysis, the number of simulations, per column length is two thousand Latin Hypercube Samples (LHS). The random variables and their distribution presented in Table 8.8 are used also for sensitivity analysis. Figure 8.32 and Figure 8.33 show the results of sensitivity analysis for the CFST with a massive inner steel core column for different lengths varying between 2 m and 12 m. For the sake of clarity, the very small values of the sensitivity indices are not depicted. In the x-axis are shown the random variables considered for reliability analysis while in the y-axis it is shown the main and the total effect of each random variable on the scale between zero and one hundred percent. *The Main Sobol index* measures the sensitivity of each random variable to the quantity of interest (load-bearing capacity)

without considering the interaction with other random variables, while the *Total Sobol index* also considers the interaction between random variables. The results indicate that, for columns with short and intermediate slenderness, the main parameters which govern the resistance (the load carrying capacity) of the CFST with massive inner steel core column under centric load, is the steel core yield strength $f_{y,tube}$, as the contribution varies between 65% and 20%, while as the length of the column is increases the resistance becomes more sensitive to the elastic modulus of steel E_y and tube thickness. On the other, also the impact of the geometric imperfection increases with the increase of the column's length as can be observed from Figure 8.32 and Figure 8.33. Moreover, if we sum up the concrete parameters f_c and E_c on one hand and the steel parameters f_y and E_y on the other, the result of sensitivity analysis indicates that, on average the concrete accounts for 10% of the load-bearing capacity of the CFST column with massive steel core under centric load, while the steel contribution is around 50%, while other percentage are attributed to geometric parameters such as tube thickness and geometric imperfection etc.

Figure 8.32 Main effect for different lengths of CFST column with massive steel core
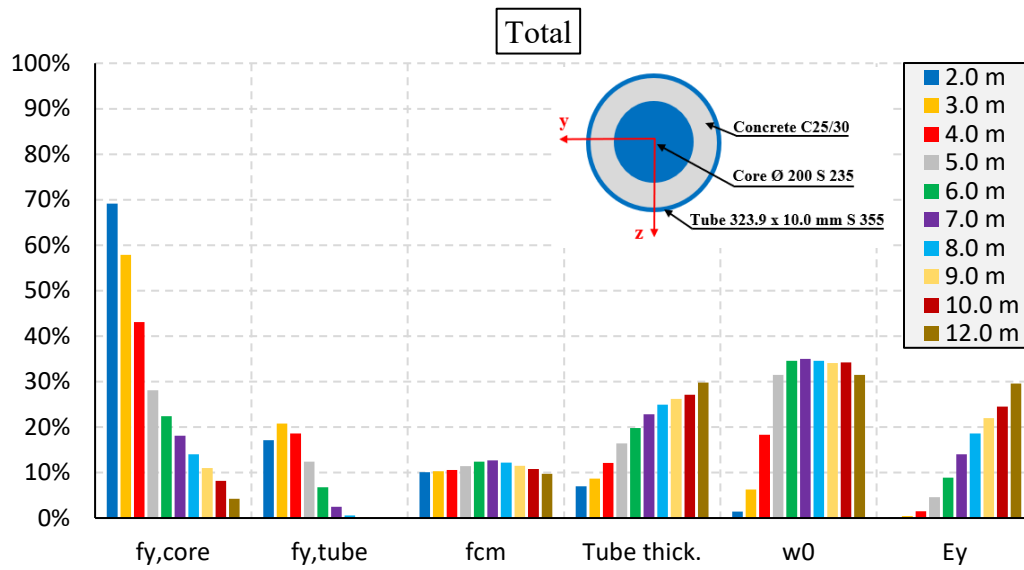
Figure 8.33 Total effect for different lengths of CFST column with massive steel core

8.7 Chapter summary

The safety and reliability assessment of the general method with the overall (safety) factor γ_0 based on strain-limited N-M interaction diagram for the design of composite columns according to prEN1994-1-1 [3] is addressed in this chapter. This is accomplished by comparing the safety level provided by [3] with 0.1 % quantile resistance of reliability analysis which corresponds to the reliability index $\beta = 3.04$ according to Eurocode 0 EN 1990 [5]. To perform reliability and sensitivity analysis, nonlinear SFEM analyses are performed. The statistical distribution of the main geometric and material parameters that carry the most uncertainties for composite columns are defined using normal and log-normal distribution based on recommendations of JCSS Model Code [46], prEN1992-1-1 [8], and prEN 1993-1-1 [9]. One of the assumptions for reliability analysis as well as sensitivity analysis is that all random variables are uncorrelated. To generate random samples, the Latin Hypercube Sampling (LHS) method is used. The considered columns are the same as the ones presented in Chapter 7. The analyses were performed by varying the length of the column to cover all the column slenderness between $0.2 \leq \overline{\lambda} \leq 2.0$.

The findings of nonlinear SFEM reliability analysis indicate that for all considered columns, both the general method based on plastic and strain-limited N-M interaction diagram, satisfy

the safety level required by EN 1990 [5] for a normal building with a reference period of 50 years at ultimate limit state. Moreover, the results show that, in case of PCEC and CFST columns with or with additional steel core/profile, across all lengths taken into consideration, the resistance follows a log-normal distribution with a small positive skewness and an almost constant reliability level, with a slightly wider distribution of the resistance for columns with short lengths. This is due to the fact that, the most material uncertainty appears in concrete compressive strength, and the primary parameter governing the resistance of the stocky columns is the concrete's compressive strength.

On the other hand, for CEC columns a non-constant reliability level through considered lengths is observed, with a significantly wider distribution of the resistance for columns with long lengths, indicating that the uncertainties have more impact in slender columns compared to stocky one. This is due to the fact that, the majority of material uncertainty are in concrete compressive strength and elastic modulus of concrete, which are the main parameters governing the resistance of the CEC columns.

The findings of the Sobol's indices [10] sensitivity analysis show that, for PCEC columns with short and intermediate slenderness ratio, the main parameters which influence the resistance are concrete compressive strength f_{cm} and steel yield stress f_y, while for columns with a high slenderness ratio the overall resistance is more sensitive to the elastic modulus of concrete E_{cm} and geometric imperfection w_0.

The same cannot be said for CEC columns, as for all considered lengths the concrete's compressive strength f_{cm} is the primary factor that determines the resistance.

In case of CFST columns with short and intermediate slenderness, the sensitivity analysis show that, the main parameters which influence the resistance is concrete compressive strength f_{cm}, while as the length of the column increases the resistance becomes more sensitive to the elastic modulus of concrete E_{cm} and tube thickness.

On the other hand, in case of CFST columns with additional steel core or steel profile, the sensitivity analysis indicates that the resistance of the column with short and intermediate slenderness ratio is influenced by the concrete compressive strength f_{cm} and the steel yield

stress f_y of the core and profile, while as the length of the column is increased, these columns are more sensitive to elastic modulus of steel E_y and concrete E_{cm}, as well as the geometric imperfection w_0.

In term of steel and concrete contribution to the load-bearing capacity, the sensitivity analysis indicates that, for PCEC columns on average the concrete accounts for 60% while the steel contribution is around 20%. In case of CEC columns on average the concrete accounts for 90% of the load-bearing capacity, while for CFST columns with additional steel core/profile the contribution is more balance between steel and concrete.

Chapter 9

Summary and Conclusions

9.1 Summary

An overview of the finding according to the objectives of the dissertation is provided below, arranged in the order that they appeared in the body of the work:

I.   In the introduction chapter, the motivation and the objectives of the dissertation are stated identifying discrepancies and the gap related to the design of composite columns according to the general method with strain-limited N-M interaction diagram. A flowchart outlining the dissertation's structure is also provided.

II.   In chapter 2, the literature review is given to discuss the fundamental concepts and the findings from previous studies on the scientific topics relevant to this dissertation. It begins with the differential equation to determine the critical buckling load and continues with the effect of initial imperfections on compressive members, the design of the composite columns, the verification again structural stability according EN 1994-1-1 [2], and ends with the basic concept regarding the probability theory and safety format according to EN 1990 [5] and *fib* Model Code [1] for composite columns in steel and concrete.

III. Chapter 3 is dedicated to the methodology and the software used in this work due to the variety of the analysis and software used in this dissertation. It begins with a detailed explanation of the geometric and material nonlinear analysis with imperfections (GMNIA) for composite columns conducted in ABAQUS/CAE [49] and OpenSees [53] given in Section 3.5 and Section 3.6, and continues with the theoretical background and software used to perform Stochastic Finite Element Method (SFEM), sampling method and sensitivity analysis for composite columns in steel and concrete.

IV.   In Chapter 4, the non-linear finite element analysis (GMNIA) conducted in ABAQUS/CAE [49] are benchmarked with experimental test results from online

existing literature to ensure that finite element model developed in ABAQUS/CAE [49] provide accurate results.

V. In Chapter 5, the non-linear finite element analysis (GMNIA) conducted in OpenSees [53] are benchmarked with ABAQUS/CAE [49] 3D model for different type of composite columns. The reason why FE model developed in OpenSees [53] is validated with ABAQUS/CAE [49] and not directly with experimental test results is because biaxial bending could not be taken into account in the FE model created in OpenSees [53], and the majority of the composite columns in the experimental test results shown in Chapter 4 are subjected to load eccentricity in two directions.

VI. Chapter 6 discusses the benchmark cases for steel and composite columns with regard to the impact of initial geometric imperfection and residual stresses. The results are presented separately for steel columns, PCEC columns, CEC column and CFST columns with massive steel core. For steel columns the results indicate that, the effect of residual stresses on flexural buckling resistance are important and cannot be neglected. This is particularly valid for columns that have an intermediate ratio of slenderness $(\bar{\lambda})$. For PCEC columns a reduction of the flexural buckling resistance is observed due to the effect of the residual stresses, however, in comparison with steel columns this reduction is smaller. On the other hand, for CEC columns the effect of residual stress is important only for columns with intermediate slenderness ratio $(0.5 \leq \bar{\lambda} \leq 1.2)$. For CFST columns with massive steel core the effect of residual stresses on flexural buckling resistance are important, but as it is reported in [30], the impact is related to the steel grade and the diameter of the massive core.

VII. Chapter 7 addresses the comparison of the flexural buckling resistance according to the general method given in prEN1994-1-1 [3] with the overall (safety) factor γ_0 based on plastic and strain-limited N-M interaction diagram and the so-called European buckling curves (the simplified method). The results are presented in non-dimensional form using reduction factor χ and relative slenderness $\bar{\lambda}$ defined according to EN 1993-1-1 [16], while the analyses were perform covering the relative slenderness between $0.2 \leq \bar{\lambda} \leq 2.0$. All the FE analysis are conducted in ABAQUS/CAE [49]. The results indicate that, in principle the simplified method is more conservative in comparison

with the general method. However, the difference between the flexural buckling resistance obtained from these two methods is influenced by the concrete class and the steel contribution (δ). In case when high class of concrete is used or steel contribution (δ) is low, the difference between these two methods increases and vice versa. On the other hand, the overall (safety) factor γ_0 based on strain-limited resistance for the general method is less conservative compared to plastic resistance for all considered composite columns. However, this difference is negligible for slender columns.

VIII.   Chapter 8 outlines and addresses the findings of the reliability and sensitivity analysis for composite columns in steel and concrete, that constitute the core of this dissertation. Stochastic Finite Element Method (SFEM) is used to perform reliability and sensitivity analysis, while to generate random samples, the Latin Hypercube Sampling method is employed. The statistical distribution related to geometry and material parameters are defined using normal or log-normal distribution as per recommendations of JCSS Model Code [46], prEN1992-1-1 [8], and prEN 1993-1-1 [9]. The results are presented separately for PCEC columns, CEC column and CFST columns with or without massive steel core or steel profile. The results of SFEM reliability analysis show that the general method based on strain-limited N-M interaction diagram satisfies the safety level required by EN 1990 [5] for a typical building with a reference period of 50 years at ultimate limit state for all considered columns. For PCEC and CFST columns a constant reliability level is observed for all considered lengths, while for CEC columns a non-constant reliability level is observed, with a significantly wider distribution of the resistance for columns with long lengths. On the other hand, based on the Sobol's indices [10] sensitivity analysis, it was possible to understand which are the main parameters which influence the resistance of the composite columns. In case of PCEC columns with short and intermediate lengths, the resistance is governed by the concrete compressive strength f_{cm} and steel yield stress f_y while for long columns the elastic modulus of concrete E_{cm} and geometric imperfection w_0 become more important. Similar results are observed also for CFST columns, while for CEC columns the main parameter for all considered length is the

concrete compressive strength. In terms of sensitivity to the variation of the material parameters, concrete is the major factor in the flexural buckling resistance of the composite columns. On average, for this case study the concrete makes up roughly 90% of a column's resistance for CEC columns, 60% for PCEC columns, roughly 50% for CFST columns, and about 40% for CFST columns with a steel profile.

9.2 Conclusions

There are various conclusions that can be drawn from the broad scope of this project considering that the aim of this dissertation was to investigate the effect of the geometric and residual stresses on steel and composite columns, the application of the general method and comparison with the European buckling curves (the simplified method), the safety and reliability of the general method based on plastic and strain-limited N-M interaction diagram, given in prEN 1994-1-1 [3], with the help of the Stochastic Finite Element Method (SFEM), which combines the Finite Element Method (FEM) with the statistical distribution of the main geometric and materials parameters.

Starting with the effect of geometric imperfection and residual stresses, the results for steel and partial concrete encased composite columns demonstrate that, for all lengths taken into consideration between $0.2 \leq \overline{\lambda} \leq 2.0$, residual stresses have a significant and undesired influence on flexural buckling under compression force and cannot be neglected, this is particularly important when dealing with columns with intermediate slenderness ratio. The same holds true also for CFST columns with or without steel profile. In addition, in case of CFST columns with massive steel core as it is reported in [30], the influence of the residual stresses on massive steel core is strictly related to the steel grade and diameter of the massive core, and in case of a larger diameter and a high steel contribution (δ), the effect of residual stresses is even more significant that the one presented in this work.

Regarding the geometric imperfection for the general method, this part is under discussion whether the imperfection value $L/1000$ which was originally measure for steel members (IPE160 – S235 mild steel) when ECCS buckling curves were developed [14], and reported in [38], [39], [32], and [36] can be applied for all composite columns. From the experimental test

conducted in CEC columns reported in [26], the average initial geometric imperfection (9 test series) is around $L/660$. In the latest version of prEN 1994-1-1 [3] it is recommended that the geometrical imperfection should be $L/400$ unless the National Annex gives a different value, and this value is reported also in Eurocode 2 EN 1992-1-1 [34] for reinforced concrete columns. Nevertheless, the reliability and sensitivity analysis conducted in this study demonstrated that the flexural buckling resistance of the composite columns under compression force is more akin to that of the reinforced concrete column than steel column, and this indicate that the geometric imperfection should fall between $L/400$ (reinforced concrete columns) and $L/1000$ (steel columns), but that no single value can be applied to all types of composite columns.

The finding from application of the general method according to prEN1994-1-1 [3] with the overall (safety) factor γ_0 based on plastic and strain-limited N-M interaction diagram indicate that, the general method provide less conservative results compared to the simplified method (European buckling curves), and the difference between the two methods increased when high-strength concrete is used or the steel contribution is low and vice versa. Related to the calculation of the overall (safety) factor γ_0, N-M interaction diagram based on the strain-limited resistance provide slightly less conservative results compared to plastic resistance for all considered column with slenderness ratio between $0.2 \leq \overline{\lambda} \leq 2.0$.

The reliability analysis using SFEM results demonstrate that for all composite columns taken into consideration, both the general method based on the strain-limited N-M interaction diagram and plastic resistance satisfy the safety level required by Eurocode 0 EN 1990 [5] for a normal building with a reference period of 50 years at ultimate limit state which corresponds to the reliability index $\beta = 3.04$. In case of PCEC and CFST columns the resistance follows a log-normal distribution with an almost constant reliability level with a slightly wider distribution for columns with small slenderness ratio, while in case of CEC columns a non-constant reliability level is observed through all considered lengths.

The results of Sobol's indices [10] sensitivity analysis provided valuable information from the statistical distribution of the main geometric and material parameters which influence the resistance of composite columns under compression force. For all considered columns, a

linear relation is observed between the variation in column's length and the main geometric and material parameters. The flexural buckling resistance of the CEC column under compression force is very similar to reinforced concrete column as the main governing parameter is the concrete compressive strength f_{cm}, with the contribution varying between 90% for 3 m column and 60% for 10 m column, while in case of PCEC and CFST columns the contribution is more evenly distributed between steel and concrete, with concrete having a slightly greater dominance which is always in a function of the column's length.

9.3 Recommendations for further research

The following recommendations are made for the research's future investigations:

−   Extensive buckling tests on various composite column types are necessary to establish statistical distribution of the main geometric and materials parameters, similar to the tests carried out for the creation of the European buckling curves for steel columns.

−   Further experimental and numerical study must be conducted regarding the initial bow imperfection and installation tolerances (position of the steel profile and reinforcement bars inside the concrete of the composite columns).

−   Additional experimental and numerical research concerns the way creep and shrinkage affect the stability of the composite columns under compression force or compression and bending moment.

List of Tables

List of Figures

Bibliography

[1]   fib Model Code for Concrete Structures 2010. fib Journal Structural Concrete, 2010.

[2]   EN 1994-1-1: 2004: Eurocode 4: Design of composite steel and concrete structures – Part 1-1: General rules and rules for buildings. CEN, 2004.

[3]   prEN 1994-1-1: 2021: Eurocode 4: Design of composite steel and concrete structures – Part 1-1: General rules and rules for buildings. CEN, 2021.

[4]   R.P. Johnson, Composite Structures of Steel and Concrete, Volume 1: beams, slabs, columns, and frames for buildings, vol. 19, no. 4. 1997. doi: 10.1016/s0141-0296(97)83368-8.

[5]   EN 1990: 2002: Eurocode 0 - Basis of structural design. CEN, 2002.

[6]   G. Hanswille, M. Bergmann, and R. Bergmann, 'Design of composite columns with cross-sections not covered by Eurocode 4', Steel Constr., vol. 10, no. 1, 2017, doi: 10.1002/stco.201710004.

[7]   Joint Committee on Structural Safety (JCSS), Probabilistic Model Code – Part 3: Material properties. 2000.

[8]   prEN 1992-1-1: 2019: Eurocode 2: Design of concrete structures - Part 1-1: General rules, rules for buildings, bridges and civil engineering structures. CEN, 2019.

[9]   prEN 1993-1-1: 2019: Eurocode 3 — Design of steel structures — Part 1-1: General rules and rules for buildings. CEN, 2019.

[10]   I. M. Sobol, 'Global sensitivity indices for nonlinear mathematical models and their Monte Carlo estimates', Math. Comput. Simul., vol. 55, no. 1–3, pp. 271–280, 2001, doi: 10.1016/S0378-4754(00)00270-6.

[11]   Leonard Eulero, Methodus inveniendi lineas curvas maximi minimive proprietate gaudentes sive solutio problematis isoperimetrici latissimo sensu accepti. 1744.

[12]   Z. P. Bazant, L. Cedolin, and J. W. Hutchinson, Stability of Structures: Elastic, Inelastic, Fracture, and Damage Theories. 1993. doi: 10.1115/1.2900839.

[13]   A. Henriksson and J. Panarelli, 'Initial bow imperfection for flexural buckling of steel members', Chalmers University of Technology, 2017.

[14]   ECCS (1978), European Recommendations for Steel Construction, European Convetion for Constructional Steelwork, Brussels. Brussels, 1978.

[15]   S. Jerath, Structural Stability Theory and Practice: buckling of columns, beams, plates, and shells. 2021. doi: 10.1002/9781119694489.

[16]   EN 1993-1-1: 2005: Eurocode 3: Design of steel structures - Part 1-1: General rules and rules for buildings. CEN, 2005.

[17]   J. Jönsson and T. C. Stan, 'European column buckling curves and finite element modelling including high strength steels', J. Constr. Steel Res., vol. 128, pp. 136–151,

2017, doi: 10.1016/j.jcsr.2016.08.013.

[18]   Sfintesco D., 'Fondement expérimental des courbes européennes de flambement, Construction Métallique', no. 3, pp. 5–12, 1970.

[19]   H. Beer and G. Schulz, 'Bases Théoriques des Courbes Européennes de Flambement Construction Métallique', 1970.

[20]   R. Bjorhovde, 'Deterministic and probabilistic approaches to the strength of steel columns, PhD Thesis', Lehigh University, 1972.

[21]   J. Strating and H. Vos, 'Computer Simulation of the E. C. C. S. Buckling Curve Using a Monte-Carlo Method.', 1973.

[22]   A. Taras, 'Contribution to the Development of Consistent Stability Design Rules For Steel Members, PhD Thesis.', Technischen Universität Graz, 2010.

[23]   G. Schulz, 'Traglastermittlung von planmäßig mittig belasteten Druckstäben aus Baustahl unter Berücksichtigung von gometrischen und strukturellen Imperfektionen', 1968.

[24]   prEN 1993-1-14 2021: Eurocode 3: Design of steel structures — Part 1-14: Design assisted by finite element analysis. CEN, 2021.

[25]   Bergman R, 'Traglastberechnung von Verbundstuetzen', PhD thesis, The Ruhr University Bochum, 1981.

[26]   T. Bogdan et al., 'Load bearing behavior of concrete encased composite columns with high-performance materials', Ce/Papers, vol. 6, no. 3–4, pp. 314–319, 2023, doi: 10.1002/cepa.2705.

[27]   C. Bernuzzi and B. Cordova, Structural Steel Design to Eurocode 3 and AISC Specifications. 2017.

[28]   C. G. Salmon, J. E. Johnson, and F. A. Malhas, 'Steel Structures - Design and Behavior'. 2009.

[29]   ECCS (1984), Ultimate Limit State Calculation of Sway Frames with Rigid Joints, European Convetion for Constructional Steelwork - TC 8, Brussels. 1984.

[30]   M. Lippes, 'Zur Bemessung von Hohlprofil – Verbundstützen aus hochfesten Stählen und Betonen', PhD thesis, Bergische Universität Wuppertal, 2008.

[31]   P. Zogu and M. Schäfer, 'Safety and reliability assessment of composite columns according to Eurocodes using stochastic finite element method', 2024.

[32]   G. Hanswille, M. Schäfer, and M. Bergmann, Eurocode 4 - DIN EN 1994-1-1 Bemessung und Konstruktion von Verbundtragwerken aus Stahl und Beton, Teil 1 1: Allgemeine Bemessungs und Anwendungsregeln für den Hochbau. Kommentar und Beispiele. 2020.

[33]   K. Roik and R. Bergmann, 'Harmonisation of the European Construction Codes', 1989.

[34]   EN 1992-1-1: 2004: Eurocode 2: Design of concrete structures - Part 1-1: General rules and rules for buildings. CEN, 2004.

[35] D.-I. M. Chanou, 'Zum Tragverhalten von Hohlprofil-Verbundstützen mit Mehrkernquerschnitten, PhD Thesis', Bergische Universität Wuppertal, 2018.

[36] P. Zogu and M. Schäfer, 'Determination of overall factor for the application of the General Method based on plastic and strain-limited N-M interaction for composite compression members', Ce/Papers, vol. 6, no. 3–4, pp. 95–100, 2023, doi: 10.1002/cepa.2665.

[37] prEN 1992-1-1: 2021: Eurocode 2 Design of concrete structures – Part 1-1 General rules, rules for buildings, bridges and civil engineering structures. CEN, 2021.

[38] H. Unterweger and M. Kettler, 'Design of composite columns based on Eurocode – comparison between general and simplified methods', pp. 757-, 2018, doi: 10.4995/asccs2018.2018.7064.

[39] G. Hanswille, Eurocode 4 Composite Columns - Background and Applications. 2008.

[40] Q. Zhang, 'Moment and Longitudinal Resistance for Composite Beams Based on Strain Limited Design Method-Elastic-Plastic Design for Composite Beams', 2020.

[41] M. Schäfer, Q. Zhang, P. Zogu, and M. Bergmann, 'Assessment of General Method for Composite Column Design in EN 1994-1-1 and Comparison with Simplified Method', 9TH Int. Conf. Compos. Constr. STEEL Concr., vol. 6, no. 1, pp. 195–206, 2021, doi: https://doi.org/10.1002/cepa.1904.

[42] Q. Zhang, 'SL.com'. University of Luxembourg, 2021.

[43] S.-K. Choi, R. V. Grandhi, and R. A. Canfield, Reliability based structural design. 2006.

[44] M. Furu and R. Möse, 'Evaluation of Safety Formats for Nonlinear Finite Element Analysis of Concrete Structures', 2010.

[45] M. Holický, A. Materna, G. Sedlacek, L. Sanpaolesi, and Ton Vrouwenvelder, Guide to the basis of structural reliability and risk engineering related to Eurocodes, supplemented by practical examples. 2005.

[46] Joint Committee on Structural Safety (JCSS), Probabilistic Model Code – Part 1: Basic of design. 2001.

[47] V. Cervenka, 'Global Safety Format for Nonlinear Calculation of Reinforced Concrete', Beton- und Stahlbetonbau, vol. 103, no. S1, pp. 37–42, 2008, doi: 10.1002/best.200810117.

[48] V. Cervenka, 'Reliability-based non-linear analysis according to fib Model Code 2010', Stuctural Concr. J. fib, vol. Volume 14, no. 1, pp. 19–28, 2013, doi: DOI: 10.1002/suco.201200022.

[49] Dassault Systemes Simulia Corp, 'ABAQUS/CAE 2018'. Johnston, RI, USA, 2017.

[50] M. Zhu, F. McKenna, and M. H. Scott, 'OpenSeesPy: Python library for the OpenSees finite element framework', SoftwareX J., vol. 7, no. 2018, pp. 6–11, 2018, doi: https://doi.org/10.1016/j.softx.2017.10.009.

[51] F. McKenna, S. Yi, A. B. Satish, K. Zhong, Adam Zsarnoczay, and W. Elhaddad, 'NHERI-

SimCenter/quoFEM: Version 3.3.0 (v3.3.0)'. 2023. doi: https://doi.org/10.5281/zenodo.10443180.

[52] F. Williamson, 'Richard courant and the finite element method: A further look', Hist. Math., vol. 7, no. 4, pp. 369–378, 1980, doi: 10.1016/0315-0860(80)90001-4.

[53] G. L. F. Silvia Mazzoni, Frank McKenna, Michael H. Scott, 'Open System for Earthquake Engineering Simulation (OpenSees)'. University of California, Berkeley, 2006.

[54] J. D. Arregui-Mena, L. Margetts, and P. M. Mummery, 'Practical Application of the Stochastic Finite Element Method', Arch. Comput. Methods Eng., vol. 23, no. 1, pp. 171–190, 2016, doi: 10.1007/s11831-014-9139-3.

[55] P. H. Warts, 'Stuctural reliability using Finite Element Analysis', Delf University of Technology, 2000.

[56] J. Králik, 'Reliability Analysis of Structures using Stochastic Finite Element Method', 2009.

[57] J. Schneider and T. Vrouwenvelder, Introduction to safety and reliability of structures. 2017.

[58] H. Eklund Astrid Skorve Arne Strand, M. Engen, and K. Jochen Köhler, 'Reliability assessments of concrete structures using non-linear finite element analyses', NTNU6 Norwegian University of Science and Technology, 2017.

[59] N. L. Tran, C. A. Graubner, and G. Rombach, 'An efficient latin hypercube sampling for probabilistic nonlinear finite element analysis of reinforced concrete structures', - Proc. 7th Int. Conf. Struct. Eng. Mech. Comput. 2019, no. 1, pp. 543–548, 2019, doi: 10.1201/9780429426506-95.

[60] M. D. McKay, R. J. Beckman, and W. J. Conover, 'A comparison of three methods for selecting values of input variables in the analysis of output from a computer code', Technometrics, vol. 42, no. 1, pp. 55–61, 2000, doi:10.1080/00401706.2000.10485979.

[61] S. Shayan, 'System Reliability-Based Design of 2D Steel Frames By Advanced Analysis', PhD Thesis, The University of Sydney, 2013.

[62] B. M. Adams et al., Dakota, A Multilevel Parallel Object-Oriented Framework for Design Optimization, Parameter Estimation, Uncertainty Quantification, and Sensitivity Analysis: Version 6.16 User's Manual. 2019.

[63] D. Li, L., Papaioannou, I. and Straub, 'Global sensitivity analysis', 2019.

[64] Z. Hu and S. Mahadevan, 'Probability models for data-Driven global sensitivity analysis', Reliab. Eng. Syst. Saf., vol. 187, no. December, pp. 40–57, 2019, doi: 10.1016/j.ress.2018.12.003.

[65] H. Wang, J. Li, and Y. Song, 'Numerical Study and Design Recommendations of Eccentrically Loaded Partially Encased Composite Columns', Int. J. Steel Struct., vol. 19, no. 3, pp. 991–1009, 2019, doi: 10.1007/s13296-018-0179-7.

[66] M. Begum, R. G. Driver, and A. E. Elwi, 'Finite-Element Modeling of Partially Encased

Composite Columns Using the Dynamic Explicit Method', J. Struct. Eng., vol. 133, no. 3, pp. 326–334, 2007, doi: 10.1061/(asce)0733-9445(2007)133:3(326).

[67]	M. Begum, R. G. Driver, and A. E. Elwi, 'Behaviour of partially encased composite columns with high strength concrete', Eng. Struct., vol. 56, pp. 1718–1727, 2013, doi: 10.1016/j.engstruct.2013.07.040.

[68]	V. Terzic, 'Structural Modeling With Examples in OpenSees'. University of California; Berkeley, 2012.

[69]	A. Poursadrollah, 'Flexural Buckling of Steel Cold-Formed Hollow Profiles in the framework of Eurocodes', University of Naples Federico II, 2021. doi: 10.13140/RG.2.2.17654.11849.

[70]	J. Frólo and Š. Gramblička, 'Steel core in composite steel-concrete columns', Key Eng. Mater., vol. 691, pp. 195–206, 2016, doi: 10.4028/www.scientific.net/KEM.691.195.

[71]	J. Frólo and Š. Gramblička, 'The steel core covered by reinforced concrete in the composite steel-concrete columns', in 22nd International Conference ENGINEERING MECHANICS, 2016.

[72]	M. Johansson and K. Gylltoft, 'Mechanical Behavior of Circular Steel–Concrete Composite Stub Columns', J. Struct. Eng., vol. 128, no. 8, pp. 1073–1081, 2002, doi: 10.1061/(asce)0733-9445(2002)128:8(1073).

[73]	Bridge RQ., 'Concrete filled steel tubular columns. Tech rep. R283', 1976.

[74]	R. Gonçalves and J. Carvalho, 'An efficient geometrically exact beam element for composite columns and its application to concrete encased steel I-sections', Eng. Struct., vol. 75, pp. 213–224, 2014, doi: 10.1016/j.engstruct.2014.05.042.

[75]	Y.-L. Pi, M. A. Bradford, and B. Uy, 'Second Order Nonlinear Inelastic Analysis of Composite Steel–Concrete Members. II: Applications', J. Struct. Eng., vol. 132, no. 5, pp. 762–771, 2006, doi: 10.1061/(asce)0733-9445(2006)132:5(762).

[76]	B. . Young, 'Steel Column Design', PhD thesis, Cambridge University, 1971.

[77]	J. B. Dwight, 'Use of Perry-Roberstson Formula to Represent the New European Strut Curves', in International Colloquium on Column Strength, Paris, 1972, pp. 399–411.

[78]	P. Zogu and M. Schäfer, 'Numerical Study of Non-linear Buckling Analysis for Steel and Partial Concrete Encased Composite Columns', Ce/Papers, vol. 5, no. 4, pp. 778–786, 2022, doi: 10.1002/cepa.1819.

[79]	G. Hanswille and R. Bergmann, 'Ermittlung geometrischer Ersatz-imperfektionen für Verbundstützen mit hochfesten Stahlen', 2001.

[80]	EN 1992-2: 2005: Eurocode 2: Design of concrete structures - Part 2: Concrete bridges - Design and detailing rules. CEN, 2005

[81]	Knobloch, M., Bureau, A., Kuhlmann, U., da Silva, L.S., Snijder, H.H., Taras, A., Bours, A.-L. and Jörg, F. (2020), Structural member stability verification in the new Part 1-1 of the second generation of Eurocode 3. Steel Construction, 13: 98-113.